Performance evaluation of the photovoltaic system

Submitted by

John Penman

to

the University of Exeter as a thesis for the degree

of

Doctor of Philosophy in Renewable Energy

in July 2022.

I certify that all material in this thesis that is not my own work has been identified. No material has previously been submitted and approved for the award of a degree by this or any other University.

Signature: ……..

Abstract

The various renewable energy source technologies, Photovoltaics (PV) transforming sunlight directly into electricity, have become standard practice worldwide, especially in countries with high solar radiation levels. PV systems have been developed rapidly over recent years, and many new technologies have emerged from different producers. For each type of PV module, manufacturers provide specific information on rated performance parameters, including power at maximum power point (MPP), efficiency and temperature factors, all under standard solar test conditions (STC) 1000 W/m². Air. In addition, the mass (AM) of 1.5 and the cell's temperature was 25℃.

Unfortunately, this grouping of environmental conditions is infrequently found in outdoor conditions. Also, the data provided by the manufacturers are not sufficient to accurately predict the performance of photovoltaic systems in various climatic conditions. Therefore, monitoring and evaluating the performance of the off-site systems is necessary.

This thesis aims to overview various photovoltaic technologies, ranging from crystalline silicon (c-SI) to thin-film CdTe and GiCs. The following are the main parameters for evaluating the external units' performance to describe the PV systems' operation and implementation. In addition, a review of the impacts of various environmental and operational factors, such as solar radiation, temperature, spectrum, and degradation.

Dedication

This dedication is to my late father, John and my mother, Nancy. Who was there for me in my darkest time and gave me unwavering encouragement and confidence throughout my life.

My dedication also extends to my beloved wife for her understanding, patience, care and love. Zhenny's reassurance was influential to me while pursuing this degree and writing my treatise.

And to all my family: I am incredibly grateful.

Acknowledgements

It is a long and lonely road full of sweat, blood, tears, and sleepless nights to achieve a Ph.D. But, of course, this is only the half-truth, partially true because my Ph.D took about seven years and logged at least 100,000 miles. Yet, despite the length of this journey, I never felt alone. The doctorate is a path that I was fortunate enough to walk with many supportive people with only encouragement to achieve by my side. I think everyone I have met has added their input in many ways to improve this work: without them, this thesis would not be the work you are about to read.

Firstly, I must thank Professor Tapas Mallik for entrusting my submission to such an important assignment. Despite my mistakes and oversights, Tapas was fully supportive. It did not matter what the issue was; I am eternally grateful. Next, I thank Dr Senthilarasu Sundaram for being a thoughtful second. Good luck with your new position. And to Dr Mohammad Abusara for all his understanding.

PhDs take up most of my time and make decisions that strongly impact my life. So it's not just a job; it's a journey; I met some delightful people and new friends, Eduardo, Nadia, and Leonardo, on this journey. So my acknowledgements give me two good feelings: firstly, the satisfaction of completing my long journey, and secondly, these friends are forever friends, never mind the distance; as they will only ever be a phone call away, as friendships are for life.

Now is the time to thank the most important people in my life. My family has always been the foundation, allowing me to develop into today's person. To my wife Zhenny, I can only thank her for her support and understanding: when I felt I had no free time for her other than studying and writing. Thanks to my sister Fiona and her husband, Peter, for their support and feedback.

Last but not least, my mother, Nancy and father, John, helped me through the darkest periods. And for that, I can never thank you enough. I have always felt loved and supported in all my choices, no matter what. You have always been an example to follow in challenging times and circumstances. I dedicate these seven years of work and 100,000 miles to you for your continuous support.

Contents

List of Tables.

List of Figures

Nomenclature

Symbol	Definition	Unit
A_{cell}	Cell's active area	m^2
A_{fins}	Area of the finned Surface	m^2
A_i	Area of the i-surface of the fins	m^2
CL	Characteristic length	M
c_p	Specific heat capacity	J/K
D	Diameter	M
E_{ref}	AM1.5 reference spectrum	W/m^2nm
FF.	Cell's fill factor	
$F_{i,k}$	View factor between the surfaces i and k	
g	Gravitational acceleration	m/s^2
Gr	Grashof number	
h	Heat transfer coefficient	W/m^2K
H	Fin height	M
h_{fins}	Heat transfer coefficient of a micro-finned surface	W/m^2K
h_m	Mass specific heat transfer coefficient	W/kgK
h_{tot}	Average heat transfer coefficient	W/m^2K
I_{DC}	Currant provided by the DC supply	A
I_F	Diode's forward current	A
I_R	Diode's reverse current	A
I_S	Cell's short circuit current	A
J	Current density	A/m^2
k	Thermal conductivity	W/mK
k_B	Boltzmann constant	J/K
Kn	Knudsen number	
L	Length of the micro-fins	M
l	Length	M
L_{max}	Maximum length	M
n	Ideality factor	
N_{cell}	Number of cells	
N_{fins}	Number of fins	
Nu_{loss}	Nusselt number of the insulating case surfaces	
N_w	Number of wires	
Pr	Prandtl number	
Q	Heat power	W
q	Conduction heat flux	W/m^2
q_{el}	Elementary charge	C
Q_{cell}	Waste heat produced by the cell	W
Q_{fins}	Heat dissipated by a micro-finned surface by convection	W
Q_{in}	Heat produced by the heater	W
$Q_{J.}$	Heat generated because of the Joule losses	W
Q_{loss}	Heat lost by the insulating case	W

Q_r	Heat dissipated by a micro-finned surface by radiation	W
Q'_v	Volumetric heat source	W/m^3
r	Hydraulic radius	m
R	Thermal resistance	K/W
R*	Thermal resistance per unit of Surface	Km^2/W
Ra	Rayleigh number	
R_{el}	Electrical resistance	Ω
s	Spacing between the fins	m
SR.	Spectral response	A/Wnm
T	Temperature	K
t	Thickness	m
t_b	Fin base thickness	m
T_{back}	Temperature of the back surface of the insulating case	K
T_{cell}	Cell's Temperature	K
T_{fins}	Temperature of a micro-finned surface	K
v_{air}	Kinematic viscosity of the air	m^2/s
V_{DC}	Voltage provided by the DC supply	V
$V_{F.}$	Diode's forward voltage drop	V
V_{fins}	Volume of the fins array	m^3
V_{OC}	Cell's open-circuit voltage	V
V_{OCS}	Subcell's open-circuit voltage	V
$V_{R.}$	Diode's reverse voltage drop	V
w	Electrical conductor's width	m
W	Fin array's width	m
x	Concentrations	suns
z	Electrical conductor's thickness	m

Greek symbols

α	Coefficient of linear thermal expansion	1/K
α_D	Thermal diffusivity	m^2/s
β	Coefficient of volumetric thermal expansion	1/K
ΔL_{max}	Maximum expected deformation	m
ΔT	Temperature difference	K
ε	Material's emissivity	
ε_{fins}	Fin effectiveness	
θ	Tilt angle	rad
μ_G	Mean of the Gaussian distribution	
ν	Kinematic viscosity	m^2/s
ρ	Electrical resistivity	Ωm
ρ_D	Density	kg/m^3
σ	Stefan-Boltzmann constant	W/m^2K^4
σ_{el}	Electrical conductivity	S/m
σ_G	Standard deviation	

Subscripts

air	Air
amb	ambient
c	Convective
d	Layer below the thin resistive layer
d	Power dissipated
fins	Micro-fins
flat	Flat silicon wafer
g	Power generated
HP	Heat path between the cell and the ambient
loss	Losses happening on the insulating case
OC	Open circuit
p	Peak power (under standard test conditions)
r	Radiative
S	Surface
SC	Short-circuit
Syl	Sylgard
Tot	Combination of radiation and convection
trl	thin resistive layer
u	Layer over the thin resistive layer
w	Wire
Ω	Ohmic losses

Prefixes

U	Uncertainty

Abbreviations

ASTM American Society for Testing and Materials International (USA) CNT Carbon nano-tubes
CPC Compound Parabolic Concentrators
CPV Concentrating Photovoltaics (or Concentrator Photovoltaics) C.R. Concentration Ratio
CSTCs Concentrator Standard Test Conditions
CTE Coefficient of Thermal Expansion
CVD Chemical Vapour Deposition
DBC Direct Bonded Copper
DC Direct current
DNI Direct normal irradiance
DRIE Deep Reactive Ion Etching
DST Department of Science and Technology (India)
DWCNT Double-walled carbon nanotubes
ENEPIG Electroless Nickel/Electroless Palladium/Immersion Gold
EPSRC Engineering and Physical Sciences Research Council (UK.)
EVA Ethylene-Vinyl Acetate
FF Fill factor
FR4 Flame Retardant, type 4
HCPV High Concentrating Photovoltaics
HiPco High-pressure carbon monoxide HS Heat Sink
IEC International Electrotechnical Commission (Switzerland)
IEEE Institute of Electrical and Electronics Engineers (USA) IMM Inverted Metamorphic Multijunction
IMS Insulated Metal Substrate
IPC Association Connecting Electronics Industries
I.R. Infrared
LCPV Low Concentrating Photovoltaics
LED Light Emitting Diode
LM Lattice-matched
MCHS Microchannel heat sink
MCPV Medium Concentrating Photovoltaics
m-EDWM Micro-electro discharge wire machining
MEMS Microelectromechanical systems
MHP Micro-heat pipes
MJ Multijunction
MWCNT Multi-walled carbon nanotubes

NREL	National Renewable Energy Laboratory (USA)
PCB	Printed Circuit Board
PDMS	Polydimethylsiloxane
PMMA	Poly (methyl methacrylate)
PPMS	Poly (p-methylstyrene)
PV	Photovoltaics
PV/T	Photovoltaic/Thermal collectors
RIE	Reactive Ion Etching
SEM	Scanning Electron Microscope
SWCNT	Single-walled carbon nano-tubes
TIM	Thermal interface material
UHCPV	Ultra-High Concentrating Photovoltaics
UV	Ultraviolet

List of publications

Publications included in the thesis

Chapter 1: Introduction.

The Earth-Sun, our sun, is a star, in many ways, the most significant star in the solar system. The sun is a unique energy source for our universe and our planet. It radiates more energy in one hour than is used globally in one year; currently, solar power is sufficient, in theory, to meet all humankind's current and future requirements.Renewable energies are the foreseeable future for energy generation. They are the cleanest and most abundant in the octave of renewable energies with increasing energy demands. Therefore, the electricity sector plays a critical role in supporting economic recovery and a more and more crucial long-term role in providing the current and future world requirements.

Photovoltaics: is the method to convert the sunlight for power generation directly; it is still limited; however, there are multiple ways to generate electricity from the earth's sun.
Direct photovoltaics or solar thermal energy used to drive turbines, battery storage, and fuel cells are not fully explicitly developed for solar generation. Some of these technologies have some far-reaching issues in extreme climatic environments.This technology lags in solar cell manufacturing from common and or inexpensive materials. We also require a greater understanding of the environmental conditions, such as temperature, humidity, wind, and dust, which cause significant performance degradation and losses to the PV systems. During a recent overview of renewable energy and photovoltaics, describing this solution's limits and current progression for future generation projects, in 2020, solar PV was recognised as the cheapest electricity source in history.

This section will consider the challenges of developing solar panels to incorporate temperature and environmental conditions. The solar community, engineers, designers, and manufacturers can improve solar panels' performance and reduce production costs.

1.1 Introduction.

Renewable energy provides an alternative solution to conventional power. Renewable energy is energy created from a naturally replenished renewable resource. There is an octave of carbon-neutral renewable resources; solar, wind, wave, hydro, biomass, and geothermal power.The most energy productive of these renewables is solar. According to Prof. Washington Taylor, MIT, the sun produces 173,000 terawatts of solar energy, 10,000 times more than the world energy use [1]. We can utilise solar cells to capture this free energy. Solar power has been increasing research to understand and resolve the associated problem with actual environmental conditions. Temperature, humidity, wind, dust, and solar panel output show that ecological conditions temperature, humidity, wind, and dust cause significant performance degradation.

The phenomenon is called soiling, which is a challenging and complex issue. The soiling impact refers to the power that introduces the above influencing issues affecting the PV panel's output performance. These complex issues create critical attenuation to solar panels' optimal performance worldwide, consequently, more significant in arid climatic conditions. Soiling problems are commonly overlooked and overestimated. Many factors influence the soiling: climatic changes, geography, dust particle properties, PV panel type, panel angle, and urbanisation [2,3]. Many studies have been carried out on the impact of soiling on PV panels; however, future studies on soiling effects are critical. Reducing performance requires quantification to allow future developments optimal performance.

1.2 World energy consumption.

One of the critical issues for any country's social and economic development is energy. Worldwide global energy consumption and demand increased by 2.3 % in 2018; this is the fastest growth rate within a decade, causing an increase in fossil fuel usage of 70%. Renewable energy growth was 31%; however, that was still insufficient to increase global demand. Electricity continues to be the fuel of the future [4]. In 2019, the worldwide global market grew by 0.9 %, caused by a reduction in economic growth and milder weather condition, which affected the decline in heating and cooling. Still, renewable energy continues to grow [4].

In 2020, the Covid-19 crisis underlined the importance of a reliable, affordable, and secure electricity supply that can accommodate sudden changes in performance and economic activity. The electricity sector will substantially support economic renewal with a crucial long-term role in providing the world's energy [5].Global electricity demand recovers in the Stated Policies Scenario (STEPS) and surpasses pre-Covid-19 levels in 2021. Electricity demand growth in India will grow faster than in other regions by 2030, after which change is most noticeable in Southeast Asia and Africa [6]. China sees the most extensive individual increase in demand, accounting for over 40% of the global growth to 2030. Electricity demand growth worldwide overtakes all fuels.

Electricity will meet 21% of global energy consumption by 2030. Renewable electricity sources have been resilient during the Covid-19 crisis. They are set for healthy growth, increasing by two-thirds from 2020 to 2030 in the STEPS. Renewables achieve 80% of worldwide electricity demand growth. Renewable energy will surpass coal by 2025 as the primary method of generating electricity during the next decade. By 2030, all renewables, hydro, wind, solar PV, bioenergy, geothermal, concentrating solar, and marine power will provide nearly 40% of the electricity supply [7].

By 2020 Solar PV will become the leading provider of electricity generation and looks set for colossal expansion. Estimates for 2020 - 2030, solar PV grows by 13% per year, and solar PV in 2020 is now the cheapest electricity.

1.3 History of Photovoltaics.

The "photovoltaic" means the creation of voltage caused by the exposure to sunlight, or direct conversion of sunlight or solar radiation into electricity. This was observed by Henri Becquerel in 1839, and the beginning of solar cell technology. From its inception there was progression and further developments [8].

- 1878, Mouchet at el; solar-powered engines
- 1888, Aleksnadr Staetov; solar cell
- 1891, Clarence kemp; solar water heater
- 1905, Albert Einstein; how light packet carry energy
- 1954, Bell laboratories; modern solar cell

In 1950, a change occurred with the advent of silicon technology; a solar cell's efficiency of 10% was developed in Bell Laboratories in 1954 [9]. In the '70s, oil shortages created a

reinterest in solar energy as a renewable source, increasing efficiency by 17%. In 2010 the efficiency reached 40.7%.

The global production data for 2010 was between 18Gw and 27Gw; between 2012 and 2017. Although, the increase in renewable electricity production reduced global primary energy intensity by an estimated 1.2%. The world's total immediate energy demand increased by 2.3% in 2018, the most significant increase since 2010, driven by global economic growth [10, 11]. Improvements in primary energy intensity helped limit the growth in demand. Global direct energy intensity decreased more than 10% during the five years between 2013 and 2018, at a mediocre annual rate of 2.1%.On a year-to-year basis, energy intensity improvement has slowed more recently, falling from 3.0% in 2015 to 1.2% in 2018 [12].

More than 200 GW of new renewable power generating capacity was installed in 2019, raising the global total to 2,588 GW [13]. Installations were well above 2018 levels, maintaining the more than 8% average growth rate of installed renewable power capacity over the previous five years. Around 115 GW of solar PV was added worldwide in 2019, cementing the technology's status as the leader in new electricity generating capacity [14]. During the year, 57% of renewable power capacity additions were of solar PV (direct current), followed by wind power (around 60 GW for 30%) and hydropower (some 16 GW for 8%) [15].

The remaining 5% of additions were from bio-power, geothermal power, and concentrating solar thermal power (CSP). However, improvements in primary energy intensity helped limit the growth in demand. Global solar photovoltaics additions were stable or even diminished slightly in 2019. The solar PV market grew approximately 12% to around 115 GW (GRS 2020 report), ending with firm orders in Europe, the United States, and developing global markets. The global market for solar PV expanded by about 44% in 2019. Power generating capacity was installed in 2019, raising the global total to 2,588 GW.

For the fifth year, net additions of renewable power generation capacity outpaced net fossil fuel installation and nuclear power combined [16,17].Overall, worldwide new investment in renewable power and fuels grew 2%. Compared to 2018, costs continued to decrease, reaching some USD 301.7 billion; nearly all were in wind and solar power.

Wind power investment overshadowed solar energy investment for the first time since 2009 [18]. Several significant countries and regions, such as China, Europe, and the United States, have propelled these trends to have an enormous impact in 2019. Renewable power is growing in all corners worldwide. Globally, 32 countries had a minimum10 GW of renewable power capacity in 2019, which increased from only 19 countries a decade earlier [19].

1.3.1 Middle east solar development.

The Middle East and Africa noticed a significant solar PV installation in 2019; an estimated 6.7 GW increased to 15.1 GW, an 80% increase in cumulative capacity across these two regions [20v]. As of 2018, the Middle East's largest installer was the United Arab Emirates, aiming to achieve 50% renewable energy by 2050 [21].

Commercial operations began at the 1,177 MW Sweihan facility in Abu Dhabi. Expected to cover the electricity requirements of 90,000 people [22]. Dubai allocated the fifth phase (0.9 GW) of its 5 GW Mohammed bin Rashid Al Maktoum Solar Park [23]. United Arab Emirates had more than 1.7 GW of solar PV in operation, including at least 125 MW of rooftop capacity under Dubai's Shams initiative [24].

Saudi Arabia, the country's first grid-connected solar PV plant (0.3 GW Sakaka) in late 2019. In Jordan (added 0.6 GW), when at least two large plants were completed, efforts continued towards installing solar PV on all the nation's 7,000 mosques. Israel met its largest solar PV park (120 MW) and added 0.8 GW [25]. Kuwait and Oman added more significant developments to their pipelines, and Iraq launched a tender for a 755 MW capacity [26].

1.3.2 European solar development.

In European countries, the shift was even more dramatic; Denmark, for example, went from 39% to 77%, Germany (16% to 42%) and the United Kingdom (8% to 38%) [27]. In 2019, an estimated 18 countries improved at least 1 GW of new capacity, increasing from 11 countries in 2018.

All continents contributed significantly to global growth [28]. By the end of 2019, 39 countries had amassed a capacity of 1 GW or more, an increase from 31 countries one year earlier, or at least 5% [29]. The current trend among major energy companies to invest in renewable energy highlights renewables' cost-competitiveness and public appeal.

The world's largest oil and gas companies, particularly Europe-based, are moving into solar project development and operation. Using solar PV to power their operations worldwide

Solar PV has an increasing effect on electricity systems. Raising the importance of integrating solar energy under varying technical and market conditions equitably and sustainably [30].

Many utilities are actively involved in solar PV deployment and operations [31]. Challenges to tackling solar PV become a primary electricity source globally, including policy and regulatory insecurity in many countries' financial and bankability challenges [32]. Subsidy solar PV schemes and adequate regulatory frameworks and policies governing grid connections are still required [33].

1.3.3 Government policies.

Mainstream feed-in tariffs (FITs), feed-in premiums, and tenders – continued to drive most of the global market in 2019 [34]. Corporate purchasing of solar PV grew considerably, and self-consumption was an essential driver of new distributed systems in several countries [35].

Although still a small stake in the annual market, several private large-scale systems in 2019 were interested in this significant multiplying concept [36]. In addition to driving the building of new and more efficient manufacturing services. Competition and price pressures have supported investment in solar PV technologies across the entire value chain. Particularly in solar cells and modules, to improve efficiencies further and reduce the LCOE [37].

In 2019, new records were achieved for cell and module efficiencies [38]. Monocrystalline cell technology, which lost its lead to multi-crystalline in 2002, raced ahead for the majority share of global shipments [39]. Demand for higher-efficiency modules has shifted towards Passivated Emitter Rear Cell (PERC) technology.

The next generation of technologies PERC has become the new standard for the monocrystalline silicon solar cell variety because it increases efficiencies [40]. After all, the cell's efficiency influences the production cost at all stages. Therefore, substantial effort is directed toward efficiency improvement, making it an economically attractive option for many projects [41].

Manufacturers of PERC (particularly China's LONGi) have participated dramatically in its commercialisation [42]. While monocrystalline PERC focuses on significant expansions and substantial commercial ability that came online in 2019, the industry is already looking ahead to PERC [43].

In 2019, several manufacturers converted or built new factories to produce hetero-junction cell technology (HJT), which offers higher efficiencies and occurs at low temperatures and fewer production steps than other high-efficiency cell technologies. Several China-based

companies were actively looking into HJT, and some had small production lines in operation [44]. European manufacturers were considering HJT (and other technologies) as an option to regain market quantity [45].

In late 2019, REC (Norway) began production at an HJT cell and module facility in Singapore [46]. Researchers also conquered the theoretical efficiency limits of silicon-based solar cells by stacking cells of different varieties and developing new, more efficient cell technologies [47].

Perovskites use crystalline silicon, or a thin-film base attracts substantial research funding and increases efficiencies [48]. Researchers continued to concentrate on the long-term stability of perovskites [49]. More than a dozen companies worldwide worked on perovskites in 2019 [50]. Improvements in-cell technology and module design have enabled modules with higher power ratings [51].

In 2019, for example, Sun Power (United States) launched the industry's most potent residential panel at 400-plus watts. In addition, Canadian Solar unveiled what it claimed was the first poly bifacial module of 400-plus watts for large projects [54]. Increasing the power rating increases electricity output. Reducing the number required for a project means less space is needed, and associated land, installation, and other costs are reduced [55].

Bifacial modules capture light on both sides and offer potential gains in output (and thus a lower LCOE).With even more significant performance gains if used in installations with trackers. However, there are ongoing uncertainties about incorporating climatic and environmental conditions [56].

1.4 Photovoltaics development.

Today 2020, Silicon solar cells account for 90% of all solar cells manufactured [57]; however, efficiency is around 15%; 85% of the light received is not converted. Silicon is a leading technology in manufacturing solar cells due to its high efficiency. However, due to their high price, more manufacturers and researchers are looking for new technology and materials to reduce solar cells' production costs. The thin-film solar cell has created exceptional attention due to its promising performance. With the possibility of manufacturing cost reduction, the cost reductions are thin-film solar cells use fewer materials. The layers are thinner than mono and poly-crystalline solar cells; however, these technology-based solar cells' efficiency is low (12%-15%) [58].

1.4.1 New developing materials and technology for PV cells.

New developing technology and materials. They were allowed for the introduction of the third generation PV, Nanotubes (CNT), quantum dots (QDs), hot carriers (HC), and the latest solar cell materials. Such as perovskite, these are all promising; however, all of these are still to be proven commercially viable [59]. These three new technologies, Nanotubes (CNT), quantum dots (QDs), and hot carriers (HC). They are used in nanotechnology for PV cell manufacturing. In addition, they are used to increase the efficiency since the bandgap can adjust by nanoscale components [60,61]. The technological advantages of third-generation solar cells or thin-film are reducing the material required to manufacture and having low costs, lightweight, and good electrical performance.

1.4.1.1 Carbon nanotubes (CNT).

Sumio Iijima discovered carbon nanotube in 1991 [62]. These nanotubes have promising applications in nanoscience. Over the decade, carbon nanotube solar cells, extensively researched for their exceptional and highly desirable thermal, electrical, and mechanical properties [63-65],

They have a bandgap of 2.0 eV. Thin-film photovoltaic materials are better than conventional solar cell materials such as silicon because they are lighter, more flexible cheaper to manufacture; these factors are essential. Furthermore, the development of technologies such as photovoltaic material is continually increasing. For example, the latest development is Nanotubes (CNT), which cools the solar cell by 10 degrees Celsius, improving efficiency (KAUST 2019).

1.4.1.2 Quantum dots (QDs).

Over the past decade, photovoltaic devices using nanoscale materials, such as semiconductor quantum dots. Quantum dots are a material that, combined with various substances, creates a unique semiconductor that can control light absorption and emission spectra and has a bandgap of 1.4 eV [66-68].

1.4.1.3 Hot carriers solar cell.

Hot compassion of carrier cells is challenging compared to CNT and QD; it requires selective energy contact to convert light into electrical power without producing heat. HC has a bandgap of 1.1 eV. Nevertheless, its efficiency level achieved 66%, significantly higher than existing silicon cells due to a lack of suitable materials with lower carrier cooling rates. As a result, HC is not commercialised; however, still are an experimental technology.

1.4.1.4 Latest solar cell materials.

As solar technologies develop using new materials, such as perovskite, it has a suitable bandgap of 1.52 eV. This new material has increased the efficiency to around 20%; this material still has advantages and disadvantages [69,70]. Perovskite benefits are low carrier recombination rates. However, it is precarious and unreliable and degrades under high humidity, moisture, UV, and hysteresis; however, it is a promising new technology [71]. The latest development, 21st December 2020, Oxford PV, produced a revolutionary technology, a perovskite solar cell achieving 29.52 % efficiency, a new world record.

1.5 Choice of photovoltaic panels.

Many types of PV cells are available. This section details the PV cells currently in the manufacturing, research, and development stages. Solar cells are categorised as first, second, and third-generation solar cells. First-generation; is a solar cell that is expensive to manufacture and has low-efficiency levels. Second-generation; solar cells have lower efficiency and are cheaper to manufacture. Third-generation solar cells are not commercialised and are more efficient. Most of these are ongoing research; however, the third-generation solar cells aim to reduce manufacturing and production costs. A crystalline silicon-based solar cell, in comparison with others, has the highest efficiency and is the second most straightforward raw material to be found in the world.

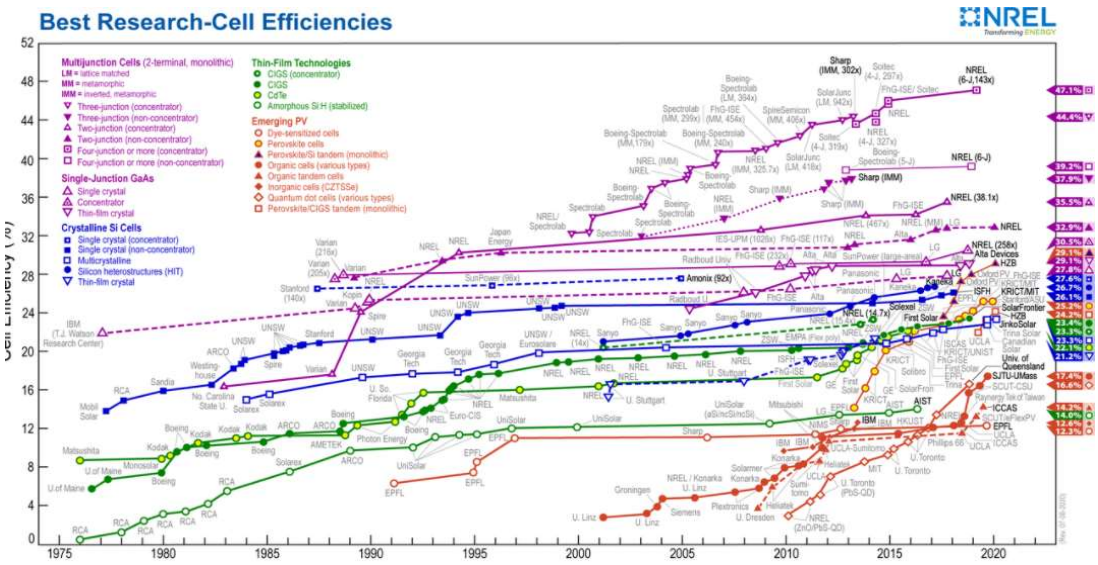

Figure 1.1: Reported timeline of research solar cell energy conversion efficiencies (NREL).

The figure overleaf solar cells used in solar cell manufacturing are from all types of silicon PV Materials. These are classified based on their generation type.

- First-generation solar cells; are single and multi-crystal solar cells.
- Second-generation solar cells; A-Si thin film, mc-Si solar cells, CdTe, CIS, and CIGS solar cells.
- Third generations solar cells; Nanocrystal based, polymer-based, Dye-sensitized, and concentrated solar cells.

All of these different types have different properties that affect the output power.

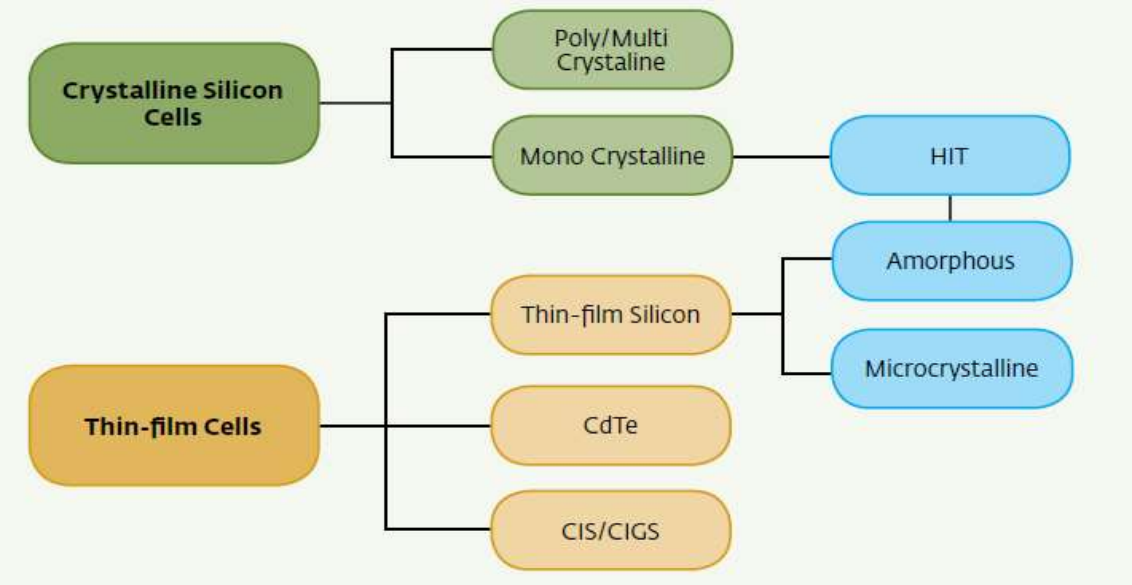

Figure 1.2: PV Technology class.

Mono-crystalline, poly-crystalline, and amorphous-crystalline silicon solar cells are the most widely used commercial solar cells group. Since these solar cells have stable characteristics over a long time, they have good reliability during operation and mass production as developed in microelectronics technology. Allows fast and relatively cheap solar cells based on silicon. The decreasing trend in the price of solar cells continues, and the technology improves so that the efficiency of solar cells improves significantly. One of the improvements is technologies based on single crystalline silicon (monocrystalline silicon) layer with a thin amorphous layer. The subsequent structure is HIT solar cell (hetero junction with an amorphous intrinsic thin layer) produced by Sanyo Ltd. The efficiency of commercially produced HIT solar cells is over 20%, with plenty of room for improvement [72,73].

HIT solar cells use a thin intrinsic amorphous silicon layer (a-Si: H(i)) which is made on both sides of the wafer (Czochralski n-type c-Si), using a low-temperature PECVD process that takes place at 175oC or 250oC [74]. This way, they avoid high-temperature processes that degrade the amorphous film and crystalline bulk interface surface. The HIT structure achieved in such a way has multiple advantages over the standard approach. First, the width of a bandgap Eg of amorphous silicon is 1.55eV to 1.87eV, increasing efficiency at lower wavelengths, where the most concentrated intensity of terrestrial solar radiation can be acquired. The HIT structure shows better temperature characteristics and a higher VOC voltage (open circuit) because of a significant decrease in surface and interfaces recombination.

1.5.1 Crystalline Materials.

The different crystalline materials used for solar cell manufacture are shown above with a concise overview; crystalline silicon-based solar cell has the highest efficiency compared to others [75]. Recent studies have identified that silicon's band gap of 1.12eV is not optimal. Materials with band gaps nearer to 1.5eV have higher theoretical efficiencies.

1.5.2 Mono-crystalline.

Monocrystalline is fabricated from pure monocrystalline silicon. Silicon has a single crystal lattice structure with virtually no defects or impurities [76]. Monocrystalline cells' main advantage is that their high efficiency is typically 15%, with a bandgap energy of 1.1 eV. This material in developing solar cells has been extensively used, and its efficiency compared to other solar cells; monocrystalline cells have the highest efficiency, greater than 20%. However, manufacturers recommend 15%-17%. The disadvantage of these cells is a complicated manufacturing process which incurs slightly higher costs to produce monocrystalline silicon.

1.5.3 Poly or multi-crystalline.

A less expensive material. Polycrystalline Silicon does not require the costly and energy-intensive crystal growth process. Instead, multi-crystalline is constructed using numerous monocrystalline silicon grains, sliced into fragile wafers and manufactured into complete cells. As a result, poly-crystalline cells are less expensive to develop and manufacture than monocrystalline. However, 12-15% are less efficient, with a bandgap of 1.2 eV. Therefore, this material is suitable for reducing the cost of developing PV Modules; it's 12-15% efficiency is low compared to monocrystalline cells and other developing materials [77,78].

1.5.4 Gallium arsenide (GaAs).

GaAs is a compound formed by gallium (Ga) and arsenic (As) with a similar structure as silicon. Its bandgap energy is 1.42 eV. Compared to silicon-based cells, GaAs is typically used for concentrator PV modules and space applications. They have high heat resistance properties [78]. It is also higher than poly and monocrystalline silicon; however, material and production are costly [79].

1.5.5 Thin-film solar cells.

Thin film technology solar cells are less expensive. They use fewer materials, allowing the cell thickness between 35-260nm and a bandgap around 1.5 eV -1.75 eV [80].

Above is that of a crystalline structure. Amorphous silicon cells are composed of silicon atoms in a thin homogenous layer. Amorphous silicon absorbs light more efficiently than crystalline silicon, which allows for more delicate cells, producing amorphous silicon (a-Si) thin-film PV[81]. Thin-film technology has approximately 15% market share, and the other 85% is crystalline silicon, which Is very Amorphous silicon [82].

The main difference between amorphous silicon and the previous ones mentioned is popularity compared with CIS/CIGS and CdS/CdTe; in comparison with efficiency. It has a relatively high bandgap of 1.7eV [83,84]. Amorphous Silicon is a non-crystalline structure. With forty times more light absorptivity than either monocrystalline silicon Cadmium telluride (CdTe) or cadmium sulphide (CdS). This material has a low efficiency of 6% and an ideal bandgap of 1.45 eV. The direct absorption coefficient is high, which is the most significant advantage of amorphous cells incorporated into a range of flexible and rigid materials [85].

1.5.6 Copper Indium gallium selenide (CiGs) / copper indium selenide (CiS).

From its inception, Thin-film technology copper indium selenide (GiS) has been encouraging as a solar cell of its optical properties and good electronics. Changing gallium (Ga) for Indium (In), improved bandgap adjustment to achieve 1.04 eV to around 1.68 eV. As a result, the laboratory's cell efficiency has exceeded 20%; however, commercially, CiGs efficiencies are between 12% -14% [86]. Three materials, CdTe, CiGs, and Si solar cells. Can enhance efficiency using inherent characteristics such as stability and performance yields; CiGs cells are the most promising group [87]. The CiGs solar cell has a high coefficient (a $>10^5$ cm^{-1}); its conversion efficiency reached 22.6% in 2016 [88]. Considering the future development with CiGs, this will improve the efficiency of multi-junction due to its bandgap. Which can achieve 1eV; however, limited production due to rare earth elements, indium, and gallium will prevent large-scale production [89].

1.5.7 Organic and polymer cells.

Today's primary trend concerns organic and polymer cells. The lure of these technologies is that they offer low cost and fast production compared to crystalline silicon; however, it has typically 4% efficiency with a bandgap of 1.65 eV. Expensive raw materials have halted the organic solar cell research, longevity issues, stability, degradation issues, and lower power conversion efficiency than inorganic solar cells [90].

1.5.8 Hybrid solar cells.

These hybrid solar cells are manufactured by combining crystalline with non-crystalline silicon; these solar cells have a bandgap of 1.75 eV and have developed a solar cell with an efficiency of 21% [91].

1.5.9 Dye-sensitised solar cells.

Dye-sensitised solar cells (DSCs) have solar cells with a bandgap of 1.72 eV, which have attracted much awareness in recent years. Because of their excellent photovoltaic performance, specifically under low-light conditions. These are their flexibility in colours and appearance, relatively simple fabrication procedures, and potentially low cost. Dye-sensitised solar cells are an excellent competitor to the existing materials list in producing solar cells [92].

Photovoltaic cells conception to capture the photons of the solar spectrum. When a photon hits a PV cell [93]:

- If the photon has less energy than the bandgap, it is not collected and passes through the cell.
- The extra energy is lost as heat if the photon has more energy than required.
- The energy conversion works at maximum efficiency if the photon has the same energy as the bandgap.

Silicon has been the most used material for photovoltaic cells because it is inexpensive and relatively well understood. The bandgap of silicon is estimated to be 1.1eV. In contrast, the solar spectrum contains energy between 0 and 4eV, with 2.5eV at the spectrum's peak; this means that most infrared spectrum is not collected by silicon cells, limiting the maximum achievable efficiency [94]. The solar spectra are divided into several regions by increasing the conversion rate. Rather than converting the photon energies with a single cell exploiting a single bandgap, solar energy is converted by several cells, each tuned for a different spectrum region. The spectrum is separated across various semiconductors through two approaches: a spatial configuration (Figure 1.3a) or a stacked configuration (Figure 1 . 3 b) overleaf [93].

In the first case, an optical device distributes photons with different energies into various locations, where they hit the "most appropriate" subcell [95]. This approach has recently shown high-efficiency potential for unconcentrated or low-concentration PV applications. However, it is still considered complex to be practical in a tracked HCPV [96-100]. The

preferred approach in CPV is to arrange the cells in a stacked configuration, where different layers of semiconductors are stacked. Due to this geometry, these cells are usually called multi-junction (MJ) cells. The band gaps must decrease from the top to the bottom of the cell: this way, considering the light hitting the top of the cell, the top subcells act as low-pass photon energy filters, transmitting to the subcells below only the sub-bandgap photons.

Larger wavelengths (with lower energy) pass through the upper subcells and are absorbed below. They are comprised of the following elements: gallium indium phosphate (GaInP), gallium indium arsenide (GaInAs), and gallium arsenide (GaAs). This architecture can also transfer to other solar cell technologies and multijunction cells made from CIGS, CdSe, Silicon, organic molecules, and other materials.

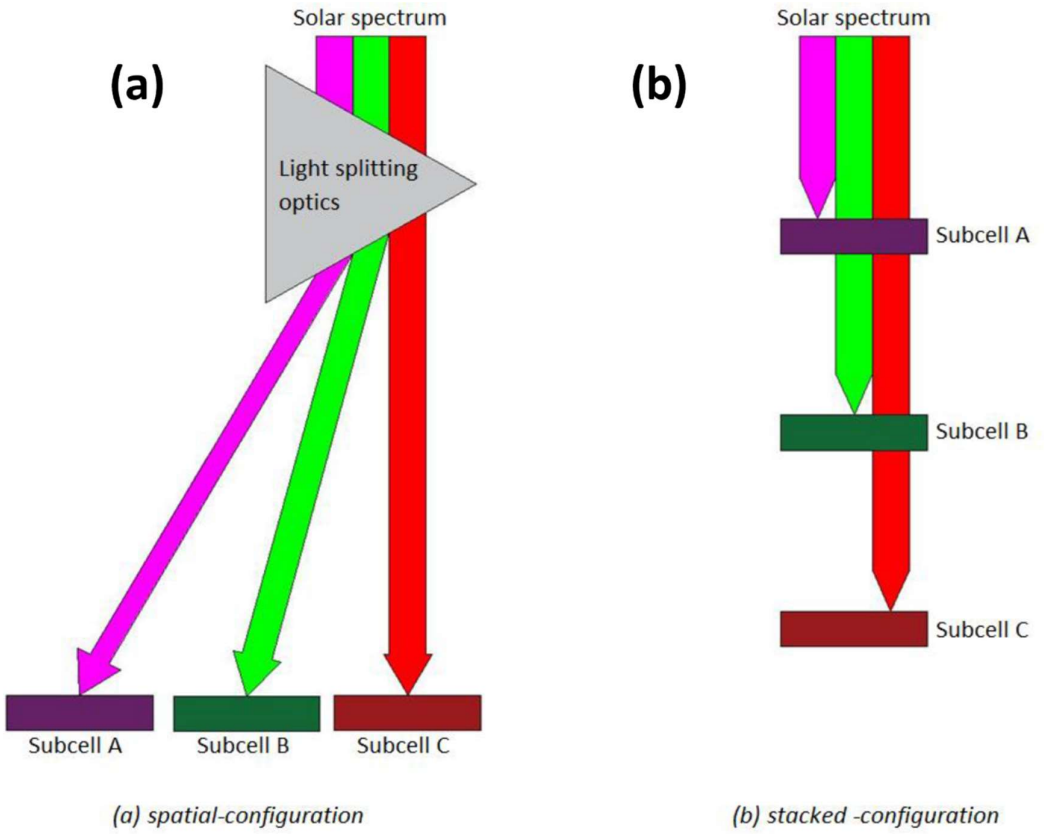

Figure 1.3: Configurations for multijunction spectrum splitting, adapted from [91].

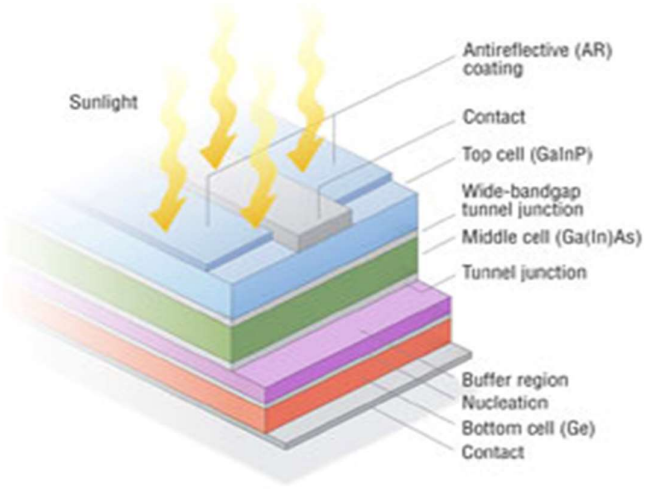

Figure 1.4: Multijunction III-V photovoltaic cell structure [NREL].

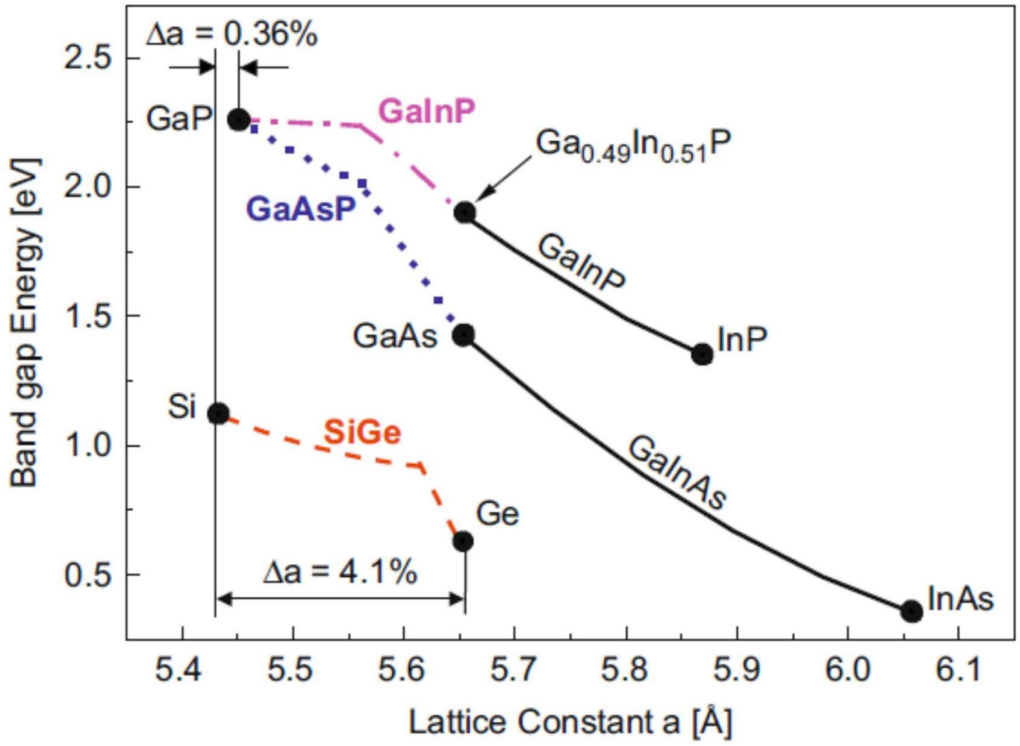

Figure 1.5: Semi-conductors lattice constants [94].

Nowadays, lattice-matched GaInP/GaAs/Ge triple-junction cells are the most common MJ cells [101]. From top to bottom, arranged by the following layers, represented in Figure 1.5:

- **GaInP** is a semiconductor composed of indium, gallium, and phosphorus. It is a high-energy junction. It absorbs the ultraviolet and visible part of the solar spectrum (bandgap ≈ 1.85eV);
- **GaAs** is an III-V semiconductor composed of gallium and arsenic. It absorbs in the near-infrared spectrum (bandgap ≈ 1.42eV).
- **Ge** absorbs lower photon energies in the infrared spectrum (bandgap ≈
    - 0.67eV).

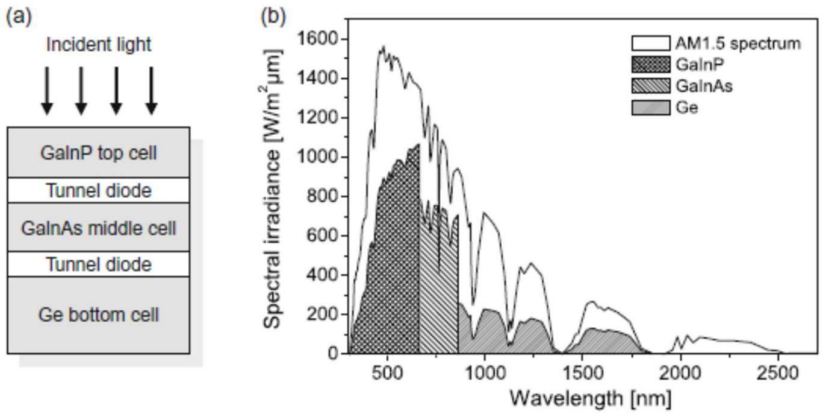

Figure 1.6: Spectral Irradiance of the AM1.5 spectrum and the parts of the spectrum that can be used by a triple-junction solar cell [94].

An additional optimization characteristic for MJ cells is the current matching. Due to the series-connected configuration, the output current of a Multi-junction (MJ) cell is equal to the smallest one among the currents produced by any subcell. Thus, it is essential to design each junction to produce the same amount of photocurrent [94]. Each layer's thickness is selected to best match the currents of the other two subcells. The absorption coefficient for solar cell materials is not infinite: a cell of limited thickness will not attract all the incident light above the bandgap [14]. A fraction of that light will be transmitted. The thinner the cell, the greater the transmission: thinning a subcell will decrease its current, instead increasing the lower subcell current.

For this reason, correct subcell sizing is essential to obtain the current matching. The terrestrial sun spectrum contains less high-energy light than the AM0[i] spectrum. Thus, to satisfy the current matching requirements, the top terrestrial subcell's thickness must be greater than that of a space cell [14].

Multijunction cells' efficiencies have recently increased at a rate of about 0.5-1% yearly [101]. At the end of 2014, the highest efficiencies achieved 27.6% and 46.0% for silicon single-junction and multijunction cells under concentrated sunlight.

Traditional GaInP/GaAs/Ge cells were fabricated to have the same lattice constant in all the subcells. As a result, the semiconductors in these cells can be grown with high-quality [102]. However, the bandgap combination of the lattice-matched triple-

junction cells leads to a large excess current in the Ge layer. Therefore, a different set of semiconductors would grant a better bandgap combination. Therefore, many MJ cells other than the GaInP/GaAs/Ge ones are being investigated and might find application soon. Such as the metamorphic and inverted metamorphic (IMM) cells [103].

In contrast to LM cells, subcells of a metamorphic cell do not have the same lattice constant [104]. Massively growing materials with different lattice constants lead to misfit dislocations that deteriorate the material quality. The introduction of buffer structures between the Ge bottom cell and the GaInAs middle cell is required to reduce the effects of the dislocations. The top subcell is first grown on a lattice-matched substrate in the IMM cells, followed by the other subcells [105]. This way, the upper subcells' material quality is enhanced compared to the conventional MJ cells [106]. Alternatively, the subcells can be separately fabricated and then mechanically stacked [107]. Despite the high efficiencies, high mechanically stacked cells' high costs have limited their diffusion.

1.6 Review on CiGs, CdTe and SiHi Solar Cells.

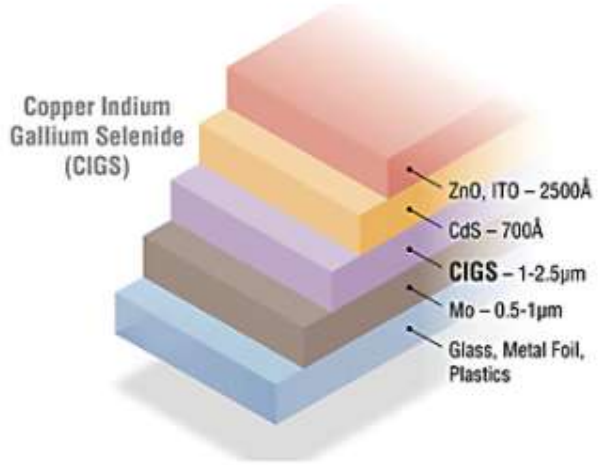

Figure 1.7: Structure of CiGs thin-film solar cell [21].

Copper Indium Gallium Selenide (CIGS) solar cell, also known as CI(G)S or CIS cell. It is a categorised thin-film photovoltaic cell that transforms ultraviolet light into electrical energy. CIGS has a chalcopyrite crystal structure and is tetrahedrally bonded. It possesses a notably improved absorption coefficient of about 105 cm^{-1} for 1.5eV and higher energy photons. It exhibits high proficiency. CIGS photovoltaic cells' current efficacy on a small area device was 21.7% (Mansfield et al., 2015). CIGS is more advantageous than conventional PV technologies because it yields a greater measured energy level,

significantly displays a reduced temperature coefficient for power loss, decreased detectability to shadowing and short energy settlement time.

CIGS is a good substitute for silicon due to its commensurable efficiency and production cost. It can be lowered considerably by utilizing economical substrates and foils made of glass and plastic, apart from its high efficiency and reasonable manufacturing cost. CIGS material for photovoltaic cells is that the material responsible for absorption wastage is minimised compared to 1G solar cells (i.e. C-Si). Fabricating a solar cell requires only around 2mm thick CIGS absorber film. Recently, an amended photocurrent in CIGS photovoltaic cells proficiency of 21.7%. It records promising results with Voc of 717mV, Jsc of 37.2mA/cm2, and FF of 78.6%. Its key novelty includes alkaline Post-Deposition Treatment (PDT) of CIGS with the proficiency of solar film, produced by thermal co-evaporation of Copper, Indium, Gallium and Selenium. The CIGS cell's alkaline composition in the PDT procedure is altered by adding alkaline essentials from the film's superficial adjacent. The multi-junction is established with a fine buffer layer. The high photocurrent in CIGS solar cell was obtained by decreasing CdS buffer width and an enhanced steeper.

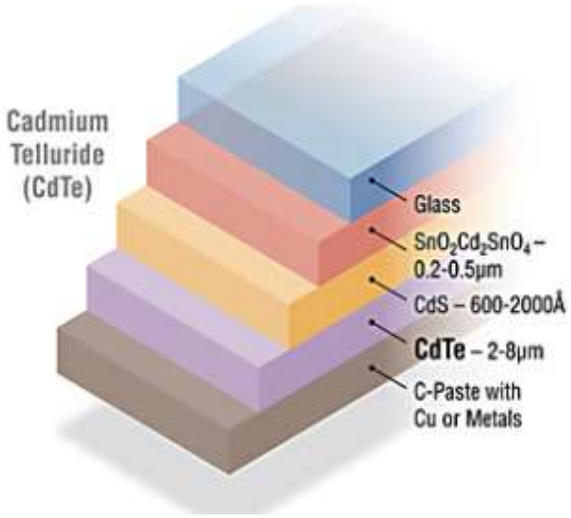

Figure 1.2: Structure of CdTe thin-film [NREL].

CdTe material is promising for producing solar cells at a low cost with a low efficiency of 13%. (Tamboli et al., 2017) Achieving a better efficiency rate in a single junction solar cell generic structure is rigid. (Romeo et al., 2004) developed a CdTe hetero-junction flexible

solar cell where the absorber layer was fabricated from CdTe. CdTe has the highest absorption coefficient, which leads to an efficiency of 16.5%.

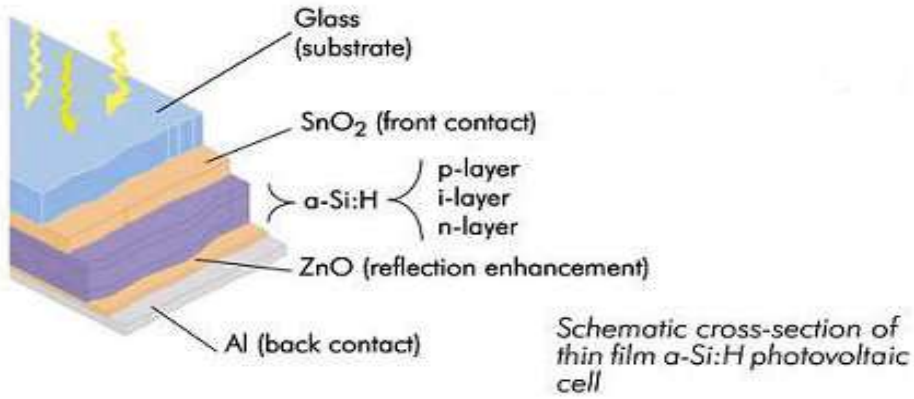

***Figure 1.3*: Structure of SiHi thin-film solar cell.**

The Copper Indium Gallium Selenide (CIGS) cell was fabricated using vacuuming manufacturing procedures. Deposit a thin layer of 2 μm copper, indium, gallium and selenide on glass or plastic backing and electrodes on the front and back sides. The produced current flows via the electrodes.

The manufacturing cost is lower than the crystalline silicon PV cells but more expensive than other single-junction thin-film cell-like Cadmium Telluride. Over the years, the CIGS cell was perceived as a promising cell. Thus many companies and research institutes took particular interest in it. The companies and institutes drive research towards improving the lifecycle reliability, power output efficiency, and cost of modules made using the cells [108,109]. CIGS has a bandgap energy of 1.45 eV, a high sunlight absorption coefficient and PCE of 20%, and EPBT of 1 year [110, 111]. Its performance is slightly affected by shading.

CIGS solar cells are alleged to have a very high potential against CiGs and CdTe solar cells. They are achieving low production cost with high module efficiency. The CIGS possesses a better absorption coefficient (lower material usage) and requires a lower thermal budget than c-Si solar cells. Its record efficiency (22.6%) has surpassed CdTe (22.1%).

In conclusion, flexible CIGS cell efficiency is comparable to conventional Si solar cells, and stability is not a concern; however, Si solar cells require less energy to deposit CIGS film.

The Flexible CdTe cell has demonstrated successful manufacturing. The use of simple components, high production rate, high efficiency and fabrication in single-layer and multilayer configurations. The flexible a-Si: H, since PECVD is the standard technique used for fabrication with processing temperature around 200 °C, temperature-sensitive plastic foils can be used. The success of flexible a-Si: H cell is due to high throughput, large area, and longtime PECVD deposition without downtime. Therefore, future progress is bright for flexible CIGS, CdTe and a-Si: H solar cells.

	Band-gap	**Linear thermal expansion at 25°C**	**Lattice constant at 300K [siliconfareast.com]**
GaAs	1.4 eV	$5.7 * 10^{-6}$ °C^{-1}	5.653 Å
Ge	0.7 eV	$5.9 * 10^{-6}$ °C^{-1}	5.646 Å
Si	1.1 eV	$2.6 * 10^{-6}$ °C^{-1}	5.431 Å
SiHi	1.7eV		
GiCs	1,.2eV	$5.0 * 10^{-6}$ °C^{-1}	
CdTe	1,45eV	$5.6 * 10^{-6}$ °C^{-}	6.481 Å

Table 1.1. Semiconductors' properties comparison.

.

	Conventional PV	Thin film solar cells		
	c-Si	a-Si	CdTe	CIGS
Best research cell efficiency	25.7% [37]	14% [37]	22.1% [37]	22.6% [37]
Best module efficiency	24.4% [36]	12.3% [36]	18.6% [36]	15.7% [36]
Theoretical efficiency limit	29.43% [52]	20% [51]	32.8% [51]	33.5% [51]
Absorption coefficient	10^4 cm^{-1} [40]	(5×10^4) cm^{-1} [40]	10^5 cm^{-1} [40]	$>10^5$ cm^{-1} [40]
Current PV market share	92% [32]	<1% [32]	5% [32]	2% [32]
Annual production	~71.76 GW	~0.78 GW	~3.9 GW	~1.56 GW
Energy payback time	~2 years [42]	~1.5 years [42]	~7 months [42]	~1 year [42]
Major manufacturer	Jinko Solar [33]	Sharp [10]	First Solar [10]	Solar Frontier [10]

Table 1.2. Introduction on the production, efficiency of conventional PV (c-si) and thin-film solar cells (a-si, CdTe and CiGS [112].

1.7 Improvement in efficiency.

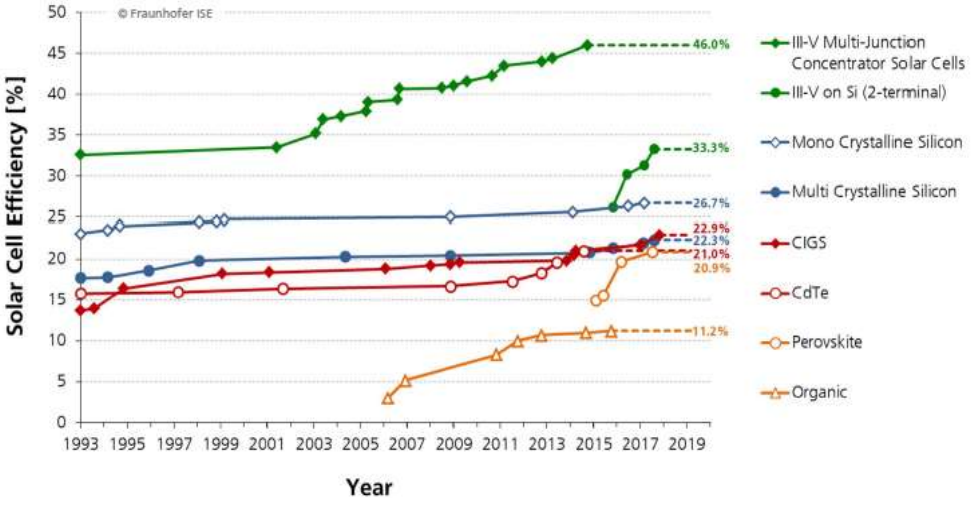

Figure 1.4: Development of laboratory solar cell efficiencies.

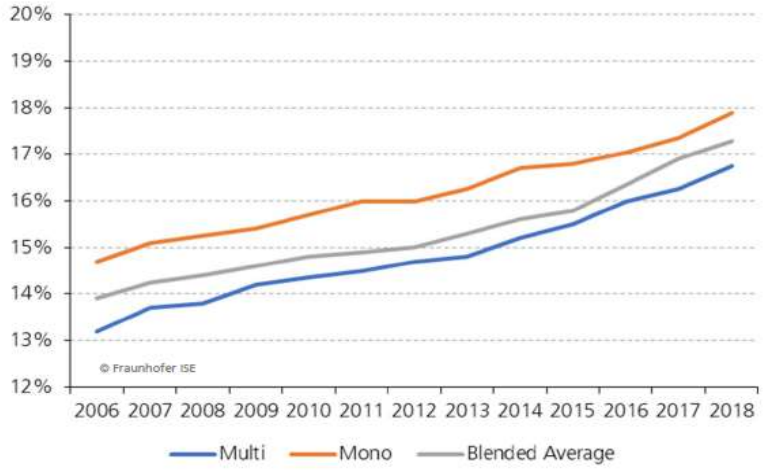

Figure 1.5: Average Crystalline –Silicon PV module efficiency [1].

1.7.1. Solar cells efficiency.

Practically all photovoltaic devices integrate a p-n junction in a semiconductor across which the photovoltage is developed. A cross-section through a typical PV solar cell is shown below in Figure 1.12.

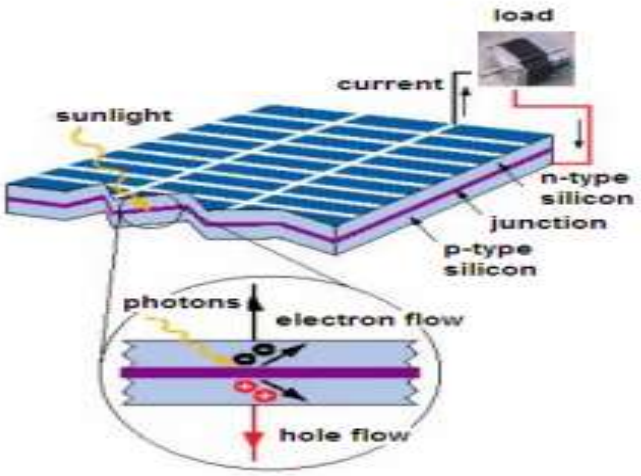

Figure 1.6: A schematic layer of a PV cell [113].

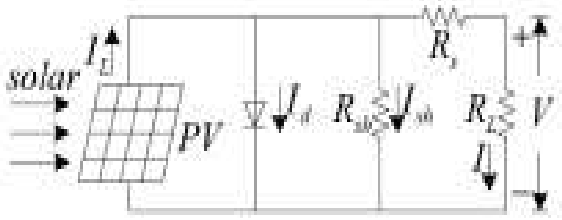

Figure 1.7: The equivalent circuit of a PV cell [114].

The I-V characteristic of the PV solar cell changes with the sunlight intensity $S/(W/m^2)$ and cell temperature $t\ °C$ that is $I = f(V, S, t)$. According to the electronics theory, the solar cell's actual equivalent circuit is shown in Figure 1.13 when the load is a pure resistance.

IL is current supplied by the solar cell.

$$\boldsymbol{I = IL - Io\left[exp\left(\frac{q(V+IRs)}{AkT} - 1\right)\right] - \frac{V+IRs}{RSH}} \qquad \textbf{(1.1)}$$

where Id , the junction current of the diode,

$$Id = Io\left[exp\left(\frac{q(V + IRs)}{AkT}\right) - 1\right]$$

I = the load current

I_L = the photovoltaic current,

I_o = the reverse saturation current

q = electronic charge,

k = boltzmann constant,

T = absolute temperature,

A = factor of the diode quality

RS = series resistance,

RSH = parallel resistance

Another critical parameter is open-circuit voltage Voc ;

$$Voc = \frac{kT}{q} In\left(\frac{IL}{Io} + 1\right) = \frac{kT}{q} In\left(\frac{IL}{Io}\right) \qquad \textbf{(1.2)}$$

Figure 1.14 shows an I-V characteristic and the power curve to illustrate the maximum power point position.

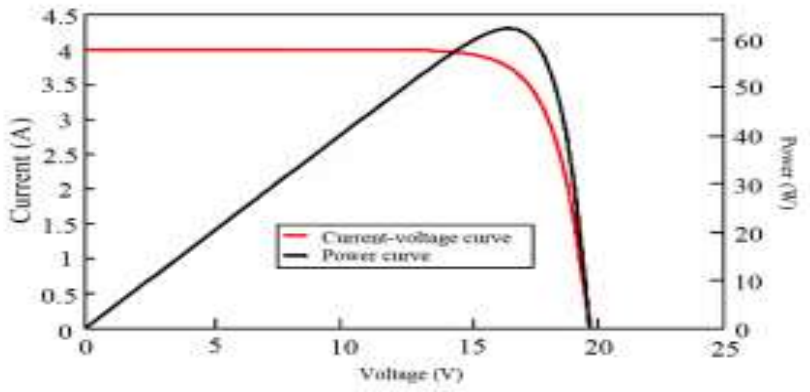

Figure 1.8: I-V characteristics of a crystalline silicon module with power variation [115].

As temperature increases, the intrinsic semiconductor bandgap shrinks, and the open-circuit voltage (Voc) decreases following the p-n junction voltage temperature dependency identified in the diode factor $^{q}/_{kT}$.

Solar cells have a negative temperature coefficient of Voc (β). Moreover, a lower output power results in the same photocurrent because the charge carriers are liberated at a lower potential. Using the convention introduced with the Fill Factor calculation, a Voc reduction results in a minor theoretical maximum power $Pmax = Isc \times Voc$ given the same short-circuit current Isc [116,117].

The intrinsic semiconductor bandgap shrinks as temperature increases, meaning more incident energy is absorbed. As a result, a more significant percentage of the incident light has enough power to raise charge carriers from the valence band to the conduction band. Therefore, more significant photocurrent results; thus, Isc increases for given insolation, and solar cells have a positive temperature coefficient of Isc (α).

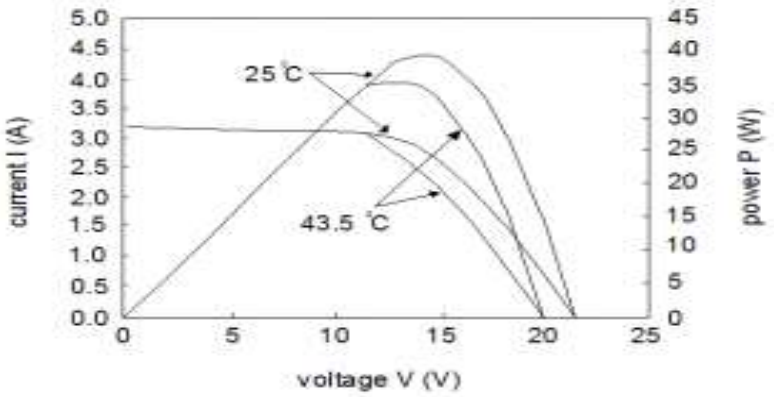

Figure 1.9: I-V and P-V characteristics of a PV solar cell [118].

Figure 1.15 shows I-V and P-V characteristics when the temperature alternates at continuous illumination. The effects result from features of crystalline silicon cell-based modules. Which produce a higher voltage as the temperature drops and, equally, lose voltage in high temperatures; therefore, solar panel or system derating calculation requires an adjustment for this temperature effect.

Two primary factors are establishing efficiency:

- The cell efficiency is utilising silicon type N-type or P-type and cell design. Therefore, to increase cell efficiency is imperative to find new materials to make more efficient photovoltaic cells

- The total panel efficiency ensures the necessary energy by using the cell layout, panel size, and configuration. The maximum power (Pmax) generated by the photovoltaic panels has to increase, increasing the active area of the photovoltaic cells.

Firstly, cell efficiency is the cell structure. Silicon choice, N-type or P-type, cell efficiency is defined as the fill factor (FF), the maximum efficiency conversion of the cell at the optimum voltage and current. Cell design is an essential part of the panel efficiency: important factors; are silicon type, number of busbars (MBB), and passive type (PERC).

Solar panels are tested under laboratory conditions using Standard Test Conditions (STC) of 1000 W/m², 25°C cell temperature, with a 1.5 air mass spectrum. Electrical incident solar irradiance performance, influenced by the chosen photovoltaic panel type's output power, varies among manufacturers 350W-400W. The efficiency is 20.4% to 22.6%. The efficiency of the panel is the maximum power rating (Watts) divided by the area M;

$$\textbf{Efficiency} = \frac{\boldsymbol{Pmax}}{(\boldsymbol{Area\ x\ 1000W/m^2})}\ \boldsymbol{X\ 100}$$

1.7.2 Actual efficiency.

Actual efficiency is the operating efficiency influenced by several factors: irradiance, shading panel, orientation, temperature, location, dust, dirt, and time of year. The temperature will be greater than 25°C and cannot compare actual energy production from the PV under test. In general, solar cells' efficiency decreases with an increase in temperature. Therefore, the temperature is a critical factor that leads to a loss in PV efficiency and power output. Causing a temperature increase and causing bandgap shrinkage; therefore, the open-circuit voltage will drop [119].

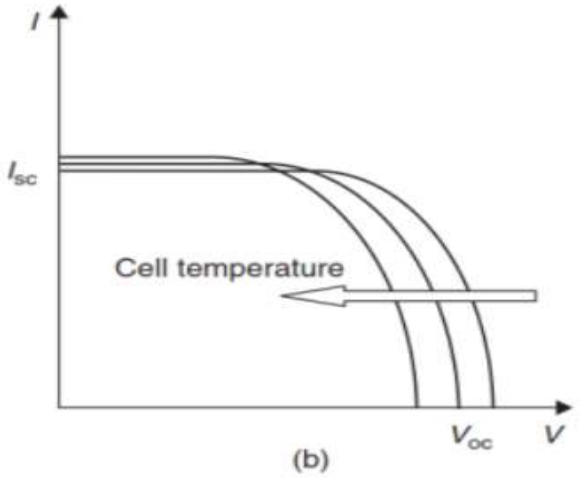

Figure 1.10: Effects of Temperature on PV cell characteristics [8].

Figure 1.16 shows the effects of Temperature on PV characteristics. Temperature influence greatly impacts monocrystalline silicon compared to all other types of silicon

solar cells. For example, the efficiency decreases by 15% and 5% in monocrystalline silicon and thin-film solar cell [120].

1.7.3 Maximum Powerpoint.

The maximum power point (MPP) is the point at which the solar cell outputs the maximum net power. However, the MPP voltage can drift based on various factors, including irradiance intensity, device temperature, and device degradation. Therefore, one crucial part of PV module engineering is ensuring the MPP (maximum power point) is tracked continuously to maximise the net power output. An MPP tracking system (MPPT) should also consider unforeseen events such as poor operating conditions and individual cell failures. The MPP can be obtained through passive or active methods. For example, the MPP can be passively traced through a constant voltage source or by placing a resistor in series with the load. These methods are simpler and cheaper to implement. Still, they might not produce the maximum possible power output since many variables, such as the device quality, degradation, and input parameters, can affect power output.

1.7.4 Sun Trackers.

Solar tracking systems have many bases of classification. For example, it can be classified based on the control system, drivers, tracking strategy, or the degree of freedom of the movement exhibited by the system.

1. based on the control system used.

2. Closed-loop tracking system.

Irrespective of the above driving system used for the movement of the tracker. Be it some passive system or some pre-defined algorithm based on mathematical calculations based on the sun's trajectory, when sensors are deployed to detect the sun's position. This is then feed-backed to the system so that the comparator/ microprocessor is used. Can see the error and give the required actuating signal to the motors to correct the error; then, the system is said to be working on the principles of the feedback control system. And the trackers deploying the above scenario are known as closed-loop sun trackers. Stamatescu et al. (2014) propose a dual-axis tracking system consisting of 4 PV cells as sensors, two motors and a tri-positional control mechanism. Sensors measure the radiation, and the motors are controlled accordingly.

1.7.4.1 Open-loop tracking system.

This type of system uses a controller which gives the driving signal to the motor purely based on current data inputs and the operating algorithm of the system alone. It has no feature of observing and evaluating the output data regarding the desired output. Thus it is cheaper and simpler to implement than the closed-loop tracking system. Still, it involves no rectification process; therefore, the algorithm alone has to ensure that it achieves the desired goal. Al-Naima and Yaghbian (1990) constructed a dual-axis microprocessor-based sun tracker which used a tracking strategy purely based on the calculations of the astronomical coordinates of the sun. It showed better tracking capability than the conventional sensor-controlled counterparts.

1.7.4.2 Active solar tracking systems.

These systems use electrical drives and mechanical gear trains to orient the panels typical to the sun's radiations. It uses sensors, motors and microprocessors for tracking and is more accurate and efficient than passive solar trackers. But on the other hand, they are needed to be powered and consume energy. When the trackers are not in proper alignment with the sun. The sensors receive different illumination and create a differential signal which is then used by a comparator or a microprocessor to determine the appropriate movement in the proper direction. The required signal is then given to the motors to work accordingly. This process stops at a point where the sensors receive equal illumination. The PV module is typically aligned with the sun's radiations. Abdelghani-Idrissi et al. (2018) used an active sun tracker while experimenting with thermal efficiency enhancement. They found that the tracker-based system showed an overall gain of 40% in stored thermal energy compared to the fixed one.

1.7.4.3 Passive solar tracking system.

This system does not use mechanical devices to orient the panel toward the sun's radiation. Alternatively, some pressurized low boiling point gaseous liquids or shape memory alloys are used as actuators which, upon receiving unbalanced illumination, force the plate to undergo some angular motion to re-equilibrate the radiation by inducing thermal expansion in the expandable gases or the shape memory alloys. When one side of the liquefied gas receives more thermal energy than the other, the gas expands and moves to the other side of the tracker. The light weight of the panel causes it to be pulled towards the light source, tilting it until it reaches an equilibrium. Though less complex and compelling, it fails to give high efficiency at low temperatures. Poulek (1994) developed a new low-cost shape memory alloy-based sun tracker, which could collect up to 40% surplus energy compared to the fixed-tilt collectors.

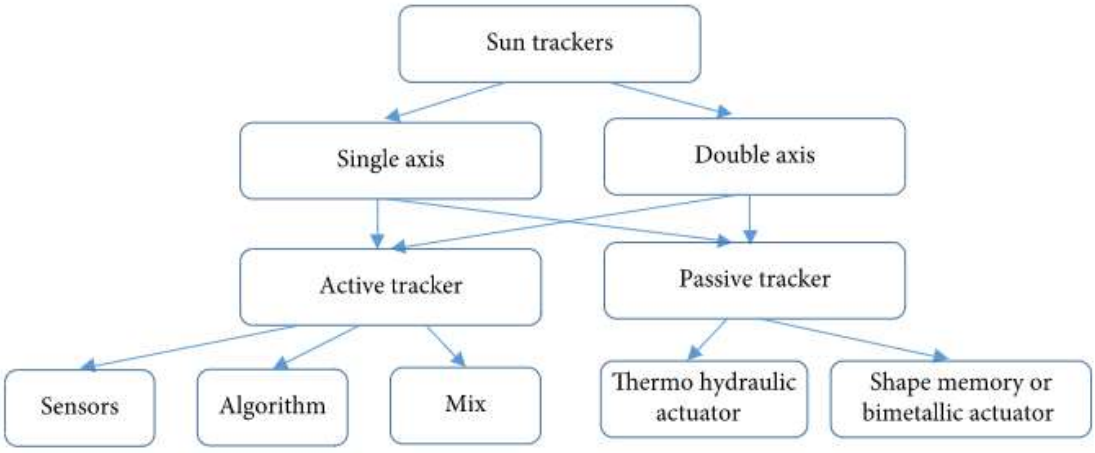

Figure 1.11: Sun trackers classification.

1.8 Conclusions.

Solar energy is sufficient; in theory, it meets all our current and future energy requirements. Many solar cells, monocrystalline, poly-crystalline, and thin-film are available. Nevertheless, the technology lags, hindered by a complicated process to produce highly efficient monocrystalline cells. Poly or multi-crystalline are cheaper to manufacture; however, they are less efficient. The monocrystalline cell has an efficiency of approximately 15% to improve this performance; multi-junction cells with differing bandgaps are used and developed; however, there are disadvantages. Once again, this will result in more complex and expensive to produce.

Manufactures will have to decrease manufacturing costs and increase output power. Manufacturers must develop and increase wafer size; this allows larger panel formats to build the compelling panel with a rating of up to 600Watts. Therefore, larger cells have a greater surface area. Combined with the latest cell technologies, multi busbar (MBB), PERC and tiling ribbon, they can increase the efficiency by up to 22%. New technology allows further developments in better materials for solar cells or Increasing efficiency. Alternatively, inexpensive or common materials for cell production combined with a reduced thickness reduce manufacturing costs.

The latest developments allow further advances in research and development in cell metasurface structures and cell efficiencies. According to Carlos II de Madrid University, 9th February 2021 has allowed multiple performance improvements with up to 40% efficiency improvement. Metasurfaces; once this design is implemented in manufacturing, there will be a significant improvement in future solar cell field performance. Reducing the layer's thickness will efficiently generate the current, saving on materials and manufacturing costs. Reduced thickness and the extraction of electrons generated by light are also more effective. They have fewer paths to cross where they will be reabsorbed. The absorption in the layers surrounding the active layer creates a warming effect. Which reduces the defect in the long term and can be applied to future solar installations to achieve better energy efficiency and increase cell efficiency.

The latest research and development in perovskite solar cell efficiency: The newest achievement for increased efficiency was achieved by Oxford PV Scientists on 21st December 2020. Developed a record-breaking perovskite cell. Sustainable and affordable solar power technology with an efficiency of 29.52%; Oxford PV "believes that future solar cells will be improved significantly."

1.9 Research Methodology.

Reviewing the literature, past milestones in PV technology and current developments in soil degradation were examined. To understand the most established technologies and identify development trends. In addition, research into the existing and new potential materials was also undertaken and highlighted as a new area for PV development. Finally, methods for theoretically and experimentally investigating soil degradation were explored, and critical parameters for analyse were identified.

1.10 Contribution in the field.

- A thorough characterisation of PV cells and PV degradation caused by soiling, how the degradation should be associated, noticeable trends, and their future outlook.

- A method aimed at optimising PV soiling while incorporating realistic surface soiling data, temperature, and other practical concerns.

- Understanding the impact of PV soiling and temperature effects on different PV cells compared to its theoretical predictions.

1.11 Overview of Thesis Structure.

Chapter 1 introduces the topic of solar energy, world energy consumption, and the history of Photovoltaics, incorporating current world and European solar development, their benefits, and the many challenges in harvesting light for electricity.

An updated literature review of the different types of solar PV incorporating new developing materials and technology research incorporating improvements in efficiency, and solar cell efficiency increasing with the use of tracking systems

The importance of material choice and surface temperature is highlighted, along with suggestions for furthering PV soiling and temperature research to investigate the environmental effects on PV performance.

Chapter 2 deals with the challenges and limitations of temperature predictions in large plants using weather forecasts and solar predictions and the output parameters of solar cells incorporating temperature effects, irradiation, and cooling systems and effects.

Chapter 3 deals with the challenges and limitations of correlation of soling, optical losses on PV performance, dust causes and effects on PV plants, environmental conditions and PV performance and cooling systems, outcomes, cleaning procedures, and site-based research.

Chapter 4 carries on from chapters 2 and 3, detailing how the relative humidity incorporating thermal losses affects different PV panels used on PV plants. Again, the impact of temperature, water vapour and the effect of the operational temperature.

Chapter 5 gives a thorough example of the Spectral analysis on PV plants including Pv degradation and the most recent spectral analysis developments on solar panels

Chapter 6 introduces and summarises the use of a small central control mechanism for large scale PV plants. The use of different controllers and various inverters types, thus the effect on the controller on maximum power and the impact of soiling losses on the controller.

Chapter 7 is a case study carried out in Kuwait, detailing the experimental methodology, spectral characterisation, particle characterisation of PV yield and economic analysis

Chapter 8 concludes the chapters and gives recommendations for future work. Overall this work identifies soiling and temperature defects. A broad literature review explores the soiling and temperature issues; thus, challenges have been demonstrated theoretically and experimentally due to soiling and temperature limitations. Solutions are proposed using new methods and concepts. The procedures and results of soling and temperature presented should be helpful in many areas of PV, designers, manufacturers, and even further research, with additional detailed data on improving PV cells.

Chapter 2: Temperature prediction for large-scale PV plants.

2.1 Introduction

This chapter gives an overview of the temperature predictions for large-scale PV plant technologies. It is reporting the most widely accepted definitions and resuming the most commonly employed components and materials with particular attention to solar power plant performance degradation. Based on solar collector type, geographical location, local climate, and the collectors' exposure period without manual cleaning. Moreover, it reviews the state-of-the-art cooling systems that maintain photovoltaic systems' temperatures within the acceptable operating range. The analysis of the advantages of cleaning operations includes natural, manual, automatic and passive methods. The goal is to provide solar power plant designers with the ability to forecast projected pollution losses in different parts of the world and evaluate effective cleaning methods to restore system energy productivity.

The solar industry has started considering solar forecasting with increasing installed utility-scale PV plants and a growing necessity for predictable energy generation. The reasons are:

- Solar generation is variable.
- Prediction of solar output will make the electric grid perform better under variable conditions.

Solar forecasting provides grid operators with a method to forecast and balance power generation and consumption. Assuming the grid operator has a mix of generation assets at his disposal, reliable solar forecasting allows the operator to optimise how he reports to his controllable units. Of course, the capabilities will vary from network to network, but the application of solar prediction remains essentially static.
Some essential components make up the solar prediction tools.

Firstly, there is the weather model, and solar power generation is inherently variable. Cloud cover causes this contrast by blocking the sun's rays from the solar panels; however, the weather is predictable with great certainty.

Secondly, a solar forecast factor is a model used to convert the weather into utility plant power output. The solar industry practises these "PV simulation" models to predict a PV plant's performance under environmental conditions such as irradiance, wind speed, temperature, and relative humidity. PV simulation models also include important plant behaviours. Such as tracking, which predicts PV panels' orientation mounted on uniaxial or dual-axis trackers. Therefore, accurate weather models and PV simulation tools are needed to produce an accurate and valuable solar energy forecast.
The first is associated with the forecast horizon. The time between the forecasting and the prediction is theoretically crucial; the regulatory framework requires accurate assessment to set up the algorithm consistently with the electricity market rules. Multiple philosophies exist, according to [1,2].

There are four different modes:

- Very short-term - forecast horizon of up to 6 hours, usually performed with higher accuracy, is fit for real-time electricity transmission, optimal reserves, and smooth power production for solar energy.

- Short-term - forecast horizon between 6 hours and up to 3 days. is advantageous to increase the stability of the grid

- Medium-term - forecast horizon between 3 days and several months, maintains the power system planning and maintenance schedule by predicting the available electric power.

- Long-term - forecast horizon between months and years helps transmission and distribution authorities in electricity generation planning, energy bidding, and security operations [3].

Satellite forecasts are effective in the short term, usually 4-6 hours ahead. It is the best way to spot small cloud forecast horizons (1 day or more). The model's Numerical Weather

Prediction (NWP) has insufficient ability to anticipate smaller drawdowns. Satellite Cloud Transmission Predictions use satellite imagery to predict cloud movement in the near term with geostationary satellites.

Numerical Weather Prediction (NWP) inaccuracies and the satellite models arise mainly from model biases and local weather conditions. Statistical methods combine the inputs of multiple prediction models or computer vision techniques. Such as artificial neural networks can increase accuracy; however, a perfect weather forecast can still lead to wrong solar forecasts. PV simulation tools are needed to translate weather conditions into suitable performance for the solar power plant. PV Systems made of wired-to-transformer units have a complex response to environmental conditions. Physical and experimental models do better at translating requirements into expected outcomes. However, statistical methods linking PV behaviour to radiation (or other weather variables) fail due to that relationship's nonlinearity [4].

Forecast predictions for a group of distributed plants yield better results when Numerical Weather Prediction (NWP) data is affected due to spatial averaging [5]. However, to reduce spatial resolution and increase accuracy, these complex algorithms use detailed meteorological data resulting in increased costs for the facilities that need to be anticipated PV. Thus, they can be replaced by commercially available weather forecast services, improving economic efficiency, limiting accuracy, and increasing time accuracy.

Errors in solar forecast accuracy occur from the weather prediction or PV simulation step. The solar industry has advanced in creating better weather forecasts. However, much work is left to do with fundamental model development, application and analysis.
Multiple weather forecast techniques are used to predict cloud cover and irradiance. These could include Numerical weather predictions (NWP) models, which use physical relationships to predict large-scale atmospheric trends, and are suitable for prolonged use.

However, the prediction error increases with the observed horizon. Each type serves a specific purpose; The short-range forecast is valid to ensure the power system's security in extreme weather conditions. Short-term forecasts have the most comprehensive implementation; Producers and consumers use them to optimise their profits, unit distribution, and load balancing. Medium-term forecasts are primarily intended for asset

management. In contrast, long-term forecasts analyse resources and select future publication locations. Therefore, the most crucial focus of the research is on short-term forecasting measures. This relatively short window allows more accurate weather forecasting and is directly related to power grid operation.

Regarding the technique used to perform the forecast, categorised models are: physical, statistical, data-driven, and hybrid. The Physical methods, established on numerical weather predictors (NWPs), sky imagery, and satellite imaging based on the area modelled, can be global or mesoscale. However, PV forecast should be used only mesoscale with a resolution of up to 50 km [6].

Compared with large-scale dispatchable plants, distributed solar photovoltaic (PV) forecasts are more challenging to produce because of the relatively small size and many solar PV sites. However, such predictions are most accurate. This is because nearly real-time power generation and detailed static data (e.g., location, hardware information, panel orientation) are available for all connected systems [7].

Large-scale solar power plants are generally located in semi-arid and desert lands where sunlight is abundant to convert solar energy. However, these plants suffer from two main factors of environmental degradation: high ambient temperature and high concentration of atmospheric dust. The degradation of solar collector performance results from the pollution results in a significant energy productivity loss in all solar power plants.

In most solar cells, the short circuit current (Isc) goes up as the temperature increases, while the open-circuit voltage (*Voc)* and the fill factor (FF) decrease as the temperature decreases (Figure 2.1). The Isc of a solar cell generally increases due to the temperature-dependent bandgap narrowing, increasing photons absorption. The Isc can also decrease as the temperature increases. There is bandgap narrowing in a filter layer or an optical element that impedes the absorption of additional photons. The temperature-dependent decrease of the Voc and FF are primarily due to the increasing the reverse saturation current density (Jo) and the standard operating cell temperature (NOCT). Additional temperature-dependent factors can also reduce the FF.

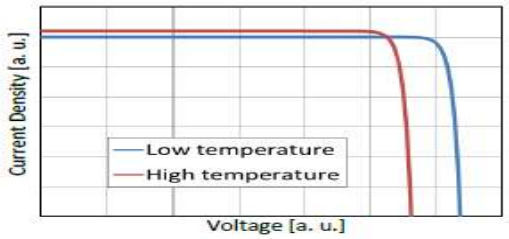

Figure 2. 1: I-V curves of a solar cell at two values. In most solar cells, the Isc increases as the temperature increases, while the Voc and FF typically decrease as the temperature decreases.

Most solar cells' efficiency (η) will decrease as the temperature increases. While some characteristics can improve the efficiency (*η*) as the temperature increases, such as the short circuit current (*Isc*), other essential terminal characteristics, such as the open-circuit voltage (*Voc),* can reduce the efficiency (*η*) more quickly. These temperature-dependent terminal characteristics will be explored later in the sections, as well as examples for the S-Q detailed balance limit. IV curve of a solar cell showing the open-circuit voltage in Figure 2.2.

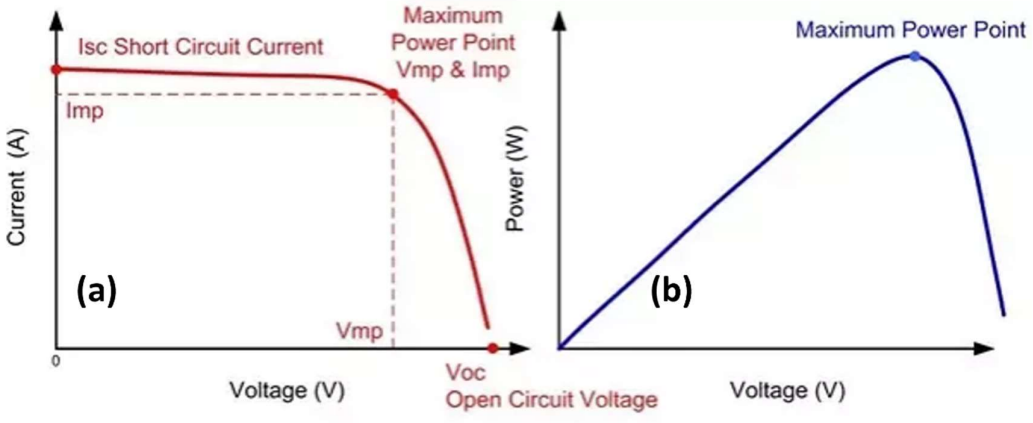

Figure 2. 2: (a,b): IV curve of a solar cell showing the open-circuit voltage [8].

2.1.1 Equivalent Circuit of a PV Cell.

The equivalent electronic circuit of a PV cell is in figure 2.3.

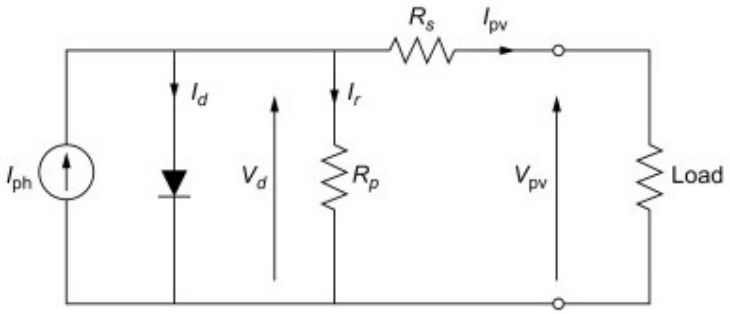

Figure 2. 3: Equivalent circuit of a PV Cell [1].

Originated for Kirchoff's first law, the output current is given by

$$\boldsymbol{I = I_{ph} - I_D - I_p} \quad \textbf{(2.1)}$$

$$\boldsymbol{I = I_{ph} - I_{sat*}\left(exp\frac{(q*(V_0 + I*Rs))}{n*K*T_{cell}*N_s} - 1\right) - \frac{V_0 + I*R_s}{R_p}} \quad \textbf{(2.2)}$$

Where Id, Is the junction current of the diode,

$$\boldsymbol{I_d = I_{sat}\left[exp\left(\frac{q(Vo + IRs)}{nKTcell}\right) - 1\right]} \quad \textbf{(2.3)}$$

Another critical parameter is the Open circuit voltage (Voc),

$$\boldsymbol{Voc = \frac{kT}{q} In\left(\frac{Iph}{Isat} + 1\right) = \frac{kT}{q} \ln\left(\frac{Iph}{Isat}\right)} \quad \textbf{(2.4)}$$

I = *output current,*
Isat = *Diode reverse saturation voltage*
Iph = *photo current*
V_o = *Output Voltage*

Rs = Series resistance (represents Voltage loss on the way to external connector)

Rp = Parallel resistance (representing leakage currents)

K = Boltzmann's constant

Q = charge on electrons

Ns = Number of cells in series

N = deality factor

Tcell = Solar panel temperature

2.1.2 Parameters of Solar Cell.

The main parameters used to describe solar cells' performance are:

the peak power Pmax. the short circuit current, ***Isc****; the maximum power,* ***Pmax****; the open-circuit Voltage,* ***Voc****; the fill factor,* ***FF****; the standard operating cell temperature,* ***NOCT;*** *the efficiency,* ***η****; the series resistance,* ***Rs****; the shunt resistance* ***Rsh****; the ideality factor of the diode,* ***m****; the reverse saturation* ***Io*** *and photo-generated current;* ***Iph*** [8]

The short-circuit current density Isc, the open-circuit voltage Voc, fill factor FF, and the conversion efficiency η. This becomes apparent from the illuminated I-V characteristic. Standard test conditions for a reliable test of the I-V characteristics are vital to performing the Standard Test Conditions (STC). The total irradiance on the solar cell under test equals 1000 W/m², and the spectrum should match the AM1.5 spectrum. Finally, the temperature of the solar cell should be constant at 25°C. As the performance of a solar cell strongly depends on the temperature.

2.1.3 Output parameters of the solar cell.

2.1.3.1 Short circuit current (Isc).

The short-circuit current (Isc): is the maximum current at zero voltage. The short-circuit current is dependent on the photon flux incident on the solar cell, determined by the incident light spectrum. For standard solar cell measurements, the spectrum is standardised to the AM1.5. Therefore, the short-circuit Voltage, Isc, is the maximum current through the solar cell at zero voltage. The short circuit current is dependent on the lowing factors,

- The area of the solar cell, cell area, to remove the dependence of the solar cell area then Jsc, the current density in M.A./cm².
- The number of photons, Isc, from the solar cell depends on the light intensity.

- The spectrum of light is the standard ATM 1.5.
- The optical properties.
- The collection probability depends upon the surface passivation.
- This details that the short circuit current is dependent on the generation rate and the diffusional length.

According to the "peak power," a photovoltaic panel's performance recognises the maximum power the panel provides when it receives solar radiation of 1 kW/m² at a cell temperature of 25°C. However, these conditions are insignificant because solar radiation has a variable intensity, with considerable temperature changes to the exposed panel [9].

Two crucial considerations of the I-V curve of a PV module are the short-circuit current and the open-circuit voltage. But, of course, that alters with the solar irradiance and the ambient air temperature [10].

Andreev et al. stated, "the photocurrent increases the temperature by 0.1%°$C^{-1,}$ causing a reduction in the solar cell gap [11]. Thus, reducing the open-circuit voltage by −2 mV °C^{-1} between 20°C and 100°C and an increased saturation current ". These two effects cause a reduction in the maximum power by 0.35%°C^{-1} ". This change is estimated between −0.3 and −0.5%°C^{-1}; these influences on the solar cell have specific consequences on the PV cell's electrical efficiency or module [12].

2.1.3.2 Open circuit voltage (Voc).

The maximum voltage produced is the open-circuit voltage (Voc): the voltage at which no current flows through the external circuit. Voc parallels the forward bias voltage, at which the dark current density compensates for the photocurrent density. Voc depends on the photo-generated current density and can be calculated, assuming zero net current.

2.1.3.3 Fill factor (FF).

$$\boldsymbol{Pmax = Vmax\ Imax} \qquad \textbf{(2.5)}$$

$$\boldsymbol{FF = \frac{I_{mp}V_{mp}}{I_{sc}V_{oc}} = \frac{P_{mp}}{V_{oc}I_{sc}}} \qquad \textbf{(2.6)}$$

FF = Fill factor

Imp = Current at Maximum power

Isc = Short circuit current

Voc = open circuit voltage

Vmp = Voltage at Max power

Pmp = Maximum power point

The efficiency of the Fill factor is defined as the ratio of the maximum power output (Pmax) at the maximum power point to the product of the open-circuit voltage, and short circuit current density is expressed as;

$$ϩ = \frac{I_{sc}V_{oc}}{P_{in}} = \frac{P_{mp}}{P_{in}} \qquad \textbf{(2.7)}$$

This calculation is more suited for calculating the FF of an experimental I-V curve of the solar cell. It considers the effects of the series resistance (Rs) and the shunt resistance (Rsh) to calculate the theoretical FF on the cell's performance.

Green gave the Fill factor calculation expression to provide greater accuracy, which offers the maximum possible value of FF. And does not consider resistive losses, the series resistance (Rs) and the shunt resistance (Rsh) [13].

$$\boldsymbol{FF} = \frac{\boldsymbol{Voc - In\,(Voc + 0.72)}}{\boldsymbol{Voc + 1}} \qquad \textbf{(2.8)}$$

To calculate the temperature dependence of the FF with T

$$\frac{\boldsymbol{dFF}}{\boldsymbol{dT}} = \frac{\left(\frac{\boldsymbol{dVoc}}{\boldsymbol{dT}} - \frac{\boldsymbol{Voc}}{\boldsymbol{T}}\right)}{(\boldsymbol{Voc - Vth})} \qquad \textbf{(2.9)}$$

$$\left(\frac{{}^{\boldsymbol{Voc}}/_{\boldsymbol{Vth - 0.28}}}{{}^{\boldsymbol{Voc}}/_{\boldsymbol{Vth - 0.72}}} - \boldsymbol{FF}\right) \qquad \textbf{(2.10)}$$

The efficiency of the solar cell: ratio of the power output corresponding to the maximum power point to the power input, where Pin is the intensity of the incidental radiation.

$$\eta = \frac{P_{max}}{P_{In}.\ Area} \quad \text{or} \quad \eta = \frac{Voc*Isc*FF}{P_{In}}$$

2.1.3.4 Maximum power (Pmax).

The maximum power, ***Pmax,*** Is the maximum power output at optimal operating conditions

$$\boldsymbol{Pmax = Vmax\ Imax} \qquad \textbf{(2.11)}$$

The most significant material parameter is diffusion length and surface passivity when comparing similar material types of solar cells. For example, in a cell with a perfectly passivated surface and uniform generation, the equation for the short-circuit current is defined as:

$$\boldsymbol{Isc = Q^G\ (Ln + Lp)} \qquad \textbf{(2.12)}$$

2.1.3.5 Equivalent Circuit of a PV Cell.

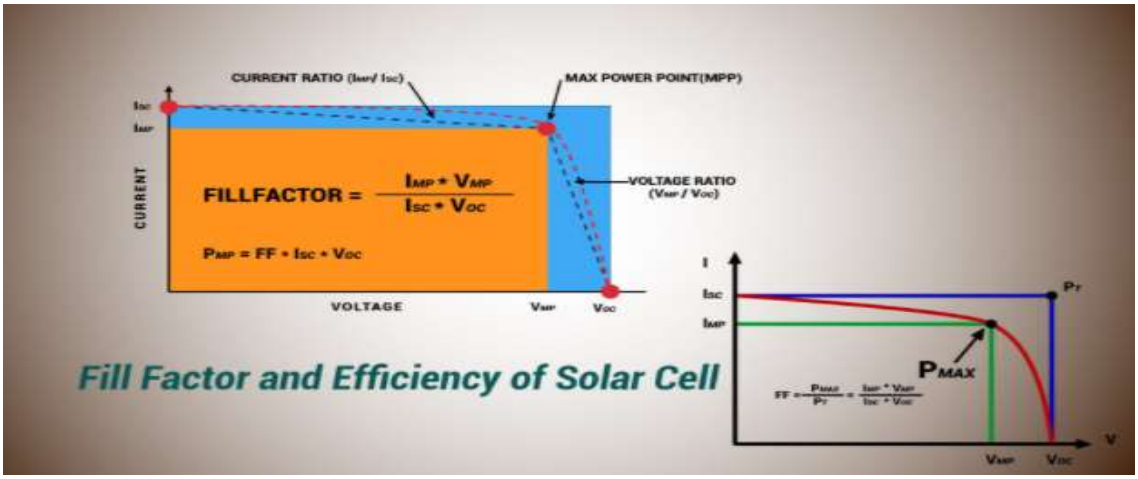

Figure 2. 4: Fill factor and Efficiency of the Solar Cell.

A more substantial potential from only a fraction of solar irradiation requires an examination of the PV module performance parameters. Voc, Isc and the FF are three significant essential parameters. Maximising all three parameters is necessary for an efficient operation. The fill factor and Efficiency graph of the Solar Cell is shown in Figure 2.4.

- F.F.
- Voc.
- Isc.

The F.F. measures the efficiency of a solar PV module, The F.F. and the ratio of Pmax to the product of Voc & Isc, the percentage of the actual ultimate achievable power.

$$\boldsymbol{Fill\ Factor\ (FF) = \frac{Pmax}{Voc\ x\ Isc}} \qquad \textbf{(2.13)}$$

The performance of a photovoltaic panel is according to the “peak power”. The panel’s maximum electric power receives solar radiation of 1 kW/m² at a cell temperature of 25°C. These conditions are insignificant because the insolation has a variable intensity, and the panel is exposed to considerable temperature changes [14].

Two critical factors of the I-V curve for a PV module; are the short-circuit current (Isc) and the open-circuit voltage (Voc) that change with solar irradiance and ambient air temperature [15]. Andreev et al. identify a photocurrent temperature increases at 0.1%◦C−1, reducing the solar cell gap, causing the open-circuit voltage to decrease at −2mV◦C−1 between 20 and 100◦C gap and an increase in the saturation current [16]. Both effects lead to a

decrease in the maximum available power equal to 0.35%∘C−1. This influence has been estimated between −0.3 and −0.5%∘C−1 [17]. These influences on Isc and Voc have significance on the electrical efficiency of the PV cell or module.

Several authors have proposed and used many correlations for calculating the electrical performance of a PV module, as defined by Skoplaki and Palyvos [18].

These relations especially emphasise the silicon temperature's role that is deemed the main parameter modifying the conversion efficiency. For example, the expression planned by Evans to describe the module's efficiency η in equivalence of given values of the operating temperature Tc and insolation G is well known [19]:

$$\boldsymbol{\eta = \eta_{ref}\left[1 - x(T_C - 25) + \varepsilon log_{10}\left(\frac{G}{G_{ref}}\right)\right]} \qquad \textbf{(2.14)}$$

Based on ηref, is the efficiency at Standard Test Conditions (STC) in which the solar irradiance Gref is 1000W/m^2, and the cell temperature is 25∘C. The insolation coefficient ε and temperature coefficient χ the have values of 0.12 and 0.004K$^{-1,}$ respectively, for crystalline silicon modules [20]. Other correlations, recently proposed in Mattei et al., Koehl et al. and Skoplaki and Palyvos, use experimental constants whose values only refer to a few models of PV panels [21].

The cell temperature appears to be an essential parameter to study. The solar cell operating temperature is one of the critical parameters in establishing the energy conversion efficiency of a Solar cell panel: the efficiency of a Solar cell device is a decreasing function of the Tc temperature (23).

Several available empirical correlations in the literature obtain the PV panel operating temperature. These correlations have advanced for common geometries and standard weather variables. From a mathematical point of view, the correlations for the PV operating temperature are either obvious in form. Giving Tc directly or implicit in form; they involve variables that depend on Tc; in the last case, a repetition procedure is essential. Most relationships typically include the reference condition and the appropriate variables' corresponding values [22].

The typical procedure to determine the cell temperature Tc consists of using the Normal Operating Cell Temperature (NOCT) [23-25].

The PV module manufacturer gives the value of this parameter: Tc is then dependent on the ambient temperature Ta and the ratio of insolation G [W/m^2] to the standard value of 800W/m2, according to

$$\boldsymbol{T_C = T_a\,(T_{NOCT} - 20)\frac{G}{800}} \qquad \textbf{(2.15)}$$

Therefore, to predict the yield output of the PV system, it is essential to evaluate the operating conditions under the following conditions. Insolation, panel temperature, wind speed, air temperature electrical load operating time while producing electricity [26]. The analysis proposes that $V/V_{mmp,panel}\ \ (G_s\ T_c)$. The ratio is characterised by the electricity produced by a PV panel [27].

These parameters are well-defined in the paragraphs below.

2.1.3.6 Isc.

The short-circuit Voltage, Isc, is the maximum current through the solar cell at zero voltage. The short circuit current is dependent on the lowing factors,

- The area of the solar cell, cell area, to remove the dependence of the solar cell area then Isc, the current density in M.A./cm²
- The number of photons, Isc, from the solar cell depends on the light intensity.
- The spectrum of light is the standard ATM 1.5
- The optical properties
- The collection probability depends upon the surface Passivation

$$\boldsymbol{Isc = Q^G\ (Ln + Lp)} \qquad \textbf{(2.16)}$$

This details that the short circuit current is dependent on the generation rate and the diffusional length.

2.1.3.7 Pmax.

The maximum power, ***Pmax.*** Under these conditions, the maximum electrical energy is called peak power (Pmax) in Wp (Watt-peak). The idea of watt-peak compares the

performance of the PV installations and, under optimal conditions, predicts the amount of electricity they can create.

2.1.3.8 Voc.

The open-circuit voltage, ***Voc,*** is the maximum voltage available from the solar cell with no load when the current is zero.

Open circuit voltage how many volts the PV will produce with no load. Measuring with a voltmeter across the plus and minus leads; will show the Voc. The solar panel has no load on it, producing no current. This is the maximum voltage the PV can create under standard test conditions(STC). When determining how many solar panels can be wired in series, this is the number to use going into the inverter or charge controller.

2.1.3.9 Fill factor.

The fill factor, ***F.F.,*** is the maximum power. This is the ratio of the maximum output power (***Pmax)*** at the maximum power point to the product of the open-circuit voltage (***Isc)*** and the short circuit current ***(Isc) density***.

$$FF = \frac{Pmax}{Voc\ Isc} \qquad (2.17)$$

Green gave an expression for the calculation of FF to excellent accuracy.

$$FF = \frac{Voc - In(Voc + 0.72)}{Voc + 1} \qquad (2.18)$$

Equation (2.17) is suitable for calculating FF as an experimental I-V curve of the solar cell. However, equation (2.18) gives the maximum possible FF valve as it does not consider resistive losses.

2.1.3.10 NOCT.

The Shockley-Queisser (S.Q.) limit gives the maximum efficiency for a single-junction photovoltaic device, 33.8% under 1,000 W m^{-2} solar irradiation with AM1.5G spectral distribution.

The standard operating temperature, ***NOCT,*** is crucial for its energy output. I*t is* usually rated in Standard Test Conditions (STC = 1000W/m², Am 1.5, 25°C). However, their

operating temperatures are generally significantly higher and thus indicate the cell's temperature. However, this is not constantly occurring with actual operating temperatures. They may be far exceeded, depending on several factors wind speed, irradiance, and ambient temperature.

First-generation silicon solar cells, although this technology has high conversion. However, its raw material has associated high costs, and the manufacturing process is complex, with several issues impacting the efficiency:

- The photons' energy hitting the solar cell is less than the bandgap, so the light cannot be converted into electricity and is lost.
- The incoming photons' energy is greater than the bandgap, so the excess energy is lost as heat.

- The Fermi levels (the energy level occupied by the electron orbital at temperature) equals 0K. The occupancy level determines the conductivity of different materials) Both n-type and p-type silicon is always inside silicon's bandgap, so the open circuit voltage is smaller than the bandgap.

Second-generation thin-film solar cells have lower efficiency levels. And are cheaper to manufacture; these types of thin-film solar cells have both advantages and disadvantages:

Advantages:

- It has high absorption co-efficient
- It can occupy both vacuum and non-vacuum processes.
- Lower cost in comparison to Si-based solar cell.
- Low-cost substrate (Cu tape)

Disadvantages:

- Environment Contamination starts from the fabrication process.
- Materials are hard to find.

Third-generation solar cells Polymers and organics types have advantages and disadvantages

Advantages (Polymers):

- Raw materials are easy to find
- Easier fabrication process rather than the other two technology
- Cost is minimal

Disadvantages (organic):

- Liquid electrolyte (low Temperature) High cost, Ru (dye) and Pt (electrode)

An effective way of increasing the efficiency level is to reduce the operating temperature; by cooling the module and the heat stored inside the PV system during its operation.

2.2 Temperature effects.

2.2.1 The effects of temperature.

The weather conditions influence solar cell performance, mainly the solar irradiance and temperature [28]. Reducing irradiance involves a reduction in solar cell output current and voltage. On the other hand, increasing cell temperature consists of a slight increase in the output current and a considerable reduction in voltage output, resulting in an overall decrease in output power. These effects are illustrated in Figures 2.5 and 2.6.

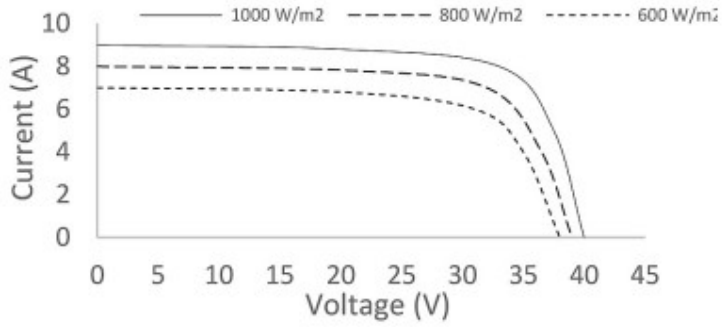

Figure 2. 5: Effect of irradiance on solar cell I-V curve.

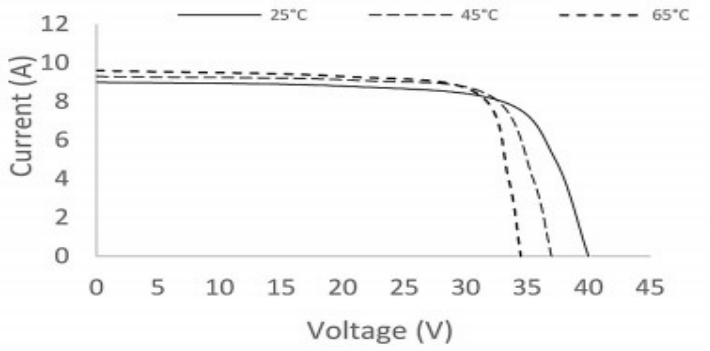

Figure 2. 6: Effect of temperature on solar cell I-V curve.

Solar panels were tested in a laboratory setting under the Standard Test Conditions (STC) of 1000 W/m^2 incident solar irradiance, cell temperature 25°C, wind speed 0.0 and air mass spectrum1.5. STC seldom occur in actual outdoor conditions; therefore, the cell temperature, most of the time, under actual operating conditions, will be greater than 25°C, especially in hot environments. Consequently, they cannot be used to evaluate the actual performance and energy yield of a PV System [29]. Various solar cell technologies have different responses to temperature variations. Hamrouni et al. explored ambient temperature and solar irradiance on the solar pumping system's performance [30]. They concluded that high ambient temperature decreased the pump flow rate and overall system efficiency. Priyanka and Ravindra studied the solar cell's critical characteristics' temperature dependence (in the range of 273–523 K). Namely, the short circuit current density, open-circuit voltage, fill factor and efficiency [31].

Module temperature conditions affect a PV power system output. These conditions will affect its overall performance as it modifies the system efficiency and output energy. As temperature increases, the bandgap lessens, and the open-circuit voltage Voc decreases.

2.2.2 Temperature effects on various solar cell technologies.

Solar cells of various semiconductor materials such as. Si, GaAs, InP, CdTe and CdS. They determined that the overall performance decreases with the increase in temperature. Dubey et al. reviewed literature investigating the relationship between cell temperature and solar cell performance. And established when using the data found in the literature to

estimate solar cell temperature provided consideration since those terms apply only for restricted mounting [32]. Tobnaghi et al. experimentally accomplished coefficients to evaluate the electrical parameters of solar cells with temperature discrepancies. The most significant coefficient obtained described the decrease of maximum power output with the increase in temperature, with a coefficient factor of -0.005 mW/°C [33].

2.2.3 Measurement of cell temperatures.

2.2.3.1 Ambient Temperature.

Temperature effects result from all the conditions of crystalline silicon modules. As the temperature increases, it loses voltage and conversely generates a higher voltage as temperature decreases.

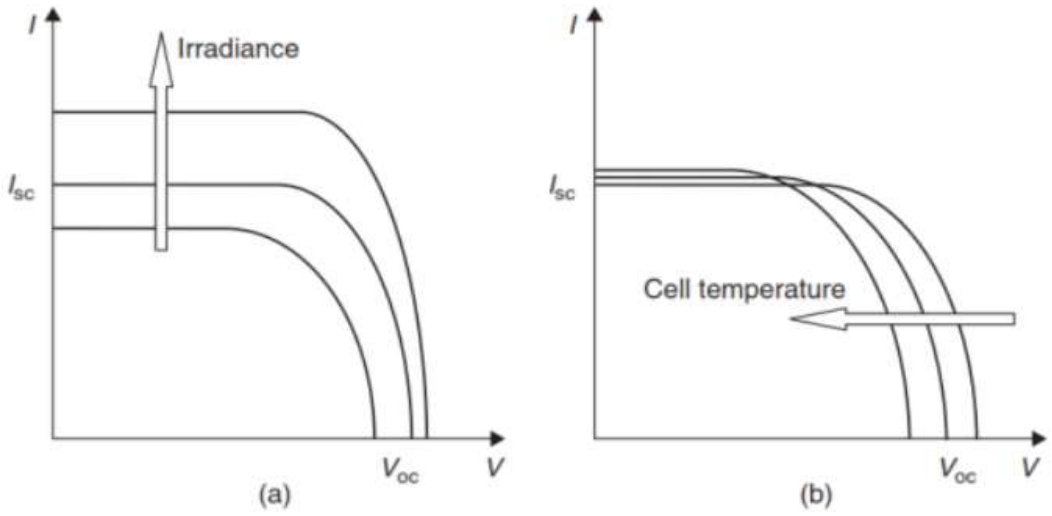

Figure 2. 7: Effects of irradiation and cell temperature on PV cell characteristics, (a) effect of increased irradiance and (b) effect of increased cell temperature [10].

Figure 2.7 above details the effects of increased temperature and irradiance on the cell characteristics. In particular, in Figure 2.7(a), the open-circuit voltage increases logarithmically by increasing the irradiance. Nevertheless, the short circuit current has achieved a linear increase. The cell temperature effect on the cell characteristics is detailed in Figure 2.7(b). The main impact of the rise in cell temperature is the open-circuit voltage,

decreasing linearly with the cell temperature. As a result, the efficiency drops; the short circuit current increases slightly with cell temperature [34].

The procedure to determine the expected operating cell temperature (NOCT) of a PV module included in the IEC standards; is based on the fact that the difference between module temperature (T*m*) and ambient temperature (T*amb*) can be measured independent of the ambient temperature and linearly proportional to the irradiance level above 400W/m^2 [35].

$$\boldsymbol{Tm = Tamb + (NOCT - 20)\frac{E}{800}} \qquad \textbf{(2.19)}$$

$\boldsymbol{E}$ is the Irradiance in W/m^2.

A PV cell's energy conversion efficiency (η) is the percentage of power converted (from absorbed light to electrical energy) and collected.

This term was calculated using the ratio of maximum PowerPoint. Pmax, divided by the input light irradiance (E, in W/m^2 under standard test conditions, and the surface area of the PV cell (AC in m^2).

$$\eta = \frac{\boldsymbol{Pmax}}{\boldsymbol{EAc}} \qquad \textbf{(2.20)}$$

The efficiency in a PV module decreases with increasing the module temperature Tm.

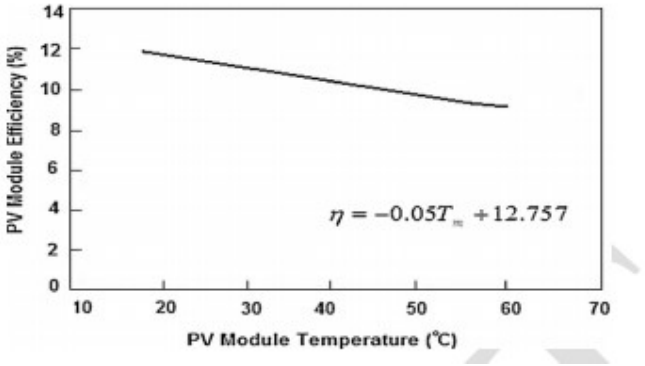

Figure 2. 8: Relationship of the PV module efficiency (η) and the PV module Temperature (Tm) [10].

One of the essential factors in increasing efficiency is Improving solar cell efficiency and reducing production costs. Research is ongoing to increase the efficiency of commercial solar cells. To improve efficiency and reduce the rate of thermal degradation, an effective way to achieve this is by lowering the surface operating temperature, which will be discussed later in this thesis.

2.2.4 The influence of irradiation.

Solar radiation has a direct effect on the Panel output power. Which varies caused of the location and the time of the day; Figure 2.8 (a) shows a logarithmically increase in the open-circuit voltage (Voc) and a linear increase in short circuit current (Isc).

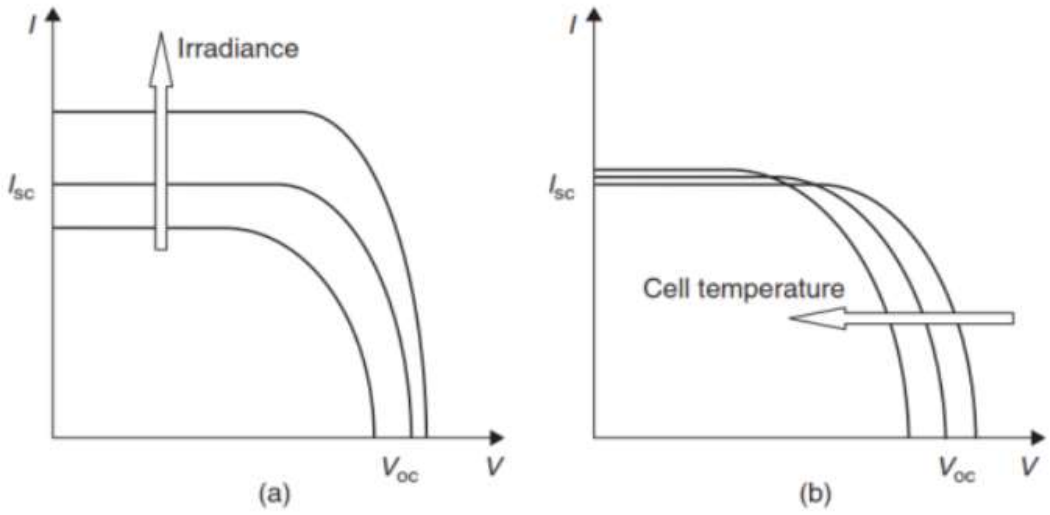

Figure 2. 9: Effects of irradiation and cell temperature on PV cell characteristics, (a) effect of increased and (b) effect of increased cell temperature [8].

2.2.5 Inverter efficiency.

Inverters are essential for autonomous or grid-connected photovoltaic (PV) systems. These inverters affect the overall performance of the PV system. Inverter problems and problems are difficult to notice unless the inverter shuts down. Solar inverters are very efficient. Depending on the make and model, 93-96 per cent (not 100 per cent), some of the input DC power utilised to run about 10-25 W. However, you can improve efficiency using an electronic technology called Maximum Power Point Tracking (MPPT). The combination of

current or voltage determines the maximum output of the solar cell. It constantly changes depending on the level of light, shade, temperature, and the characteristics of the PV panel. The MPPT system continuously searches this point to extract the maximum power available from the cell. Multiple MPPT systems can maximise yield even if the array is partially shaded.

As with any grid-connected photovoltaic (PV) system, the inverter is a crucial device that converts the photovoltaic array's direct current (DC) to the alternating current (AC) used in the grid. Inverters convert direct current to alternating current and condition the photovoltaic system to get the maximum power. Power is the product of current (I) times voltage (V). Therefore, inverters have electronics that regulate the DC voltage to maximise the production of current and voltage (I*V). This process is called Maximum Power Point Tracking (MPPT).

The electricity or current produced by solar cells is direct current (DC). The electricity produced is not constant over time, as the intensity of sunlight depends on weather conditions. Since the energy generated by PV systems changes frequently, it is not easy to use the power obtained from PV units directly. In general, the output characteristics of solar cells depend on the solar radiation, the cleanliness of the surface of the solar cells, and the environmental aspects of the solar cell group, such as the operating temperature of the cell surface [36].

Energy losses in PV systems are significant factors affecting energy production. It is essential to convert DC uneven energy into constant energy DC or AC. An integral component of stable power transmission is the inverter. The inverter is responsible for the regular output power from PV units. The inverter’s efficiency is good when there is little difference between the input and output power. However, due to the nature of the device, power loss is inevitable. System losses occur while converting DC, produced by PV panels and solar cells, into AC, a consumable form. All power losses that occur in an inverter are considered system losses. No transformer can achieve 100% efficiency when converting from direct to alternating current. Therefore, the output power (AC) is not as high as the input power (DC).

Inverter efficiency ranges from 95 to 98%, and efficiency may vary depending on DC input power and voltage. The research was carried out to maintain the productivity of the inverter

by isolating the maximum power from the solar panel using the Maximum Power Point Tracking (MPPT) algorithm [37,38].

Determining the actual efficiency of an inverter Rather than relying on the efficiency provided by the manufacturer, the solar energy produced must be estimated first [39]. The power output varies mainly with environmental factors. Solar radiation is a significant factor affecting energy production. Some studies are underway to estimate solar radiation to predict future energy production [40-42]. Studies on estimating the power output based on ambient temperature, wind speed, and incident light [43-45]. Methods based on historical weather data; There is a significant correlation between present or past and future solar energy generation weather conditions. Machine learning Artificial neural networks and Support Vector Machines (SVM) [46-48] can be suited for solar energy estimation. Techniques that utilise long short-term memory (LSTM) are a method for analysing time series of weather data using past and current weather data [49,50]. Other studies present methods using an adaptive linear time-series model and a technique for applying past data and predictions to the fuzzy decision tree model [51-53]. Further studies have been conducted based on the linear regression model used to study the sun.

2.2.6 Energy production and losses.

2.2.6.1 Mismatch losses.

Two modules of the same type from the same manufacturer are not perfectly identical; manufacturing variation leads to minor variation in the electrical parameters of the modules. This loss represents these manufacturing variations. However, these losses are not applied to designs using microinverters or DC optimisers. Because these module-level power electronics isolate the modules from one another.

2.3 Temperature coefficient.

One of the main parameters affecting solar cell performance is temperature; the solar cell output decreases with the temperature increase. Therefore, selecting the proper solar cell technology that performs better at a specified location considering its average temperatures is crucial.

Tobnaghi et al. obtained coefficients to estimate the variations in solar cells' electrical parameters with temperature. The most significant coefficient obtained described the

decrease of maximum power output with the increase in temperature, with a coefficient of -0.005 mW/°C.

Ye et al. performance monitoring different solar cell technologies in Singapore (tropical climate). Including monocrystalline Si, heterojunction crystalline Si, multi-crystalline Si, double-junction Si, single-junction/double-junction amorphous Si, CdTe and CIGS. In this work, the degradation rates were calculated using Statistical decomposition methods. As a result, the degradation rates for monocrystalline Si modules establish to be less than or equal to -0.8% per year, multi-crystalline Si modules -1% for, amorphous Si -2% for CdTe modules and CIGS modules -6% [54].

2.4 Types and performance of cooling systems.

Cooling methods and systems are identified in Figure 2.10 below:

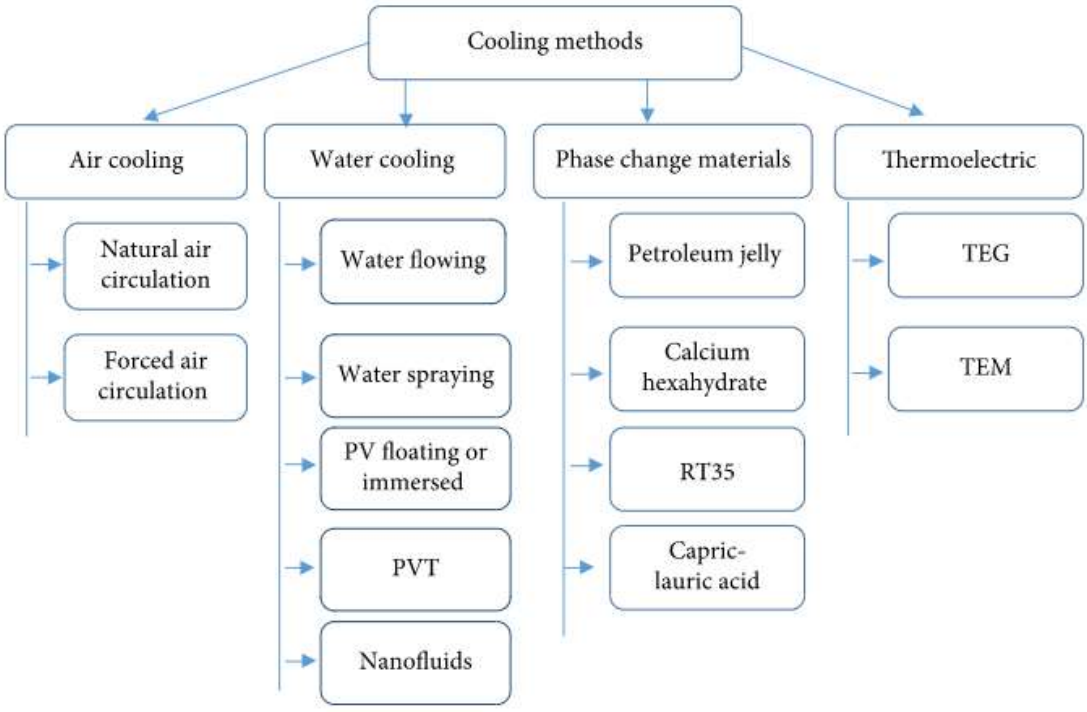

Figure 2. 10: The main cooling methods [8].

Cooling systems are classified further as either *passive* or *active*. Passive cooling does not require mechanical or electrical power input because it exploits natural laws. Active

cooling instead is obtained using a fraction of the cell power output. It is usually easily controllable and independent of the work conditions. The use of part of the energy output reduces the overall system efficiency.

2.4.1 Passive cooling systems.

2.4.1.1 Air Cooling.

These air-cooling systems are clarified as Natural airflow and Forced air circulation.

2.4.1.2 Natural airflow.

It is the most common method for cooling the PV panels due to its simplicity, no extra materials, and relatively low cost. However, photovoltaic panels' cooling can be improved if metallic materials with fins installed on the back of PV panels are installed to ensure excellent air circulation [55]. Using natural airflow between the vertical building walls and the PV system mounted on them, the photovoltaic panels' temperature can be maintained at less than 40°C lower by almost 20°C [56].

2.4.1.3 Forced air Circulation.

Forced air circulation is an effective method to cool the photovoltaic panels. However, there are other methods to air circulation, such as an open channel beneath, a steel plate with an air-channel below, and an array of air ducts below the PV panels with ideal fins [57,58]. Teo et al. used the array ducts, notably decreasing the temperature of the photovoltaic panels. Their efficiency increased between 12 and 14%.

2.4.1.4 Water Cooling.

These water-cooling systems Can be further defined as water flowing, Water spraying, PV floating or immersed, PVT and Nanofluids.

Cooling using water for photovoltaic panels has been studied since the late 1960s when the first hybrid photovoltaic panel and solar thermal collector panels (PVT) were fabricated. This technology underwent rapid development after the 1990s. Nowadays, there are many PVT types, such as natural and forced water circulation, non-concentrated and concentrated sunlight, glazing, without glazing, with and without absorber plate, and other types [59].

These hybrid panels produce electric and thermal energy, utilising almost the same space. He et al. studied a PVT consisting of a monocrystalline silicon panel placed on the absorber plate with a water pipe attached underneath. The water circulation is a natural one. The photovoltaic panel's efficiency is comparable with the one without a solar collector fitted; a Photovoltaic panel with the solar collector installed is approximately 40% efficient.

The hybrid system's efficiency is greater than that of a conventional system [60]. Yang and Yin found that the PV panel's maximum power in hybrid systems increases by 23% compared to a single PV panel. The solar thermal collector generated 661 W/m^2 [61]. Xu et al. recommended a concentrated PVT system. The Fresnel lenses and an optical prism concentrate the sunlight up to 1090 suns. The efficiency of photovoltaic cells is 28%, and the thermal efficiency is 60% [62].

2.4.1.5 Water flowing or spraying.

Several studies have examined the performance of the PV cells experimentally with active cooling water. Nizetic et al. investigated water spray cooling's impact on the PV panel's performance in the highest solar irradiation level environment [63]. Both sides of the PV panel cooled simultaneously by utilising twenty nozzles, ten on each side, as shown in Fig. 2.10. The results of three different cooling cases: front side cooling, rear side cooling and both sides are compared with a non-cooling case. The research suggested that the water spray cooling had a practical effect on the performance of PV panels. The best case was the simultaneous front and back side cooling of PV panels. Lastly, depending on the investigational results, the water spray cooling system had a good impression on the PV panel performance.

Abdolzadeh et al. studied the impact of water spray cooling on the performance of photovoltaic water pumping experimentally [64]. The configuration with two modules and a 25 lit/h/ water spray was called 'A'. The design with three modules, five lit/h/module and 25 lit/h/module water spray were called the 'B1' and 'B2', respectively, were used in the test. In "A" and "B1", the module temperature was decreased, reduced in case A was more significant than "B1", as shown in Fig. 2.11.

The experimental results suggested that spraying water on the PV module significantly improved system performance. Therefore, Irwan et al. studied the PV panel's performance using the water-cooling method [65]. A solar simulator carried out an indoor test consisting of twenty 500 W halogen lamps and two 50W Monocrystalline PV panels used in the trial. A DC water pump is used to spray water and connected to one of the panel's front surfaces,

and the other panel is used as a base panel. It was seen from the experimental results that the operating temperature of the PV panel incorporating the water-cooling system was reduced by 5–23°C. And the power output was increased by 9–22%; therefore, water cooling is one way to enhance the PV panel's electrical efficiency, as shown in Figs. 2.12–13.

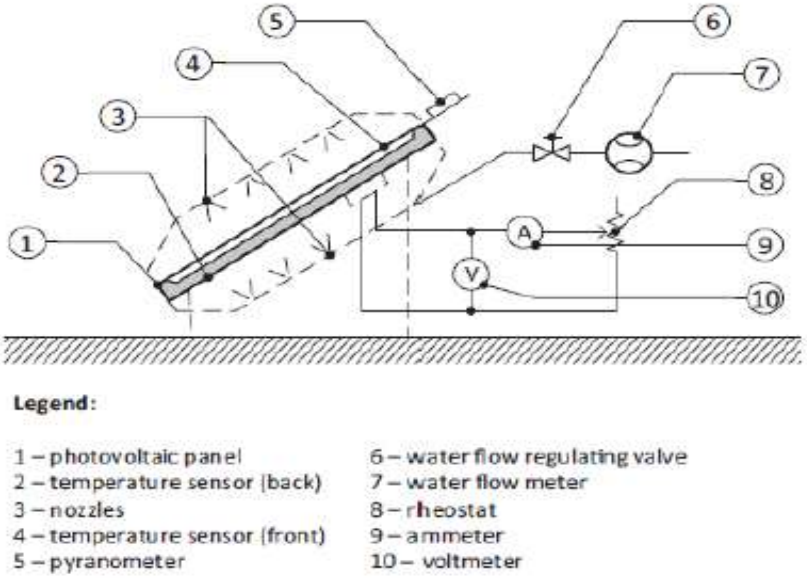

Figure 2. 11: Schematic layout of the specific experimental setup.

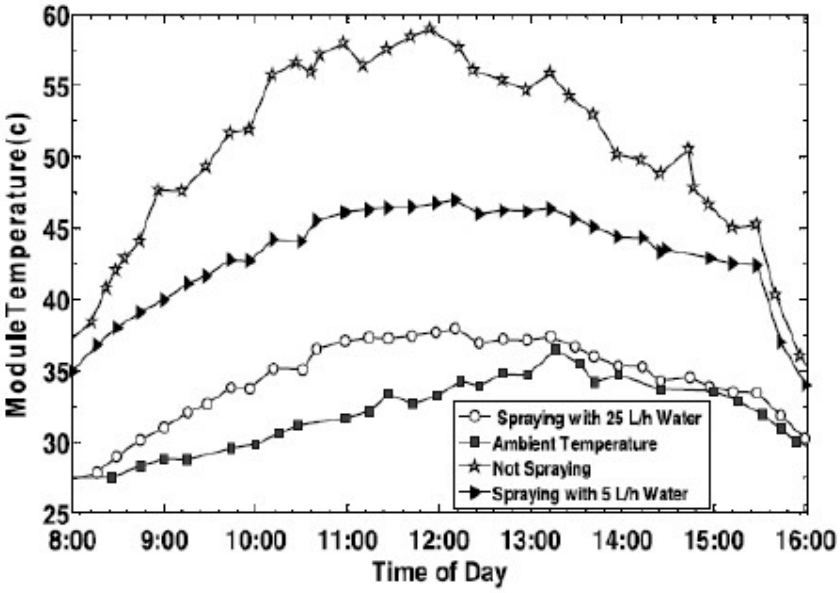

Figure 2. 12: Water spray affects the module temperature.

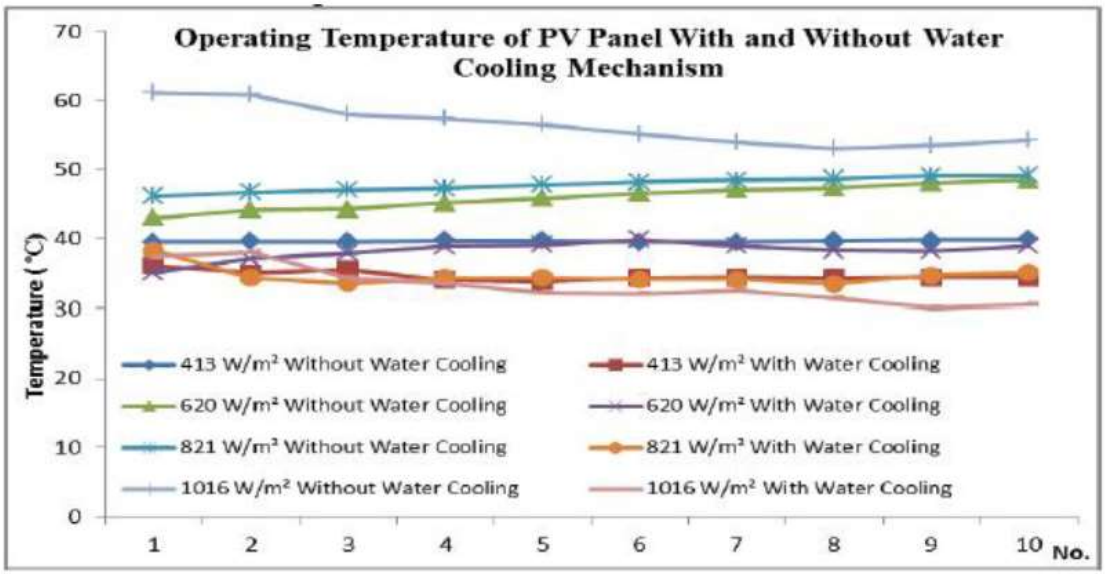

Figure 2. 13: Operating temperature of PV panel with and without water cooling mechanism.

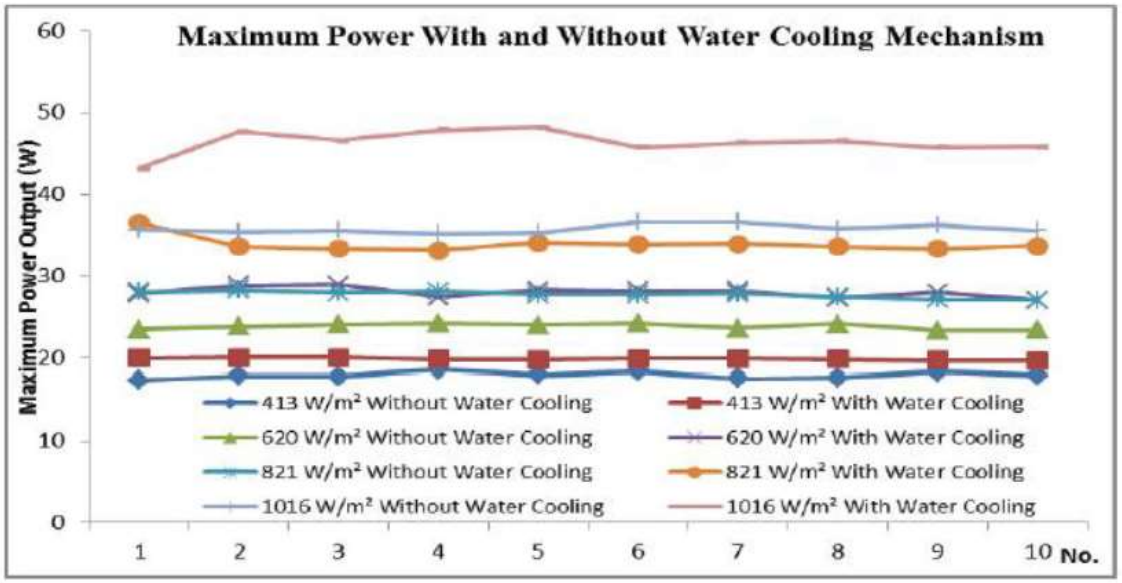

Figure 2. 14: The maximum power output of PV panel with and without water cooling mechanism.

2.4.1.6 PV floating or immersed.

Clot et al. studied the PV single crystalline silicon panel's behaviour submerged in water. IN NATURAL CONDITIONS, the PV panel temperature is around 70°C, but the temperature decreases to 30°C if submerged at 4 cm. The efficiency of the panel submerged increases by 11%. This increase is limited by water absorption. If the PV panel is submerged at 40 cm, the efficiency decreases by 23%.

Floating photovoltaics are another possibility of lowering the temperature of photovoltaic panels. Cazzaniga et al. described a floating PV photovoltaic facility that operates at low flow rates in concentrated light. Photovoltaic panels Sacramento et al. cooled using a watering device. Two polycrystalline silicon panels were used to compare their behaviour when mounted on the ground, the other floating on water. The efficiency of floating PV panels is 12.5% higher than other PV panels.

2.5 Photovoltaic thermal systems (PVT).

Karami and Rahimi used water-based boehmite at 0.01% by weight to cool the PV modules, and the efficiency gain was 27%. Hussien et al. used $A_{l2}O_3$ water nanofluid with a concentration ratio of 0.3% to improve the performance of the PV / T hybrid panel. The

tests were carried out at 1000 W/m^2 and a mass flow rate of 0.2 L/s for 24 minutes. As a result, the photovoltaic module temperature drops from almost 79°C to 35°C.

2.5.1 Nanofluids.

The solar cell module illuminated 917 W/m^2 cooled with a concentration ratio of water, TiO_2 / water, ZnO / water, Al_2O_3 / water, 0.2%. The most significant improvement in electrical efficiency was 6.36% Al_2O_3 / water, and the lowest with 5.48% water. Rostami et al. The solar cell module was cooled using nanofluids and ultrasonic waves simultaneously. The study found that:

The PV panel efficiency increases from 8% without nanofluid to 12% incorporating nanofluid; this means a 50% improvement in performance.

The variations of the nanoparticle concentration of 0.01% - 0.8%,

A flow rate from 0.4 ^{m3}/h to 12.5 m^3/h,

The level of illumination is 1000 W/m^2.

PV temperature results are influenced strongly by flow rate and 0.8% nanoparticle concentration rate. PV temperature dropped from 49°C to 24°C, and flow rate increased from 0.4 m3 / h to 12.5 m3 / h, the temperature dropped again from 36°C to 24°C, concentration rate changed from 0.01% To up to 0.8% at a flow rate of 12.5 m3 / h.

2.5.2 Thermo Electric Generator (TEG).

The thermoelectric generator (TEG) is a device for directly converting thermal energy into electrical energy based on the Seebeck effect. It has presented urgent potential in the case of waste heat recovery. The TEGs have many advantages: no moving mechanical parts, are long-lived, quiet, environmentally friendly, and require little maintenance [66]. As a significant cause of the fuel crisis and environmental pollution, the internal combustion engine (ICE) drives vehicles with only 30% of the total heat generated by gasoline. During this process, 40% of the heat escapes through the waste gas exhaust and the remaining 30% by the coolant [67]. The TEG using automobile waste exhaust as a heat source assumed a new alternative way to reduce ICE loads and decrease fuel consumption and environmental pollution.

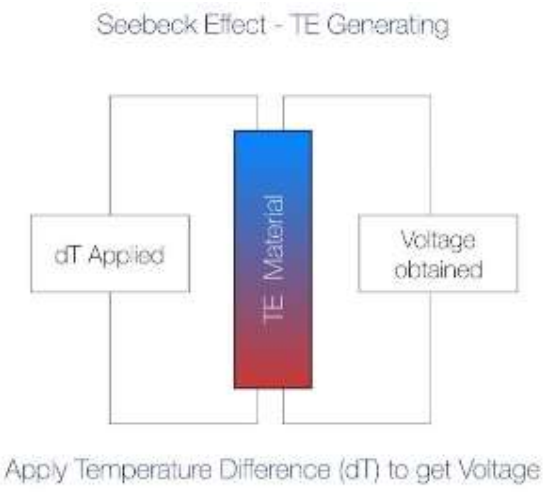

Figure 2. 15: ***Seed back effect illustration.***

A thermoelectric cooler (TEC) is a small cooling device that relies on a Peltier junction. Composed of two conductors made of different materials, a Peltier junction (J.C. Peltier1833) acts as a heat pump that can warm or cool. When current passes through the contacts of two dissimilar conductors in a circuit, a temperature differential appears between them. This briefly described phenomenon is the basis of thermoelectricity and is applied actively in the so-called thermoelectric coolingmodules. In contrast to the Joule heating, which is proportional to the square of the current:

$$Q = R \times I^2$$

the Peltier heat (Qp) varies as a linear function of the current and changes its sign with it:

$$Q_p = P \times q$$

Q is the charge that passes through the junction (q = I x t), and P is the Peltier coefficient, whose value depends on the contact materials' nature and temperature. The typical way of presenting the Peltier coefficient is the following:

$$P = \alpha \times T$$

Here, α - alpha is the Seebeck coefficient defined by contacting materials, properties, and temperature. T is the junction temperature in Kelvins.

2.5.3 Active cooling systems.

2.5.3.1 Passive and active cooling.

Usually, cooling systems are classified as *passive* or *active*. Passive cooling does not require mechanical or electrical power input because it exploits natural laws. Active cooling instead is obtained using a fraction of the cell power output. As a result, it is independent of the work conditions and easily controllable. However, using part of the energy output reduces the overall system efficiency.

In 2005, published a complete review on the cooling system for photovoltaic cells under concentrated illumination. Royne *et al.* stated that passive cooling was not feasible for densely packed cells or linear concentrators with temperatures above 20 suns. They concluded that micro-channel heat sink or impinging jets, both active cooling systems, were the

In 2008, Yeom and Shannon [68] reviewed micro-coolers, but only a few reported technologies were passive. In 2007, Tseng *et al.* applied Taguchi's statistical method to optimise the passive cooling systems for electronic devices. Passive cooling is more reliable than active cooling and reduces the potential damage caused by cooling failure.

Some references use different definitions for passive and active cooling. Active cooling refers only to the so-called *photovoltaic/thermal* (PV/T) technology, where the PV waste heat; is recycled for water heating and other purposes.

Specially designed PV/T collectors can facilitate the replacement of the outer walls and roof coverings. These collectors used the following: hospitals, schools, hotels, private houses, and flat developments for water heating and electrical power supply. With their great application and potential, hybrid collectors have been the subject of intensive scientific research and technical development for many years. Researchers and manufacturers; to increase the efficiency of PV modules and thermal absorbers by using new designs and material types and their proper integration into the PV/T collector. It is necessary to reduce the manufacturing cost of these systems to make them more competitive in the market.

2.5.4 Key characteristics.

2.5.4.1 Heat pipes.

Micro-heating tubing (MHP) can provide good heat transfer and reduce the thermal resistance between the cell and the cooler. Couture [69] defined a micro-heat pipe as a heat pipe "small enough. That the mean curvature of the vapour-liquid interface is necessarily comparable in reciprocal magnitude to the hydraulic radius of the total flow channel."

In the scientific literature, microscopic temperature pipes are active and passive configurations [70]. Yeom and Shannon summarised MHP's efforts from 1996 to 2007 and reported that the heat flux removed from MHP ranged from a few watts / cm^2 to over 300 W / cm^2. Given this high heat output level, micro heat pipes can be viable for passive CPV cooling.

2.5.4.2 Cross-sections.

Hung and Sang [71] reported that micro heat pipes' thermal output is closely related to the cross-section's geometry. Various cross-sections have b designed and tested to improve the return flow of the working fluid. Peterson et al. Showed that a triangular section micro heat pipe's performance was superior to a rectangular section due to the more significant capillary pump effect [72].

Moon et al. confirmed this result with MHP with curved sections [73]. Suman and Kumar developed an analytical model to study MHP performance. They considered MHP with two cross-sections: an equilateral triangle heat pipe with a 400 μm side and a 400 μm rectangular heat pipe [74]. Pentane is used as the working fluid and silicon as the substrate. Suman and Kumar showed that heat pipe performance deteriorated as the number of sides increased.

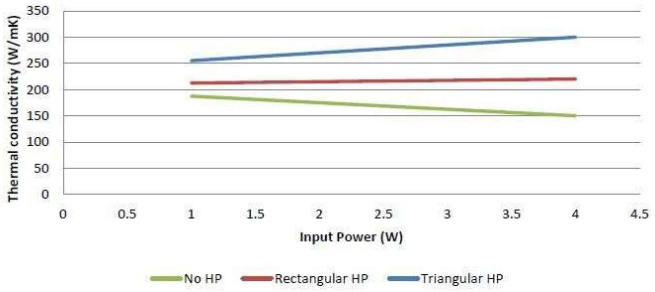

Figure 2. 16: Thermal conductivities of a silicon wafer with a rectangular heat pipe array, with a triangular heat pipe array and without heat pipe array, adapted from [72].

Kang and Huang produced MHP with star grooves and MHP with diamond grooves [75]. They reported an increase in thermal conductivity of 33.6% for stellar-grooved MHP and 39.1% for rhombus-grooved MHP compared to conventional triangular MHP. The authors stated that better achievement in capillary action in more star and diamond groove devices with more acute angles and improved gaps. As reported by Hung and Tseng, the sharpness and the number of sharp corners. Two critical source geometries determine the capillary pumping capacity and thus, determine the performance of the micro heat pipe. For common polygonal shapes, the corner's sharpness depends on the number of corners: the corner angle decreases as the number of corners increases. With the asterisk groove MHP, the number of corners and the corner angle do not interact.

For these reasons, Hung and Tseng found that star-gauge micro heat pipes offer greater capillary pumping capacity and increased heat transport capacity than ordinary polygonal micro-heat pipes. Also, they found that an increase in the overall length of the micro heat pipe caused a decrease in its heat transport capacity.

Wang and Peterson proposed a wire-bonded aluminium-acetone micro-heat pipe obtained by sandwiching an array of cylindrical wires between two flat plates [76]. Wang and Peterson discovered that the maximum heat transfer capacity increased when the wire diameter and operating temperature increased. Also, they demonstrated that increasing the spacing between wires could raise the maximum heat transport capacity. In their following work, Wang and Peterson confirmed this statement. Still, they added a spacing value where this improvement, overshadowed by the decrease in the number of heat pipes in the array's maximum heat transfer capacity, became limited [77]. The optimum spacing distance will vary with the diameter.

2.5.4.3 MHP with arteries.

This design consists of one vein channel: the traditional MHP and two neighbour arterial channels distributed on both sides of the vein and connected at both ends. Vapour carries the latent heat to the cold end in the vein, where it condenses.

The liquid is transported to the hot end by the V-grooves' capillary force in the micro-triangle pipes in the arteries. Due to the liquid pressure difference between the cold end of the artery and the MHP. The fluid accumulated in the condenser section is recycled in the evaporator sections.

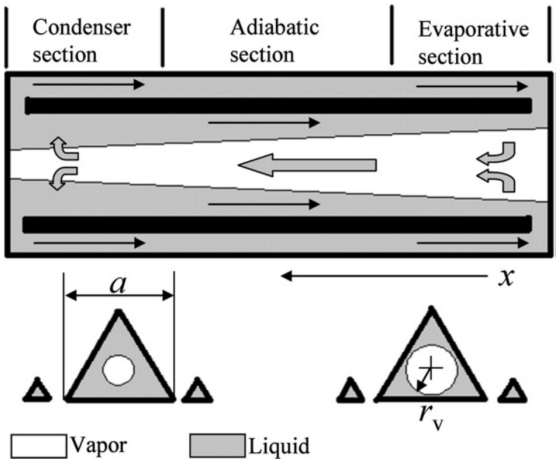

Figure 2. 17: Working principle of MHP with arteries [78].

Liu *et al.* compared MHPs with and without arteries, concluding that implanted arteries could effectively enhance the capillary force, improve the capability to transport the liquid from the cold end back to the hot end, and limit the propagation of the dry-out region [78].

2.5.4.4 Working fluids.

The working fluid is essential for micro-heat pipes' efficiency, a two-phase cooling device. In 2003, Chien *et al.* proposed nanofluids in micro-heat pipes [79]. Using nano-gold particles suspended in water, the authors obtained an average decrease of 40% in the MHP thermal resistance instead of pure water. Over 30 papers on nanofluids' application into heat pipes were published when this investigation was conducted. Only the works on heat pipes micro-grooved have been considered in this review. A summary of the results is presented in Table 1.3: each study improved MHP heat transfer through nanofluids' use. Liu Z.H. and Li Y.-Y. Cited three main reasons for this improvement in heat transfer: the effective thermal conductivity of nanofluids; the physical proprieties of nanofluids have changed, the capillary force in HP increases, and the fluid pressured to disperse through the micro-grooves; The nanoparticles form a thin porous layer on the wall, increasing the capillary strength [80].

Shape of micro-grooved heat pipe	**Best performing working liquid type (nanoparticle size and optimal concentration**	**Maximum reduction in thermal resistance (fluid compared with)**	Researchers
Disk-shaped	Au/Water (17 nm)	Average of 40% (DI water)	Chien et al. [299]

Cylindrical	Ag/Water (10nm) Ag/Water (35nm)	50% (water) 80% (water)	Kang *et al.* [301]
Cylindrical	Ag/Water (10nm)	44% (water)	Wei *et al.* [302]
Cylindrical	CuO-water (50nm, 1.0wt%)	39% (water)	Yang *et al.* [303]
Flat	Al2O3-water (38.4 nm, 0.8wt%)	47.7% (DI water)	Do K.H. and Jang S.P. [304]
Flat-shape	TiO2-water (20nm, 4.0wt%)	27% (water)	Shafahi et al. [305]
Cylindrical	TiO2-water (10nm, 4.0wt%)	25% (water)	Shafahi et al. [306]
Cylindrical	CuO-water (50nm, 1.0wt%)	About 50% (water)	Liu et al. [307]
Cylindrical	CuO-water (50nm, 1.0wt%)	50% (water)	Wang et al. [308]

Table 1.3 - Nano-fluids in micro-grooved heat pipes publications, adapted from [80].

2.5.5 MHP Fabrication.

The manufacture of micro heat pipes usually involves standard microsystem technologies. Ivan et al. Deep plasma etching was used to obtain a microcapillary wick, laser-drilled in a wafer to fill small holes. The two wafers were mounted using a silicon direct bond technique. Finally, thermal annealing using inert gas resulted in irreversible bonding due to the formation of covalent bonds between both surfaces

In 2002 Le Berre *et al.* manufactured and tested two types of silicon micro-heat pipes [81]. The first one (shown in Figure 2.17a) consisted of 55 parallel triangular channels, 230μm-wide, 170μm-deep, and 20mm-long channels micro-machined on a silicon wafer, a separation of 130μm. Next, a second wafer was then sealed to the first

to seal the device hermetically. The second design (Figure 2.17b) incorporated liquid transport arteries: the liquid circulated to the evaporator through etched channels. In this case, the first wafer consisted of 25 triangular grooves 500µm-wide and 320µm-deep etched into the wafer. The second wafer also contained 25 triangular tracks. Fabrication began with the thermal growth of a 1.5µm oxide layer on the wafer of the device. The oxide on both sides of the device wafer is designed as an etch mask. The triangular grooves were etched using a 40wt% aqueous KOH solution at 60°C. Finally, a simple silicon wafer seals the MHP *(Si-Si direct bonding*) matrices.

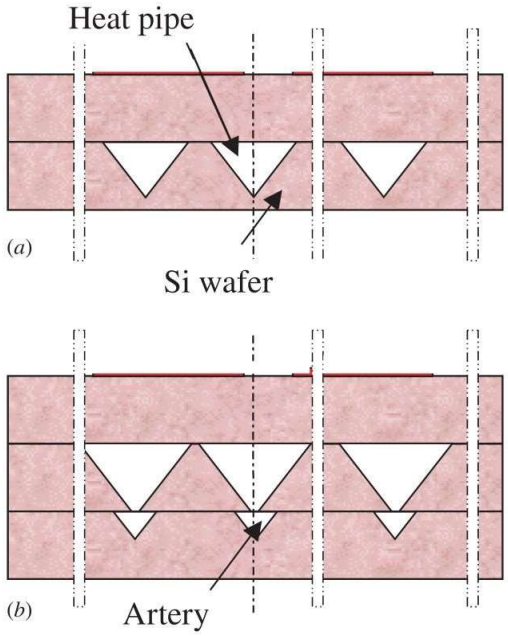

Figure 2. 18: Transverse cross-sections of an MHP developed by Le Berre et al. MHP [81].

A star fluted MHP forged by three silicon wafers, Kang and Huang. They use the wet etching technology of photolithography to construct a series of 31 parallel V-grooves. Next, three layers of wafers were eutectic bonded to form the MHP. The whole process is presented in Figure 2.18.

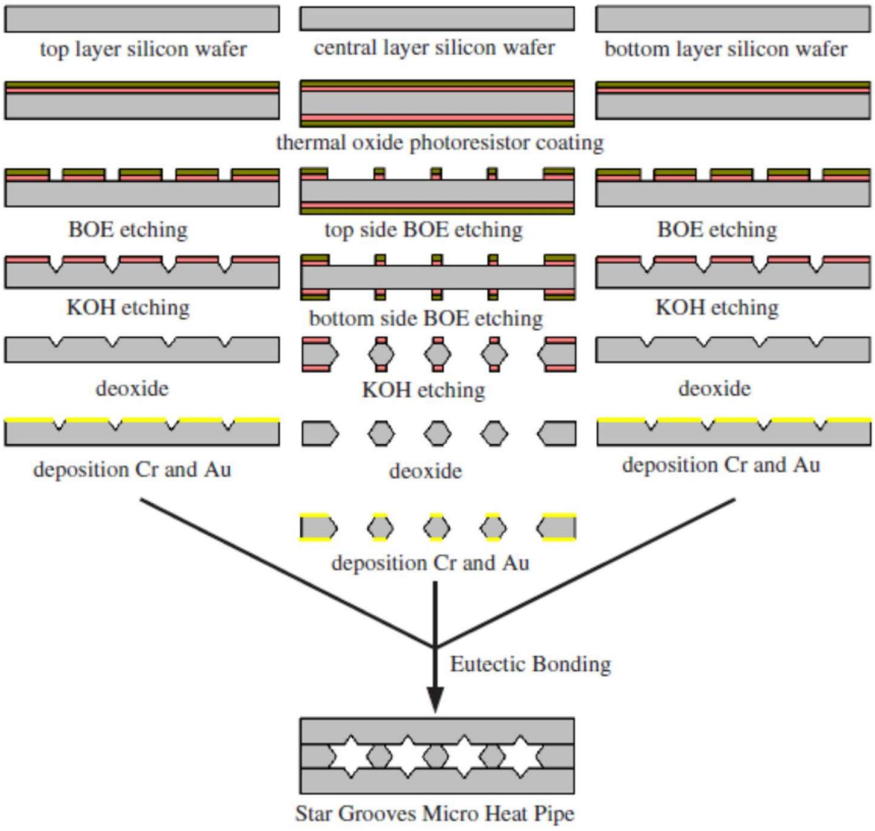

Figure 2. 19: Fabrication process of the star grooved MHP [75].

2.5.5.1 Miniature two-phase closed thermosyphon

Two-phase closed thermosyphons are also known as *wickless heat pipes* (Figure 2.19). Lee defined them as heat pipes that do not use capillary force. Thermosyphons exploit gravitational laws: therefore, they cannot be used in orientation-dependent applications [82].

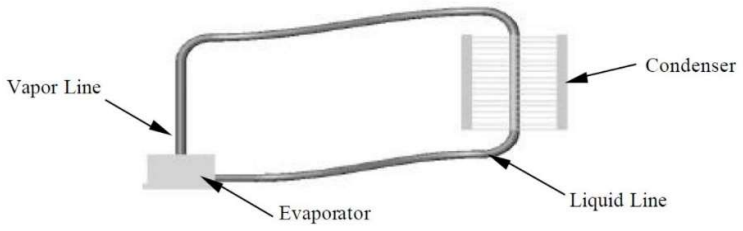

Figure 2. 20: Conceptual Design of the Loop Thermosyphon.

2.5.5.2. Heat exchangers.

Several studies have investigated the PV cells' numerically and experimentally performance. They were using active cooling water with a heat exchanger's aid. Using the water-cooling technique, Hussien et al. implemented an experimental investigation to improve the photovoltaic/thermal system's electrical efficiency [83]. The cooling mechanism consisted of a heat exchanger and seven water pipes attached to the PV panel's back. The PV panel's electrical efficiency was increased in the case of 0.3 L/s water flow rate compared to the other water flow rate cases, as shown in Fig. 12. Bahaidarah. compared the PV panel's performance with rectangular heat exchanger cooling (RHX) attached to the PV panel's back without cooling [84]. The maximum cell efficiency for the rectangular heat exchanger cooling was 13.07%, while for uncooled PV cells was 7.82%, as shown in Fig. 13. Bahaidarah et al. studied experimentally and numerically. The performance of a hybrid PV water-cooled system [85]. A heat exchanger was connected to the rear of the PV cells to enhance the PV panel's performance for the climate of Dhahran, Saudi Arabia. The hybrid PV-water cooled system consisted of a 230Watt monocrystalline type. A cooling panel (heat exchanger) is connected to the rear of the PV module, and an insulated tank to store the cooling water. The water-cooled PV panel's operating temperature was remarkably reduced to approximately 20%, as shown in Fig. 2.22. The increase in electrical efficiency was around 9%. Also, the water-cooled PV system's energy collection was almost four times more than the PV-only system.

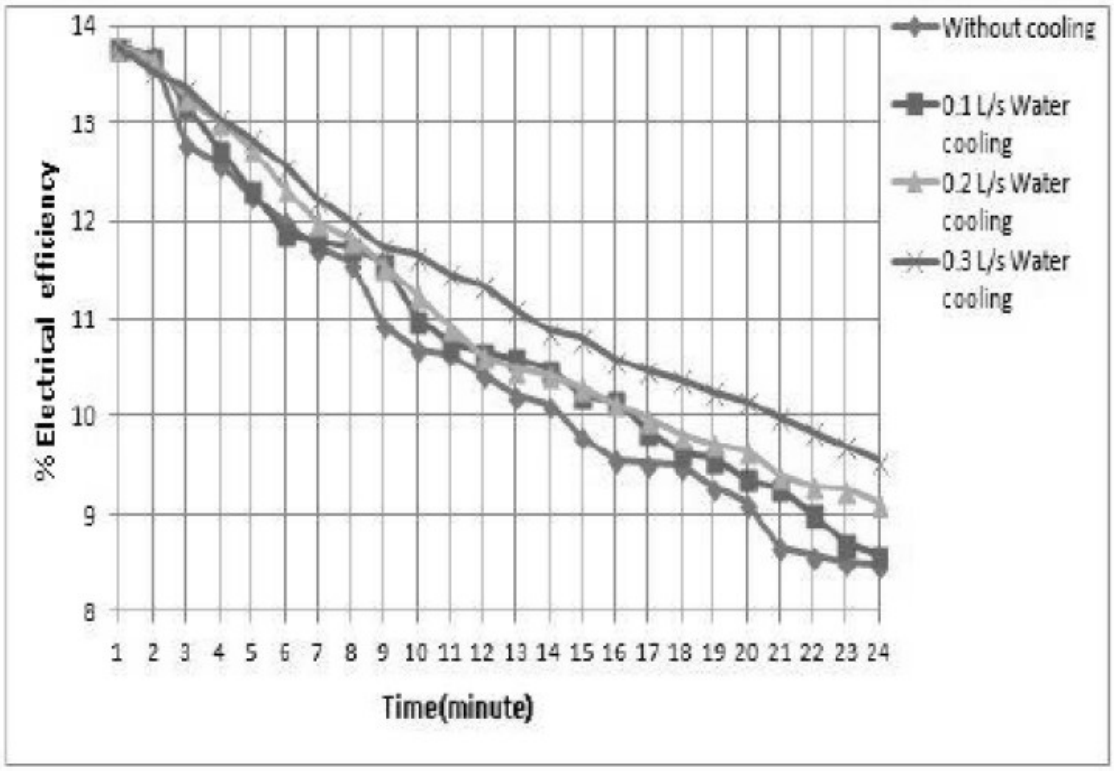

Figure 2. 21: *Water mass flow rate effect on electrical efficiency of the PV panel.*

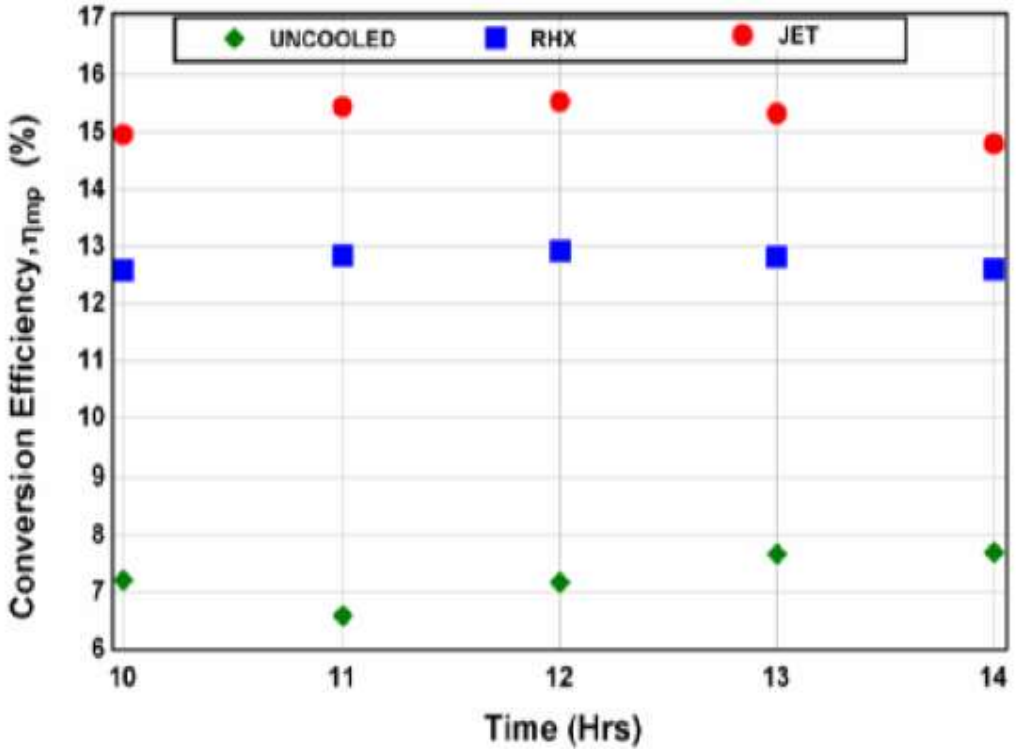

Figure 2. 22: *Efficiency conversion variation for PV with jet cooling, RHX cooling and an uncooled panel.*

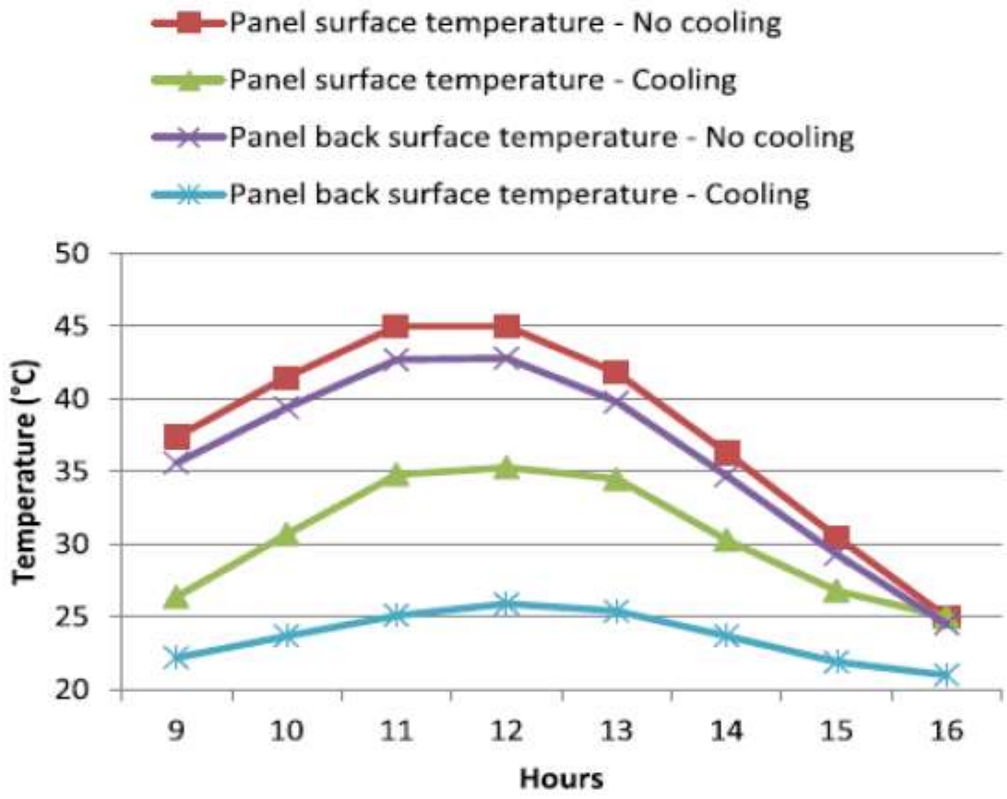

Figure 2. 23: Conversion Efficiency variation for PV with jet cooling, RHX cooling and an uncooled panel.

2.5.5.3 Air channels.

Several studies investigated the PV cells' performance with active cooling using air channels connected to the PV panel's back. Teo et al. compared the PV electrical efficiency with and without active cooling; the influence of the operating temperature on the hybrid photovoltaic/thermal solar system's efficiency [86]. The electrical efficiency decreased when the cells operating temperature increased for both cooling and non-cooling cases. Still, the electrical efficiency was higher for the cooling case, as shown in Fig. 2.21. The experiments also found a linear proportional relationship between the PV panel temperature and the irradiation, as displaced in Fig. 2.22. Tonui et al. investigated the performance of PV/T solar collectors using forced or natural air circulation to extract heat [87]. The air channel improved two ways to boost the heat transfer from the channel walls to airflow. The first one was inserting a thin flat metallic sheet in the middle of the channel (TMS system). The second one is connected to rectangular fins at the rear of the channel (FIN system), as shown in Fig. 5. This achievement modified PVT/Air systems would considerably enhance the performance of larger applications of PV systems. Finally, Ameri et al. investigated the performance of photovoltaic/thermal air collectors experimentally [88].

The panels were installed on the air channel and the top of a thin metal (aluminium) sheet (TMS). The study indicated that the system's electrical efficiency is directly associated with solar radiation concentration, PV cells temperature, and fans' power rate. Therefore, the electrical efficiency in the case of forced convection fluctuated with several fans; however, there was an optimum number of fans for high electrical efficiency. The cross-sectional view of PVT/AIR collector models.

2.5.5.4 Heat spreading.

2.5.5.4.1 Cooling fins.

Several studies have investigated the cells' performance. Numerically and experimentally using different cooling fin types and profiles. Chandrasekar et al. used aluminium fins merged with the cotton wick as a passive cooling system to maintain the PV panel's temperature [89]. The cooling system consists of three aluminium fins (630 × 100 × 60 mm) with a cotton wick attached to the underside of the crystalline silicon PV cells, shown in Fig. 2.23.

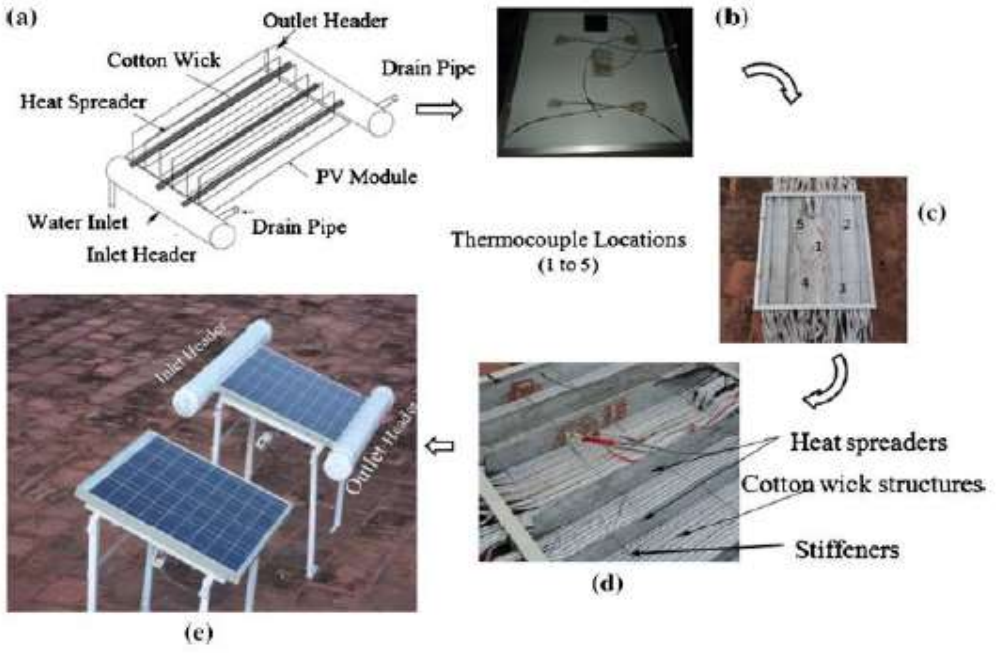

Figure 2. 24: Photographic view of the experimental PV module with stages of fabrication. (a) Desired rear side of PV module (b) location of thermocouples (c) fins in conjunction with wick structures (d) details of the stiffeners, and (e) final fabricated experimental setup with headers.

Figure 2.24. Photographic view of the experimental PV module in fabrication stages. (a) Preferred underside of PV module (b) thermocouple's location (c) fins in conjunction with wick structures (d) details of the stiffeners, and (e) final fabricated experimental setup with headers. The results identified that the PV panel's maximum temperature decreased by 12% using the cooling system, and the output power was increased by 14%. Nehari et al. numerically investigated the fins' proper length to identify the PV panel output power improvement during the passive cooling phase change material (PCM) [90]. The fins have remarkably decreased the temperature of the PV cells compared to the case without fins.

The 25, 30, and 35 mm fins length provided a preferable PV cell cooling. Got more et al. studied the performance enhancement of PV cells experimentally by using fins cooling under natural convection [91]. Two 37 W PV panels were used in the test, and nine aluminium fins were attached to the back of one panel. The experimental results indicated that the PV panel's cell temperature with fins cooling was decreased by 4.2% compared with the panel without fins. In addition, the average output power was enhanced by 5.5% in the case of the PV panel with fin, shown below in Figs. 2.24–2.25.

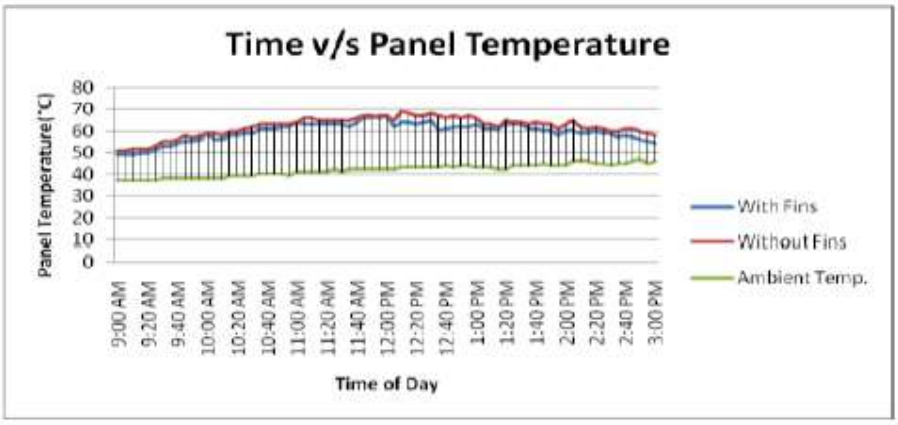

Figure 2. 25: Comparison of PV panel temperatures with & without fin cooling.

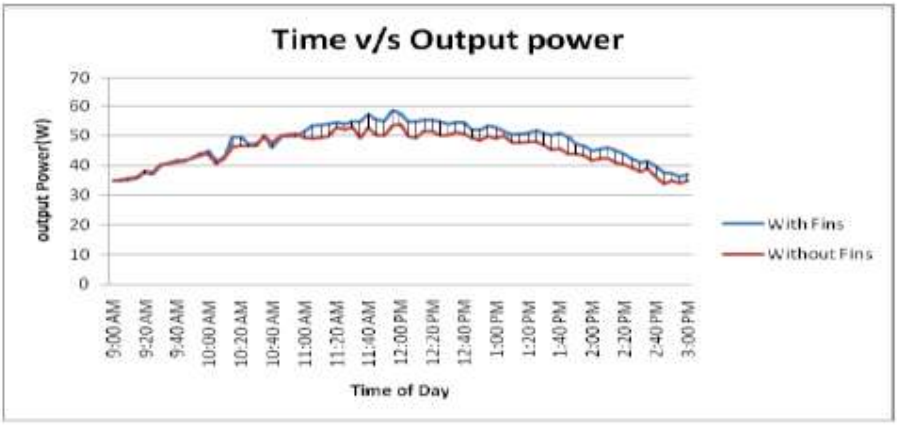

Figure 2. 26: Comparison of output power with & without fin cooling.

2.7 Knowledge gap.

Following the extensive literature review, the knowledge gap and the motivation to carry out the thesis.

- A detailed literature review has been carried out in this work
- An analysis of the photovoltaic performance is unknown for the Kuwait climatic conditions
- Methodologies for analysis of soiling performance and analysis of soiling characteristics is not evident for Kuwait climatic conditions.
- The dependencies of solar technologies for its performance considering the soiling is not clearly reported.

2.8 Research question.

Research questions have been developed based on the thesis's comprehensive literature review.

- How the different photovoltaic technologies are performed inn different climatic conditions.
- What impact does the photovoltaic performance have considering the soiling losses of the solar modules.
- How to analyse different soiling characteristics for the improvement of efficiency and photovoltaic performance of the solar energy.

2.9 Research aims and objectives.

The research aims to develop an efficient,

- Review of different photovoltaic system for analysing its performance in different conditions.
- Methodology for developing techniques of understanding performance of photovoltaic systems.
- Developing and understanding effect of photovoltaic system by analysing the effect of soiling losses for different conditions.

2.10 Conclusions.

The present article highlighted different cooling techniques for small domestic photovoltaic panels. The PV cell temperature decreases by about 12° C using a heat sink with air cooling. However, the system's electrical efficiency in air cooling does not always increase with increasing the air's mass flow rate. Still, there is an optimum mass flow rate value.

Water spray cooling considerably affects the PV cell's performance; the system's performance enhances remarkably even for the water spray's low flow rate. In addition, water cooling significantly reduces the PV cell's operating temperature and improves the PV panel's electrical performance. A cooling system with fins reduces the PV panel's temperature and enhances its electrical efficiency.

Chapter 3: Correlation of soiling, optical losses on PV performance and Dust effects on PV Plants.

This chapter summarises the significant deteriorating dust effects on PV plants in the Middle East; Kuwait reports the most widely accepted cleaning of the most employed components and materials. Moreover, it reviews the state-of-the-art cleaning systems used to maintain photovoltaic systems to achieve optimum performance. Particular attention is committed to the latest cleaning developments, enhanced output power, lower costs and material usage. A system containing three 5cm x 5cm low iron glass coupons were exposed in Kuwait City for three months (February to April) during the spring at three angles (Horizontal, Tilt-45°, Vertical) to study the effect of soiling on PV performance through optical losses.

3.1 Introduction.

In the recently completed COP26 in Glasgow, about 200 nations agreed to accelerate actions of reducing CO_2 emissions and meet up 2025 target in 2022. Kuwait is rapidly deploying resources to increase clean energy contribution to the electricity supply. To achieve the target through multi-billion pounds investment in solar energy technology to develop a 5GW asset. However, the technology is facing a severe challenge (PV soiling) that has devastatingly influenced its performance. A 10 MW pilot project comprising 5 MW polycrystalline and 5 MW is facing serious soiling challenges.

PV soiling reduces the yield of the technology depending on several factors such as site, particulate matter, climatic conditions, and angular positioning. The country experience extreme dust activities with varying levels of aerosol deposition and entrainments from a storm, haze, rising, and suspended dust leading to about 26 severe dust storms in 137 days/year, which drop visibility about 150 m and sometimes to as low as 1.8 m. PV soiling is forecasted to cause 4-7 billion euros revenue losses by 2023.

Several studies have already been conducted on the performance of the popular solar installation in Kuwait (Al-Shegaya); mere attention has been given to the impact of soiling on the asset. However, considering the above highlights, a huge investment such as Al-Shegaya in Kuwait requires continuous research and monitoring to sustain its performance. Therefore,

this study investigated the effect of soiling on PV performance through optical losses and relates it to the asset's economic failures.

Moreover, module cleaning is a simple but essential task. It can produce significant and immediate benefits in terms of energy yield. The soiling effect refers to particulate contaminations of the optical surface. It has been identified to have a considerable deterioration impact on the energy yield. Due to the incident light's high absorption and scattering losses, these power losses vary according to world location. As the dust accumulation differs caused by dust accumulation on solar collector surfaces [1].

Dust usually applies to microscopic sold particles with a diameter of less than 500 u.m; it occurs in the atmosphere from various sources. Dust is a thin layer covering the PV module's surface. The typical dust particles are less than 10 μm in diameter, depending on the location and the local environment. Many sources produce dust from pollution by wind, volcanic eruptions, and vehicular movements, among many others. The accumulated dust over time intensifies the soiling effect. The volume of accumulated dust on the surface of the PV module affects the overall energy produced from the PV module on a daily, monthly, seasonal and annual basis [2]. Nathar, Gupta and Said stated that the performance might decrease by up to 20% every month by layer upon layer of dust on uncleaned cell surfaces [3,4]. Experiments by Goossens and Van Kerschaever indicated that high wind speeds promote dust accumulation on surfaces [5].

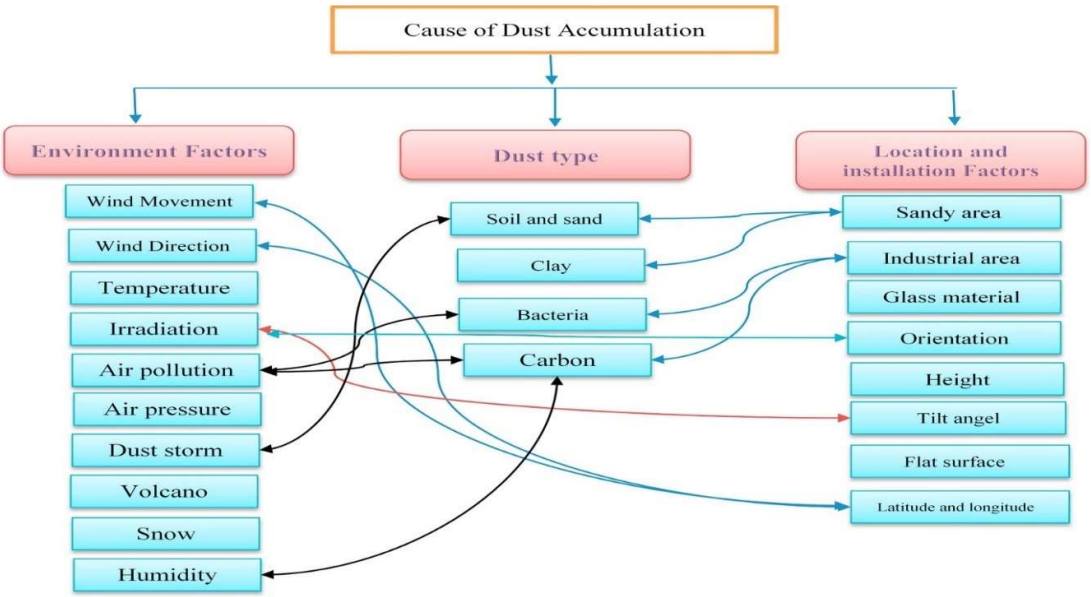

Figure 3. 1: Factors were producing dust accumulating on the surface of PV modules[a].

Zaki Ahmad et al. in 2014, researched the effects of contaminants related to physiognomies of dust on solar arrays [6]. In further research, fifteen types of dust physiognomies were acknowledged: ash, calcium carbonate, carbon limestone, cement, mud, red soil, silica, sand, sand clay, soil, and coarser mode airborne dust and harmattan dust. Six physiognomies, ash, calcium, limestone, soil, sand, and silica, significantly affected PV. They also found that the material's impact on PV characteristics was restricted as most studies considered artificial dust rather than natural dust accumulation. The findings used different physiognomies and other PV technologies further investigated in future studies.

Investigation of many studies; interestingly, the impact of the dust on performance is attributed to the immense solar potential averaging 6KWh/m²/day; however, there are many different variations. Each study has its unique parameters, testing equipment, and relevant standards; therefore, it is impractical and difficult to compare these studies' results [7]. What can be accepted if there are losses, and how do we reflect the correct parameters?

3.2 Middle Eastern critical dust studies.

Most of the research on the effect of dust on solar power has taken place in the Middle East, encouraging solar potential to incorporate an arid desert environment [8]. In regions where rainfall is restricted and the dry season lasts several months, soil accumulation on solar panels can significantly impact PV's performance. Sanaz Ghazi et al. investigated the pattern of dust distributed in different parts of the world. And found that the Middle East and North Africa have the worst dust accumulation zones in the world; Sarver et al., [9,10].
Studies introduced critical contributions to understanding these problems' performance effects and mitigation. These contributions spanned a technical history of almost seven decades of previous studies. That reported losses due to dust in many places, including dusty regions such as Saudi Arabia and Kuwait. For example, Salim et al. showed a reduction of power efficiency between 26% and 40% over six months in thermal collectors and PV panels [11]. In Kuwait, it was observed that over six days of duration, a 17 % power reduction was identified. Interestingly, the study also indicated that the dust influence increased in spring and summer by 20%.

3.2.2 Dust deposit.

The dust settlement on solar cells is explained as two primary factors influencing the dust and the local environment. The local environment consists of site-specific factors influenced by human activities, built environment characteristics, surface finishes orientation and height of installation environmental features, vegetation types and weather conditions. the property of dust type and chemical, biological and electrostatic properties size shape. Weight is as essential as accumulation/aggression. The finish of a solar cell surface is a rough surface that is likely to produce more significant dust accumulation. It is also well known that dust promotes dust, accounting for the effects it promotes dust deposition or settlement on the solar cell surface and the consequences of gravity [12-14].

A structure to understand the various factors that govern the assimilation of dust is illustrated in Figure 3.2. it is all too easy to differentiate the phenomenon of dust. However, it is extraordinarily complex and challenging to comprehend, considering all the factors that influence dust settlement practically.

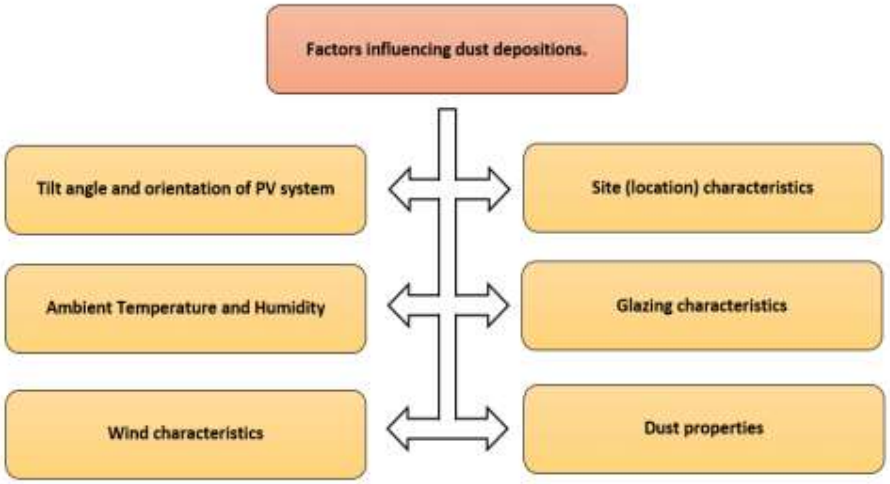

Figure 3. 2: Factors influencing dust depositions on the surface of PV panels [2].

3.2.2.1 Inclination angle.

The PV modules' tilt angle (β) strongly influences dust deposition [15-17]. For collectors installed at a fixed angle, with no solar tracking system, accumulation decreases when the inclination angle increases from horizontal (0°) position to vertical (90°)

The projected solar collector's surface area decreases with the angle of inclination β from 0° to 90°. When the unit PV is installed vertically, particle diffusion's primary sedimentation mechanism for contamination. Since the rate of gravitational pollution is proportional to d^2

where d; the equivalent diameter of the particle, one can see that the larger the particle size, the greater the velocity of precipitation. Thus, with fewer fine particles, most of the particles deposited on a horizontal surface will be necessary. In contrast, diffusion, including perturbed diffusion, is inversely proportional to d; Hence the dust deposited on a vertical surface will often be fine particles.

The angle of inclination of the fixed plate to set at $\beta = (L \pm 10)$where *L* is the latitude of the location of the solar power plant, the surface area of the collector projected up would be $\mathrm{A}\ cos\ \mathrm{B}$, where A is the area of the solar collector. Both mass concentration densities are in (g/m^2) Furthermore, the particle size distribution of sediment particles will depend on the angle β. Both gravitational stability and diffusion are considered primary sedimentation mechanisms under clean conditions.

The effect of airborne dust, containing the wind velocity component perpendicular to the surface of the collector, results in the aggregation of large particles. In these cases, there will be additional dust deposition if the particles are charged, caused by particle collision with the assistance of electrostatic adhesion forces.

In arid regions, most dust particles gain much electrostatic charge as they erode. Wind also removes the deposited dust. The dust removal rate at relatively high wind speed will be more effective at a greater inclination angle. The removal of deposited dust also depends on the particle diameter d and dust layer structure.

A thin layer of dust accumulated on a horizontal surface that is not easily removed by wind, even at a relatively high speed $(50m/s)$ Ineffective for particles with $d < 50\mu m$ when the free vapour velocity is less than $(50m/s)$ The main reason for the inefficiency of low wind removal is that the force of adhesion of the particles to the surface is proportional to d, while the force of removal is proportional to d^2 in wind force cases, therefore. When d is minor, the adhesion force is greater than the removal force [18].

Due to the forces of gravity, some larger particles can roll off the surface of the plate or move to the lower parts as the angle of inclination increases. Cleaning panels with rain and wind also depends on the angle and direction of the roofs concerning the wind direction. As the accumulation of large particles decreases with increasing the inclination angle, the relative concentration of fine particles on the inclined surfaces increases. In a study conducted in Minya, Egypt (Hegazy, 2001). It was observed that the surface densities of the collected particles of small diameters (< one μm) were higher on the panels with higher angles, while

the coarse dust particles (average diameter three μm) were deposited at Higher proportions on lower slabs [19].

3.2.2.2 Pmax.

The changes observed in temperature, humidity and solar radiation vary either parameters: short circuit current (Isc) or open-circuit voltage (Voc) or Fill Factor (FF). In turn, this decreases the maximum power point from STC characterisation.

The PV cell parameters: open-circuit voltage (Voc), short circuit current (Isc), and fill factor (FF). Vary almost linearly with the temperature variation explained by the decrease in the bandgap [20]. However, the reduction in the power of PV cells is primarily caused by the reduction in Voc and FF with increasing temperature [21].

Similarly, a high humid environment also harms PV cells' performance. The experimental results show that the short circuit current (Isc) decreases significantly with high relative humidity; the current leakage explains mee due to increased moisture content [22].

3.2.2.3 Tracking effects.

Most PV large units; are commonly installed with a fixed tilt angle. Photovoltaic systems with solar-powered trackers produce maximum output power and reduce dust build-up. Tracking can also provide plate orientation that can be used for comfortable cleaning and to hide panels at night and during dust storms. Promising results and achievements regarding dust accumulation, the variable tilt/azimuth angle in solar systems with tracking capabilities make the cleaning role of gravitational forces or natural cleaning agents more appropriate in removing sediment particles from the surfaces of collectors. At a pilot site in Hermosillo, Sonora, Mexico Cabanillas and Munguia 2011 [23].

The loss of relatively low dust accumulation after 20 days of exposure was due to the solar tracking system compared to the fixed-tilt angled methods. In another study,

Salim et al.,1988[11] four identical PV systems were exposed to the outdoor environment for one year near Riyadh, Saudi Arabia. The test results showed that the power gain from the uniaxial solar tracking system ranges between 16% and 21%, with an average of roughly 18% per month, compared to the array with a constant inclination angle of 24.6 ° (site latitude).

Moreover, the performance of the dual-axis tracking system showed an approximate 2% increase in power output compared to the single-axis tracking system. These differences are attributed to the reduced dust accumulation and increased absorption of sunlight in solar tracking systems for fixed units. However, tracking systems may show a slightly lower energy

conversion efficiency due to the higher temperature of the solar cell and its exposure to a DNI elevation because it continuously tracks the sun.

Theoretically, the solar irradiance that strikes the PV cells is the input power. In contrast, the output power can be defined as the multiplication of its developed current and induced voltage per the cell's impedance at a particular instant. The ability to convert input solar energy into electrical energy is known as the conversion efficiency of that specific solar cell. Solar cells are characterised. As monocrystalline, polycrystalline, thin-film amorphous, perovskite, organic or plastic based on a different semiconductor substrate, doping material, and manufacturing processes solar cells. The conversion efficiency varies accordingly [24]. As per a study, the efficiency of a cell can be increased significantly by doping some organic polymers as luminous-down-shifting (LDS) materials [25]. Recognising that the application of LDS technology reveals. There can be an increase of 10-20% efficiency in Cd-Te devices having layers of Cadmium sulfide (CdS) buffer layer.

In contrast, the most commonly used silicon wafer-based technologies are benefited up to 0.5 -3% [26]. Table 3.1 shows various kinds of PV technologies with their respective efficiencies. Mono and polycrystalline technology have more than 40% market share among all technologies listed due to material availability and economic constraints [27]. With recent advancements in thin-film technology. Now commercialization of solar cells has higher efficiency be with the pricing in the same range that would have cost for conventional wafer-based technology [28].

PV Technology	Efficiency (%)
Carbon nanotubes (CNT)	3-4
Amorphous silicon	5-7
Polycrystalline silicon	8-12
Dye synthesized	11.1
Monocrystalline silicon	15-18
Other thin film (CdTe, CIS, etc.)	16-20
Triple junction under concentrated Sun	up to 37.4
Hot carrier solar cell	66

Table 3.1. Different technologies are incorporating performance efficiencies [6].

3.3 Environmental conditions and PV performance.

A PV module is based on the Standard Testing conditions Case (STC). It is considered a reference point from which performance deviates concerning the environmental impacts it is exposed [29]. The atmospheric condition and the radiation profile vary from place to place, and the performance of a solar PV plant in a particular location is solely dependent on such environmental constraints. The temperature, humidity and solar radiation changes vary on either parameter. Short circuit current (Isc) or open-circuit voltage (Voc) or Fill Factor (FF), which in turn happen to decrease the maximum power point from STC characterisation. Solar radiation is the source of energy harvest action composed of energy-carrying photons, releasing electrons from PV cells through the photoelectric effect. The intensity of the solar radiation entering the PV cell determines the output current so as the output power.
The solar energy input to the PV cell is measured in Watts per meter square area, often termed Solar Irradiation. Solar irradiation varies from place to place, mainly for a particular location. It changes with the time of day; with the increase in solar irradiance, both short circuit current and open-circuit voltage parameters increase to maximum power point [30]. However, the change in short circuit current was discovered to be more prominent than that in open-circuit voltage [31, 32].

Despite the specific air mass of any particular place, the resultant solar irradiation also varies with the number of atmospheric particles: dust and water vapour content present [33]. Besides this, the orientation and tilt angle of the solar module also affects the amount of incident light. Intensity falls upon it to face the module at an optimal angle defined by the latitude of the site minus ten degrees [34]. Even though the optimum tilt angle might vary seasonally or monthly according to the location, a two-axis tracking system's feasibility must be achieved before implementation [35]. Subsequently, the temperature of the solar PV cell is one of the performance determining parameters. The ambient temperature to which the PV modules are exposed. It does not directly impact the performance metrics of the PV cell; instead, the rise in the cell operating temperature concerning laws of thermodynamics explains it. The PV cell parameters: open-circuit voltage (Voc), short circuit current (Isc), and fill factor (FF). Vary almost linearly with the temperature variation explained by the decrease in the bandgap [20]. However, the reduction in the power of PV cells is primarily caused by the decrease in Voc and FF with increasing temperature.

Similarly, a high humid environment also harms PV cells' performance. The experimental results show that the short circuit current (Isc) decreases significantly with high relative

humidity; the current leakage explains mee due to increased moisture content. Additionally, water vapour contents in high humidity cause the scattering of solar radiation. Consequently, the module's performance reduces with the reduced short circuit current [36]. According to the experimental observation made in Karachi, Pakistan (305K), with an increase of humidity by 25%, the output power seems to be reduced by 29.92% [37]. Likewise, a case study of Sohar City-Oman showed a significant reduction of 44% in the output current when RH increased from 67% to 95% [38]. Although places with high wind velocity seem to provide a better PV energy harvest action environment, They reduce relative humidity and lower cell temperature.

The above-discussed parameters: solar radiation, ambient temperature, and relative humidity, do also exhibit variations during different seasons of the year as well as due to weather perturbations like precipitation, change in wind patterns and cloudiness. Spectral gain/loss of PV cell technology (a-Si and CdTe) with stronger sensitivity at a shorter wavelength is seen with several per cent of seasonal variation [39]. In a study by Sohar-Oman, the increment of solar intensity by 101.6% was seen in the summer compared to the winter [40]. Adversely panel temperature was reduced by 97.6% due to a decrease in ambient temperature during the winter. Similarly, in a study of seasonal effect in a si-PV technology, the change of about -3% in temperature effect, 16% in spectral effect and 2.5% in irradiance effect were seen in summer compared to the winter season [41].

3.4 Cleaning Systems.

To improve the solar panels PV's overall efficiency, they require frequent cleaning, which is costly and time-consuming in terms of energy. Therefore, new and innovative cleaning methods that do not take time and do not consume much energy require investigation. Figure 3.3 illustrates several solar PV cleaning strategies: automatic, natural and self-cleaning self-remediation. These include electrostatic and mechanical self-cleaning and plating methods; these methods apply mechanical vibration, air blowing, water blowing and ultrasound techniques. In addition, the coating methods use a hydrophobic substance covering the panel's glass, which carries the dust away from the solar panels [42,43].

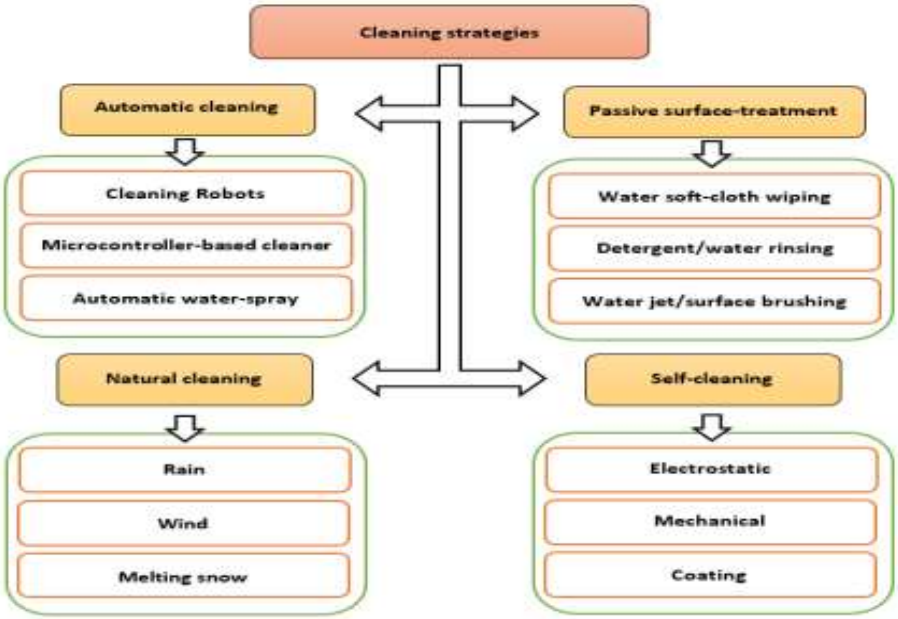

Figure 3. 3: Different cleaning strategies for removing dust from solar PV panels [2].

3.4.1 Cleaning agents

Solar panel performance also differs from other site-specific influences. Such as temperature, humidity, dust density, air mass and panel orientation: these parameters might vary drastically in different seasons. Despite these factors, various forms of precipitation, clouding, and wind also affect the yearly energy production from solar panels. Soiling is a significant influence that directly blocks solar panels and reduces energy conversion efficiency.

Dust accumulation most often leads to temperature rise resulting in reduced efficiency. Various studies have concluded that soiling harms solar cell output performance, explained mainly by the reduced solar intensity and the rise in cell temperature [44-49].

The effect of performance degradation, in turn, affects the economics of larger PV plants more prominently, thereby increasing the levelised Cost of Energy (LCoE). Different dust prevention and cleaning technologies have been evolving ever since PV plants have come into their use. Robotic cleaners, electrostatic removal, self-cleaning layer, and automated water cleaning are the current technologies. Selecting an appropriate cleaning mechanism is crucial for the specific plant size and location. Besides the cleaning mechanism, the essence of the optimal time for cleaning is a concern that needs to be dealt with since visual inspection for cleaning decisions shall not be appropriate in terms of energy economics. With data science and machine learning advancements, their application for cleaning operation decisions can be a significant leap in advancing solar PV energy systems. Such an optimised cleaning decision would undoubtedly help to reduce the LCoE.

3.4.2 Automated cleaning systems.

3.4.2.1 Current Technologies and Practices of Solar Panel Cleaning.

Megaprojects of energy generation from the Solar PV panel constructed in semi-arid or desert receives plenty of solar radiation throughout the year. Nevertheless, with higher possibility comes a more significant challenge. In these deserted places with a higher concentration of atmospheric dust with seldom rain, soil on the panel's surface is inevitable. Cleaning these panels is a must for maximum energy harvesting from solar cells. Different manual and automated technologies are available to clean the solar panel. Cleaning expenses in a solar plant account for almost half of the O&M cost.

3.4.2.2 Current Technologies.

Rainwater has been a medium for a long time to clean solar panels. Harness of energy from sunlight is more from a clean panelwhich generates more electricity. With advancements in material science and robotics, manual cleaning of solar panels is replaced with new technology like EDS, Robots, and cleaning kits to effectively clean a panel. Some of the practices and technologies are discussed in the sub-sub sections below.

3.4.3 Surface coating

3.4.3.1 Surface coatings on glass.

Developing renewable energy surface coatings technologies is essential in the current global scenario that presents environmental problems and problems incurred. Photovoltaic technologies (PV) stand out because they are renewable, safe, and environmentally friendly energy sources [50]. Increasing PV energy production, technological efforts are directed toward developing high-performance and reliable PV solar cells and mitigating external factors that can reduce the conversion efficiency of PV units. One of these factors is the effect of pollution resulting from dust accumulation on the surface of the unit, which reduces the transparency of the cover glass PV over time and thus reduces the photovoltaic output of the unit [51].

Dust is deposited on the glass surface as a thin layer of particles with a diameter of fewer than ten μm; its accumulation depends mainly on the environment's location and condition [51]. Dirt deposition on PV units has been extensively studied in the literature [52-54]. However, most of the contributions analysed the effect of dust accumulation in reducing the efficiency of PV modules or transporting glass units. At the same time, a smaller number evaluated alternatives to anti-pollution coatings by testing them in different environmental conditions outdoors [55-56].

3.4.3.2 Sol-gel method

The sol-gel method has been a relatively advanced TiO2 thin film preparation technology. Its method is titanium alkoxide (tetrabutyl titanate, isopropyl titanate) as raw material. The hydrolysis and polycondensation reaction in an organic solvent by sol, and then sol evenly coated method (pulling method, spin coating and spraying. The gel film formed on the base plate, and then after drying, heat treatment can form TiO_2 thin film. It has the advantage of low synthesis temperature. Easy control of reaction conditions, high purity, substantial uniformity, and the preparation process is simple, without special and expensive instruments. Convenient for multiple coating, it can effectively control the film thickness. However, the sol-gel method has the disadvantage of high cost, the cost of titanate precursors is expensive, and many organic solvents are needed.

Many reports about the sol-gel coating on different carriers at home and abroad in recent years, the preparation of TiO_2 thin films with unique surface chemical composition by the sol-gel method by doping other ions or compounds [19.20] has become one of the research hotspots because of the advantages of the sol-gel process, such as substantial similarity, easy doping and modification. And the sol-gel method can, by adding different particles such as template agent, surfactant, preset and conveniently control the surface of the thin-film structure. For example, by adding polystyrene (PS), polyethene glycol (PEG), polypropylene glycol (PPG), polyoxyethylene (PEO), polymethyl methacrylate (PMMA), hexadecyl trimethyl ammonium bromide (CTAB) and sodium dodecylbenzene sulfonate (DBS). In addition, the preparation of porous or high surface roughness of TiO_2 thin film is beneficial to improving the thin film super hydrophilicity [57].
Preferentially in its anatase polymorphic form, titanium oxide exhibits a photo-induced super-hydrophilicity, i.e. a surface showing a water contact angle close to 0° after UV exposure [58].

The development of the following gel substances; TiO2/SiO2 super hydrophilic sol-gel films (ST1 and ST2), TiO_2 super hydrophilic e-beam evaporation film (T) and functionalized-SiO_2 hydrophobic sol-gel films (SM). TiO^2/SiO^2 films showed a persistent super hydrophilic character with water contact angles close to 0°, while functionalized-SiO_2 presented hydrophobic properties [59]. These anti-soiling coatings composed of superhydrophobic /hydrophobic thin films have been successfully synthesised, characterised and tested in different locations.

3.4.4 Mineral coatings.

In the Megaptojects of solar panels PV, it is more expensive to use hydrophobic coatings PV to clean panels because this method consumes no energy for cleaning nor causes scratches on PV surfaces, thus conserving panels' energy production [60]. Using self-cleaning hydrophobic nanomaterials to encapsulate the surface of solar panels PV is an effective way to increase the overall efficiency of the panels over a long lifespan, as shown in Figure 3.4.

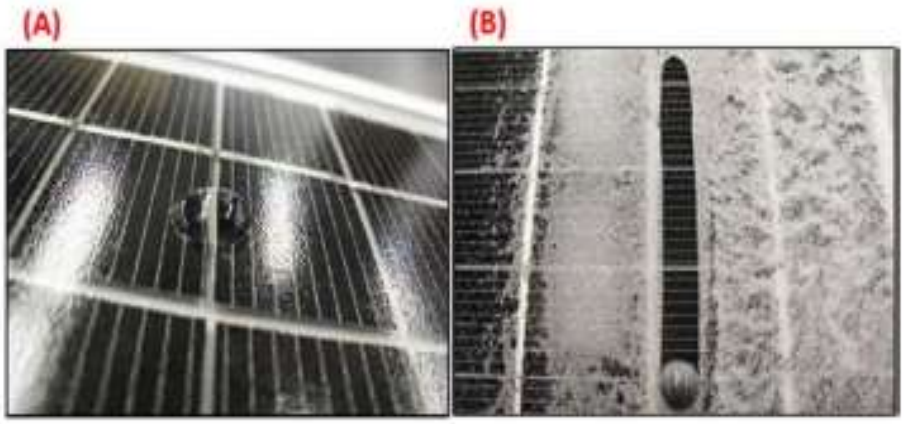

Figure 3. 4: Self-cleaning hydrophobic coatings; (A) A solar panel coated with a PV nanomaterial; and (B) Water rolls off the surface like a ball rolling down a slide [61],[62].

The main working principle of using hydrophobic coating nanomaterials is that the layer forms a barrier so that water accumulates in a spherical shape. As a result, water rolls off the panel surface when solar panels are installed at a tilted angle, a sphere rolling down, as depicted in Figure 3.4 [61,62].

3.4.5 Future proposed cleaning methods

3.4.5.1 Piezoelectric system.

Piezoelectric actuators are utilised in various optical adjustments, biomedical manipulation, space explorations and other areas; due to higher torque to volume ratio, flexible structure, and high positioning precision, the piezoelectric system is employed in the cleaning of solar panels. The acoustic piezoelectric system with water as a cleaning agent spreads 0.1 to 1 mm depth of water around the surface of the solar panel cleans during the rarefaction cycle of the compression waves. A vacuum created in liquid during the rarefaction is called an ultrasonic cavity. This cavity cleans the panel by sucking the dust on the solar panel surface.

For the air medium, the mechanism is similar to the change in the cleaning medium only. Linear Piezoelectric actuator-based solar PV panel cleaning system. As a proper pressure force between the wiper and solar panel is adjusted. The actuator can drive the wiper to effectively clean and wipe a dust layer by vibrating the dust away from the solar panel's surface [63, 64]. Figure 3.5 shows a linear piezoelectric system.

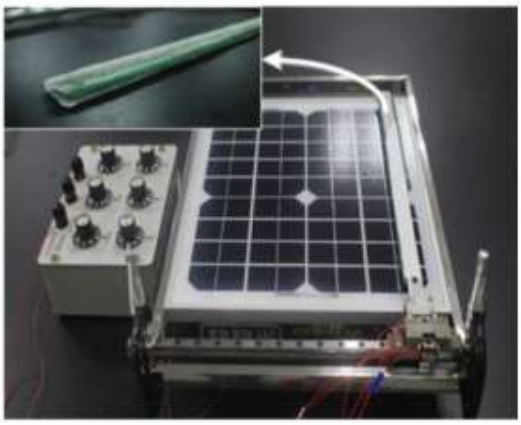

Figure 3. 5: linear piezoelectric system [63].

3.4.6 Electric curtain system.

Places with dry dust are addressed with a phenomenon explained by applying an appropriate electric field to the dust particles on the module surface. This phenomenon of charging dust particles is an electrostatic concept. Where charged dust particles are bound to form a standing wave-type electric curtain at any point. An electric field with amplitude and direction oscillating at the imposed frequency exists. Furthermore, the frequency of oscillation is fixed, that the dust particle moves along the line of an electric field to one of the modules' edges, thereby cleaning the surface. Uncharged particles that fail to form the electric curtain are soon charged through either polarization or electrostatic induction and removed from the module [65].

An ElectroDynamic Screen (EDS) is one of a kind that uses the same principle of standing wave-type electric current. However, a high voltage three-phase electric source is used to form a travelling wave with intense translational energy [66]. The application of different phases to the substrates of a module and respective lines of force is shown in Figure 3.6.

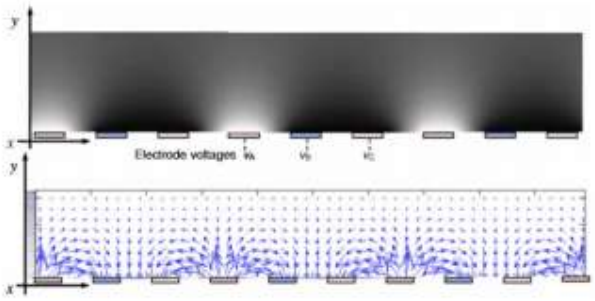

Figure 3. 6: Electrodynamic screen [64].

This kind of cleaning mechanism requires a dry module surface. To avoid any vapour-based bonding of dust particles with the module: recommended to use such systems where humidity is meagre and almost negligible precipitation. A study on concentrated solar power plants reported that its applicability is limited to locations with less than 60% relative humidity. Such a system is expected to have 90% efficiency in regaining the reflectance lost due to soiling [67]. The dry condition of MARS is suitable for applying this technology [68].

3.4.7 Self-cleaning mechanism.

A translucent self-cleaning nano-film can be coated to the surface of a solar panel to avoid dust deposition in the panel. The self-cleaning nano-film is made from super hydrophilicity or superhydrophobic material. In the super-hydrophilicity method, the rainwater gets scattered throughout the solar module and cleans the dust. Thus, this method is not popular, and various research is going on. In superhydrophobic material, the water droplets quickly fall off, carrying dust particles like in the leaf of a lotus plant. Multiple studies are going on to realise superhydrophobic surfaces by forming microstructures or nanostructures. However, using these materials on the solar panel surface would be questionable as solar farms are situated where seldom rains are present. Thus, these materials need to be studied in depth [69,70].

3.4.8 Robotic system.

The robotic system is the most challenging technology, more than all other technologies discussed above since it has a wide range of applicability in small and large PV systems. The robotic system consists of actuators, drives, gears having some movement above the module surfaces, and a virtual operator that cleans the module even better than manual hand cleaning. With advancements in 3D printing, nanotechnology is aiding in making very complex robots which can operate as efficiently as a human would do the work. The recent development in automation makes the cleaning job even more manageable and straightforward, reducing the complexity between the robot and the operator. Integration of

automation in the robotic system has allowed a robot to self-decide and act when needed lowering the human-machine interfacing time and humanitarian aid for the entire cleaning operation. Robotic cleaners can see microcontrollers and programmable logic controllers to ease the solar panel cleaning process [71, 72]. The fuzzy logic controlled algorithm discussed deals with the fuzzification of the solar irradiance value and the output current value such that defuzzification would result in decision-making to clean or not [73,74]. The rising Internet of Things (IoT) in the technological field can substantially turn in the solar panel cleaning process. Distant monitoring of the PV system is achieved by employing required sensors to feed the real-time data to the operator through the cloud.
Such an IoT-enabled system reduces inspection costs, and cleaner teams can go with their robots only at the time of need. With the application of IoT, a reduction in site visits will be possible. Human intervention in the cleaning process shall only be limited to complete supervision, achieved by employing decision-making automation with pre-installed robots mounted over the solar array/s.

This idea was demonstrated in prototyping a system named after Smart Solar Photovoltaic Panel Cleaning System, as depicted in Figure 3.3 [75]. This system consists of two central units: Robotic and Autonomous units, functioning cleaning and decision-making. The autonomous team took solar radiation as an input parameter and generated power as an output parameter and compared it with the calibrated model to decide whether to perform a cleaning action. Consequently, robotic units act as the slave unit and perform the cleaning as commanded by the autonomous team. A person supervises the whole system. Only the cleaning system and the supervisor access internet connectivity in any world location.

A practical experiment to study dust effects and optical losses have been examined in this work.

3.5 Methodology.

3.5.1 Experiment.

Three 5cm x 5cm low iron glass coupons were exposed. In Kuwait city with proximity to Shegaya solar farm (29°12'19", 047°03'06") for three months (February to April) during the spring, which is considered to be the period with the most significant dust storm activity in the region [76-80]. The coupons were positioned at three angles (Horizontal, Tilt-45°, and Vertical) and after the expiration of the exposure period. Coupons were returned to the solar laboratory at the University Exeter in the United Kingdom for characterisation to obtain optical losses information and deposited material. The optical losses data were collected to analyse the PV soiling of the Al-Shegaya solar farm installation.

3.6 Spectral Characterisation.

The exposed coupons were examined using a spectrophotometer (Perkin Elmer Lambda 1050 UV/VIS/NIR). An unexposed clean coupon was used as a benchmark. To measure transmittance change (Δτ) from 250nm to 1250 nm, the spectral wavelength to which all installed PV systems in Al Shegaya solar farm respond. The relative transmittance change in percentage was calculated using Eq. 3.1, where the τ_x is transmittance data of coupon relative to its angular positioning and $\tau_{Unexposed}$ Represents the baseline coupon, which is clean and was not exposed.

$$\textbf{Relative } \boldsymbol{\Delta\tau_x}(\%) = \frac{(\boldsymbol{\tau_{Unexposed} - \tau_x})}{\boldsymbol{\tau_{Unexposed}}}(\mathbf{100}) \qquad \textbf{(3.1)}$$

The optical losses based on the optimum angle were calculated using the linear interpolation technique provided in Eq. 3.2, where $\Delta_{\tau_{(Optimum)}}$ is the calculated change of transmittance of a coupon at an optimum angle, $\beta_{(31)}$ is the optimum tilt angle of Al Shegaya based on GSA, $\beta_{(45)}$ is the angular position of 45° that a coupon was exposed, $\beta_{(0)}$ is the horizontal angle at which a coupon is positioned, $\Delta_{\tau_{(0)}}$ is the optical loss for horizontally positioned coupons, and $\Delta_{\tau_{(45)}}$ Is the optical loss recorded on the coupon positioned 45° angle [81].

$$\Delta_{\tau_{(Optimum)}} = \frac{(\beta_{(31)} - \beta_{(45)})\,(\Delta_{\tau_{(0)}} - \Delta_{\tau_{(45)}})}{(\beta_{(0)} - \beta_{(45)})} + \Delta_{\tau_{(45)}} \qquad \textbf{(3.2)}$$

3.7 Particles characterization.

The morphological characterisation was conducted using the electronic scanning microscope (SEM Quantal FEG 650). Before scanning, a soiled coupon was carbon coated with an Emi-Tech K950 machine. Two images (backscattered electron and secondary electrons) were obtained, and the latter was used for morphological analysis. The element study of accumulated particles was conducted with an Energy Dispersive X-ray (EDX) attached to the SEM. Backscattered images from the SEM were adopted to determine the accrued elements of the coupons.

X-ray powder diffraction (XRD - Siemens D5000 diffractometer) was employed for mineralogy characterisation. Due to the number of samples, smear sample preparation was conducted to transfer the particles from the coupon to the diffractometer grey plastic holder. The transparency of minerals recorded was further determined using online databases such as mindat.com and minerals.net.

3.8 PV yield.

Power losses using exposed coupons were calculated using two approaches. The first uses an experimental approach where coupons were placed on top of a high-efficiency solar cell under a solar simulator (Wacom WXS 2105-20 AM1.5G) to measure yield and estimate reductions by calculating the percentage difference between the soiled exposed coupon and a clean unexposed one using Eq. 3.3, where PV_{SL} is the soiling losses based on the coupon placed on top of the cell, PV_{Out} is the yield of the cell without any coupon on top, and PV_{Out+SL} is the cell yield with soiled coupon relative to the type of coupon.

$$\mathbf{PV_{SL}}\ (\%) = \frac{|(\boldsymbol{PV_{Out}} - \boldsymbol{PV_{Out+SL}}|}{\left[\frac{\boldsymbol{PV_{Out}} + \boldsymbol{PV_{Out+SL}}}{\mathbf{2}}\right]} \times (\mathbf{100}) \quad \textbf{(3.3)}$$

A correlation was conducted using Optical losses data from this study, which was used as the soiling losses value and annual PV yield data of Al Shegaya solar energy park from Global solar atlas and PVSyst. Soiling losses were calculated using Eq. 3.3 and compared with the estimated losses presented by GSA.

3.9 Economic analysis.

The economic analysis of the losses was conducted to determine the simple payback time of the installation. And compared it with the assumed payback time estimated by both GSA and TSK. Considering the losses determined from this study. The simple payback time was calculated using Eq. 3.4, where the IC is the initial installation cost, AEP is the annual energy production, and $x.$ is the price of energy displaced.

$$\boldsymbol{SP} = \frac{\boldsymbol{IC}}{\boldsymbol{AEP} \times \boldsymbol{x./kWh}} \qquad \textbf{(3.4)}$$

3.10 Results.

The optical results provided the anticipated data pattern where the coupon exposed on the horizontal plane shows higher accumulation and reduces when tilted towards the vertical plane. The most extraordinary optical loss record is 52% when the coupon is exposed horizontally, as shown in Figure 3.7. The most negligible loss is recorded from the coupon on the vertical with about a 25% reduction. The calculated optical loss for the optimum tilt angle is 46.4% based on the annual optimum angle of 31° for the region.

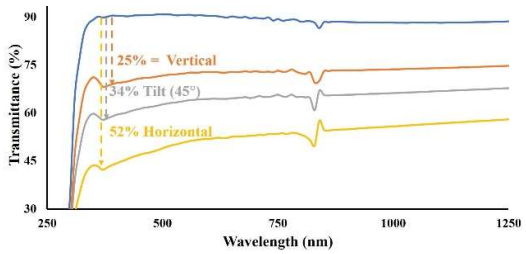

Figure 3. 7: Optical losses variation highlight losses relative to angular positioning.

The size of particles and the space they occupied on the coupon represent the optical losses recorded. The accumulation appears to be having a significant amount of PM10 and PM2.5 particles. Although the accumulation pattern was observed to be non-uniform, having larger particles in layers could reduce the photon influx. Refer to Figure 3.8 for an SEM imaging of accumulated dust. The majority of the particles have aggregated structures that could affect light transmittance.

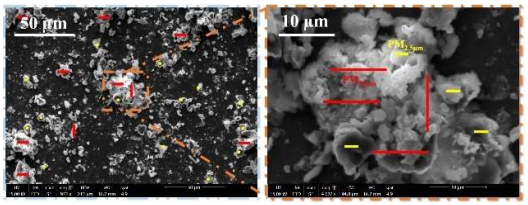

Figure 3. 8: SEM imaging illustration particles sizes, shapes and accumulation pattern.

The backscattered image was further characterized using the EDX for elementology analysis. Finding shows elements belonging to varying groups with some metalloids (Si), transitional metals (Mo and Fe), alkaline metals (Na, K, and Al), alkaline earth metals (Mg and Ca), and halogens which are known as reactive non-metals (Cl and Br). Figure 3.9 shows the elements recorded from the EDX analysis. The discussion section of this report provides a detailed explanation of the various aspects.

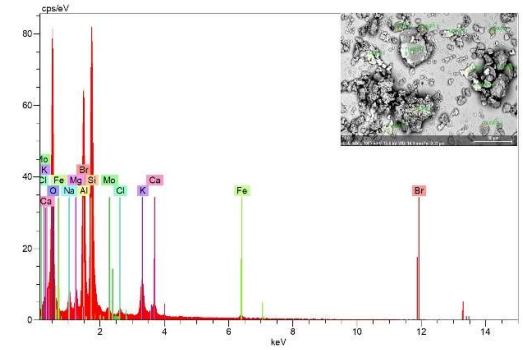

Figure 3. 9: EDX graphs illustrating elements recorded on the exposed coupon.

The recorded minerals, through XRD analysis, show particles having diaphaneity to be transparent to translucent (Actinolite, Calcite, Clinochlore, Dolomite, Gypsum, Lizardite and Muscovite), transparent to opaque (Quartz), and opaque (Kaolinite) properties. All these minerals could affect the transmittance at varying capacities, where some will complete attenuate an influx of photons. The diffractometer chart is provided in Figure 3.10.

Yield losses determine using a simulator show a similar trend of losses considering the optical losses. The most significant PV power yield loss was recorded horizontally on the coupon with about 53% reduction, followed by 38%. In comparison, the lowest was 25% from the vertical plane. The PV performance reduction due to soiling was closely similar to optical losses.

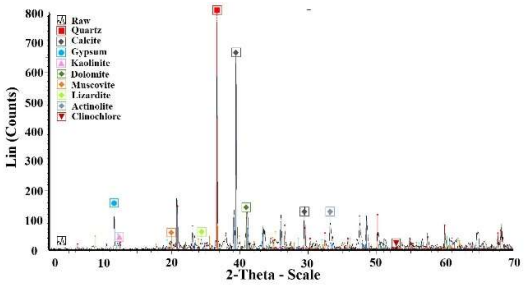

Figure 3. 10: Diffractometer illustrating peaks of minerals accumulated on the exposed coupon.

Figure 3.11 illustrates the performance parameter where short circuit currents (ISC) are highlighted to demonstrate the impact of soiling losses on PV performance. The loss from the optimum tilt angle of the region was calculated, and findings show that about 43% soiling loss could occur when a coupon is positioned on the plane (31]. In addition, significant variation was observed in the short circuit current, which reduced the power out.

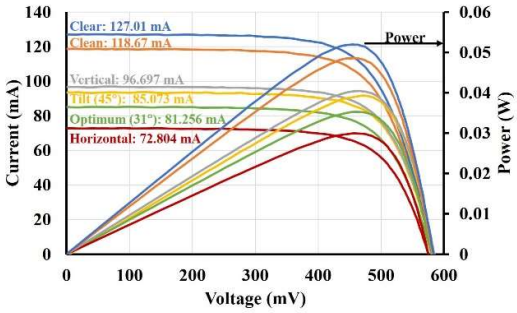

Figure 3. 11: IV Curves illustrating PV yield variation.

Al Shegaya energy park PV yield losses correlated with optical losses to determine possible soiling losses. Employing 46% as the calculated soiling losses, a reduction from 17,760,000 to 9,519,360 kWh/10MWp was estimated. This reduction is further translated into economic losses, where a simple payback time analysis was calculated. The findings show that it would take about 45 years before the installation will attain a return on investment. This simple payback calculation ignored operations and maintenance (OM), regaining performance due to other seasonal effects and factors that could reduce the impact of soiling.

3.11 Discussion.

The results exhibit comparable findings where the optical losses are in relatively good agreement with PV yield losses and could be related to an asset yield loss.
Morphology, elementology and mineralogy studies highlight that PV yield losses drove optical losses through the attenuation, scattering, and reflection of influx photons. It was observed that most of the accumulated particles are of larger grain sizes, aggregated in conglomerate clusters, and non-uniform deposition. Some elements recorded are highly reactive and conductive metals, while others (halogens) are reflective. Most of the minerals recorded were around translucent, some opaque. These transparency levels could disrupt light transmittance, mainly when accumulated in aggregated patterns observed from the SEM imaging. Reduction of light transmittance means PV performance reduction.

Optical losses and PV yield results highlighted alarming losses, which render the technology unprofitable. However, an installed PV system exposed under normal conditions will last 25 years. The results show that simple payback using the GSA atlas soiling level could reach 24 years and 45 years when adopting the optical data from this study. This indicates that the investment is not viable and would return the investment. However, the soiling losses are not

expected to remain at this level since seasonality tends to cause variation. In addition, the site was reported by AL-Rasheedi et al. to adopt mitigation techniques using a semi-automated system attached to a tractor. However, the cleaning is only conducted five times a year, which is assumed inadequate. Other methods were reported by Chanchangi et al. to have the capacity to mitigate these losses with different performance efficiency, and some are natural (rain and wind) [82]. However, cementation and calcification are extremely resistive simple detachment forces. Therefore, it is recommended to investigate the adhesion forces and the factors influencing them in the region.

The results presented demonstrated the adequacy and efficacity of the comprehensive approach implemented considering the data limitation. However, the finding shows discrepancies from the expected asset performance. Even though several factors such as the effect of seasonality, climatic conditions, operational maintenance cost, and variation of accumulation concerning time were ignored. The full potential of this approach could be achieved if all the above-listed factors are considered; as such, this report must interpret these limitations.

3.12 Conclusions.

Module cleaning is a simple but essential task. It can produce significant and immediate benefits in terms of energy yield. The frequency of module cleaning will be determined by local site conditions and the time of year. The level of module soiling is site-specific; therefore, the interval between cleans will vary considerably between sites. The frequency of cleaning solar cell modules is governed by the site's location and the surrounding ground material. These sites can be dusty and arid sites resulting in increased soiling) Moreover, the local rainfall patterns in dry areas will result in more soiling [83].

This review discusses various parameters of the solar photovoltaic panel and different cleaning systems developed and used up to the present day. The critical points of the topics addressed are:

1. The rise in cell temperature and soiling of the module are the two major issues of the PV systems.
2. Active and passive cooling techniques can deal with places with extensive temperature rise. In contrast, soiling issues rectify using by cleaning the modules' surfaces.
3. Cleaning can be achieved by natural rainfall, manual hand cleaning, water jet/sprinklers, and robots.

4. Standing wave-type electric curtain system can be applied in areas with water-scarce, like solar panels on Mars.
5. To obtain optimum cleaning instant for a particular case scenario, the use of machine learning application to develop a decision-making model with the help of parameters affecting the performance of PV plant: solar irradiance, output power, temperature, humidity, air mass, dust density, seasonal and weather patterns. The complexity and accuracy of the system are defined mainly by power plant size, vulnerability to soiling, seasonal patterns and weather perturbations.
6. For distant solar farms with no rainfall and prone to frequent sand/dust deposition, the Internet of things (IoT) based cleaning system with a pre-installed robot in the solar array shall avoid the multiple site visit costs [84].

Therefore, for large solar farms, solar panel cleaning shall only be carried out if the reduced efficiency is below the critical level. The investor must ensure that the investment made for the cleaning purpose has a modest rate of return. Further research and development on a decision-making model considering cost worth evaluation are essential for the evolving solar panel cleaning technology.

Moreover, a practical approach to dust effect and optical transmittance losses at varying angular positions in Kuwait was investigated and further employed to determine PV yield performance reduction. Findings show alarming declines where about 52% transmittance losses were recorded on a horizontally exposed coupon. The laboratory PV performance experiment results highlighted a similar trend (53% power reduction for the same coupon). A simple economic analysis of the pilot project in the region shows that the asset requires considerable continuous maintenance to sustain its performance; otherwise, a return on investment would not be achieved.

Chapter 4: Relative humidity effects on PV Plants.

4.1 Introduction.

Let us talk about the energy we receive from the sun. The earth receives approximately 1,413 W/m^2, and actual consumption is around 1,050 W/m^2 as recorded in 1972 by the Forest Service Pacific Northwest Forest and Range Experiment Station, USDA, Portland, Oregon. Of the 100% of the solar energy produced, approximately 30% is reflected or absorbed by clouds, oceans, and landmasses in cities where the humidity is more significant than other resources. For example, in areas such as Mumbai, Malaga, Hamburg and Los Angeles, the average humidity ranges from (40 to 78%), resulting in a small layer of water vapour in the front solar cell directly facing the sun. As a result, solar energy hitting the solar cell experiences energy absorption/reflection loss. There were approximate losses of about 15-30% of energy plus a further 30% reflection. After the empirical analysis, one of the effects discovered was the humidity, which reduces solar energy approximately to 55-60% from just 70% of the energy used and 30% of energy loss. As per the statistical data, the top of the earth's atmosphere's sunlight intensity is about 30% denser than the earth. Therefore, in the solar panels we currently use, 70% of the energy is produced from the sun, and our solar panels achieve 30% to meet our energy requirements.

The earth's crust consists mainly of water 70%. The energy that strikes the world indirectly hits the oceans, which helps increase humidity in general. Humidity, however, poses obstacles to the power received in the upper atmosphere and affects device consumption in many aspects.

4.2 The effects of relative humidity.

The humidity on solar panels creates obstacles. The humidity creates a drastic variation in generated power, indirectly making the device work less efficiently than it would have worked without it.

In cities where the humidity level is above the average range of 30, the lower layer of water above the solar panel has lowered efficiency. According to the data: when the light consisting of energy/photon hits the water layer, which is denser, refraction appears, reducing the intensity of the light, which seems to be the root cause of the lower efficiency.

Solar cells react to the environments in which they are placed, including temperature and humidity. The thin-film technologies for photovoltaic applications include a-Si:H alloys, CdTe, Cu(In,Ga)Se2 (CIGS), poly-Si, μcSi/Poly-Si and dye/TiO2. The most advanced technologies are a-Si-alloys, CdTe and CIGS [1,2].

Cells of different materials respond differently to their operating conditions and environmental contexts. These differences can significantly impact the energy produced by other solar cells. Generally, materials with a higher bandgap are less sensitive to operating conditions. The bandgap of a semiconductor is the minimum energy required to excite an electron from a bound state into a free form where it can contribute to conduction. Compared to silicon, the reduced sensitivity of CdTe to elevated temperatures or the impact of humidity on the light available to the PV module (technically referred to as light extinction) provides CdTe thin-film modules with an advantage. Primarily when operating in hot and humid climates. The result is improved relative performance and higher comparable energy yield, defined as the total energy output from an installed solar module.

Usually, the photovoltaic solar cells are fabricated with two-layer semiconductor material under non-irradiated conditions. The concept of generating electricity through photovoltaic cells derives from solar radiation or photonic effect toward the surface of the photovoltaic cells. Piazza et al. Explain that the negatively and positively charged semiconductor treated solar grade silicon cell excites electrons flowing inside the cells through the doping process [3]. The method of electron flow from the negative (phosphorus) junction to the positive (boron) junction creates the current-producing electron-hole pair, also known as the PV effect.

Around the world, research on photovoltaic cells and processing technologies focuses on a new approach to reducing costs by reducing the number of processing steps with high consideration of overall performance and efficiency [4,5]. The light intensity factor correlates directly with the sun radiation as the primary energy source for the PV system.

Koehl et al. highlight that the water element is a vital degradation factor for PV modules. Causing hydrolysis of polymeric components and corrosion of metallic and glass features like grids and interconnectors. Wherefrom this condition, the type approval testing of the Damp-Heat test and Frost-Thaw test under IEC standards to estimate the service life of a module. Moreover, humidity using moisture weakens the reliability of PV modules. This is primarily related to the packaging process and could reflect encapsulant delamination and warping of PV cells [6].

Efficiency is the amount of light converted into a usable format of electricity. Since the efficiency depends on the value of the maximum power point of the solar cell, the maximum power point deviates due to the above effect of humidity, which indirectly reduces the efficiency of the solar cells [7].

4.2.1 Thermal losses.

Humidity is a climatic condition that affects the performance of PV systems. Kazem and Chaichan studied the effects of humidity [8]. They concluded that relative humidity has the highest impact compared to the other ambient parameters. Such as temperature and dust, Kazem And Chaichan found the inverse relation between humidity and electrical parameters. In addition, increasing the humidity during the day will result in high moisture in the PV surface, introducing mud accumulation. The resulting mud structure is intense and complicated for high wind speed to remove, resulting in partial shading to the PV [9].

4.3 Relative humidity effects on SiHi PV panel: Isc, Pmax, and Voc.

For a-Si, the goal is to reach a stable module efficiency on large areas of 10%, representing a challenging condition for competitiveness with other thin-film options. A significant problem of the amorphous silicon technology has been the degradation of the amorphous films and devices under illumination, or the so-called Staebler-Wronski effect.

The Staebler-Wronski effect is that sunlight creates light-induced metastable defects in a-Si:H was discovered very soon after the first cells were made. This light-induced degradation is called the Staebler-Wronski effect. The Staebler-Wronski effect involves an optically induced decrease in photoconductivity, dark conductivity, and restoration to the original state by annealing above 150 °C [10].

Most studies of the Staebler-Wronski effect concluded that optical exposure caused metastable states in the gap [11-14]. These metastable changes mainly increase neutral dangling bond defects' density and the dominant recombination centre. The added dangling bonds shift the dark Fermi level towards the midgap, which leads to a decrease in dark conductivity. It was also conclusively shown that recombining excess charge carriers, creates these metastable defects. In undoped hydrogenated amorphous silicon after these excess charge carriers have been generated either by illumination or by charge carrier injection. The formation of dangling bonds reduces the efficiency of the devices until the

rate of formation of the dangling bonds equals their heating rate, which increases with temperature. As a result, the stabilised efficiency is higher at higher device temperatures.

Still, the humidity factor is inversely related. For example, Xiong, Z et al. and Mekhilef, S. et al. show that power output efficiency from PV modules degrades with increased moisture content [15,16]. Due to a high percentage of surrounding humidity ingress with a very high value of efficiency drop of 63 % for mono-Si PV modules which suffers from biased damp heat tests at 85 % relative humidity condition.

4.4 Relative humidity effects on CdTe PV panel: Isc, Pmax, and Voc.

CdTe appears to be an ideal material for thin-film solar cells because its energy gap is direct and is 1.45 eV, suitable for solar energy conversion. Approximately 10-16 % efficiencies have been obtained for CdTe solar cells depending on the process used. A significant issue in the CdTe cell technology is the formation of good ohmic contacts of high stability.

Since 2010, this number has steadily increased ~15%. Since then, First Solar has contributed the most world records, including the most recent in 2019. Lab-based efficiencies demonstrate the potential of technology but are not representative of what can be achieved in a manufactured module. Scaling of cells to module areas induces additional loss mechanisms for all key metrics (current, voltage, and fill factor). The current world record efficiency for a CdTe module is 19.0% (Green et al., 2019) for a First Solar module with an area of 2.4 m^2. Also, this number has steadily increased from about 10% in 2010, with First Solar being the only contributor since 2012.

A comparison of efficiencies between CdTe and other technologies in Figure 4.1 and Table 4.1 (Fraunhofer, 2019) is shown below. Table 4.1 was adapted for this thesis, using data from multiple sources (Green et al., 2019; Geist Hardt & Topic, 2015). Note that Figure 1 only considers cells with an area above 1cm2. The highest efficiency value for a CdTe solar cell with this area is 21.0%. In contrast, the record efficiency for a smaller cell is 22.1% (both First Solar). All significant technologies contribute to utility and residential PV applications. These technologies are monocrystalline silicon, multi-crystalline silicon, CIGS and CdTe.

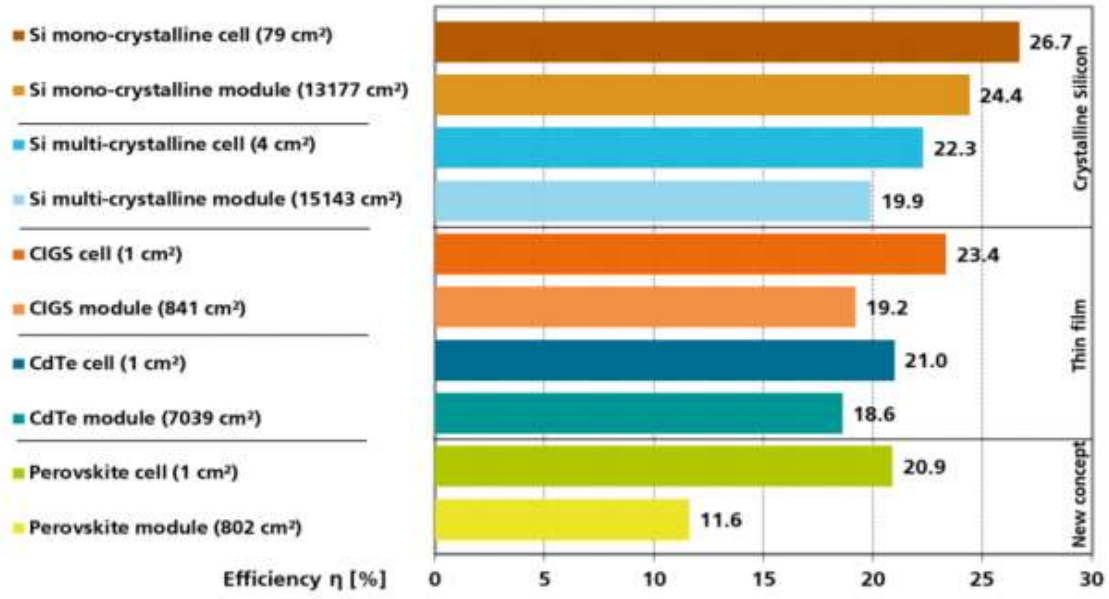

Figure 4. 1: Comparison of state-of-the-art research cell and module efficiencies for a variety of different PV technologies (Fraunhofer 2019).

Looking at some critical solar cell characteristics reveals the future potential avenues for improving CdTe efficiency. Table 4.1 shows a fraction of the potential for two metrics, open-circuit voltage (VOC) and fill factor (FF), for different technologies. CdTe solar cells have realised the least potential in FF and, more significantly, voltage. However, in Si and GaAs solar cells, more than 95% of the potential in FF has been achieved; CIGS discovered more than 91% of its potential and CdTe 88%. In VOC, CdTe has only conceded 77% of its potential, with GaAs going as high as 97% and Si and CIGS reaching 85%.

However, considering past improvements, significant advances in CdTe efficiencies for both modules and solar cells are possible.

Category	Alta GaAs -28.8%	Panasonic Hit-SI - 26.7%	Solar Frontier CIGS - 22.9%	First Solar CdTe - 22.1%
FF_{ideal} (%)	89.5	87.1	87.1	89.5
FF (%)	86.5	83.3	79.7	78.5
FF/FF_{ideal} (%)	96.6	95.6	91.5	87.7
$V_{OC,ideal}$ (V)	1.163	0.879	0.879	1.156
V_{OC} (V)	1.122	0.744	0.747	0.887
$V_{OC}/V_{OC,ideal}$ (%)	96.5	84.6	85.0	76.7

Table 4.1. Comparison of the potential for different solar cell metrics realised by other technologies (Geist Hardt & Topic, 2015).

While efficiencies are the basis for general comparison, they are insufficient to capture the complete picture of how much energy a solar cell generates under outdoor conditions. This is because most of the operational lifetime of a PV system deviates from the standard testing conditions used to determine nameplate efficiency. For example, a significant difference between CdTe and Si and CIGS is the higher bandgap of 1.54 eV (compared to around 1.1 eV for the latter two).

A higher bandgap has an overall energy yield advantage (see Figure 4.1). However, considering median values for the electricity generation potential of solar cells around the planet, there is a penalty on energy yield or harvesting efficiency.

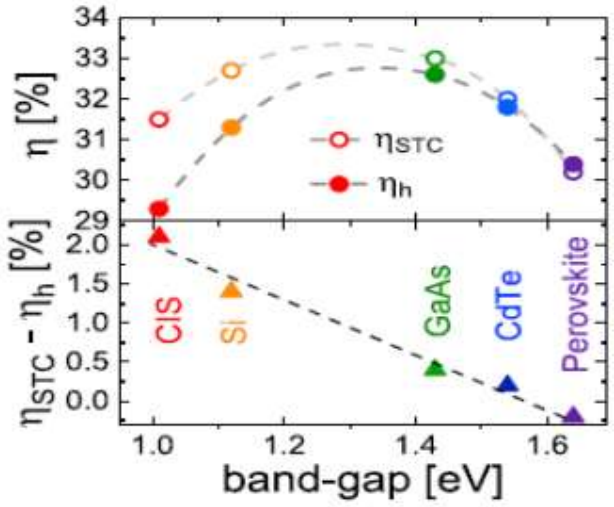

Figure 4. 2: Bandgap comparison of different PV cells.

Upper - comparison of standard testing condition efficiency ηstc and harvesting efficiency ηh for different solar cell technologies in the radiative border function of the bandgap). Lower - the difference between two efficiencies metrics is plotted, revealing a roughly linear relation between the efficiency penalty for outdoor operation and the bandgap of a solar cell. Consequently, standard testing condition efficiencies benefit cells with a smaller bandgap. In outdoor operations, performance losses for higher bandgap cells are smaller, resulting in a better performance ratio when compared to STC ratings (Peters & Buonessisi, 2018).

4.5 Relative humidity effects on CIGs PV panel: Isc, Pmax, and Voc.

4.5.1 The impact of temperature.

The impact of temperature on PV system performance is well documented (Nishioka et al., 2003; Woyte et al., 2013; Ye et al., 2013; Reich et al., 2012). Temperature impact development in predictive models (King et al., 2004; Veldhuis et al., 2015; Sandia National Laboratories, 2020). The solar-cell output voltage and the current generation are affected via temperature and materials-specific factors (the kT dependence of Boltzmann statistics and materials-specific bandgap narrowing or widening) and device-architecture-specific factors (Peters et al., 2018). Figure 16 shows several PV materials' radiative efficiency changes as a temperature function. Figure 16 directly compares the temperature dependence of performance ratios of state-of-the-art CdTe and PERC-type silicon PV modules as a function of temperature. This function is often linearly approximated, and the slope is called the power temperature coefficient.

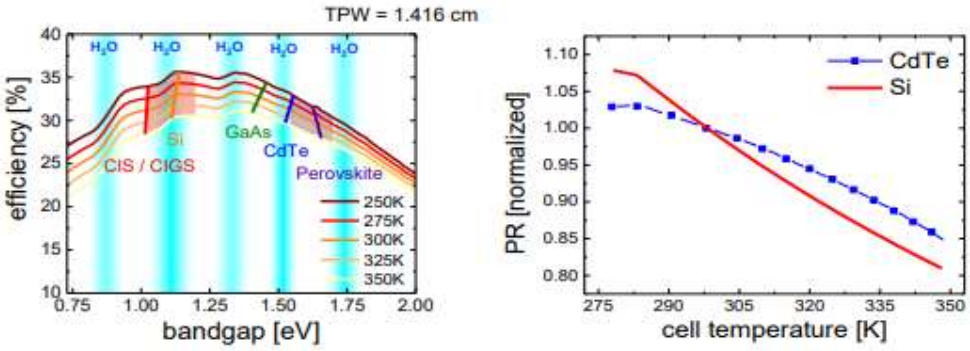

Figure 4. 3: Cell efficiencies at different band gaps.

Left - Limiting efficiency as a function of bandgap and temperature. Band gaps of various PV technologies as a function of temperature.

Right - Normalised performance ratio of a CdTe PV module and PERC-type silicon solar cells. CdTe is less sensitive to changes in temperature and has a comparably higher performance ratio at high temperatures (Peters et al., 2018).

Table 4.2 summarises the material properties of various solar cell materials. The temperature coefficient here is the most relevant parameter. Compared to mainstream silicon PV technology. CdTe has a significantly smaller temperature coefficient, resulting in a better performance ratio at temperatures above standard test conditions of 25 degrees Celsius (77 degrees Fahrenheit). However, when generating most of their power. PV modules are typically much hotter than the ambient air around them (10 degrees Celsius or greater above ambient air is not typical). Hence much of the power is generated at temperatures above 40 degrees Celsius (104 degrees Fahrenheit; 313 degrees Kelvin). Most power generation occurs at very high module temperatures between 50 and 60 degrees Celsius in hot, arid climates.

		CIS / CIGS	Si	GaAs	CdTe	Perovskite (CH_3NH_3PbI)
Band gap	E_g @ 25°C (eV)	1.010 (1.0 - 1.2)	1.125	1.431	1.540	1.639 (1.55 – 1.7)
Temperature coefficient	$D\eta/dT$ (% K^{-1})		0.3 – 0.6		0.27	
Record cell efficiency	η_{rec} (%)	14.1 (22.8)	26.7	28.8	22.1	22.1

Table 4.2. Band-gap at 25 degrees C (Eg@25 ^{o}C), power temperature coefficient (Dη/DT), and record efficiencies (η_{REC}) (Peters & Buonassisi,2018).

A smaller temperature coefficient offers a significant advantage for PV technology in hot climates; those temperature coefficients are linked to materials and depend on the architecture of the solar cell. Solar cells with a higher voltage have a smaller temperature coefficient. For example, typical values for silicon are at -0.45%/K; for CdTe, values are around -0.27%/K. However, the best silicon solar cells, heterojunction (or HIT cells), generate much higher voltages than conventional silicon solar cells (up to 750mV at an

open circuit). Moreover, have temperature coefficients as low as -0.3%/K. Therefore, further improving the voltage of CdTe solar cells should also reduce the temperature coefficient.

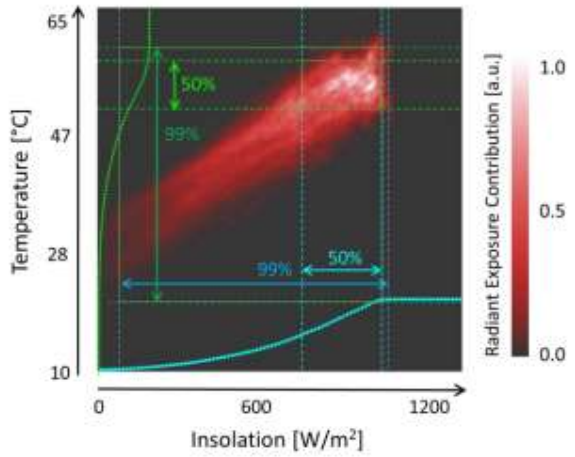

Figure 4. 4: Insolation and module temperature in a hot and arid sub-tropical environment. Most power generation occurs at module temperatures between 50°C and 60°C (Peters et al., 2018).

4.5.2 Impact of water vapour.

In addition to temperature effects, the impact of spectral variation on CdTe modules, and their differences from silicon, are well documented. Spectral effects occur because different atmospheric agents absorb light predominantly in specific spectral ranges. Water, a leading contributor to the shape of the ground reaching solar radiation, is more dominantly active in the infrared. At the same time, aerosols occur primarily in the blue. These absorptions change the percentage of available photons absorbed by a solar cell. A small bandgap cell-like silicon will see a more significant relative reduction in power for high atmospheric water concentrations than a larger bandgap cell-like CdTe. The reverse is true for aerosols. Higher levels of humidity or water vapour in the atmosphere, sometimes referred to as precipitable water, reduce the amount of sunlight that reaches the solar module as it passes through the atmosphere. Water blocks or extinguishes light through absorption or scattering. Water absorption over all wavelengths of sunlight is not equally distributed. They are still concentrated in several discrete bands called absorption bands. These absorption bands are indicated in Figure 17 as blue bars and marked with H_2O. Figure 18 shows how the limiting efficiency of the solar cell as a function of the bandgap of the solar cell material changes with increasing amounts of

water in the atmosphere. Whenever one of the blue bars is crossed, reduced efficiency occurs. Because silicon has a smaller bandgap (1.12 eV) than CdTe (1.54eV), silicon absorbs a broader range of photons, and light that Si can use is affected by more absorption bands. Consequently, as the water content in the atmosphere increases, the light intensity that silicon modules can use to create electricity is reduced more strongly than for CdTe. The greater sensitivity of silicon compared to CdTe is also shown in Figure 4.4.

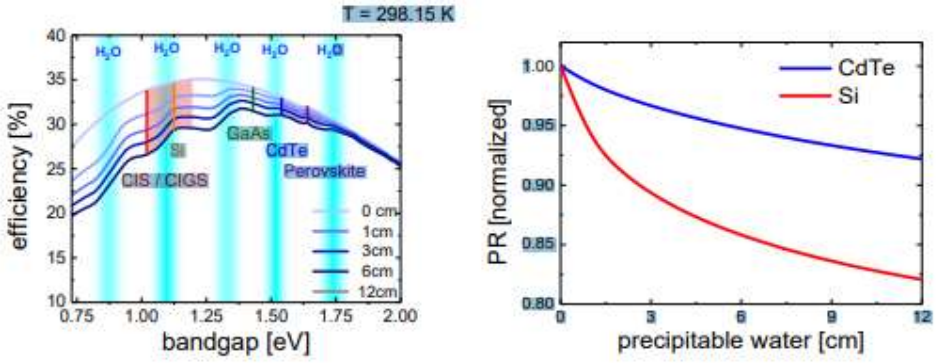

Figure 4. 5: Precipitable Water and Band Gap Effects on Efficiency.

Left - Limiting efficiency as a function of bandgap and total precipitable water. Band gaps of various PV technologies. Right - Normalised performance ratio of CdTe PV module and PERC type silicon solar cells function of full precipitable water (Peters et al., 2018).

The sensitivity to water is specific to a solar cell bandgap by its absorber material. Higher bandgap materials are less sensitive to water vapour in the atmosphere than lower bandgap materials. Consequently, all higher bandgap materials have an advantage over silicon in areas with high humidity. Because this advantage is tied to the absorbed bandgap, there are also no technological means by which lower bandgap materials could compensate. In temperate climates, the total precipitable water (i.e. the total water content of the atmosphere when condensed into a column) is below 2cm. Values can be as high as 12cm in the tropics, and the corresponding performance difference between silicon and CdTe can exceed 10%.

Figure 4.6 shows the annual decomposition rate of Pmax, Imax and Vmax broken down by technology. Despite mono-(A) and multi-Si (B) scattering, the predominant drop is in current rather than in voltage. This issue is an essential consideration for proper inverter size. More interesting is how the degradation of IV parameters varies from technology to technology. Figure 4.6 shows the degradation of Pmax, Isc, Voc, and FF for crystalline

silicon technology (a) and (b) and thin film (c). Again, thin-film technology amorphous silicon (a-Si), copper indium gallium (two), selenide (CIGS), and cadmium telluride (CdTe) have been superimposed on one map. Monocrystalline silicon and polycrystalline silicon show similar patterns. The highest Pmax degradation is closely related to Isc, followed by FF and Voc, with minimal degradation.

Typical observed Isc degradation could be due to delamination, discolouration, and cracking of individual cells. However, less likely to be due to light degradation and fouling [17,18]. FF degradation is significantly less and is usually associated with corrosion and solder bond breakage. In the thin-film technology shown in Fig. 4.6 (c), the pattern is different despite the clustering effect of the technology. All three thin-film technologies offer significantly higher FF degradation (compared to crystalline Si technology) and are often associated with photoinduced degradation of a-Si and increased series resistance in CIGS [19],

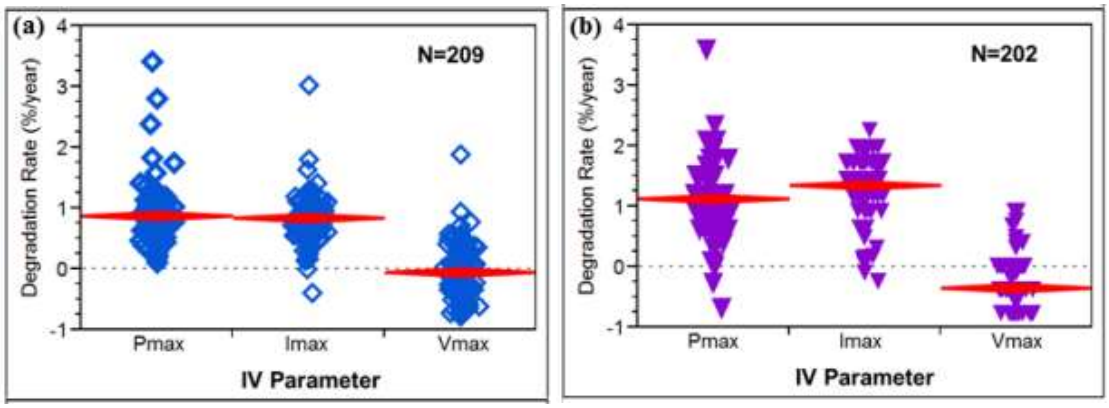

Figure 4. 6: Degradation rates of the maximum-power-point values for power, current and voltage for mono-Si (a) and multi-Si (b). Dashed lines show no degradation. A degradation that is negative indicates an improvement.

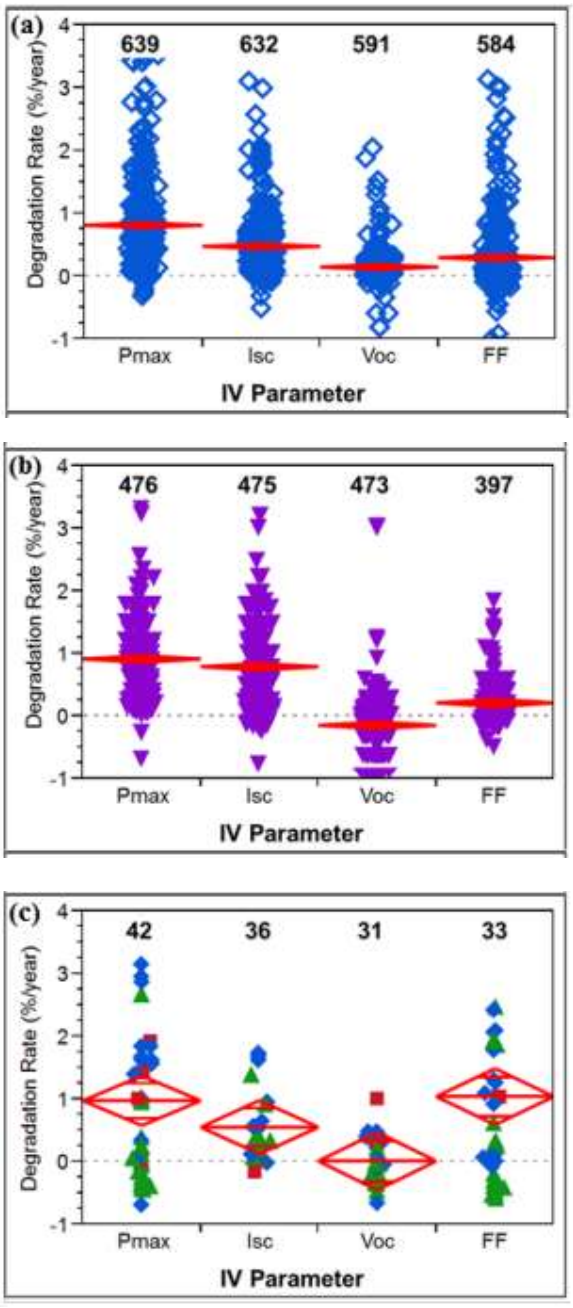

Figure 4. 7: Pmax, Isc, FF, and Voc degradation intensities for mono-Si (a), multi-Si (b), and thin-film (c) semiconductors are shown in Figure 3. (c). The thin-film layer is a Si (filled with blue diamonds), CIGS (filled with green triangles), and CdTe (red points indicated by the numbers at the top.

For most crystalline silicon modules, most degradation in Isc could be explained by discolouration of the encapsulant. The evidence supporting this theory includes:

1. That discolouration is known to cause a slight decrease in power production.

2. The discolouration is accelerated at higher temperatures, consistently observing the most increased Isc degradation in the desert.
3. That several of the reports specifically mentioned discolouration [20-24].

The decrease in Isc might also be explained by delamination and the associated loss of light transmission through the encapsulant-glass interface. Some of the reports specifically noted delamination. [25-27]

If delamination occurs, there may eventually be moisture ingress and corrosion of the internal parts of the module. Another common cause of loss of Isc can be broken cells. The effect of cell breakage may be delayed because the current can continue to flow until all metal connections fail. Still, there may be a more abrupt drop in the current output at that point because this may only affect the photocurrent in one part of the module. We expect that loss of current from one broken cell will reduce the fill factor, not the Isc. The diversity of thin-film technology complicates understanding the degradation mechanisms for the thin-film modules. The general observation that the fill factor decreases more than the other module parameters differentiates thin-film products from silicon. Still, it does not produce clear conclusions about the dominant wear-out mechanisms. The relatively small changes in open-circuit voltage simplify the system design since the match between the system voltage, and the desired input voltage of the inverter may not change much over the system's lifetime. However, a more careful evaluation of the decreases in fill factor for the thin-film modules may lead to changes in voltage; this question may benefit from the additional investigation. Similarly, as noted above, the 0.5%/yr decrease in module efficiency may correspond to significantly greater degradation rates at the system level depending on the system's design.

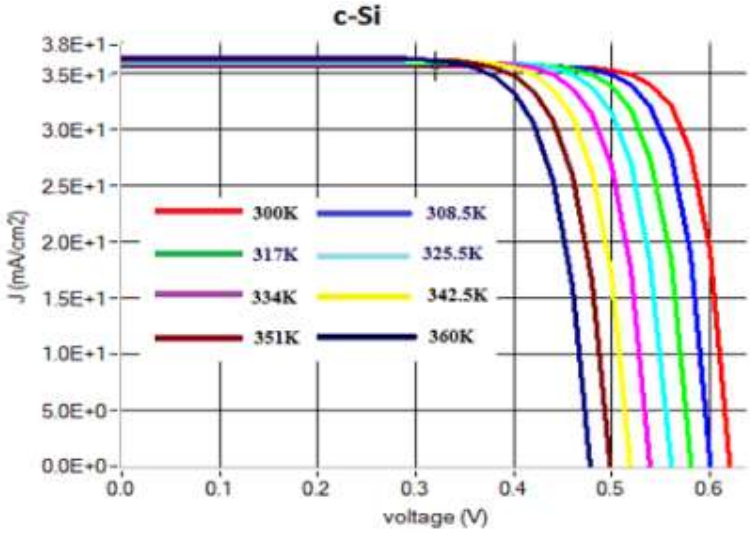

Figure 4. 8: Effect of operational temperatures on c -Si:H solar cell IV curve.

Figure 4.8 above shows the Iv curve of a c-Si solar cell at 1000 W / m² and the various operating temperatures. The open-circuit voltage (Voc) gradually decreases as the temperature rises. This is because the bandgap of semiconductors decreases at high temperatures, and Voc is proportional to the bandgap. Both Voc and Vmp decrease with increasing temperature [28].

The obtained Voc values are 0.62 and 0.48 Volts at 300 and 360K, respectively. The efficiency and fill factor (FF) also decreases with increasing temperature. As the temperature rises from 300K to 360Kas, the obtained efficiency drops from 18.42% to 14.04%. Due to the increase in carrier generation and the decrease of the high-temperature bandgap, the short-circuit current Isc increases slightly with the rise in temperature [22]. The Isc values obtained at 300K and 360K are 35.1mA and 37.3mA.

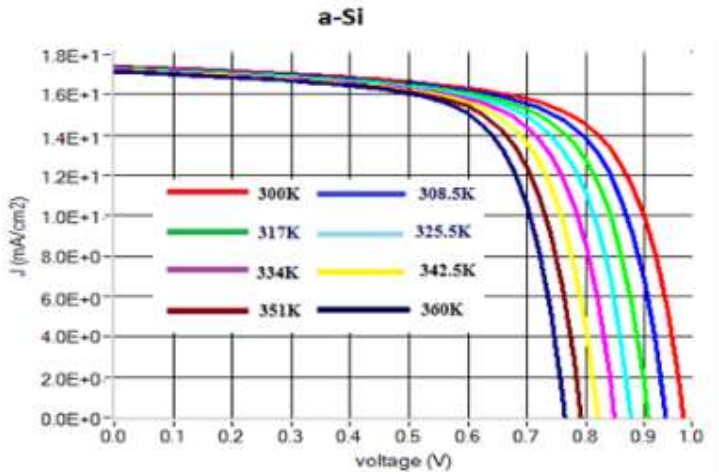

Figure 4. 9: Effect of operational temperatures on a-Si:H solar cell IV curve.

Figure 4.9 shows the IV curve of a-Si:H solar cell at 1000W/m² and different operating temperatures. The open-circuit voltage (Voc) gradually decreases as the temperature increases. This decrease is due to the bandgap of semiconductors reducing at higher temperatures, and Voc is proportional to the bandgap. Therefore, both Voc and Vmp decrease with increasing temperature [29]. The obtained Voc values are 0.55 and 0.44 volts at 300 and 360K, respectively. The efficiency and fill factor (FF) also decreases with increasing temperature. As the temperature rises from 300K to 360K, the obtained efficiency drops from 11.42% to 9.61%.

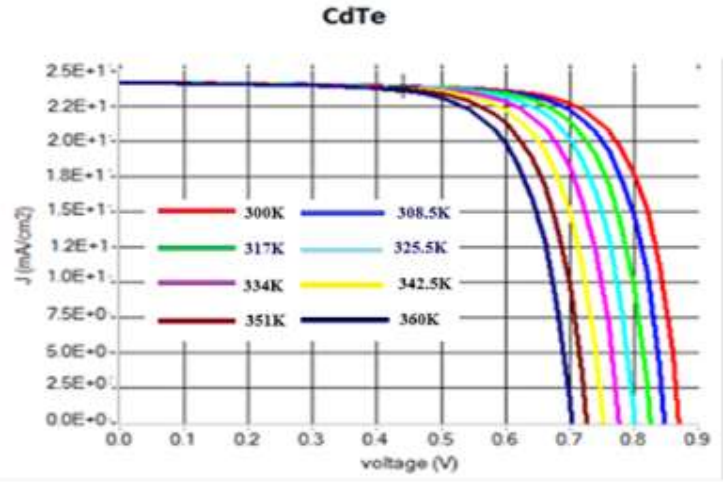

Figure 4. 10: Effect of operational temperatures on a CdTe solar cell IV curve.

Figure 4.10 shows the IV curve of a CdTe solar cell at 1000 W / m² and various operating temperatures. The open-circuit voltage (Voc) gradually decreases as the temperature

rises. This decrease is due to the bandgap of semiconductors reducing at high temperatures, and Voc is proportional to the bandgap. Therefore, both Voc and Vmp decrease with increasing temperature. The Voc values obtained were 0.75 and 0.59 volts at 300 and 360K.

Efficiency and curve factor (FF) also decreases with increasing temperature. For example, a temperature increase from 300K to 360K reduces the resulting efficiency from 7.33% to 6.79%.

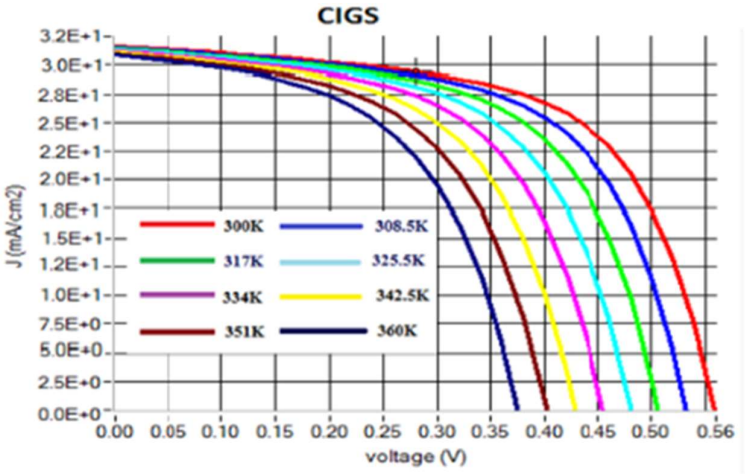

Figure 4. 11: Effect of operational temperatures on a CIGS solar cell IV curve.

The IV curve of the CIGS solar cell at 1000 W / m² and various operating temperatures are shown above in Figure 4.11. The open-circuit voltage (Voc) gradually decreases with increasing temperature. This gradual decrease is created by the semiconductor's bandgap reducing at higher temperatures, and Voc is proportional to the bandgap.

Furthermore, both Voc and Vmp decrease with increasing temperature. The Voc values obtained were 0.55 and 0.40 volts at 300 and 360 K, respectively; As shown in Figure 4.11, the efficiency and the fill factor (FF) also decrease with increasing temperature. The efficiency obtained drops from 10.86% to 6.88% due to the temperature rise from 300 K to 360 K. The Isc values obtained at 300k and 360K are 31.681 mA and 30.96 mA.

4.6 Conclusions.

The study found that c-Si solar cells perform better at higher temperatures than a-Si:H, CdTe, or CIGS solar cells, producing the following results:

The Voc, FF, Pmax and efficiency of the four solar cells decrease as the temperature increases.

The Voc of all four batteries increased slightly as the temperature increased.

The c-Si solar cell with a temperature coefficient of -0.0020/K had the lowest impact on Voc.

The Pmax temperature coefficient values for c-Si, CdTe CIGS, and A-Si are -0.0724/K, -0.0112/K, -0.0663/K and 0.0362/K. CdTe solar cells are more stable during power generation at high temperatures.

Chapter 5: Spectral analysis effects on PV Plants.

5.1 Introduction.

The spectral analysis calculates waves or vibrations in a sequence data set. This data is implemented as independent variables, such as three Cartesian space coordinates or time. It is assumed that the observation interval in space or time is constant. Purely periodic data series are rare but consider monthly averages of variables obtained over several years, such as births per 100,000 population. Data for individual years are non-cyclical. The spectrum is calculated for two reasons.

First, the normal range can bring empirical data to a simple formula with a much smaller number of members than the source data, regardless of whether the data is periodic. This one saves storage space and facilitates analysis operations. In addition, this process is used to reduce the size of image files on your computer. Second, the spectrum is an essential component of statistical descriptions.

Photovoltaic devices are affected by changes and changes in the solar spectrum. In practice, the energy produced by a photovoltaic cell or module can be calculated by integrating the spectral response and the product of the spectrum over a range of incident light wavelengths at a given temperature and irradiance level [1]. The effect of the spectrum is a technology-dependent parameter, as some technologies are more affected by spectral changes than others [2].

The spectral response of PV technology is generally known. Still, since the spectral irradiance of different installation locations is unknown, it is difficult to assess the spectral loss. The spectral content is affected by various factors, such as AM, water vapour, clouds, aerosol particle size distribution, particulate matter, and ground reflectance [3]. The spectrum is described under clear sky conditions as a function of air quality and relative humidity [4]. Spectral effects are more complex in cloudy weather. In general, light in the blue region of the spectrum is stronger than the standard AM 1.5 spectrum under these conditions. Instead, the blue areas of the range weaken as the sun moves across the sky.

Several studies have been conducted indoors and outdoors to investigate spectral effects [5-7]. The spectral response of photovoltaic cells and modules can be determined indoors using specialised equipment. Such as solar simulators and unique filters under controlled light and temperature conditions [8,9]. However, in outdoor research, the spectral

behaviour of photovoltaic devices is usually determined by mounting the photovoltaic device on a tracker. And measuring the short circuit current or I-V characteristic in combination with measurements obtained using a pyranometer and a spectroradiometer.

The influence of the spectrum is described in a variety of ways. For example, several authors have shown spectral effects by calculating each PV technique's percentage of solar radiation available [10]. Others require knowledge of the spectrum under various conditions, including average photon energy (APE) parameters [11,12].

The c-Si and CIGS technologies have broad spectral responses, which allow for sizeable spectral absorption. In the case of c-Si technology, efficiency improvements at high AM and clear sky conditions have been reported [13]. At the same time, other studies have been conducted on installations under clear sky conditions [14]. However, the performance of the tracker decreases slightly with increasing AM [15]. CdTe and a-Si technologies have approximately 350-800 nm narrow spectral responses, resulting in lower photon absorption. Compared to c-Si, a-Si modules exhibit higher energy yields in diffuse light illumination and high solar elevation angles [16].

Specifically, in a previous study in Japan, it was found that the ratio of spectral solar radiation. Available for solar cell utilisation to global solar radiation ranged from 5% for polycrystalline silicon cells to 14% for amorphous silicon cells and increased throughout the year [17,18]. Furthermore, experimental results from a study conducted in the United Kingdom showed that on an annual average basis. The available spectral fraction of solar irradiance for a-Si varied from +6% to -9%. While for CdTe and CIGS at + variation in the range of 4% to -6% and ±1.5%. Therefore, the effect of the spectrum on photovoltaic performance is essential, depending on the location, climatic conditions and spectral sensitivity of each technology.

5.2 PV degradation.

The performance of PV modules varies with climatic conditions and deteriorates over time [19-23]. An essential factor in the performance of photovoltaic technology has always been its long-term reliability, especially for emerging technologies. The most critical issue in long-term performance evaluation is degradation, which results from progress in power or performance loss, depending on several factors. Such as the battery, module, or even system level. In almost all cases, the main environmental factors associated with known degradation

mechanisms include temperature, humidity, ingress of water, and ultraviolet (UV) intensity. These factors can stress the PV device throughout its life cycle. Therefore, a detailed understanding of the relationship between external factors, stability issues, and module degradation is required.

Degradation mechanisms at the cellular level include a gradual performance loss due to the material's ageing and contact adhesion or corrosion, usually resulting from water vapour intrusion. Other degradation mechanisms include weakening the influence of the metal through the PN junction and the deterioration of the antireflection coating. The above degradation mechanisms are derived from previous experience with c-Si technologies [24,25].

In this case of amorphous silicon cells, a vital degradation mechanism occurs when the technology is subjected to sunlight. As a result, the power stabilises at approximately 70-80% of the initial energy. This decay mechanism, known as the Staebler-Wronski effect, is attributed to breaking the weak Si-Si bond [26]. This effect was introduced by photoexcited carrier recombination after the thermalisation. It results in defects that reduce carrier life [27].

Other degradation mechanisms have also occurred and were observed with CdTe and CIGS thin-film technologies at the cell level. For CdTe technology, the effect of cell degradation depends on the characteristics of the cell and the applied stress factors. CdTe technology does not enable p-type CdTe to ohm-contact with metal; hence, most devices use copper to dope the CdTe surface before contact [28,29]. Copper content can cause dramatic changes in the electrical properties of CdTe thin film.

Copper is so mobile that it diffuses along the CdTe cell's grain boundaries and recombination centres near the p-n junction. Shallow copper content reduces the conductivity of CdTe; however, copper diffusion may turn the backside contacts into non-ohmic contacts. Another effect of CdTe degradation is the applied voltage from the battery or external voltage. Copper ions are forced towards the front circuit conditions and affect cell degradation during accelerated ageing for different CdTe cell types [30]. In addition, impurity diffusion and doping distribution changes may affect device stability [31,32]. Still, the industry has addressed this problem by using special alloys.

It has long been questioned that copper atoms do not cause stability problems in CIGS cells because CIGS has a flexible structure that increases resistance to chemical changes [33]. However, wet heat tests performed on unencapsulated CIGS cells show that humidity

reduces cell performance. This is more pronounced as a decrease in VOC and FF due to increased concentration of deep acceptor states in CIGS absorbers [34]. Other essential factors include donor-type defects and the effect of Ga content on cell stability [35,36].

At the module level, in addition to the cell failure mechanism. Degradation occurs due to packaging materials, interconnects, cell cracks, manufacturing defects, bypass diode failures, encapsulants failures and delamination [37-39]. Finally, at the system level, degradation includes all cell and module degradation mechanisms, module interconnection, and inverter degradation Table 5.1 summarises the prominent thin film's failure modes and mechanisms [40].

Failure Modes	**Effect on I-V curve**	**Possible failure mechanism**
1.Cell degradation		
a.Main Junction; increased recombination	Loss in Fill Factor, *Isc* and *Voc*	Diffusion of dopants impurities, etc. electromigration
b. Back barriers; loss of ohmic contact (CdTe)	Roll over, cross over of dark and light I-V, higher *R series*	Diffusion of dopants impurities, etc. corrosion, oxidisation, electromigration
c. Shunting	*R shunt* decreases	Diffusion of metals, impurities, etc
d. Series	*R series* Increases	Corrosion and diffusion
e.De-adhesion from soda-lime glass	*Isc* decreases and *R series* increse	Na ion migrate to SnO_2/glass interface
f.De –adhesion of back metal contact	*Isc* decreases	Lamination stresses
2. Module degradation		
Interconnect resistance		
a. Interconnection resistance ZnO:Al/Mo or Mo Al interconnect	*R series* increases	Corrosion,electromigration
b. Shunting Mo across isolation scribe	R *shunt* decreases	Corrosion,electromigration

Bus bar degradation	*R series* increase or open circuit	Corrosion,electromigration
Solder joints	*R series* Increase or open circuit	Fatigue, coarsening (alloy segregation
Encapsulation failure		
a. Delamination	Loss in fill factor, *Isc* and possible open circuit	Surface contamination, UV degradation, hydrolysis of silane/glass bond, warped glass/ dinged glass edge thermal expansion mismatch
b. Loss of hermetic seal		
c. Glass breakage		
d. Loss of high potential isolation		

Table 5.1 summarises failure modes and failure mechanisms of the prominent thin film [40].

Indoor degradation investigations are performed at the modular level. In addition, adding interconnects and other materials to form the modular structure increases stability issues.

Accelerated ageing tests performed indoors and under controlled conditions can inform various degradation mechanisms. Degradation studies using indoor methodologies based on the IV curve and power acquisition at STC. The electrical properties of the PV module are firstly measured at STC. Then the module is exposed outdoors or indoors by acceleration procedures [41-43].

Finally, a solar simulator is periodically used to acquire electrical characteristics for each PV cell or module under investigation. The difference in current, voltage or power from the initial value indicates the deterioration rate continuously.

In addition, because the modules are exposed to actual outdoor conditions, many groups perform outdoor monitoring of individual PV modules by acquiring and comparing I-V curves [44-46].

Another method of investigating outdoor degradation is measuring PV systems' power and energy yields exposed to actual operating conditions. The general approach is first to establish a PR or maximum power time series normalised to photovoltaic (PVUSA) test

condition (PTC), usually monthly, with solar irradiance of 1000W/m² and temperature of 20^{O}C and wind speed of 1m/s.

Then use time series analysis like linear regression, classical sequence decomposition (CSD), and an autoregressive integrated moving average (ARIMA) to get the trend and hence the degradation rate [47].

Further testing is necessary for future exploration, so what are the current developments on the following.

5.3 Recent developments on Spectral analysis effects on a solar panel.

This research includes several significant effects affecting the performance of photovoltaic systems [48]. First, however, specified in several ways:

• Some new PV module types have a special coating or textured surface to reduce reflectance loss. Measurement data from such modules can quantify overall PV energy output improvement.

• So far, the method of estimating spectral effects has considered only single-junction PV technology. The technique used here must be changed for tandem cells and multi-junction technology.

• Some photovoltaic technologies show long-term fluctuations in unit efficiency. This is mainly the case with amorphous silicon technology and, therefore, further development of a model for operating these units.

• PV module performance is almost certainly environmentally dependent and tends to age. However, a better model of this effect must be developed before estimating the geographic variation of age-related degradation.

5.4 Conclusions.

The worldwide, Emergence and continuous spread of various photovoltaic technologies such as c-Si, thin-film, and CPV indicate photovoltaic technologies. Can become the leading energy source in the future. However, the success of each technology depends mainly on the ability to achieve goals such as improving manufacturing procedures while increasing efficiency and reducing costs.

Given the wide range of photoelectric technologies available, obtaining information on their characteristics in the open air is essential. The main performance parameters of PV systems are energy output, efficiency and PR. These parameters form the basis for all productivity estimates and loss factors studies. The main environmental factors affecting the performance of PV systems include solar radiation, ambient temperature and solar spectrum. Another essential factor to be considered is degradation. Thus, a good understanding of the characteristics of various outdoor photoelectric technologies is a critical requirement in their successful integration into other climatic conditions.

In particular, helpful information about the implementation of various photovoltaic technologies side-by-side installation has been obtained by examining their seasonal characteristics and the effects of temperature, pollution and power ratings. The results of the outdoor performance evaluation also showed that these technologies have huge potential in countries with extensive solar energy resources.

Chapter 6: Small central control Mechanism for large-scale PV plants.

This chapter summarises the central control mechanism for PV plants, reporting the most widely accepted equipment, the most employed components, and materials. Moreover, it reviews the state-of-the-art control systems to maintain photovoltaic systems to achieve optimum performance. Particular attention is committed to the latest development in control mechanisms.

6.1 Introduction to the Control Mechanism.

6.1.1 Grid-connected PV systems.

A grid-connected solar PV system comprises three parts: an array of solar cells, power electronic converters, and an integrated control system [1]. A solar cell is a semiconductor mechanism that converts sunlight into direct-current electricity. Typically, solar cells are connected in series to form a module that gives a standard dc voltage. Modules are coupled into an array to produce much current and voltage to meet demand [2]. There are two ways to connect PV modules into an array. The first approach connects modules in series into strings and then parallels into an array. The second approach first wires modules together in parallel, then those units are combined in series. PV system optimisation methods are typically employed [3]. In practice, systems sizing has been recognised based on system performance, component modelling, technical, economic considerations and system reliability [4]. PV array optimisation techniques benefit manufacturers who do not have detailed information about their future implementation. The optimum configuration depends on the 'place's general radiative characteristics, showing a clear dependence on latitude [5]. Ideally, both series-parallel and parallel-series connections are comparable if all the cells and modules are identical and work in the same condition. However, suppose sunlight is applied unevenly to different PV cells, shading or other impacts. In that case, the second connection approach could cause many problems [6].

6.2 Different types of Controllers.

6.2.1 Introduction to the Controllers.

No single inverter is best for all situations; however, there are several types: Central, String, multi-string, modular, power optimisers and micro-inverters. Distribution systems are categorised into four types: for small scale, the range up to 250 kW. For medium scale,

250kW to 1000kW, Large scale,1MW to 100MW, and mega-scale, the power capacity is more significant than 100MW [7]. Inverter technology for grid-connected solar power plants usually consists of micro-inverter, string inverters and central inverters [8-12]. Micro-inverter and string inverters are installed predominantly in small and medium-scale projects. In contrast, the central inverter is utilised in large-scale solar power projects. However, string inverters have started to be used for large-scale solar power projects [13,14].

A typical PV Plant-based system layout requires a PV array Figure 6.1, PV inverter and transformers. The connection of this equipment is based upon the location used by the PV inverter: two inverters are generally used to connect the PV plant; central or multi-string.

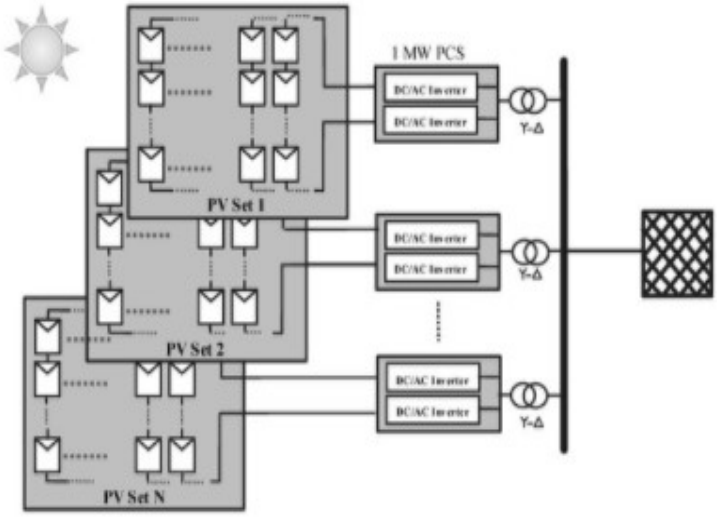

Figure 6.1: A grid-scale PV-based plant.

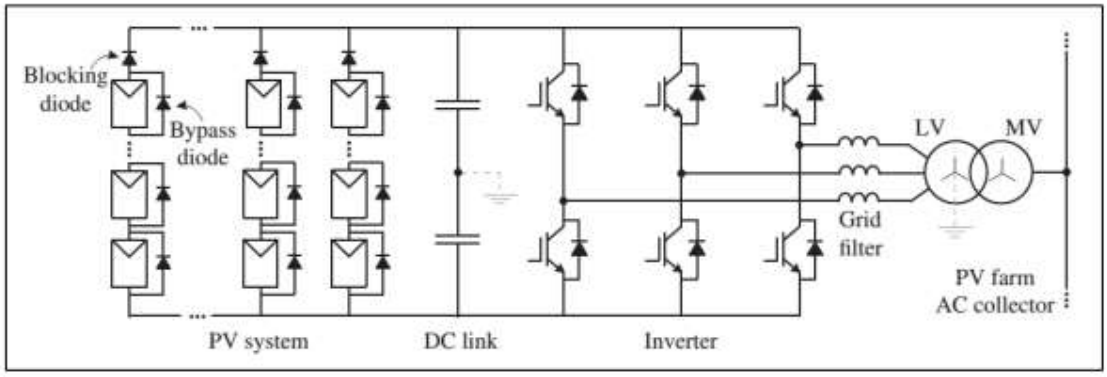

Figure 6.2: Large-scale grid-tied solar power system.

Figure 6.2 is a typical configuration of a solar power plant. The solar panels are connected in series to create strings combined in parallel before connection to the inverter. The DC/AC inverter is one of the essential components in the grid-connected solar power system. It converts DC power (solar panels) to AC (network grid) with the support of Maximum Power Point Tracking controllers (MPPT) with a grid-tied controller [15-20] with the system. The DC/AC inverter operates the MPPT of the PV array by regulating the DC-link voltage to maximum power point voltage and synchronises the AC utility grid current with the grid voltage for active and reactive power control [21]. The DC/AC inverter is linked to the grid by an inductive grid filter with an LV/MV transformer. To raise the voltage from low voltage (LV) to medium voltage (MV) of a few thousand volts (LV/MV) to reduce losses in transmitting energy to the grid.

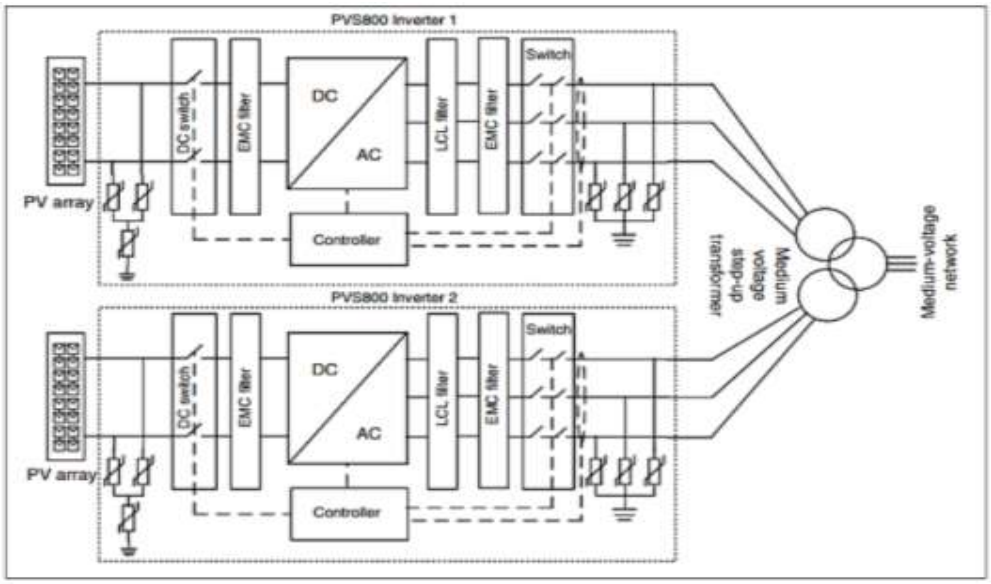

Figure 6.3: A high-level, single-line diagram shows typical voltages of operation for the AC system of a solar power plant.

6.3 Invertors.

Several inverters are central, string, multi-string, modular, power optimisers and micro-inverters. These 'inverters' objective is to convert the PV-generated DC power into AC power. To determine the PV-generated DC power required to supply a given Ac load which in turn, for specified PV array efficiency, sets the PV array size. An 'inverter's performance depends upon its point of work, the threshold of operations, grid connection system, inverter output waveform, harmonic distortion and frequency, PV efficiency, maximum power point tracker (MPPT) and transformer. The primary function is wave shaping, output voltage regulation, and operations near peak point [22].

The three significant types of inverters, sine wave, modified sine wave and square wave inverter, the primary advantage of a sine wave inverter, are the most commercially designed equipment available for sine wave operation. A modified sine wave inverter will also operate most equipment. A square wave inverter will only operate simple devices. The output square wave is converted to a sine wave. An inverter with an MPPT algorithm extracts maximum power from the PV by changing the input voltage to maintain full power point voltage (MPP) voltage on the current-voltage curve as PV output varies with insolation and module temperature [23].

6.3.1 Central inverter.

Central inverters are usually three-phase and can incorporate grid frequency transformers [24]. These transformers increase the 'inverters' weight and volume; although they provide galvanic isolation from the grid, there is no electrical bond between the input and output voltages [25].

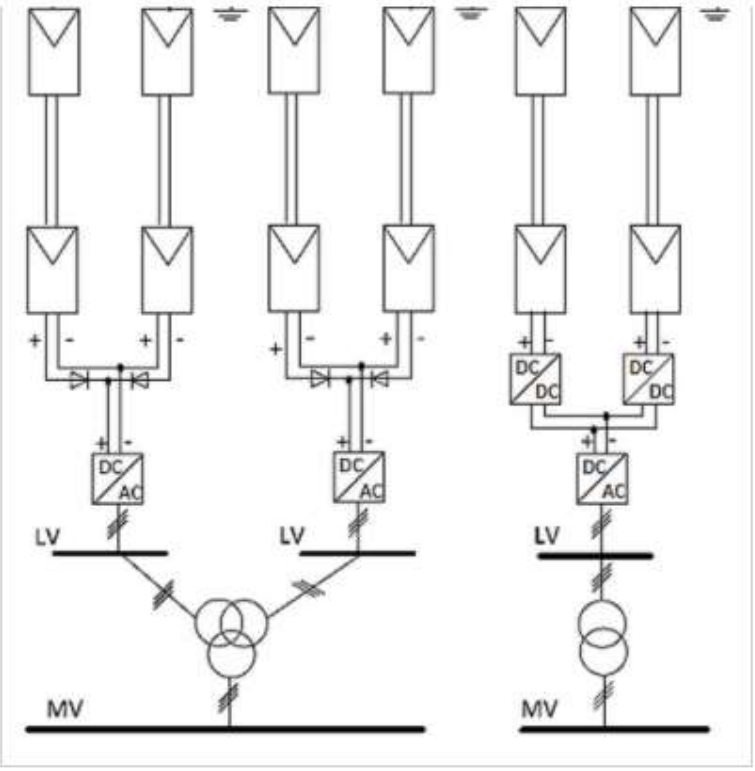

Figure 6.4: (a) Central PV inverter. (b) Mutli-string PV inverter.

6.3.2 String Inverter.

The string inverters are shown above in Figure 6.4, a smaller version of the centralised inverter, where a single string of PV modules is connected to the inverter. The input voltage may be large enough to avoid voltage amplification. No losses are associated with string diodes, and separate Maximum Power Point (MPP) tracking MPPTs can be applied to each string. Increasing the energy yield via the reduction of mismatching and partial shading losses. These superior technical characteristics increase energy yield, enhance supply reliability, increase overall efficiency compared to the centralised inverter, and reduce the price due to mass production.

The string inverter concept uses multiple inverters for multiple strings of modules. String inverters provide MPPT on a string level, with all strings being independent. It is useful when modules with different orientations. Or modules of other specifications or shading issues centralised, string, micro and power optimiser inverters produce higher power output than a string inverter.

Strings connections are in parallel to the inverter. Central inverters offer high reliability with the simplicity of installation. However, they have disadvantages. Increased mismatch losses and the absence of maximum power point tracking (MPPT) for each string may cause arrays with different module types, multiple tilts and orientation angles and shading issues [26].

6.3.3 Multi-string inverter.

The multi-string inverter in Fig. 4(a) is the further progress of the string inverter, where several strings interfaced with their DC-DC converter (separate MPP tracking systems) to a typical DC–AC inverter [27]. Compared to the centralised system, it is beneficial as individual control is achievable; therefore, a compact and cost-effective solution combines central and string 'technologies' achievements and benefits. This multi-string topology allows the integration of PV strings of various technologies.

6.3.4 Modular inverter.

Inverter systems' flexibility and adaptability increased by separating the control system's hardware. The control can be designed independently and based on functional aspects only and, in addition to that, delocalised or centralised. An important factor is the distributed control [28,29]. Defining this means that parts of the control topology are closer to the corresponding power electronic elements. Simultaneously, superordinate functions are separated and centralised, primarily supporting the modular structure. The inverter is incorporated into

hardware and software elements linked by functionalities. However, decoupled functional modules (hardware and control elements) can be treated independently. And genuine software and hardware elements are only interpreted by their detached functionalities. An example of distributed control is to locate measurements, pre-processing and post-processing functions, local control functions and supervision functions close to the concerning hardware. The primary control, management and superordinate supervision of the entire system can be decoupled and located externally, shown in the structure below in Figure 6.5.

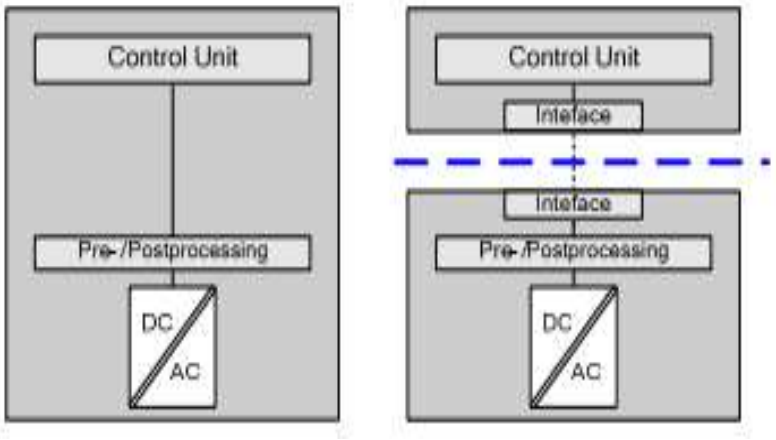

Figure 6.5: Separation of inverter control and hardware. Left: Conventional interlocked inverter structure. Right: Modular inverter structure with decoupled control and hardware.[6]

6.4 Power optimiser.

Like microinverters, power optimisers are small devices installed at each solar panel. However, instead of transforming direct current (DC) into alternating current (AC) at the solar panel, the optimiser conditions and routes the energy to the central string inverter. It is important to note that power optimisers are not inverters. Instead, as the name suggests, it optimises the energy produced by an individual solar panel and routes its DC power individually to the inverter.

6.5 Micro Solar inventors.

Different micro solar investors are classified below.

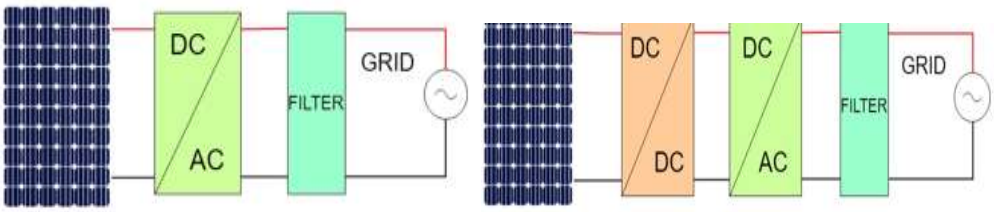

Figure 6.6: Single-stage or two-stage.

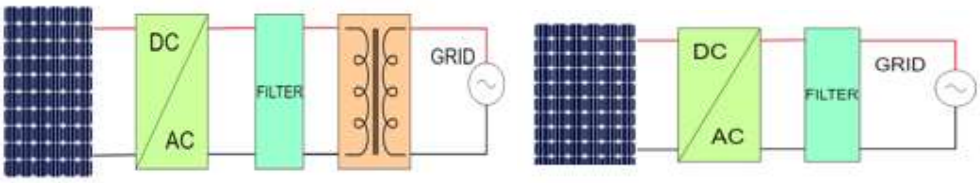

Figure 6.7: Transformer microinverter or Transformer-less microinverter.

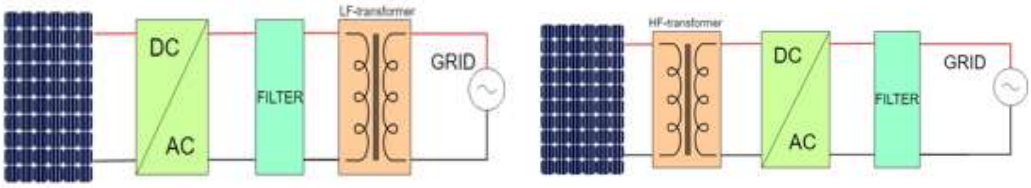

Figure 6.8: Line frequency transformer or High-frequency transformer.

Single-stage microinverters are designed to improve system efficiency by reducing the number of components. It compromises the MPPT and PWT control in one stage and performs the single-stage conversion process.

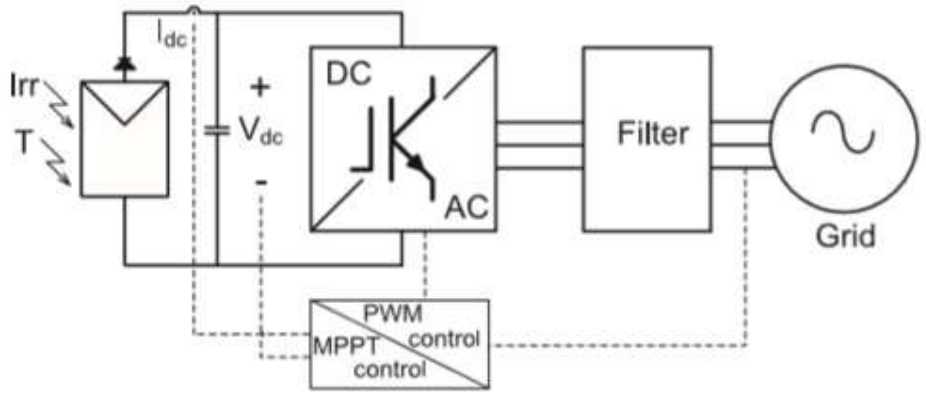

Figure 6.9: Multi-stage micro inverters [17] Mohammad Reza Aghaei, Shauhrat S. Chopra, Solar PV systems design and monitoring in Photovoltaic Solar Energy Conversion,2020D.

6.5.1 Multi-stage micro inverters.

A multi-stage micro inverter topology comprises a DC /AC stage used to boost the PV voltage to the required voltage (approximately 400v DC), incorporating a DC/AC stage that converts Dc to Ac voltage.

They convert DC electricity from PV modules into AC, ideally conforming to the local grid requirements. Also, perform a mixture of functions to maximise the plant's output. These range from optimising the voltage across the strings. Monitoring string performance to log data and providing protection and isolation in irregular grid or PV modules [30].

There are two wide-ranging classes of inverters: central inverters and string inverters. The central inverter configuration below shows the Figure remains the first choice for many medium and large-scale solar PV plants. Many modules are connected in a series to form a high voltage (HV) string.

Simple 1 or 2 stage controllers, PWM (pulse width modulation), Maximum PowerPoint

tracking (MMPT) and micro.

The local conditions and system components must be considered to tailor the specific application system. Various solar PV module technologies and layouts may suit different inverter types. Care is required in integrating modules and inverters to ensure optimum performance and lifetime. The most cost-effective inverter option requires an analysis of technical and financial factors. The DC-AC conversion efficiency directly affects the solar PV 'plant's annual revenue and varies according to several variables, including the DC input voltage and load. Extra factors should help identify inverters, such as site temperature,

product reliability, maintenance, serviceability, and total cost. Inverters also de-rate with altitude, which may be considered in mountainous locations.

Central inverters are frequently used in a "master-slave" configuration. This means that some inverters shut down when the irradiance is low, allowing the other inverters to run more closely to optimal loading. When the irradiance is high, all invertors share the load; thus, only the required number of inverters are in operation at any time. The operating time is distributed uniformly among the inverters, increasing the design life.

6.6 Effect of the controller on maximum power.

A solar PV 'system's control system contains maximum power point tracking (MPPT) and the other for grid interface control [31-34]. The control functions are achieved through power electronic converters. There are three typical power converter configurations [35]:

1) A dual-stage converter configuration including a dc/dc boost converter operating the MPPT and a grid-connected dc/ac converter using grid interface control.

2) Configuration with multi-string dc/dc inverter and a grid-connected dc/ac converter.

3) A single-stage dc/ac inverter handling all the tasks such as MPPT and grid interface control.

Figure 6.10 shows a PV array with inverter configuration 2.

For inverter configurations 1 and 2, the voltage applied to each string is

$$Vs = (1 - D) * Vdc \quad \textbf{(6.1)}$$

Vdc is the dc-link voltage, and D is the dc/dc inverter.

For configuration 3, apply the dc-link voltage.

To the parallel strings directly. The MPPT control is attained by varying the dc voltage applied to the PV generator. Typical MPPT strategies include P&O (Perturb and Observe. The Perturb & Observe algorithm states: that when a small increment perturbs the operating voltage of the PV panel. Suppose the resulting change in power (P) is positive. In that case, we are going in the direction of MPP perturbing in the same direction. If P is negative, we

are going away from the direction of MPP, and the sign of perturbation supplied must be changed [36].

6.6.1 Incremental Conductance.

Voltage-Based MPPT and Current-Based MPPT, a slight dc voltage agitation was introduced. As the output power of the PV generator increases, then the agitation is continued in that direction. Otherwise, the agitation reversed in the opposite direction. The practice continues until the maximum power point (MPP) is achieved [37].

Incremental Conductance method, the agitation voltage is calculated using the PV generator dc voltage [38]. The total Conductance method is faster and more stable in getting to the MPP. The voltage-based MPPT approach assumes that an MPP of a specific solar PV module lies about 0.8 times the 'module's open-circuit voltage. A feed-forward voltage control scheme was applied to bring the solar PV module voltage to the MPP [39]. However, the 'module's open-circuit voltage and the MPP vary with temperature and other factors; MPP for a practical PV application is challenging using this technique. The current-based MPPT approach assumes that an MPP of a PV module is about 0.9 times the 'module's short circuit current. Comparable to the Voltage-Based approach, the module's short circuit current and MPP may be affected by insolation levels. Therefore, using this method, MPP for a practical PV application, is challenging [40].

6.6.2 Power control characteristics of grid-connected dc/ac.

To study stationary and dynamic regimes in three-phase systems. The application of "vector control" (Parck vector) is a powerful tool. To analyse and control DC/AC converters, enabling the abstraction of differential equations that govern the three-phase 'system's behaviour in independent rotating shafts. However, the main disadvantage of using this control method. Is that it introduces a nonlinear part, a rotation of axes (mathematical transformations), which requires much computing power and is resolved with existing microcontrollers and DSP.

6.6.3 Power control attributes of grid-connected dc/ac converter.

The dc/ac inverter operates similarly in all three converter configurations. A control goal is to transfer the solar array's active power to the ac grid. And the reactive power of the ac Grid system at the desired value while maintaining a high-power quality in terms of harmonics and unbalance. Figure. 6.10 shows the grid-connected dc/ac converter system diagram. A dc-link capacitor is on the left. A three-phase voltage source signifies the grid voltage at the Point of Common Coupling (PCC) (right-hand side), and a grid filter is in the middle. In the d-q reference frame, the voltage balance across the grid filter [41,42].

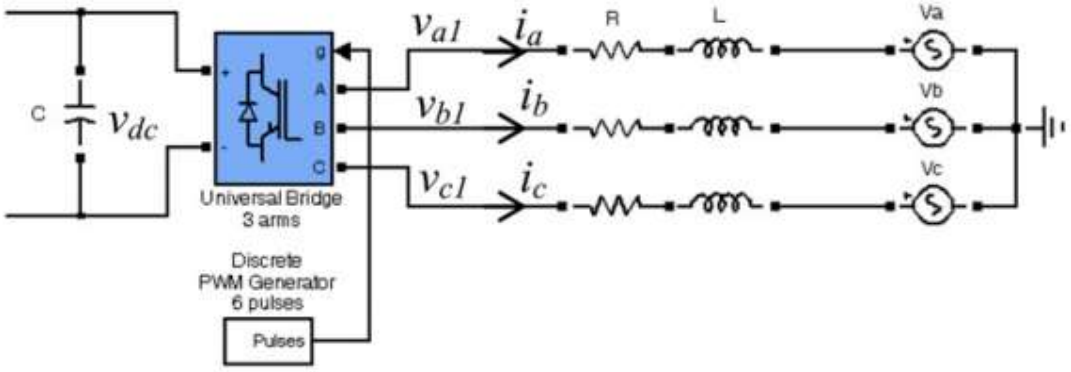

Figure 6.10: Grid-connected dc/ac converter schematic.

$$\begin{bmatrix} Vd1 \\ Vq1 \end{bmatrix} = R \begin{bmatrix} Id \\ Iq \end{bmatrix} + L \frac{d}{dt} \begin{pmatrix} id \\ iq \end{pmatrix} + wsL \begin{bmatrix} -iq \\ id \end{bmatrix} + \begin{bmatrix} Vd \\ Vq \end{bmatrix} \quad \textbf{(6.2)}$$

Here is the angular frequency of the grid voltage, and L and R are the inductance and resistance of the grid filter.

Eq. (6.2) expressed using space vectors defined by a complex Eq. (6.3)

In which Vdq, Idq, and Vdq1 are instantaneous space vectors of PCC voltage, line current, and converter injected voltage to the grid.

$$Vdq1 = R \cdot idq + L \frac{d}{dt} idq + jwsL \cdot idq + vdq \quad \textbf{(6.3)}$$

Under the steady-state condition, (6.3) becomes:

$$vdq1 = R \cdot Idq + jwsL \cdot Idq + Vdq \quad \textbf{(6.4)}$$

Vdq, Idq and Vdq1 stand for the steady-state space vectors of PCC voltage, grid current, and converter injected voltage.

The general approach used in the controller design of the grid-connected dc/ac converter is the PCC voltage-oriented frame [43],

i.e., the d-axis of the reference frame aligned with the PCC voltage position. Hence, in terms of the steady-state condition,$Vdq = Vd + j0$
Assuming $Vdq1 = Vd1 + jvq1$ and neglecting the filter resistance, then, the steady-state current flowing between the PCC and the converter, according to Eq. (6.4) is:

$$Idq = \frac{Vdq1 - Vdq}{jXL} = \frac{Vd1 - V}{jXL} + \frac{Vq1}{XL} \quad \textbf{(6.5)}$$

In which XL stands for the grid filter reactance.

Supposing generator convention is applied, i.e., power flowing toward the grid as positive; then, the power transferred from the converter to the grid is achieved from the primary complex power equation $Pg + jQg = Vdq1dg = Vd1dq.$

by solving this power equation together with Eqs. (6.5), (6.6) is obtained,

$$\boldsymbol{Pg = \frac{VdVq1}{XL} \cdot Qg = \frac{Vd}{XL}(Vd1 - Vd)} \quad \textbf{(6.6)}$$

According to Eq. (6.6), the active and reactive powers, controlled through q and d components Vq1 and Vd1 of the converter, injected voltage into the grid. The grid-connected 'converter's similar power control characteristics still exist when considering filter resistance, as shown by [44].

The converter must operate within the rated current and converter linear modulation limits for any power control conditions, as shown by Eq. (6.7). Therefore, *I rated*; the rated phase RMS

current of the converter, and *Vconv* is the phase RMS voltage of the converter output voltage [45].

$$\sqrt{\frac{I^2d + I^2q}{3}} \leq Irated, \quad Vconv = \sqrt{\frac{V^2d1 + V^2q1}{3}} \leq \frac{Vdc}{2\sqrt{2}} \qquad (6.7)$$

6.7 Seamless integration of the controller with PV plants.

Thanks to a classical P&O MPPT algorithm and a proportional-integral (PI) power controller, it is supported in MPPT and power limiting modes. Also, the seamless switch between the two methods is feasible.

The PI power controller allows for a faster dynamic response. Then the perturbation methods, due to their flexibility, PV shedding, achievable with an easy reconfiguration by reducing or raising the PV voltage.

This choice is frequently linked to the converter constraints. Nevertheless, it has an impact on the efficiency of the system. Therefore, many different types of efficiencies for inverters are defined.

These describe and quantify the efficiency of various aspects of an 'inverter's operation. However, the search for an objective quantifying inverter performance is still ongoing. As a result, new ways of measuring efficiency are frequently suggested in the literature.

The most used methods are deliberated below. Conversion efficiency measures the loss experienced during the conversion from DC to AC. These losses are due to a transformer and the associated magnetic and copper losses, inverter consumption, and losses in the power electronics. Conversion efficiency: the ratio of the fundamental component of the AC power output from the inverter, divided by the DC power input:

$$n_{Con} = \frac{P_{AC}}{P_{DC}} = \frac{Fundamental\ component\ of\ AC\ power\ output}{DC\ power\ input}$$

The conversion efficiency is not constant; it depends on the DC power input, the operating voltage, and the climatic conditions, including ambient temperature and irradiance. The variance in irradiance during a day creates variations in a PV array's output power and maximum power point (MPP).

The inverter is continuously subjected to various loads, leading to fluctuating efficiency. The voltage at which inverters reach their ultimate efficiency is a crucial design variable as it allows system planners to optimise the cabling system. Due to the energetic nature of inverter efficiency, diagrams are more suited to depiction than uniform numeric values. Figure 6.11 depicts the inverter's efficiency's dependency on the inverter load.

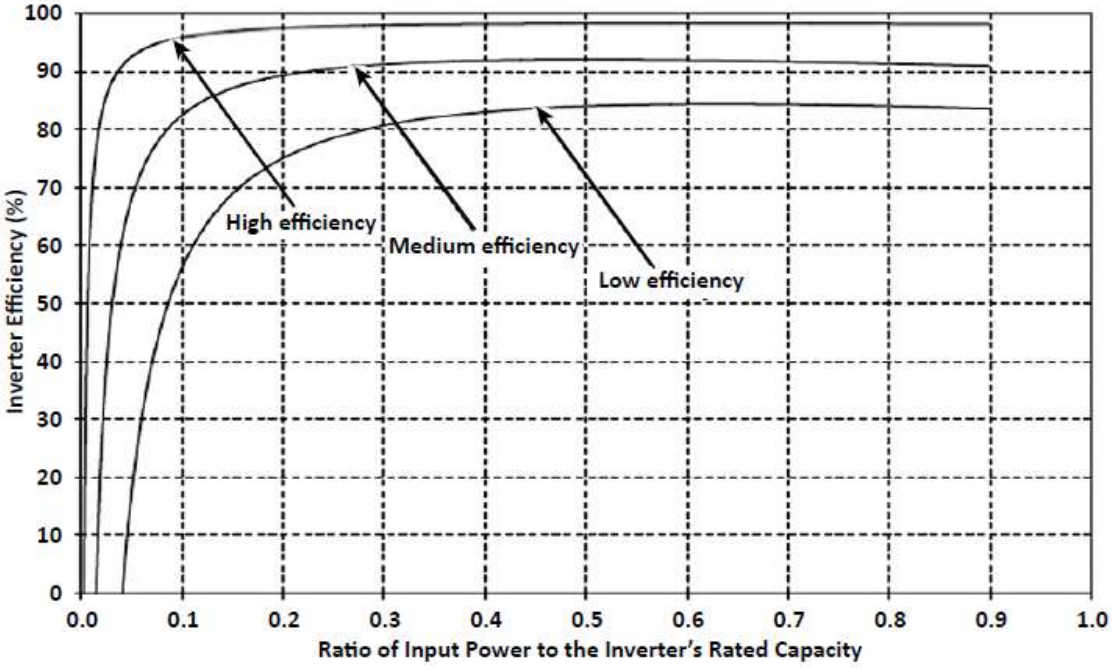

Figure 6.11: Low Medium and High efficiency 'inverters' Efficiency curves as functions of the input power to inverter rated capacity ratios [4].

6.8 Effects of soiling losses on the controller.

The conversion efficiency of a solar energy system can vary depending on environmental conditions such as; soiling, temperature and power input, and voltage. For example, the range in irradiance during a day can cause variations in a PV array's output power and maximum power point. In addition, the inverter is constantly under load, which can lead to fluctuations in its efficiency. Therefore, soiling and temperature effects directly affect the voltage at which controllers achieve their maximum efficiency.

6.9 Conclusions.

The inverter requires a dry, cool, ventilated area to achieve optimum performance. However, indoor installation is also installed outdoors. However, protection against direct sunlight, moisture, and other factors can increase the operating temperature, as this will cause affect the 'inverter's life span.

.

Chapter 7: *A case study*

Kuwait is a middle east country with a 29° 30' N latitude, with about 4.271 million population. The government has a solar PV (photovoltaic) installed capacity of 93 MW in 2019, generating 59 GWh in the same year and targeting 4 GW installation by 2030.

The country is located in a Saharan region with severe dust activity all year round, which causes a significant deteriorating influence on the PV performance. This study investigated the effect of soiling on PV performance through optical losses. Three 5cm x 5cm low iron glass coupons were exposed in Kuwait City for three months (February to April) during the spring at three angles (Horizontal, Tilt-45°, Vertical).

- The spectral characterisation was conducted using a Spectrophotometer. This yield performance reduction was determined using Wacom continuous solar simulator.
- The morphology and elemental characterisation were performed using a scanning electron microscope and energy dispersive X-ray scanning.
- X-ray powder diffraction was employed to determine the accumulated minerals. The findings show a 52% optical loss and a 53% power reduction from the coupon exposed in the horizontal position.
- Particle characterisation provided images and data minerals that cause a significant effect on light transmittance.

7.1 Introduction.

In the recently completed COP26 in Glasgow, about 200 nations agreed to accelerate actions of reducing CO_2 emissions and meet up 2025 target in 2022 [1]. Kuwait is rapidly deploying resources to increase clean energy contribution to the electricity supply. To achieve the target through a multi-million pounds investment in solar energy technology to develop a 5GW asset [2].

However, the technology faces a severe challenge (PV soiling) that has devastatingly influenced its performance [3, 4]. A 10 MW pilot project comprising 5 MW polycrystalline and 5 MW is facing serious soiling challenges [5].

PV soiling reduces the yield of the technology depending on several factors such as site, particulate matter, climatic conditions and angular positioning [3, 6, 7]. The country experience extreme dust activities with varying levels of aerosol deposition and entrainments from a storm, haze, rising, and suspended dust leading to about 26 severe dust storms in 137 days/year, which drop visibility about 150 m and sometimes to as low as 1.8 m [8, 9]. PV soiling is forecasted to cause 4-7 billion euros revenue losses by 2023 [10].

Although several studies [5, 11] have already been conducted on the performance of the popular solar installation in Kuwait [12] (Al-Shegaya), mere attention has been given to the impact of soiling on the asset. However, considering the above highlights.

A colossal investment such as Al-Shegaya in Kuwait requires continuous research and monitoring to sustain its performance. Therefore, this study investigated the effect of soiling on PV performance through optical losses and related it to the asset's economic failures.

7.2 Experimental Methodology.

Three 5cm x 5cm low iron glass coupons were exposed in Kuwait city with proximity to Shegaya solar farm (29°12'19", 047°03'06") for three months (February to April) during the spring. Shegaya solar farm is considered to be the period with the most significant dust storm activity in the region [5, 9].

The coupons were positioned at three angles (Horizontal, Tilt-45°, Vertical) and after the expiration of the exposure period, coupons were returned to the solar laboratory at the University Exeter in the United Kingdom for characterisation to obtain optical losses information and deposited material. The optical losses data were collected to analyse the PV soiling of the Al-Shegaya solar farm installation.

7.3 Spectral Characterisation.

The exposed coupons were examined using a spectrophotometer (Perkin Elmer Lambda 1050 UV/VIS/NIR). An unexposed clean coupon was used as a benchmark to measure transmittance change ($\Delta\tau$) from 250nm to 1250 nm. The spectral wavelength of all installed PV systems in the Al Shegaya solar farm response within. The relative transmittance change

in percentage was calculated using Eq. 1, where the τ_x is transmittance data of coupon relative to its angular positioning and $\tau_{Unexposed}$ Represents the baseline coupon, which is clean and was not exposed.

The optical losses based on the optimum angle were calculated using the linear interpolation technique provided in Eq. 2, where $\Delta_{\tau_{(Optimum)}}$ is the calculated change of transmittance of a coupon at an optimum angle, $\beta_{(31)}$ is the optimum tilt angle of Al Shegaya based on GSA [12], $\beta_{(45)}$ is angular position of 45° that a coupon was exposed, $\beta_{(0)}$ is the horizontal angle which a coupon is positioned, $\Delta_{\tau_{(0)}}$ is the optical loss for horizontal positioned coupon, and $\Delta_{\tau_{(45)}}$ Is the optical loss recorded on the coupon positioned 45° angle?

$$\Delta_{\tau_{(Optimum)}} = \frac{(\beta_{(31)} - \beta_{(45)})\,(\Delta_{\tau_{(0)}} - \Delta_{\tau_{(45)}})}{(\beta_{(0)} - \beta_{(45)})} + \Delta_{\tau_{(45)}} \qquad \text{Eq. 2}$$

7.4 Particles characterisation.

The morphological characterisation was performed using the electronic scanning microscope (SEM Quantal FEG 650 equipped). Before scanning, a soiled coupon was carbon coated with an Emi-Tech K950 machine.

Two images (backscattered electron and secondary electrons) were obtained, and the latter was used for morphological analysis. Next, the element study of accumulated particles was conducted with an Energy Dispersive X-ray (EDX) attached to the SEM. Again, backscattered images from the SEM were adopted to determine the accrued elements of the coupons.

X-ray powder diffraction (XRD - Siemens D5000 diffractometer) was employed for mineralogy characterisation. Due to the number of samples, smear sample preparation was conducted to transfer the particles from the coupon to the diffractometer grey plastic holder. The minerals' transparency was further determined using online databases such as mindat.com and minerals.net.

7.5 PV Yield.

Power losses using exposed coupons were calculated using two approaches. The first uses an experimental procedure where coupons were placed on top of a high-efficiency solar cell under a solar simulator (Wacom WXS 2105-20 AM1.5G) to measure yield and estimate reductions by calculating the percentage difference between the soiled exposed coupon and a clean unexposed one using Eq. 3, where PV_{SL} is the soiling losses based on the coupon

placed on top of the cell, PV_{Out} is the yield of the cell without any coupon on top, and PV_{Out+S} Is the cell yield with soiled coupon relative to the type of coupon.

$$\mathrm{PV}_{SL}\ (\%) = \frac{|(PV_{Out} - PV_{Out+SL}|}{\left[\frac{PV_{Out}\ +\ PV_{Out+SL}}{2}\right]} \times (100) \qquad \text{Eq. 3}$$

A correlation was conducted using Optical losses data from this study, which was used as the soiling losses value and annual PV yield data of Al Shegaya solar energy park from Global solar atlas and PVSyst. Soiling losses were calculated using Eq. 3 and compared with the estimated losses presented by GSA.

7.6 Economic analysis.

The economic analysis of the losses was conducted to determine the simple payback time of the installation. Considering the losses determined from this study, considering the losses with the assumed payback time estimated by GSA and TSK. The simple payback time was calculated using Eq. 4. The IC is the initial installation cost, AEP is the annual energy production, and x. is the price of energy displaced.

$$SP = \frac{IC}{AEP\ \times\ x./kWh} \qquad \text{Eq. 4.}$$

7.7 Results

The optical results provided the anticipated data pattern. The coupon exposed on the horizontal plane shows higher accumulation and reduces when tilted towards the vertical plane. The most significant visual loss record is 52% when the coupon is exposed horizontally, as shown in Figure 1.

The most negligible loss is recorded from the coupon on the vertical with about a 25% reduction. The calculated optical loss for the optimum tilt angle is 46.4% based on the annual optimum angle of 31° for the region.

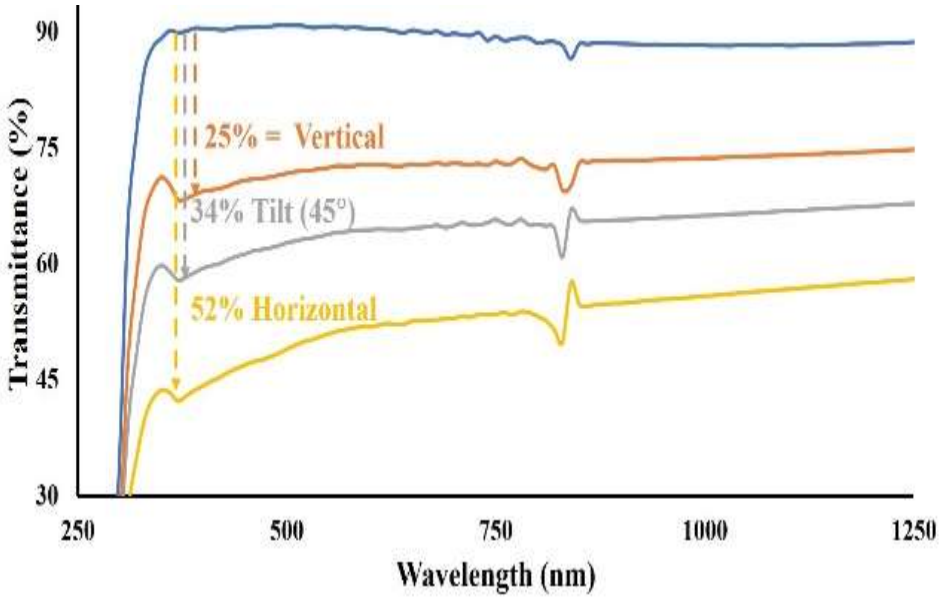

Figure 7.1: Optical losses variation highlight losses relative to angular positioning.

7.8 Particle size.

The size of particles and the space they occupied on the coupon represent the optical losses recorded. The accumulation appears to be having a significant amount of PM_{10} and $PM_{2.5}$ particles. Although the accumulation pattern was observed to be non-uniform, having larger particles in layers could reduce the photon influx. Refer to Figure 2 for an SEM imaging of accumulated dust. The majority of the particles have aggregated structures that could affect light transmittance.

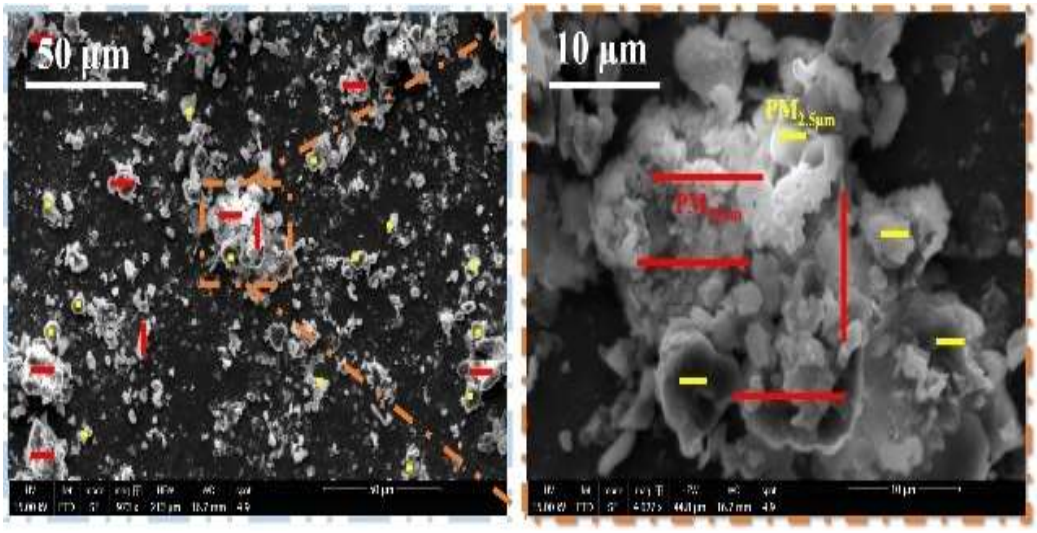

Figure 7.2: SEM imaging illustrates particle size, shapes and accumulation pattern.

7.9 Backscattering Images.

The backscatter image was further characterised using the EDX for elementology analysis. The finding shows elements belong to varying groups. For example, some metalloids (Si), transitional metals (Mo and Fe), alkaline metals(Na, K and Al), alkaline earth metals (Mg and Ca) and halogens are known as reactive non-metals(Ci and Br). Figure 3 shows the elements recorded from the EDX analysis. A detailed explanation of the various aspects is provided in the discussion section.

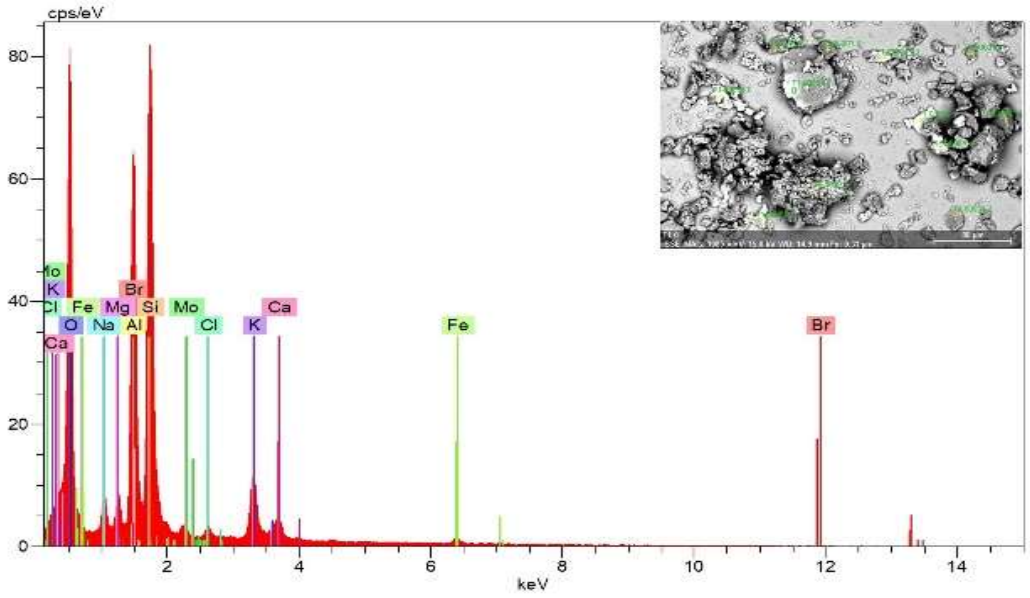

Figure 7.3: EDX graphs illustrating elements recorded on the exposed coupon.

The recorded minerals, through XRD analysis, show diaphane particles to be transparent to translucent. (Actinolite, Calcite, Clinochlore, Dolomite, Gypsum, Lizardite and Muscovite), transparent to opaque (kaolinite) properties.

All these minerals could affect the transmittance at varying capacities, where some will complete attenuate an influx of photons. The diffractometer chart is provided in Figure 4.

Yield losses determined using a simulator show a similar trend of losses considering the optical losses. The most significant PV power yield loss was recorded on the horizontal coupon with about 53% reduction, followed by 38%. In comparison, the lowest was 25% from the verticle plane. The PV performance reduction due to soiling was closely similar to optical losses.

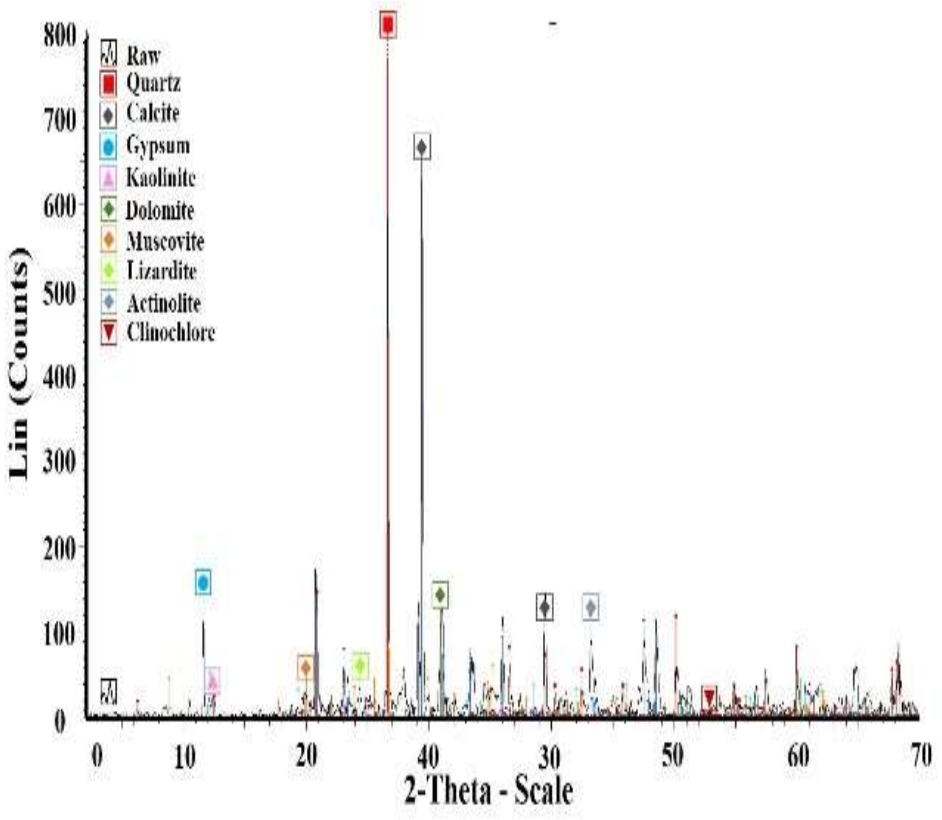

Figure 7.4: Diffractometer illustrating peaks in minerals accumulated on the exposed coupon.

7.10 Performance parameters.

Figure 5 illustrates the performance parameter where short-circuit current (ISC) is highlighted to demonstrate the impact of soiling losses on PV performance. Position loss from the optimum tilt angle of the region was calculated, finding that about 43% soiling loss could occur when a coupon is positioned on the plane (31). In addition, significant variation was observed in the short-circuit current, which reduced the power out.

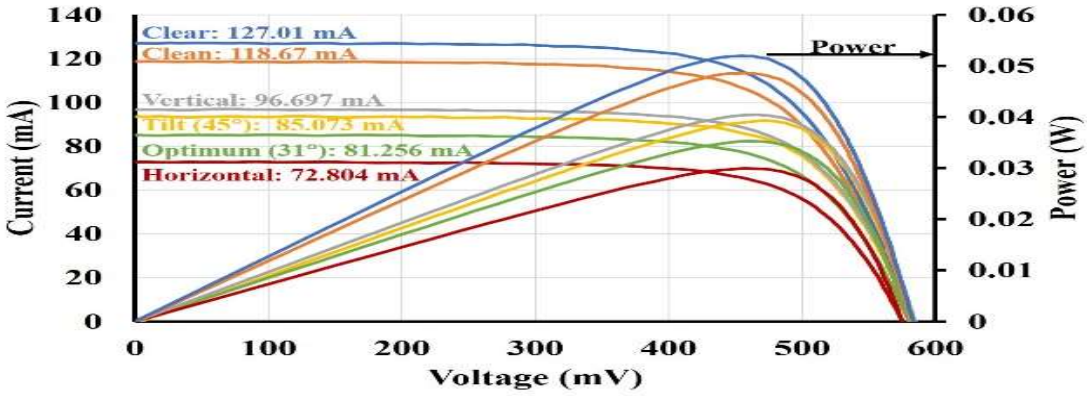

Figure 7.5: IV Curves illustrating PV yield variation.

7.11 Economic losses.

The Al Shegaya energy park PV yield losses correlated with optical losses to determine possible soiling losses, employing 46% as the calculated soiling losses. A reduction from 17,760,000 to 9,519,000 KWh/10MWp was estimated.

This reduction is further translated into economic losses, where a simple payback time analysis was calculated. The findings show it would take about 45 years before the installation will attain a return on investment. This simple payback calculation ignored operations and maintenance (OM), regaining performance due to other factors that could reduce the impact of soiling.

7.12 Discussion.

The results exhibit comparable findings where the optical losses are in relatively good agreement with PV yield losses and could be related to an asset yield loss.

The Morphology, elementology and mineralogy studies highlight that PV yield losses drove optical losses through the attenuation, scattering, and reflection of influx photons. It was observed that most of the accumulated particles are of larger grain sizes, aggregated in conglomerate clusters, and non-uniform deposition.

Some elements recorded are highly reactive and conductive metals, while others (halogens) are reflective. Most of the minerals recorded were found to be around translucent, some opaque. These transparency levels could disrupt light transmittance, mainly when accumulated in aggregated patterns observed from the SEM imaging. Reduction of light transmittance means PV performance reduction.

7.13 Optical losses.

Optical losses and PV yield results highlighted alarming losses, which render the technology unprofitable. However, an installed PV system exposed under normal conditions will last approximately 25 years. The results show that simple payback using the GSA atlas soiling level could reach 24 and 45 years.

Adopting the optical data from this study indicates that the investment is not viable and would return the investment. However, the soiling losses are not expected to remain at this level since seasonality tends to cause variation.

In addition, the site was reported by AL-Rasheedi et al. [5] to adopt a mitigation technique using a semi-automated system attached to a tractor. However, the cleaning is only conducted five times a year, which is assumed to be inadequate.

Other methods were reported by Chanchangi et al. [13] to have the capacity to mitigate these losses with different performance efficiency, and some are natural (rain and wind). However, cementation and calcification are extremely resistive simple detachment forces. Therefore, it is recommended to investigate the adhesion forces and the factors influencing them in the region.

The presented results demonstrated the adequacy and effectiveness of an integrated approach, considering the limited data. However, the output shows discrepancies with the expected performance of the assets.

Even though some factors such as seasonality, climatic conditions, operating costs for maintenance, and change in accumulation over time were ignored. The full potential of this approach can be realised if all of the above factors are taken into account; as such, this report must be interpreted in light of those limitations.

Chapter 8: Conclusion and *Recommendations.*

8.1 Conclusions.

Photovoltaics have been investigated through a comprehensive literature review as well as various theoretical and experimental studies. In addition, the impact of environmental conditions, such as soiling and temperature. Its implications on Photovoltaics have been

discussed in detail while highlighting the need for enhanced considerations towards the ecological situation and the Pv cells.

Soiling can be a severe issue for PV systems worldwide, becoming more concerning due to the rapid PV market expansion. As a result, mitigation strategies have been implemented to eliminate or reduce its effects. However, it must be tailored to the specific conditions and configuration of each PV site; in addition, the intrinsic complexity and variability of soiling make it still difficult to predict. For these reasons, it has to be constantly monitored.

Solar energy can theoretically meet all of our current and future energy needs. Many solar cells are available, including monocrystalline, poly-crystalline, and thin-film. Nevertheless, the technology lags and is hampered by the complex process of producing highly efficient single crystal cells. Polycrystalline cells are cheaper to produce, but they're not as efficient as monocrystalline cells. Multi-junction cells with different bandgaps are used to improve efficiency, but there are some disadvantages. This will lead to more complex and expensive products. The manufacturers will have to decrease their manufacturing costs and increase their output power. Manufacturers need to develop and increase the size of wafers to build larger panel formats that can generate up to 600 watts of power. Hence, larger cells have more surface area. Combined with the latest cell technology, multiple busbars (MBB), PERC and mosaic tape, they can increase efficiency by up to 22%. New technology allows for further development in materials better suited for solar cells or an increase in efficiency. Reducing the thickness of a cell produces savings in manufacturing costs.

The latest developments allow for further advances in research and development in cell metasurfaces structures and cell efficiencies. According to Carlos II University, 9th February 2021 has allowed multiple performance improvements, with up to 40% efficiency improvement possible. Metasurfaces are a new design that could significantly improve future solar cell performance. Reducing the thickness of the layer will result in more current being generated, which can be saved on materials and manufacturing costs. The reduced thickness of the film and the extraction of electrons generated by light are more effective at reducing interference. They have fewer paths to cross where they will be reabsorbed. The heat generated by light absorption in the surrounding layers causes a warming effect, which reduces the defect in long-term solar installations. And can be applied to future installations to achieve better energy efficiency and increase cell efficiency.

Chapter two discusses different ways to cool small domestic solar panels. The temperature of the PV cell decreases by about 12° C when it is cooled with air. The system's electrical

efficiency in air cooling does not always increase as the air's mass flow rate increases. There is a specific mass flow rate value that is optimum. The cooling effect of water spray on a solar cell's performance is significant; even a low flow rate of water spray has a noticeable impact. Water cooling significantly lowers the PV cell's operating temperature, improving the PV panel's electrical performance. Finned cooling system reduces the temperature of the photovoltaic panel and enhances its electrical efficiency.

Chapter three, The cleaning of your module is a simple task essential for keeping your site running smoothly. The machine produces a lot of energy quickly. The frequency of module cleaning will be determined by local site conditions and the time of year. The level of soiling on solar cell modules will vary depending on the site where they are installed. Still, the frequency of cleaning will be determined by the location and the ground material around the modules. This article discusses the various parameters of solar photovoltaic panels and different cleaning systems that have been developed up to the present day.

Chapter four established that c-Si solar cells perform better at higher temperatures than a-Si:H, CdTe, or CIGS solar cells, producing the following results:

- The Voc, FF, Pmax and efficiency of the four solar cells decrease as the temperature increases.
- The Voc of all four batteries increased slightly as the temperature increased.
- The c-Si solar cell with a temperature coefficient of -0.0020/K had the lowest impact on Voc.

The Pmax temperature coefficient values for c-Si, CdTe CIGS, and A-Si are -0.0724/K, -0.0112/K, -0.0663/K and 0.0362/K. CdTe solar cells are more stable during power generation at high temperatures.

Chapter five concluded The worldwide proliferation of various photovoltaic technologies, such as c-Si, thin-film, and CPV, confirms the viability of photovoltaic technologies. The energy source could become the leading one in the future. Each technology has a different success rate depending on whether it can help companies achieve their goals, such as improving manufacturing procedures and reducing costs. Understanding other photoelectric technologies' characteristics are essential to making informed decisions about one to use. PV systems are designed to generate energy, be as efficient as possible, and have good PR (public relations). These parameters are essential for all productivity studies of solar energy systems, including those focused on performance losses. Solar radiation, ambient

temperature, and solar spectrum all affect the efficiency of solar panels. Another essential factor to consider is how the material will degrade over time. Understanding the characteristics of different outdoor photoelectric technologies helps integrate them into other climatic conditions. For example, this information was obtained by examining their seasonal factors and the effects of temperature, pollution and power ratings.

Chapter six identified that inverter needs a cool, dry, ventilated area to work optimally. However, both indoor and outdoor installation is also possible. However, protection from direct sunlight, moisture, and other factors can increase the operating temperature, which can shorten the 'inverter's life span.

Chapter seven, the study's results showed that an integrated approach is practical and adequate when considering the limited data. However, the test results show that the assets are not performing as expected. However, some factors such as seasonality, climatic conditions, maintenance operating costs, and change in accumulation over time are ignored. The full potential of this approach can be realised if all the above factors are considered. As such, this report should be interpreted in light of those limitations.

8.2 Recommendations for Future works.

• Future work will include studying the effects of pollution on temperature and spectral fluctuations concerning parameters such as precipitation and particulate matter.

• It is expected that pollution's main effect on temperature is reducing radiation to the cell, which leads to lower unit temperature.

• Non-uniform contamination may result in mismatch effect issues between receivers, resulting in problems with hot spots. For spectral influence, the soiling tends to decrease the blue part of the spectrum the most.

• This effect may lead to a mismatch between the top and middle subcells, reducing the module's output and increasing the cell's temperature.

Bibliography

Chapter 1

[1] MIT News, MIT news office 26th October 2011.

[2] M. Mani and R. Pillai, "Impact of dust on solar photovoltaic (PV) performance: Research status, challenges, and recommendations," Renew. Sustain. Energy Rev., vol. 14, no. 9, pp. 3124–3131, 2010.

[3] H. Qasem, T. R. Betts, H.Mullejans, H. Albsairi and R.Gottschalg, "Dust induced shading on photovoltaic modules," Prog. Photovoltaics Res.Appl, vol. 22, pp. 218–236, 2014.

[4] Edinburgh Research Explorer. https://www.research.ed.ac.uk/portal/files/147360114/MuslemaniEtAlProcesses2000BusinessModelsForCarbonCapture.pdf.

[5] International Energy Agency, World Energy outlook 2020.

[6] World energy model, World Energy outlook 2020.

[7] International Energy Agency, World Energy outlook 2020.

[8] A. Luque, S. Hegedus, Handbook of Photovoltaic Science and Engineering, John Wiley & Sons, Ltd, Chichester, UK, 2003. Doi: 10. 1002/0470014008.

[9] A. Goetzberger, V. Hoffmann, Photovoltaic solar energy generation, Springer, 2005.

[10] Worldbank.org/indicator/NY.GDP.MKTP.PP.CD 20th November 2019.

[11] IEA, Energy Efficiency 2019 (Paris: 2019).

[12] IEA, World Energy Statistics and Balances, 2019.

[13] International Energy Agency, World Energy outlook, renewable power capacity in 2019.

[14] Solar PV from IEA PVPS.

[16] IEA PVPS, Snapshot of Global PV Markets 2020.

[17] IEA PVPS, Trends in Photovoltaic Applications 2019.

[18] P. Mints, SPV Market Research. The Solar Flare, no. 2 (30th April 2020).

[19] Global news investment in renewable power and fuels does not include hydropower projects larger than 50 kW Ibid.

[20] Cumulative PPA for large scale solar signed in France, PV magazine 22nd May 2019.

[21] Snapshots of Global PV markets 2020.

[22] MENA Solar is gaining traction in the MENA region-but plenty of obstacles, PV magazine 17th January 2020.

[23] MESIA Solar is gaining traction in the MENA region-but plenty of obstacles, PV magazine 17th January 2020.

[24] Latest news, Dubai electricity and water authority 8th October 2019.

[25] 300 MW solar plugs into grid renew November 2019.

[26] Iraq kicks off a substantial 755MW solar tender PV magazine 3rd May 2019.

[27] https://ens.kd/en/our-serivce/staistics-data-key-figures-and -energy -maps/annual-and-monthly -figures.

[28] IEA PVPS, Trends in Photovoltaic Applications 2018: Survey Reports of Selected IEA countries between 1992 and 2017.

[29] IEA PVPS, Trends in Photovoltaic Applications 2019.

[30] P.S. Molina, "Repsol set up renewable unit" PV magazine 9th October 2019.

[31] R. Baitelo, Associacao Brasileira de Energia Solar Fotovoltaica ABSOLAR), personal communication with REN21, 7th April 2020.

[32] Solar Power Europe Trends in Photovoltaic Applications 2019.

[33] IEA PVPS, Trends in Photovoltaic Applications 2018.

[34] IEA PVPS, Trends in Photovoltaic Applications 2019.

[35] Corporate purchasing from information and sources elsewhere in this section; self-consumption from IEA PVPS, Snapshot of Global PV Markets 2020.

[36] E. Bellini, "Italy deployed 737 MW of solar in 2019", Pv magazine, 21st April 2020.

[37] S. Chunduri, "TaiyangNews first report on high-efficiency cell technologies provides an overview from PERC to passivated contacts and HJT," TaiyangNews, 21st November 2019.

[38] S. Dutta," Global module suppliers Trina and Canadian Solar announce world record efficiencies," Mercom India, 31st May 2019.

[39] Expansions were monocrystalline from SolarPower Europe, Global Market Outlook for Solar Power 2019-2023 (Brussels: 2019).

[40] IEA, "Tracking power – solar PV," https://www.iea.org/reports/tracking-power-2019/solar-pv, viewed 17th April 2020.

[41] New standard and reasons from Solar Power Europe, 1st April 2018.

[42] M. Osborne," LONGi Solar becomes world's largest module manufacturer with the latest expansion," PV-Tech, 11th March 2019.

[43] P. Mints, Photovoltaic Manufacturer Shipments, 2017.

[44] Haugwitz, IEA, Renewables, 2017.

[45] REC," REC Group kicks off mass production of its ground-breaking Alpha module in Singapore," press release (Tuas, Singapore: 10th October 2019).

[46] The maximum theoretical efficiency of silicon solar cells is 32%; Graphene Flagship, "Graphene, perovskites, and silicon—an ideal tandem for efficient solar cells," phys.org, 3rd March 2020.

[47] J. Yoo et al., "An interface stabilised perovskite solar cell with high stabilised efficiency and low voltage loss," Energy & Environmental Science, vol. 12, no. 7 (2019), pp. 2192-99.

[49] A. Dominguez, R. Geyer. Photovoltaic waste assessment in Mexico, Resources, Conservation, and Recycling: vol 127. pp 29-41, 2017.

[50] Sergey V. Ushakov, Alexandra Navrotsky, Qi-Jun Hong, Axel van de Walle. "Carbides and Nitrides of Zirconium and Hafnium" Materials; 26th August 2019.

[51] A. Extance," The reality behind solar power's next star material," Nature, 25th June 2019, https://www.nature.com/articles.

[52] William Zappe, Machteldvan den Broek; Analysing the potential of integrating wind and solar power in Europe using spatial optimisation under various scenarios, Renewable and Sustainable Energy Reviews, Vol 94, pp 1192- 1216, 2018.

[53] J. Runyon, "SunPower releases most efficient residential solar panel on the market," Renewable Energy World, 3rd May 2019.

[54] Global Markets Outlook; Solar Power Europe 2018-2022.

[55] J. Crescenti, "Discussing bifacial project economics," Pv magazine, 19 February 2020.

[56] Rajendra S, Githin F, Alapatt A.L. Making solar cells a reality in every home: Opportunities and Challenges for Photovoltaic Device Design; IEEE Journal of Electron Devices Society 2013; 1(6): 129-144.

[57] Razykov T M, Ferekides C S, Morel D, Stefanakos E, Ullal H S Upadhyaya H M. Solar photovoltaic electricity: current and future prospects. Solar Energy 2011; 85: 1580-608.

[58] Mohammad Tawheed Kibria, Akil Ahammed, Saad Mahmud Sony, Faisal Hossain: A Review: Comparative studies on different generation solar cells technology; Proceedings of 5th International Conference on Environmental Aspects of Bangladesh [ICEAB 2014].

[59] S. Taira, Y. Yoshimine, T. Baba, M. Taguchi, H. Kanno, T. Kinoshita, H. Sakata, E. Maruyama M. Tanaka, our approaches for achieving HIT solar cells with more than 23% efficiency in: Proceedings of the 22nd European Photovoltaic SolarEnergy Conference, Milan, Italy, 3–7 September 2007, 932–935.

[60] Y. Tsunomura, Y., M. Taguchi, T. Kinoshita, H. Kanno, H. Sakata, E. Maruyama, M. Tanaka, 22%-Efficiency HIT solar cell, SANYO Electric Co., Sep. 2007.

[61] L. Zhao, C. L. Zhou, H. L. Li, H. W. Diao and W.J. Wang, Design optimisation of bifacial HIT solar cells on p-type silicon substrates by simulation, Sol. Energy Mater. Sol. Cells 92 (2008), 673–681

[61] Bhalchandra V.C, Y.A Sadawarte. The factors |affecting the Performance of Solar Cells: International Journal of Computer Applications (0975-8887); International Conference on Quality Up-gradation in Engineering Science and Technology (ICQUEST2015)

[62] Becker C, Sontheimer T, Steffans S, Scherf S, Rech B, Poly-crystalline silicon thin films by high-rate electron beam evaporation for photovoltaic applications – the influence of substrate texture and temperature. Energy Procedia 2011; 10: 61-5

[63] Kalogirou S. "Solar energy engineering: process and systems: chapter 9". Academic Press; 2009. P. 469-517.

[66] Qusay Assim Hanna Al-Naser, Noorah Mohammed Ahmed Al-barghoothi, Noor Ahmad Salman Al-Ali "The Effect of Temperature Variations on Solar Cell Efficiency," International Journal of Engineering, Business and Enterprise Applications (IJEBEA).

[67] Fundamentals of PV material (1998)

[68] Lles PA, Evolution of space solar cells, Solar Energy Materials and Solar Cells 2001; 68:1-3.

[69] VV Tyagi, Nurui A.A Rahim, N.A Rahim, Jeyraj A L, Selvara, J . Progress in solar PV technology: Research and achievements. Renewable and Sustainable Energy Reviews 20, 2013: 443-461.

[70] Soteris A. Kalogirou, Photovoltaic Systems in Solar Energy Engineering, 2009.

[71] Parida B, Iniyan S, Goic R. A review of solar photovoltaic technology. Renewable and Sustainable Energy Reviews 2011:15:1625 -36.

[72] Boutchich M, Alvares J, Diouf D, Cabarrocas P. R.I, Liao M, Masaataka J, et al., Amorphous silicon diamond-based hetero-junctions with high rectification ratio. Journal of Non –crystalline Solids 2012.

[73] Britt J, Ferekides C, Applied Physics letter 1993; 62:2851.

[74] https://www.energy.gov/eere/solar/copper-indium-gallium-diselenide.

[75] A. Morales-Acevedo, Solar cells, research, and application perspectives (Arturo morales-Acevedo: 2013).

[76] N. P. Klochko, K. S. Klepikova, I. I. Tyukhov, et al., "Structure and optical properties of sequentially electrodeposited ZnO/Se bases for ETA solar cells," Solar Energy, vol. 120, pp. 330–336, 2015

[77] X.Jiaxiong, J. Phys. Chem.solids 98.32 (2016).

[78] Itoh M, Tanahashi H, Fujii T, Takakura H, Hamakawa Y, Matsumoto Y. Evaluation of electric energy performance by democratic module PV system field test. Solar Energy Materials and Solar Cells 2001; 67:435-40.

[79] Gratzel M. Dye-sensitized solar cells. Journal of photochemistry and Photobiology C: Photochemistry Review 2003; 4:145-53.

[80] Renewable and Sustainable Energy Reviews. https://umexpert.um.edu.my/public_view.php?type=publication&row=Mjg2ODk%3D

[81] Sethi VK, Pandey M, Shukla P. Use of nanotechnology in solar cell PV International Journal of Chemical Engineering and Applications 2011; 2.

[82] Serrano E, Rus G, Garcia-Martinez J. Nanotechnology for sustainable energy; Renewable and Sustainable Energy Reviews 2009; 13:2372-40.

[83] J.P. Salvetat, appl Phys A 69(3), 255-260 (1991).

[84] M.S.Dresselhauset, R.Soc, Lond Ser A.Philos Trans A Maths Phys Eng Sci 362(1823). 2065- 2098(2004).

[85] T.W.Odem, Nature 391(6662), 62-64 (1998).

[86] E.Pop. Nano Lette, 6(1). 96-100 (2006).

[87] Chang, L. Y. et al. Low-temperature solution-processed solar cells based on PbS colloidal quantum dot/CdS hetero-junctions. Nano Lett. 13, 994–999 (2013).

[88] Strein, E. et al. Charge generation and energy transfer in hybrid polymer/infrared quantum dot solar cells. Energy Environ. Sci. 6, 769–775 (2013)

[89] Semonin, O. E. et al. peak external photocurrent quantum efficiency exceeding 100% via MEG in a quantum dot solar cell. Science 334, 1530–1533 (2011).

[90] Lucio Claudio Andreani, Angelo Bozzola, Piotr Kowalczewski, Marco Liscidini & Lisa Redorici (2019) Silicon solar cells: toward the efficiency limits, Advances in Physics:
X, 4:1, DOI: 10.1080/23746149.2018.1548305

[91] Nam-Gyu Park, Perovskite solar cells: an emerging photovoltaic technology material today Volume18, issue 2, March 2-15, Pages 65-72.

[92] Martin A. Green, Anita Ho-Baille and Hendry J. Snaith The emergence of perovskite solar cells. NATURE PHOTONICS, vol 8, July 2014.

[93] A. Luque, S. Hegedus, Handbook of Photovoltaic Science and Engineering, John Wiley & Sons, Ltd, Chichester, UK, 2003. DOI: 10.1002/0470014008.

[94] RA Messenger, J. Ventre, Photovoltaic Systems Engineering, 2005.

[95] M. a. Green, A. Ho-Baillie, Forty-three per cent composite split-spectrum concentrator solar cell efficiency, Prog. Photovoltaics Res. Appl. 18 (2010) 42–47. doi:10.1002/pip.924.

[96] B. Mitchell, G. Peharz, G. Siefer, M. Peters, T. Gandy, J.C. Goldschmidt, et al., Four-junction spectral beam-splitting photovoltaic receiver with high optical efficiency, Prog. Photovoltaics Res. Appl. 19 (2011) 61–72. doi:10.1002/pip.988.

[97] J.D. McCambridge, M.A. Steiner, B.L. Unger, K.A. Emery, E.L. Christensen, M.W. Wanlass, et al., Compact spectrum splitting photovoltaic module with high efficiency, Prog. Photovoltaics Res. Appl. 19 (2011) 352–360. doi:10.1002/pip.1030.

[98] A. Barnett, D. Kirkpatrick, C. Honsberg, D. Moore, M. Wanlass, K. Emery, et al., Very high-efficiency solar cell modules, Prog. Photovoltaics Res. Appl. 17 (2009) 75–83. doi:10.1002/pip.852.

[99] M. Stefancich, A. Zayan, M. Chiesa, S. Rampino, D. Roncati, L. Kimerling, et al., Single element spectral splitting solar concentrator for multiple cells CPV system. Opt. Express. 20 (2012) 9004–18.

[100] B. Burnett, The basic physics and design of III-V multijunction solar cells, 2002.

[101] MA Green, K. Emery, Y. Hishikawa, W. Warta, E.D. Dunlop, Solar cell efficiency tables (Version 45), Prog. Photovoltaics Res. Appl. 23 (2015) 1–9. doi:10.1002/pip.2573

[102] A.W. Bett, C. Baur, R. Beckert, F. Diimroth, Development of high-efficiency mechanically stacked GaInP/GaInAs-GaSb triple-junction concentrator solar cells, in: 17th EU-PVSEC, Munich, 2001: pp. 3–6.

[103] R.R. King, D. Bhusari, D. Larrabee, X.-Q. Liu, E. Rehder, K. Edmondson, et al., Solar cell generations over 40% efficiency, Prog. Photovoltaics Res. Appl. 20 (2012) 801–815. doi:10.1002/pip.1255.

[104] C. Chukwuka, K.A. Folly, Overview of Concentrated Photovoltaic (CPV) Cells, J. Power Energy Eng. 02 (2014) 1–8. doi:10.4236/IEEE.2014.211001.

[105] A.W. Bett, S.P. Philipps, S.S. Essig, S. Heckelmann, R. Kellenbenz, V. Klinger, et al., Overview about Technology Perspectives for High-Efficiency Solar Cells for Space and Terrestrial Applications, in 28th Eur. Photovolt. Sol. Energy Conf. Exhib., Paris, 2013: pp. 1–6. doi:10.4229/28thEUPVSEC2013-1AP.1.1.

[106] S.P. Philipps, F. Dimroth, A.W. Bett, High-Efficiency III-V Multijunction Solar Cells, in: Pract. Handb. Photovoltaics, Elsevier Ltd, 2012: pp. 417–448. doi:10.1016/B978-0-12-385934-1.00013-1.

[107] A. W. Bett, F. Dimroth, G. Stollwerck, O.V. Sulima, III-V compounds for solar cell applications, Appl. Phys. A Mater. Sci. Process. 69 (1999) 119–129.doi:10.1007/s003390050983.

[108] K. C. Pfluke, "Soldering Photovoltaic Cells," Eff. Br. mindfulness Interv. acute pain Exp. An Exam. Individ. Differ., vol. 1, 2015.

[109] K. C. Pfluke, "Photovoltaic Module Assembly Using SMT Materials and Processes," Renewable EnergyWorld,2009. [Online].Available: http://www.renewableenergyworld.com/articles/2009/05/photovoltaic-module.html.

[110] Applied materials Science Applications of Engineering Materials in Structural Electronics Thermal and other industries D@www.researchgate.net.

[111] A. Nishimura, Y. Hayashi, K. Tanaka, M. Hirota, S. Kato, M. Ito, K. Araki, and E. J. Hu, "Life cycle assessment and evaluation of energy payback time on high-concentration photovoltaic power generation system," Appl. Energy, vol. 87, no. 9, pp., 2797–2807, 2010.

[112] Kam Hoe Ong, Ramasamy Agileswari, Biancamaria Maniscalco, Panagiota Arnou, Chakrabarty Chandan Kumar, Jake W.Bowers, and Marayati Bte Marsadek "Review on Substrate and Molybdenum Back Contact in CIGS Thin Film Solar Cell" Volume 2018 |Article ID 9106269 InternationalJournal of Photoenergy / 2018 /| https://doi.org/10.1155/2018/9106269.

[113] February 2010. http://www.rise.org.au/info/Education/ SAPS/sps003.html.

[114] X.-J. Ma, J.-Y. Wu, Y.-D. Sun and S.-Q. Liu, "The Research on the Algorithm of Maximum Power Point Tracking in Photovoltaic Array of Solar Car," Vehicle Power and Propulsion Conference, IEEE, 2009, pp. 1379-1382.

[115] N. M. Pearsall and R. Hill, "Photovoltaic Modules, Systems and Applications," In: M. D. Archer, and R. Hill, Eds., Clean Electricity from Photovoltaics, World Science, Vol. 1, 2002, pp. 1-42.

[116] International Journal for Research in Engineering. https://www.ijream.org/papers/ICRTET0154.pdf.

[117] Critical Factors that Affecting Efficiency of Solar Cells. https://file.scirp.org/Html/7-6401007_1947.html.

[118] Y. Suita and S. Tadakuma, "Driving Performances of Solar Energy Powered Vehicle with MPTC," IEEE, 2006.

[119] Shenck NS. Alternative energy systems, US Naval academy Lecture Readings; 2010.

[120] Kumar R. Rosen MA. A critical review of photovoltaic-thermal solar collectors for air heating. Applied Energy 2011; 88:3603-14. (PDF) Progress in solar PV technology: Research and. https://www.researchgate.net/publication/278187510_Progress_in_solar_PV_technology_Research_and_achievement.

Chapter 2

[1] Antonanzas, J. Osorio, N. Escobar, R. Urraca, R. Martinez-de-Pison, F.J. Antonanzas-Torres, F. Review of photovoltaic power forecasting. Solar Energy 2016, 136, 78–111.

[2] Sreekumar, S. Bhakar, R. Solar Power Prediction Models: Classification Based on Time Horizon, Input, Output and Application. In Proceedings of the International Conference on Inventive Research in Computing Applications, Coimbatore, India, 11–12 July 2018. Energies | Free Full-Text | PV Forecast for the Optimal .... https://www.mdpi.com/1996-1073/13/20/5330/html.

[3] Akhter, M.N. et al. (2019), “Review on forecasting of photovoltaic power generation based on machine learning and metaheuristic techniques”, IET Renewable Power Generation, Vol. 13/7, Institution of Engineering and Technology, Stevenage, United Kingdom, pp. 1 009–1 023.

[4] Dolara, A. Leva, S.; Manzolini, G. Comparison of different physical models for PV power output prediction. Solar Energy 2015, 119, 83–89.

[5] Lorenz, E. Hurka, J. Heinemann, D. Beyer, H.G. Irradiance Forecasting for the Power Prediction of Grid-connected Photovoltaic Systems. IEEE J. Sel. Top. Appl. Earth Obs. Remote Sens. 2009, 2, 2–10.

[6] Tato, J.H. Brito, M.C. Using Smart Persistence and Random Forests to Predict Photovoltaic Energy Production. Energies, 2019, 12, 100.

[7] IRENA_Future_of_Solar_PV_2016.pdf.

[8] Chandler,S. Purohit, S. A. Sharma, A. Nehra, S. P. and Dhaka, M.S. “A study on photovoltaic .

parameters of monocrystalline silicon solar cell with cell temperature" Energy Reports, Vol.1, pp. 104-109, 2105.

[9] M. Cellura, G. Ciulla, V. L. Brano, A. Marvuglia, A. Orioli. "A Photovoltaic panel coupled with a phase-changing material heat storage systems in hot climates," in; Proceedings of the 25th Conference on Passive and Low Energy Architecture, abstract number 582, 2009.

[10] V. M. Andreev, V. A. Grilikhes, V. D. Rumyantsev, Photovoltaic Conversion of Concentrated Sunlight, John Wiley & Sons, London, UK, 1997.

[11] Andreev, V.M.etal.,Tandem GaSb/InGaAsb thermophotovoltaic cells, Proc.26th IEEE Photovoltaic specialists conference., Anahiem,1997,935.

[12] G. Ciulla, V. L. Brano, V. Franzitta, M,Trapanese. Assessment of the Operating Temperature of Crystalline PV Modules Based on Real Use Conditions, International Journal of Photoenergy, vol. 2014, Article ID 718315, 11 pages, 2014. Assessment of the Operating Temperature of Crystalline PV .... https://www.hindawi.com/journals/ijp/2014/718315/.

[13] M. A. Green, Solar Cells, Prentice-Halls, Englewood Cliffs, NJ,1982,p.88.

[14] A.Marvuglia, et al. A PV panel coupled with a phase-changing material heat storage system in hot climates," in Proceedings of the 26th Conference on Passive and Low Energy Architecture (PLEA' 08), abstract number 582, 2008.

[15] M.Mattei,G.Notton, C.Cristofari, M.Muselli, P.Poggi Calculation of the polycrystalline PV module temperature using a simple energy balance method. Renewable Energy, vol 32,no 4,pp 553-567,2006.

[16] V. M. Andreev, et al., Photovoltaic Conversion of Concentrated Sunlight, JohnWiley &Sons, London, UK, 1997.

[17] K. Emery et al., The Temperature dependence of photovoltaic cells, modules, and systems," in Proceedings of the 26th IEEE Photovoltaic Specialists Conference, pp.1275–1278, Washington, DC, USA, May 1996.

[18] SKoplaki, E. Palyvos J.A. On the temperature dependence of a photovoltaic module electrical performance. Review of the efficiency power correlations, Solar Energy, Vol 84, no 83,no5, pp.614-624,2009.

[19] D. Evans., simplified method for predicting photovoltaic array output, Solar energy, vol27, no.6, pp.555-560,1981.

[20] G. Notton., C. Cristofari., M. Mattei., P. Poggi. “Modelling a double-glass photovoltaic module using finite differences,” Applied Thermal Engineering, vol. 25, no. 17-18, pp. 2854–2877,2005.

[21] M. Koehl., M. Heck., S. Wiesmeier., J. Wirth. “Modeling of the nominal operating cell temperatures based on outdoor weathering,” Solar Energy Materials and Solar Cells, vol. 95, no.7, pp. 1638–1646, 2011.

[22] E. Skoplaki., J. A. Palyvos. “Operating temperature of photovoltaic module, a survey of pertinent correlations,” Renewable Energy, vol. 33, no. 1, pp. 23–29, 2009.

[23] J.W. Shultz, thermal and other tests of photovoltaic modules performance in natural sunlight, Journal of Energy, Vol 3, no6,pp363-372 1979.

[24] S.Pace M.Magni A new indoor procedure for the determination of NOCT, In proceedings of the photovoltaic Solar Energy Conference, Vol 5.pp667-671.1984

[25] M.K. Fuentes, thermal modelling of residential photovoltaic arrays, in proceedings of the photovoltaic specialist Conference, Vol 17, pp.1341-1346, May 1984

[26] V.Lo Brano, G Ciulla V.Franzitta A.Viola A novel implication correlation of the operative temperature of PV panel AASRI Procedia,Vol 2,pp. 112 – 120 ,2012 .

[27] D.L. King P.E Eckbert character the performance of a large photovoltaic array for all operating conditions, proceeding with the 25th IEEE photovoltaic specialists conference, pp 1385-1388 Washington, DC, USA May 1996.

[28] Sauer, D., Rau. U., Kaltschmitt, M.,photovoltaic Power Generation.In. Kaltschmitt, M., Streicher.W and Wiese, A.,(EDS), Renewable energy- Technology, Economics and Enviroment. Berlin/Heidelberg. Springer-\verlag Publishing,pp.268-271.2007

[29] Pless, S., Deru. M., Torcellini, P., Hayster, S., Procedure for Measuring and Reporting the performance of photovoltaic systems in buildings Colorado, DOE/NREL and MRI.pp.4.2005.

[30] Hamrouni, N., Jraidi, M., Cherif, A., Solar radiation and ambient temperature effect on the performance of a PV pumping system. Review des Energies Renouvelables,11(1),95-106. 2008.

[31] Priyanka, S. and Ravindra, N.M. Temperature dependence of solar cell performance- An analysis, Solar Energy Materials and Solar Cells,101,36-45.2012

[32] Dubey, S., Sarvaiya, J.N., Seshadri, B. Temperature-dependent photovoltaics (PV) Efficiency and its Effects on PV production in the world. A Review. Energy Procedia,33, 311-321.2013.

[33] Tobnaghi, D.M., Madatov, R.,Naderi, D.,. The effect of temperature on electrical parameters of solar cells. International Journal of Advanced Research in Electrical, Electronics and Instrumentation Engineering,2(12). 2013.

[34] Mehmet Emin Meral, Furkan Dincer. “Renewable and Sustainable Energy Reviews” 15 (2022)2167-2184.

[35] Bhalchandra V Chikate, Y.A. Sadwarte. “The Factors Affecting the Performance of Solar Cell,” International Journal of Computer Applications(0975-8887) International Conference on Quality Up-gradation in Engineering, Science and Technology(ICQUEST2015).

[36] Jang, S., Park, Y.M., Sung, T.K., Jung, C.B., Kim, M.S., Analysis of power conversion efficiency of inverters for photovoltaic power generation systems. In proceeding of the winter conference of the Korean Institute of Electrical Engineers, Daejeon, Korea 28 Nov 2014, pp.421-424.

[27] Tian, AQ.Chu, S.C. Pan, J.-S.; Liang, Y. “A novel pigeon-inspired optimisation-based MPPT technique for PV systems”. Processes 2020, 8, 356.

[28] G.Ali, H.V. Arbos, R.Herrera, J.Tobón, A. Peláez-Restrepo, Non-linear sliding mode controller for photovoltaic panels with maximum PPT power point tracking. Processes 2020, 8, 108.

[39] Y. Yoon. Integrated management system to improve photovoltaic operation efficiency. Internet Broadcast. Commun. 2019, 19, 113–118.

[40] McCandless, T. Detting, S. Haupt, S.E., Comparison of impact vs explicit regime identification in machine learning methods for solar irradiance prediction. Energies 2020,13, 687.

[41] Moncada, A Richardson, W., Vega Avila, R., Deep learning to forecast solar irradiance using a six-month UTSA sky imager dataset. Energies 2018,11,1988.

[42] Mfumali, P., Sigauke, C., Bere, A., Mulaudzi, S., Day ahead hourly global horizontal irradiance forecasting. Application to South African Data. Energies 2019,12,3569.

[43] Carrera, B., Kim, B., Comparison analysis of machine learning techniques for photovoltaic prediction using weather sensor data. Sensors 2020,20,3129.

[44] Rodriguez, F., Fleetwood, A., Galarza, A., Fontan, L., Predicting solar energy generation through artificial neural networks using weather forecasts for microgrid control. Renew.Energy 2018,126,855-864.

[45] Lotfi, M., Javadi, M., Osorio, G.J., Monteiro, C., Catalao, J.P.s., A novel ensemble algorithm solar power forecasting based on kernel density estimation. Energies 2020,13,2016.

[46] Dolara, A., Grimacia, F., Leva, S., Mussetta, M., Ogliari, E., A physical hybrid artificial neural network for short term forecasting of PV plants power output. Energies 2015,8,1138.

[47] Ahmad, M.W., Mourshed, M., Rezgil, Y., Tree-based ensemble methods for predicting PV power generation and their comparison with support vector regression. Energy 2018,164,465-474.

[48] Kim, S., Jung, J.Y., Sim, MK, A two-step approach to solar power generation prediction based on weather data using machine learning. Sustainability 2019,11,1501.

[49] Akandari, M., Ahmad, I. Solar power generation forecasting using ensemble approach based on deep learning and statistical methods Appl. Compt. Inform.2020.

[50] Suresh, V., Janik, P., Rezmer, J., Leonowicz, A., Forecasting solar PV output using conventional neural networks with a sliding windows algorithm. Energies 2020,13,723.

[51] Bacher, B., Madsen, H., Aalborg Nielson, H., online short-term solar forecasting. Sol. Energy 2, 2009,83,1772-1783.

[52] Detynieck, M., Marsala, C., Krishnan, A., Siegel, M. Weather-based solar-based energy prediction of the 2012 IEEEE International Conference, Fuzzy-Systems, Brisbane, Australia,10-15 June 2012; pp. 1-7.

[53] Adullah, N.A., Abd Rahim, N., Gan, C.K., Nor Azman, N. Forecasting solar power using Hybrid Firefly and Particle Swarm Optimisation (HFPSO) for optimising the parameters in a Wavelet Transform-Adaptive Neuro-Fuzzy Inference System (WT-ANFIS). Appl. Sci. 2019, 9, 3214.

[54] Ye, J.Y., Reindl, T., Aberle, A.G., Walsh, T.M. Performance Degradation of various PV module Technologies in tropical Singapore.IEEE Journal of Photovoltaics, 4(5), Sept 2014.

[55] Haidar, Z.A., Orf, J. i., Kaneesamkandi, Z. Experimental investigation of evaporative cooling for enhancing photovoltaic panels efficiency, Results in Physics, vol. 11, pp. 690–697, 2018

[56] Sato, D., Yamada, N. Review of photovoltaic module cooling methods and performance evaluation of the radiative cooling method", Renewable and Sustainable Energy Reviews, vol. 104, pp. 151–166, 2019.

[57] Teo, H.G., Lee, P.S. and Hawlader,M.N.A. "An active cooling system for photovoltaic modules," Applied Energy, vol. 90, no. 1, pp. 309–315, 2012.

[58] Mazón-Hernández, R. J., García-Cascales, R., Vera-García, F., Káiser, A. S., Zamora, B. Improving the Electrical Parameters of a Photovoltaic Panel by Means of an Induced or Forced Air Stream", InternationalJournalof Photoenergy, vol. 2013, Article ID 830968, 10 pages, 2013.

[59] Multiconcept Methods to Enhance Photovoltaic System Efficiency. https://www.hindawi.com/journals/ijp/2019/1905041/

[60] S.S. Joshi and A.S. Dhoble, "Photovoltaic-thermal systems (PVT): technology review and future trends," Renewable and Sustainable Energy Reviews, vol. 92, pp. 848–882, 2018

[61] D.Yang and H.Yin, "Energy conversion efficiency of a novel hybrid solar system for photovoltaic, thermoelectric and heat utilisation," IEEE Transactions on Energy Conversion, vol. 26, no. 2, pp. 662–670, 2011.

[62] N.Xu, J. Ji, W.Sun, W.Huang, J.Li, and Z.Jin, "Numerical simulation and experimental validation of a high concentration photovoltaic/thermal module based on point-focus Fresnel lens," Applied Energy, vol. 168, pp. 269–281, 2016.

[63] S. Nizetic, D. Coko, A. Yadav, F. Grubiši-Cabo, Energ. Convers. Manage, 108 (2016).

[64] M. Abdolzadeh, M. Ameri, M.A. Mehrabian, Energ. Source, (2011).

[65] Y.M. Irwan, W.Z. Leow, M. Irwanto, M. Fareq, A.R. Amelia, N. Gomesha, I. Safwati, Energ. Procedia, 79 (2015).

[66] R. Ahiska, S. Dislitas Computer-controlled test system for measuring the parameters of the real thermoelectric module Energy Convers. Manag., 52 (2011), pp. 27-36

[67] C. Yu, K.T. Chau Thermoelectric automotive waste heat energy recovery using maximum power point tracking Energy Covers. Manag., 50 (2009), pp. 1506-1512

[68] J. Yeom, M.A. Shannon, 3.16 Micro-Coolers, in Y. Gianchandani, O. Tabata, H. Zappe (Eds.), Compr. Microsystems, Elsevier, New York, 2007: pp. 499–550.

[69] T. Cotter, Principles and prospects for micro heat pipes, 1984.

[70] C.B. Sobhan, R.L. Rag, G.P. Peterson, A review and comparative study of the investigations on micro heat pipes, Int. J. Energy Res. (2007) 664–688. doi:10.1002/er.

[71] Y.M. Hung, Q. Seng, Effects of geometric design on the thermal performance of star-groove micro-heat pipes, Int. J. Heat Mass Transf. 54 (2011) 1198–1209. doi:10.1016/j.ijheatmasstransfer.2010.09.070.

[72] G.F. Peterson, A.B. Duncan, M.H. Weichold, Experimental investigation of micro heat pipes fabricated in silicon wafers, J. Heat Transfer. 115 (1993) 751–756.

[73] S.H. Moon, G. Hwang, S.C. Ko, Y.T. Kim, Experimental study on the thermal performance of micro-heat pipe with a cross-section of polygon, 44 (2004) 315–321. doi:10.1016/S0026-2714(03)00160-4.

[74] B. Suman, P. Kumar, An analytical model for fluid flow and heat transfer in a micro-heat pipe of polygonal shape, Int. J. Heat Mass Transf. 48 (2005) 4498–4509. doi:10.1016/j.ijheatmasstransfer.2005.05.001.

[75] S. Kang, D. Huang, Fabrication of star grooves and rhombus grooves micro heat pipe, J. Micromechanics Microengineering. 12 (2002) 525–531.

[76] Y.X. Wang, G.P. Peterson, Analysis of Wire-Bonded Micro Heat Pipe Arrays, J. Thermophys. Heat Transf. 16 (2002) 346–355. doi:10.2514/2.6711.

[77] Y. Wang, G.P. Peterson, Optimisation of micro heat pipe radiators in a radiation environment, J. Thermophys. Heat Transf. 16 (2002) 537–546.

[78] W. Liu, J. Kang, X. Fu, C. Stefanini, P. Dario, Analysis on the heat resistance of the micro heat pipe with arteries, Microelectron. Eng. 88 (2011) 2255–2258. doi:10.1016/j.mee.2011.02.082.

[79] H. Chien, C. Tsai, P. Chen, P. Chen, Improvement On Thermal Performance Of, Micro. (2003) 389–391.

[80] Z.-H. Liu, Y.-Y. Li, A new frontier of nanofluid research – Application of nanofluids in heat pipes, Int. J. Heat Mass Transf. 55 (2012) 6786–6797. doi:10.1016/j.ijheatmasstransfer.2012.06.086.

[81] M. Le Berre, S. Launay, V. Sartre, M. Lallemand, Fabrication and experimental investigation of silicon micro heat pipes for cooling electronics, J. Micromechanics Microengineering. 13 (2003) 436–441. doi:0960-1317/13/3/313.

[82] Y.-S. Lee, Y.-P. Lee, Y. Lee, The effects of surface tension and wire diameter on the rise velocity of a bubble in a miniature two-phase closed thermosyphon, Appl. Therm. Eng. 16 (1996) 655–668. doi:10.1016/1359-4311(95)00081-X.

[83] H.A. Hussien, A.H. Numan, A.R. Abdulmunem, Mater. Sci. Eng. 78 (2015).

[84] H.M.S. Bahaidarah, IEEE, (2015).

[85] H. Bahaidarah, A. Subhan, P. Gandhidasan, S. Rehman, Energ. 59 (2013).

[86] H. G. Teo, P.S. Lee, M.N.A. Hawlader, Appl. Energy. 90 (2012).

[87] J. K. Tonui, Y. Tripanagnostopoulos, Renew. Energy, 32 (2007).

[88] M. Ameri, M.M. Mahmoudabadi, A. Shahsavar, Energy. Source, (2012).

[89] M. Chandrasekar, T. Senthilkumar, Heat Mass Transfer, (2016).

[90] T. Nehari, M. Benlakam, D. Nehari, 60 (2016).

[91] J.A. Gotmare, D.S. Borkar, P.R. Hatwar, Int. J. Adv. Manuf. Tech, (2015).

Chapter 3

[1] Arash ayyaah, M.N.Horenstein, Malay K. “Energy yield loss caused by dust deposition on photovoltaic panels” Solar Energy, Volume 107, September 2014, Pages 576-604.

[2] E. Asl-Soleimani, S. Farhangi, M. Zabihi. The effect of tilt angles, air pollution on the performance of photovoltaic systems in Tehran, Renew energy, 24 (2001), pp. 459-468

[3] Nathar NM, Gupta JP. Effects of dust transmittance of glazing materials for solar collectors under arid zone conditions of India.Solar and wind Technology,1990;7:237-243.

[4] Said SAM. Effects of dust accumulation on performances of thermal and photovoltaic flat plate collectors. Applied Energy:1990;37(1);73-84

[5] Goossens D, Van Kerschaever E. Aeolian dust deposits on photovoltaic solar cells: the effects of wind velocity and airborne dust concentration on cell performance. Solar Energy:1999,66(4):277-289.

[6] Z.A. Darwish, H.A. Kazem, K. Sopian, M. Al-Goul, H. Alawadhi Effect of dust pollutant types on photovoltaic performance Renew Sustain Energy Rev, 41 (2015), pp. 735-744

[7] Denholm P, Drury E, Margolis R, and Mehos M, Solar Energy: the largest energy resource. In: Sioshansi FP, editor. Generating electricity in a carbon-con-strained world. California: Academic Press; 2010. p. 271-302.

[8] M. Mani and R. Pillai, "Impact of dust on solar photovoltaic (PV) performance: Research status, challenges, and recommendations," Renew. Sustain. Energy Rev., vol. 14, no. 9, pp. 3124–3131, 2010.

[9] Ghazi S, Sayigh, Ip K "Dust effect on flat surfaces – a review paper. Renew Sustainable Energy Review 2014; 33; 742-51.

[10] T. Sarver, A. Al-Qaraghuli, and L. L. Kazmerski, "A comprehensive review of the impact of dust on the use of solar energy: History, results, literature, and mitigation approaches," Renew. Sustain. Energy Rev., vol. 22, pp. 698–733, 2013.

[11] Salim A, Huriab F, Eugenio N. PV power-study of system options and optimisation. In: Proceedings of the 9th European PV solar energy conference; 1988

[12] Syafiq, A.; Pandey, A.K.; Adzman, N.N.; Abd Rahim, N. Advances in approaches and methods for self-cleaning of solar photovoltaic panels. Solar Energy 2018, 162, 597–619

[13] Ziedan, H.A.; Elbaset, A.A.; Mourad, A.N. Optimization of PV/wind power system case study: supplying large industry load in Egypt. J. Eng. Appl. Sci. 2020, 15, 1014–1020.

[14] Monto Mani R.Pillai Impact of dust on solar photovoltaic (PV) performance: Research status, challenges and recommendations, Renewable and Sustainable Energy ReviewsVolume 14, Issue 9, December 2010, Pages 3124-313.

[15] Cano, J. Photovoltaic Modules: Effect of Tilt Angle on Soiling. Master's thesis, Arizona State University, Tempe, AZ 2011.

[16] J.Y. Hee, L.V. Kumar, A.J. Danner, H. Yang, C.S. Bhatia The effect of dust on transmission and self-cleaning property of solar panels Energy Proc., 15 (2012), pp. 421-427

[17] Arash, S, M.Nhorenstein, Malay K.Mazumber. Yield loss of photovoltaic panels caused by depositions. http://www.alionenergy.com/wp-content/uploads/2016/03/Yield-Loss-of-PV-Panels-Caused-by-Depositions_Sayyah_201409.pdf

[18] W.C. Hinds Aerosol Technology: Properties, Behavior, and Measurement of Airborne Particles(second ed.), Wiley, New York (1999

[19] A.A. Hegazy Effect of dust accumulation on solar transmittance through glass covers of plate-type collectors Renew. Energy, 22 (4) (2001), pp. 525-540.

[20] O. Dupré, R. Vaillon, and M. A. Green, ‘‘Physics of the temperature coefficients of solar cells,’’ Sol. Energy Mater. Sol. Cells, vol. 140, pp. 92–100, 2015.

[21] F. Dinçer and M. E. Meral, ‘‘Critical factors that are affecting the efficiency of solar cells,’’ Smart Grid Renew. Energy, vol. 1, no. 01, p. 47, 2010.

[22] C. M. Tan, B. K. E. Chen, and K. P. Toh, ‘‘Humidity study of a-Si PV cell,’’ Microelectron. Rel., vol. 50, nos. 9–11, pp. 1871–1874, Sep. 2010.

[23] R.E. Cabanillas, H. MunguiaDust accumulation effect on the efficiency of Si photovoltaic modules. Renew. Sustain. Energy, 3 (4) (2011), p. 04311.

[24] M. R. Maghami, H. Hizam, C. Gomes, M. A. Radzi, M. I. Rezadad and S. Hajighorbani, “Power loss due to soiling on a solar panel: A review”, Renew. Sustain. Energy Rev., vol. 59, pp. 1307-1316, Jun. 2016.

[25] J. R. Caron and B. Littmann, “Direct monitoring of energy lost due to soiling on first solar modules in California”, IEEE J. Photovolt., vol. 3, no. 1, pp. 336-340, Jan. 2013.

[26] M. Tilli, M. Paulasto-Krockel, T. Motooka and V. Lindroos, Handbook of Silicon-Based MEMS Materials and Technologies, Norwich, NY, USA: William Andrew, 2015.

[27] F. Mejia, J. Kleissl and J. L. Bosch, “The effect of dust on solar photovoltaic systems”, Energy Procedia, vol. 49, pp. 2370-2376, Oct. 2014.

[28] B. R. Paudyal and S. R. Shakya, “Dust accumulation effects on the efficiency of solar PV modules for off-grid purpose: A case study of Kathmandu”, Sol. Energy, vol. 135, pp. 103-110, Oct. 2016

[29] N. Khadka, A. Bista, B. Adhikari, A. Shrestha, D. Bista and B. Adhikary, “Current Practices of Solar Photovoltaic Panel Cleaning System and Future Prospects of Machine Learning Implementation,” in IEEE Access, vol. 8, pp. 135948-135962, 2020, doi: 10.1109/ACCESS.2020.3011553

[30] M. N. Islam, M. Z. Rahman, and S. M. Mominuzzaman, ‘‘The effect of irradiation on different parameters of a monocrystalline photovoltaic solar cell,’’ in Proc. 3rd Int. Conf. Develop. Renew. Energy Technol. (ICDRET), May 2014, pp. 1–6.

[31] D. M. Tobnaghi and D. Naderi, ‘‘The effect of solar radiation and temperature on solar cells performance,’’ Extensive J. Appl. Sci., vol. 3, no. 2, pp. 39–43, 2015.

[32] R. Gottschalg, T. R. Betts, D. Infield, and M. J. Kearney, ‘‘Experimental investigation of spectral effects on amorphous silicon solar cell in outdoor operation,’’ in Proc. 29th IEEE Photovoltaic Spec. Conf., Dec. 2002, pp. 1138–1141.

[33] S. Mekhilef, R. Saidur, and M. Kamalisarvestani, ‘‘Effect of dust, humidity and air velocity on the efficiency of photovoltaic cells,’’ Renew Sustain Energy Rev., Vol. 16, no. 5, pp. 2920–2925, Jun. 2012.

[34] Ì. Portolan dos Santos and R. Räther, ‘‘Limitations in solar module azimuth and tilt angles in building-integrated photovoltaics at low latitude tropical sites in brazil,’’ Renew. Energy, vol. 63, pp. 116–124, Mar. 2014.

[35] M. Kacira, M. Simsek, Y. Babur, and S. Demirkol, ‘‘Determining optimum tilt angles and orientations of photovoltaic panels in Sanliurfa, turkey,’’ Renew. Energy, vol. 29, no. 8, pp. 1265–1275, Jul. 2004.

[36] B. A. L. Gwandu and D. J. Creasey, ‘‘Humidity: A factor in the appropriate positioning of a photovoltaic power station,’’ Renew. Energy, vol. 6, no. 3, pp. 313–316, Apr. 1995.

[37] M. K. Panjwani and G. B. Narejo, ‘‘Effect of humidity on the efficiency of solar cells (photovoltaic),’’ Int. J. Eng. Res. Gen. Sci., vol. 2, no. 4, pp. 499–503, 2014.

[38] H. A. Kazem and M. T. Chaichan, ‘‘Effect of humidity on photovoltaic performance based on an experimental study,’’ Int. J. Appl. Eng. Res., vol. 10, no. 23, pp. 43572–43577, 2015.

[39] D. Dirnberger, G. Blackburn, B. Müller, and C. Reise, ‘‘On the impact of solar spectral irradiance on the yield of different PV technology,’’ Sol. Energy Mater. Sol. Cells, vol. 132, pp. 431–442, Jan. 2015.

[40] M. T. Chaichan and H. A. Kazem, ‘‘Experimental analysis of solar intensity on photovoltaic in hot and humid weather conditions,’’ Int. J. Sci. Eng. Res., vol. 7, no. 3, pp. 91–96, 2016.

[41] J. Merten, ‘‘Clear separation of seasonal effects on the performance of amorphous silicon solar modules by outdoor I/V-measurements,’’ Sol. Energy Mater. Sol. Cells, vol. 52, nos. 1–2, pp. 11–25, Mar. 1998.

[42] Tsamaase, K.; Ramasesane, T.; Zibani, I.; Matlotse, E.; Motshidisi, K. Automated dust detection and cleaning system of PV module. IOSR J. Electr. Electron. Eng. 2017, 12, 93–98.

[43] Alghamdi, A.S.; Bahaj, A.B.S.; Blunden, L.S.; Wu, Y. Dust removal from solar PV modules by automated cleaning systems. Energies 2019, 12, 2923.

[44] M. N. Islam, M. Z. Rahman, and S. M. Mominuzzaman, ‘‘The effect of irradiation on different parameters of the monocrystalline photovoltaic solar cell,’’ in Proc. 3rd Int. Conf. Develop. Renew. Energy Technol. (ICDRET), May 2014, pp. 1–6.

[45] Ì. Portolan dos Santos and R. Räther, ‘‘Limitations in solar module azimuth and tilt angles in building-integrated photovoltaics at low latitude tropical sites in brazil,’’ Renew. Energy, vol. 63, pp. 116–124, Mar. 2014.

[46] M. Kacira, M. Simsek, Y. Babur, and S. Demirkol, ‘‘Determining optimum tilt angles and orientations of photovoltaic panels in Sanliurfa, Turkey,’’ Renew. Energy, vol. 29, no. 8, pp. 1265–1275, Jul. 2004.

[47] M. Lave and J. Kleissl, ‘‘Optimum fixed orientations and benefits of tracking for capturing solar radiation in the continental united states,’’ Renew. Energy, vol. 36, no. 3, pp. 1145–1152, Mar. 2011.

[48] B. Elhab, ‘‘Optimising tilt angles and orientations of solar panels for Kuala Lumpur, Malaysia,’’ Sci. Res. Essays, vol. 7, no. 42, pp. 3758–3765, 2012.

[49] D. Goossens and E. Van Kerschaever, ‘‘Aeolian dust deposition on photovoltaic solar cells: The effects of wind velocity and airborne dust concentration on cell performance,’’ Sol. Energy, vol. 66, no. 4, pp. 277–289, Jul. 1999.

[50] A.Solklie, M. Tasbihi, M.Kete, U.L. Stanger,. Deposition and possible influence of a self-cleaning thin Tio2/Sio2 film on a photovoltaic module efficiency, Catal. Today 252,2015, 54-60.

[51] M.R. Maghami, H.Hozam, C.Comes, M.a. Radzi, M.I. \Rezadad, S.Hajighorbani,. Power loss due to soiling on solar panel a review, Renew.Energy Rev.59,2016,1307-1316.

[52] A.Rao, R.pillai, M. Mani, P.Ramamurthy,. Influence of dust deposits on photovoltaic panel performance. Energy Procedia 54,2014,690-700.

[53] S. Mekhilef, R.Saidur, M. Kamalisarvestani,. Effect of dust, humidity and air velocity on efficiency .16 2013of photovoltaic cells. Renew, Sustain Rev.16 2012, 2920-2925.

[54] F.Mejia, j.Kleissi, J.L. Bosch. The effect of dust on solar photovoltaic systems, Energy Procedia 49 2014,2370-2376.

[55] T.Sarver, A. Al-Qaraghuli, L.L. Kamerski,. A complete review of the impact of dust on the use of solar energy, history, investigations, results, literature and mitigation approaches, Renew, sustain Energy review, 22, 2013, 68-733.

[56] K.Midtdal, B.P. Jelle. Self-cleaning glazing products state-of-the-art review and future research pathways, Sol, energy Mater, sol. cells 109,2013,126-141.

.

[57] Kai Guo, Bo Jiang, Peng Zhao, Yaping Wu, Shuang Tian, Zhiyue Gao, Lijun Zong and Shuo Yao. Review on the Superhydrophilic coating of Electric insulator 3rd International Conference on Green Energy and Sustainable Development IOP Conf. Series: Earth and Environmental Science 651 (2021) 022037 IOP Publishing doi:10.1088/1755-1315/651/2/022037.

[58] Jesus, M.A.M.L., Neto, J.T.d.S., Timò, G. et al. Superhydrophilic self-cleaning surfaces based on TiO2 and TiO2/SiO2 composite films for photovoltaic module cover glass. Appl Adhes Sci 3, 5 (2015). https://doi.org/10.1186/s40563-015-0034-4.

[59] M.Houmard, G. Berthome, J.C. Joud, and M. Langlet. Enhanced cleanability of super-hydrophilic TiO2–SiO2 composite surfaces prepared via a sol-gel route. Surface Science, Vol 605 issue 3-4 2011.pp.456-462 .

[60] Al-Housani, M.; Bicer, Y.; Koç, M. Assessment of various dry photovoltaic cleaning techniques and frequencies on the power output of CdTe-type modules in dusty environments. Sustainability 2019, 11, 2850.

[61] Mohsin, L.; Sakhrieh, A.; Aboushi, A.; Hamdan, A.; Abdelhafez, E.; Hamdan, M. Optimised cleaning and cooling for photovoltaic modules on the output performance. Therm. Sci. 2018, 22, 237–246.

[62] Ghazi, S.; Sayigh, A.; Ip, K. Dust effect on flat surfaces—A review paper. Renew. Sustain. Energy Rev. 2014, 33, 742–751.

[63] P. Vasiljev, S. Borodinas, R. Bareikis, and A. Struckas, ‘‘Ultrasonic system for solar panel cleaning,’’ Sens. Actuators A, Phys., vol. 200, pp. 74–78, Oct. 2013.

[64] X. Lu, Q. Zhang, and J. Hu, ‘‘A linear piezoelectric actuator based solar panel cleaning system,’’ energy, vol. 60, pp. 401–406, Oct. 2013.

[65] H. Kawamoto and T. Shibata, ‘‘Electrostatic cleaning system for removal of sand from solar panels,’’ J. Electrostatics, vol. 73, pp. 65–70, Feb. 2015.

[66] M. Mazumder, ‘‘Electrostatic removal of particles and its applications to self-cleaning solar panels and solar concentrators,’’ in Developments in Surface Contamination and Cleaning: Methods for Removal of Particle Contaminants. Amsterdam, The Netherlands: Elsevier, 2011, pp. 149–199.

[67] M. N. Horenstein, M. K. Mazumder, R. C. Sumner, J. Stark, T. Abuhamed, and R. Boxman, ‘‘Modeling of trajectories in an electrodynamic screen for obtaining maximum particle removal efficiency,’’ IEEE Trans. Ind. Appl., vol. 49, no. 2, pp. 707–713, Mar. 2013.

[68] G. A. Landis and P. P. Jenkins, ‘‘Dust mitigation for mars solar arrays,’’ in Proc. 29th IEEE Photovolt. Spec. Conf., 2002, pp. 812–815.

[69] M. Mazumder, M. Horenstein, J. Stark, J. N. Hudelson, A. Sayyah, C. Heiling, and J. Yellowhair, ‘‘Electrodynamic removal of dust from solar mirrors and its applications in concentrated solar power (CSP) plants,’’ in Proc. IEEE Ind. Appl. Soc. Annu. Meeting, Oct. 2014, pp. 1–7.

[70] J. Son, S. Kundu, L. K. Verma, M. Sakhuja, A. J. Danner, C. S. Bhatia, and H. Yang, ‘‘A practical super hydrophilic self-cleaning and anti-reflective surface for outdoor photovoltaic applications,’’ Sol. Energy Mater. Sol. Cells, vol. 98, pp. 46–51, Mar. 2012.

[71] G. He, C. Zhou, and Z. Li, ‘‘Review of the self-cleaning method for solar cell array,’’ Procedia Eng., vol. 16, pp. 640–645, 2011.

[72] S. M. Al-Dhaheri, L. A. Lamont, L. El-Chaar, and O. A. Al-Ameri, ‘‘Automated design for boosting offshore photovoltaic (PV) performance,’’ in Proc. IEEE PES, 2010, pp. 1–6.

[73] E. Al-Qubaisi, M. Al-Ameri, A. Al-Obaidi, M. Rabia, L. El-Chaar, and L. Lamont, ‘‘Microcontroller based dust cleaning system for a standalone photovoltaic system,’’ in Proc. Int. Conf. Electr. Power Energy Convers. Syst., 2009, pp. 1–6.

[74] C. H. Huang, M. R. Lee, Y. F. Su, C. C. Huang, Y. T. Su, W. H. Su, and F. Z. Cai, ‘‘Development of intelligent solar panel cleaning system with fuzzy logic theorem,’’ Appl. Mech. Mater., vols. 479–480, pp. 565–569, Dec. 2013.

[75] G.-C. Hsieh, L.-R. Chen, and K.-S. Huang, ‘‘Fuzzy-controlled li-ion battery charge system with active state-of-charge controller,’’ IEEE Trans. Ind. Electron., vol. 48, no. 3, pp. 585–593, Jun. 2001.

[76] Al-Rasheedi, M., Christian, A. G., Mohammad, A., Alaa, I., Jared, A., Hamad, A., Performance evaluation of a utility-scale dual-technology photovoltaic power plant at the Shagaya Renewable Energy Park in Kuwait. Renewable and Sustainable Energy Reviews, 2020. 133: p. 110139.

[77] Zaihidee, F.M., Mekhilef, S. Seyedmahmoudian, M. and Horan, B., Dust as an unalterable deteriorative factor affecting PV panel's efficiency: Why and how. Renewable and Sustainable Energy Reviews 2016. 65 (2016): p. 1267-1278.

[78] Gupta, V., Sharma, M., Pachauri, R. K., and Babu, K. N. D. , Comprehensive review on effect of dust on solar photovoltaic system and mitigation techniques. Solar Energy, 2019. 191(2019): p. 596-622.

[79] Steensma, G., Román, R., Marshall, C., Bermejo, J., Iyer, K., Al-Hajraf, S., and Al-Qattan, A., Shagaya renewable energy park project. AIP Conference Proceedings, 2019. 2126(1): p. 040003.

[80] Al-Hemoud, A., et al., Socioeconomic effect of dust storms in Kuwait. Arabian Journal of Geosciences, 2017. 10(1): p. 18.

[81] GSA. Kuwait. 2022 [cited 2022; Available from: https://globalsolaratlas.info/detail?s=29.205142,47.051536&m=bookmark&pv=ground,180,31,10000&c=29.329279,47.97781,13.

[82] Chanchangi, Y.N., et al., In-situ assessment of photovoltaic soiling mitigation techniques in northern Nigeria. Energy Conversion and Management, 2021. 244: p. 114442.

[83] R. Gottschalg, T. R. Betts, D. Infield, and M. J. Kearney, ‘‘Experimental investigation of spectral effects on amorphous silicon solar cells in outdoor operation,’’ in Proc. 29th IEEE Photovoltaic Spec. Conf., Dec. 2002, pp. 1138–1141.

[84] N. Khadka, A. Bista, B. Adhikari, A. Shrestha, and D. Bista, ‘‘Smart solar photovoltaic panel cleaning system,’’ IOP Conf. Ser., Earth Environ. Sci., vol. 463, Apr. 2020, Art. no. 012121.

Chapter 4

[1] W. Fuhs and R. Klenk, Proc. 2nd World Conference on Photovoltaic Solar Energy Conversion, Vienna, Austria, 1998, pp. 381-386.

[2] W. H. Bloss, F. Pfisterer, M. Schubert, and T. Walter, Progress in Photovoltaics: Research and Applications 3 (1995) 3.

[3] Di Piazza, M. C., & Vitale, G. (2010). Photovoltaic field emulation, including dynamic and partial shadow conditions. Applied Energy, 87(3), 814-823.

[4] Iyengar, V. V., Nayak, B. K., & Gupta, M. C. (2010a). Optical properties of silicon light-trapping structures for photovoltaics. Solar Energy Materials and Solar Cells, 94(12), 2251-2257.

[5] Iyengar, V. V., Nayak, B. K., & Gupta, M. C. (2010b). Silicon PV devices are based on a single step for doping, antireflection and surface passivation. Solar Energy Materials and Solar Cells, 94(12), 2205-2211.

[6] Tan, C. M., Chen, B. K. E., & Toh, K. P. (2010). Humidity study of an a-si PV cell. Microelectronics Reliability, 50(9–11), 1871-1874.

[7] Ravi Prakash Tiwari, Rajesh M, K. Sudhakar" Energy and energy analysis of solar photovoltaic system", 2012 Bhopal.

[8] Kazem, H.A.; Chaichan, M.T. Effect of humidity on photovoltaic performance based on experimental study. Int. J. Appl. Eng. Res. 2015, 10, 43572–43577.

[9] Kazem, H.A.; Chaichan, M.T. The effect of dust accumulation and cleaning methods on PV panels' outcomes based on an experimental study of six locations in Northern Oman. Sol. Energy 2019, 187, 30–38.

[10] D. L. Staebler and C. R. Wronski, Applied Physics Letters 31 (1977) 292.

[11] R. S. Crandall and W. Luft, Progress in Photovoltaics: Research and Applications 3 (1995) 315.

[12] F. Kampas, J. del Cueto, R. Romero, and J. Xi, Proc. AIP Conference No. 268, 1992, pp. 33-38.

[13] E. S. Sabisky, Journal of Non-Crystalline Solids 87 (1986) 43.

[14] D. Wagner, Acta Physica Austriaca 57 (1985) 251.

[15] Xiong, Z., Walsh, T. M., & Aberle, A. G. (2011). PV module durability testing under high voltage biased damp heat conditions. Energy Procedia, 8(0), 384-389.

[16] Mekhilef, S., Saidur, R., & Kamalisarvestani, M. (2012). Effect of dust, humidity and air velocity on the efficiency of photovoltaic cells. Renewable and Sustainable Energy Reviews, 16(5), 2920-2925.

[17] M.A. Quintana et al., Commonly observed degradation in field-aged PV modules, 29th Photovoltaic Specialists Conference, New Orleans, 2002; 1436.

[18] Sakamoto et al., Field Test Results on the Stability of c-Si PV Modules Manufactured in the 1990s, 3rd World Conference on Photovoltaic Energy Conversion, Osaka, Japan, 2003, 1888.

[19] J.A. del Cueto et al., Stability of CIGS Modules at the OTF over 2 Decades, 33rd Photovoltaic Specialists Conference, San Diego, 2008, 1.

[20] P. Sanchez-Friera, et al., Analysis of degradation mechanisms of crystalline silicon PV modules after 12 years of operation in Southern Europe, Progress in Photovoltaics: Research and Application 2011.

[21] A.M. Reis, et al., Comparison of PV module performance before and after 11-years of field exposure, Proceedings of the 29th Photovoltaic Specialists Conference, New Orleans, LA, USA, 2002, 1432–1435.

[22] D. Berman, et al., EVA Laminate Browning after 5 years in a Grid-connected, Mirror-assisted, Photovoltaic System in the Negev Desert: Effect on Module Efficiency, Solar Energy Materials and Solar Cells 1995, 36, 421–432.

[23] R.M. Smith et al., Outdoor PV Module Degradation of Current-Voltage Parameters, World Renewable Energy Forum, Denver, CO, USA, May 2012.

[24] A. Skoczek, et al., The Results of Performance Measurements of Field-aged Crystalline Silicon Photovoltaic Modules, Progress in Photovoltaics, 2009, 227.

[25] Sakamoto et al., Field Test Results on the Stability of c-Si PV Modules Manufactured in the 1990s, 3rd World Conference on Photovoltaic Energy Conversion, Osaka, Japan, 2003, 1888.

[26] C.E. Chamberlin, et al., Comparison of PV module performance before and after 11 and 20 years of field exposure, 37th Photovoltaic Specialists Conference, Seattle, WA, USA, 2011, 101-105.

[27] A. Skoczek, et al., The Results of Performance Measurements of Field-aged Crystalline Silicon Photovoltaic Modules, Progress in Photovoltaics, 2009, 227.

[28] S. Dubey, J.N. Sarviya, and B.seshadri. "Temperature-Dependent Photovoltaic (PV) Efficiency and its effect on PV Production in the World-A Review", Energy Procedia Vol 33, pp311-321.2013.

[29] S. Ahmed, F. Jannat, M.A.K. Khan and M.A. Alim" Numerical development of eco-friendly Cs" TiBr6 based perovskite solar cell with all-inorganic charge transports materials via SCAPS-ID", Optik, vol 225,p.165765,2021.

Chapter 5

[1] Suri, Marcel,Remund, Jan,Cebecauer, Tomas, Hoyer-Click, Carsten.Dumortier, Dominique, Huld, Thomas, Stackhouse, Pau. A simple model for estimating the influence of spectrum variations on PV performance 24th European Photovoltaic Solar Energy Conference, 21-25 September 2009, Hamburg, Germany.

[2] D. L. King, J. A. Kratochvil and W. E. Boyson, "Measuring solar spectral and angle-of-incidence effects on photovoltaic modules and solar irradiance sensors," Conference Record of the Twenty-Sixth IEEE Photovoltaic Specialists Conference - 1997, 1997, pp. 1113-1116, DOI: 10.1109/PVSC.1997.654283.

[3] Myers D. R. Emery K. Gueymard C. 2002 Terrestrial Solar Spectral Modeling Tools and Applications for Photovoltaic Devices, Proceedings of the 29th IEEEPhotovoltaic Specialists Conference, 1683 1686, 0-78037-471-1 Orleans, USA, May 2002.

[4] C.A. Gueymard, D. Myers, K. Emery, Proposed reference irradiance spectra for solar energy systems testing, Solar Energy, Volume 73, Issue 6,2002, Pages 443-467.

.

[5] Hanan Al Buflasa, Ralph Gottschalg, Tom Betts, Modeling the effect of varying spectra on multi-junction A-SI solar cells, Desalination, Volume 209, Issues 1–3,2007, Pages 78-85.

[6] J Merten, J Andreu, Clear separation of seasonal effects on the performance of amorphous silicon solar modules by outdoor I/V-measurements1This work has been financed by the project JOU2-CT92-5103 of the EU.1, Solar Energy Materials and Solar Cells, Volume 52, Issues 1–2,1998, Pages 11-25.

[7] Zanesco I. Krenziger A. 1993 The Effects of Atmospheric Parameters on the Global Solar Irradiance and the Current of a Solar Cell. Progress in Photovoltaics: Research and Applications, 1 3 July 1993.

[8] T W Cannon and RL Hulstrom, Atmospheric Optical Calibration System for Outdoor Testing of Photovoltaic Devices 1993, Metrologia 409.

[9] A.Virtuani, H.Mullejans, E.D. Dunlop.Progress in photovoltaics.Comparison of indoor and outdoor performance measurements of the recent commercially available solar module. Volume 19, Issue 1. January 2011 Pages 11-20.

[10] R. Gottschalg, D.G. Infield, M.J. Kearney, Experimental study of variations of the solar spectrum of relevance to thin-film solar cells, Solar Energy Materials and Solar Cells, Volume 79, Issue 4,2003, Pages 527-537.

[11] R. Gottschalg, T.R. Betts, D.G. Infield, M.J. Kearney, The effect of spectral variations on the performance parameters of single and double junction amorphous silicon solar cells, Solar Energy Materials and Solar Cells, Volume 85, Issue 3,2005, Pages 415-428.

[12] A.Dobbin, M.Norton, G.E.Georgiou, M.Lumb, T.N.D.Tibbits, Energy Harvest predictions for a spectrally tuned multiple quantum well device utilising measured and modelled solar spectra, AIP Conference Proceedings 1407, 21 (2011).

[13] J.H.King, N.E. Papitashvili, Solar wind spatial scales and compares hourly Wind and ACE plasma and magnetic field data. Space Physics, Volume 110, Issue A2, February 2004.

[14] T. Zdanowicz, T. Rodziewicz and M. Z. Waclawek, "Effect of air mass factor on the performance of the different type of PV modules," 3rd World Conference on Photovoltaic Energy Conversion, 2003. Proceedings of, 2003, pp. 2019-2022 Vol.2.

[15] Kenny et al., 2006, A practical method for the energy rating of C-SI photovoltaic modules based on standard tests, Progress in Photovoltaics, Volume 14 Issue 2 March 2006 pages 155-166.

[16] Grunow, P., Preiss, A., Koch, S., & Krauter, S. (2009). Yield and spectral effects of a-Si modules. In Proceedings of the 24th European Photovoltaic Solar Energy Conference (pp. 2846-2829).

[17] Yuichi Hirata, Tatsuo Tani, Output variation of photovoltaic modules with environmental factors—I. The effect of spectral solar radiation on photovoltaic module output, Solar Energy, Volume 55, Issue 6,1995, Pages 463-468,

[18] Adelstein & Sekulic, 2005, J. Adelstein and B. Sekulic, "Performance and reliability of a 1-kW amorphous silicon photovoltaic roofing system," Conference Record of the Thirty-first IEEE Photovoltaic Specialists Conference, 2005., 2005, pp. 1627-1630, doi: 10.1109/PVSC.2005.1488457.

[19] Cereghetti, N., A. Realini, D. Chianese, and S. Rezzonico. "Power and Energy production of PV modules." In 3rd World Conference on PV Energy Conversion, Osaka (J). 2003.

[20] E. D. Dunlop, D. Halton and H. A. Ossenbrink, "20 years of life and more: where is the end of life of a PV module?," Conference Record of the Thirty-first IEEE Photovoltaic Specialists Conference, 2005., 2005, pp. 1593-1596, DOI: 10.1109/PVSC.2005.1488449.

[21] C.R.Osterwald, J,Adeistein,J.A.del Cueto,W.edulic,D. Trudell, P.McNutt, R.Hanson, S.Rumel,A.Anderberg, T.Moriarty.Progress in Photovoltaics, Resistive loading of photovoltaic modules and arrays for long-term exposure testing., Volume 14 Issue 6 September 2006 pages 567-575.

[22] L. J. Caballero, P. Sanchez-Friera, B. Lalaguna, J. Alonso and M. A. Vazquez, "Series Resistance Modelling of Industrial Screen-Printed Monocrystalline Silicon Solar Cells and Modules Including the Effect of Spot Soldering, 2006 IEEE 4th World Conference on photovoltaic energy Conference,2006, pp.1388-1391, DOI:101109/WCPEC.2006.279710.

[23] A.K. Som, S.M. Al-Alawi, Evaluation of efficiency and degradation of mono- and polycrystalline PV modules under outdoor conditions, Renewable Energy, Volume 2, Issue 1,1992, Pages 85-91.

[24] G.Makrides, B.Zinsser, N.Norton, G.E.Georgiou. Performance of Photovoltaics under actual operating conditions.Third-generation photovoltaics,2012.

[25] M. A. Quintana, D. L. King, T. J. McMahon and C. R. Osterwald, "Commonly observed degradation in field-aged photovoltaic modules," Conference Record of the Twenty-Ninth IEEE Photovoltaic Specialists Conference, 2002., 2002, pp. 1436-1439, DOI: 10.1109/PVSC.2002.1190879.

[26] C.R.Wronski,Chapter 10 The Staebler-Wronski Effect,Editor(s): Jacques I. Pankove,Semiconductors and Semimetals,Elsevier,Volume 21, Part C,1984,Pages 347-374.

[27] Stutzmann, M. and Jackson, W. B. and Tsai, C. C. 1985, Light-induced metastable defects in hydrogenated amorphous silicon: A systematic study, Phys. Rev. B, volume 32, issue 1, pages 23--47,1985, Jul, American Physical Society,doi10.1103/PhysRevB.32.23.

[28] Chin K. K. Gessert T. A. Su-Huai W. 2010 The Roles of Cu Impurity States in CdTe Thin Film Solar Cells, Proceedings of the 35th IEEE Photovoltaics Specialists Conference, 1915 1918, 978-1-42445-890-5 Honolulu, USA, June 2010.

[29] Dobson K. D. Visoly-Fisher I. Hodes G. Cahen D. 2000 Stability of CdTe/CdS Thin-Film Solar Cells. Solar Energy Materials and Solar Cells, 62 3 May 2000, 295 325.

[30] Powell R.C. Sasala R. Rich G. Steele M. Bihn K. Reiter N. Cox S. Dorer G. 1996 Stability Testing of CdTe/CdS Thin-Film Photovoltaic Modules, Proceedings of the 25th IEEE Photovoltaic Specialists Conference, 785 788, 0-78033-166-4 USA, May 1996.

[31] Batzner D. Romeo A. Terheggen M. Dobeli M. Zogg H. Tiwari A. N. 2004 Stability Aspects in CdTe/CdS Solar Cells. Thin Solid Films, 451-452, March 2004, 536 543

[32] Degrave S. Nollet P. Stojanoska G. Burgelman M. Durose K. 2001 Interpretation of Ageing Experiments on CdTe/CdS Solar Cells. Proceedings of 17th International Photovoltaic Science and Engineering Conference, 1058 1061, Fukuoka, December 2007.

[33] Guillemoles J.F. Kronik L. Cahen D. Rau U. Jasenek A. Schock H.W. 2000 Stability Issues of Cu(In, Ga)Se2-Based Solar Cells. Journal of Physical Chemistry B, 104 20 April 2000, 4849 4862.

[34] Schmidt M. Braunger D. Schäffler R. Schock H. W. Rau U. 2000 Influence of Damp Heat on the Electrical Properties of Cu(In,Ga)Se2 Solar Cells. Thin Solid Films, 361-362 , February 2000, 283 287.

[35] Igalson M. Wimbor M. Wennerberg J. 2002 The Change of the Electronic Properties of CIGS Devices Induced by the Damp Heat Treatment. Thin Solid Films, 403-404, February 2002, 320 324.

[36] Malmström J. Wennerberg J. Stolt L. 2003 A Study of the Influence of the Ga Content on the Long-Term Stability of Cu(In, Ga)Se2 Thin Film Solar Cells. Thin Solid Films, 431-432 May 2003, 436 442.

[37] King D. Kratochvil J. A. Boyson W. E. 1997 Measuring the Solar Spectral and Angle of Incidence Effects on Photovoltaic Modules and Solar Irradiance Sensors, Proceedings of the 26th IEEE Photovoltaic Specialists Conference, 1113 1116, 0-78033-767-0 USA, September 1997.

[38] Pern F. J. Czanderna A. W. Emery K. A. Dhere R. G. 1991 Weather Degradation of EVA Encapsulant and the Effect of its Yellowing on Solar Cell Efficiency, Proceedings of the 22nd IEEE Photovoltaic Specialists Conference, 557 561, 0-87942-636-5 Vegas, USA, October 1991.

[39] Wenham S. R. Green M. A. Watt M. E. 2007 Applied Photovoltaics, (Second edition), Earthscan, 978-1-84407-401-3 London, UK.

[40] McMahon T.J. 2004 Accelerated Testing and Failure of Thin-film PV Modules. Progress in Photovoltaics: Research and Applications, 12 23 2004, 235 248.

[41] Carr A. J. Pryor T. L. 2004 A Comparison of the Performance of Different PV Module Types in Temperate Climates. Solar Energy, 76 1-3, January-March 2004, 285 294.

[42] Meyer E. L. van Dyk E. E. 2004 Assessing the Reliability and Degradation of Photovoltaic Module Performance Parameters.IEEE, Transactions on reliability,53,1 March 2004, pp,83-92.

[43] Osterwald C. R. Anderberg A. Rummel S. Ottoson L. 2002 Degradation Analysis of Weathered Crystalline-Silicon PV Modules, Proceedings of the 29th IEEE Photovoltaic Specialists Conference, 1392 1395, 0-78037-471-1 Orleans, USA, May 2002.

[44] Akhmad K. Kitamura A. Yamamoto F. Okamoto H. Takakura H. Hamakawa Y. 1997 Outdoor Performance of Amorphous Silicon and Polycrystalline Silicon PV Modules. Solar Energy Materials and Solar Cells, 46 3 (June 1997), 209 21.

[45] Ikisawa M. Nakano A. Igari S. Terashima H. 1998 Outdoor Exposure Tests of Photovoltaic Modules in Japan and Overseas. Renewable Energy, 14 1-4, May-August 1998, 95 100.

[46] King D. L. Kratochvil J. A. Boyson W. E. 2000 Stabilisation and Performance Characteristics of Commercial Amorphous-Silicon PV Modules, Proceedings of the 28th IEEE, Photovoltaic Specialists Conference,446 1449,0-78035-7772-8 USA, September 2000.

[47] Jordan D. C. Kurtz S. R. 2010 Analytical Improvements in PV Degradation Rate Determination, Proceedings of the 35th IEEE photovoltaic Specialist Conference, 2688 2693,978-1-42445-890 Honolulu, USA, June 2010.

[48] Thomas Huld and Ana M. Gracia Amillo. Estimating PV Module Performance over Large Geographical Regions: The Role of Irradiance, Air Temperature, Wind Speed and Solar Spectrum Energies 2015, 8, 5159-5181; doi:10.3390/en8065159 OPEN ACCESS energies ISSN 1996-1073 www.mdpi.com/journal/energies Article.

Chapter 6

[1] Masters GM. Renewable and efficient electric power systems. Wiley-IEEE Press, ISBN 978-0-471-28060-6; 2004

[2] The Interplay of Contact Layers: How the Electron https://pubs.acs.org/doi/suppl/10.1021/acs.jpclett.8b02824/suppl_file/jz8b02824_si_001.pdf.

[3] Kalaitzakis K. Optimal PV system dimensioning with obstructed solar radiation. Renew Energy 1996;7(1):51-6.

[4] Shuhui Li, Timothy A. Haskew LI, Fei HU. Integrating photovoltaics and power converters characteristics for energy extraction study of solar PV systems.

[5] Badescu V. Simple optimisation procedure for silicon-based solar cell interconnection in a series-parallel PV module. Energy Conversion Manage 2006; 47:1146-58.

[6] Lorenzo E, Araujo G, Cuevas A, Egido M, Miñano J, Zilles R. Solar electricity: engineering of photovoltaic systems. Progensa; 1994.

[7] Cabrera-Tobar, A.; Bullich-Massagué, E.; Aragüés-Peñalba, M.; Gomis-Bellmunt, O. Topologies for large scale photovoltaic power plants. Renew. Sustain. Energy Rev. 2016, 59, 309–319.T.

[8] D. Pal, H. Koniki, P. Bajpai. Central and Micro Inverters for Solar Photovoltaic Integration in AC grid. Proceeding of 2016 National Power Systems Conference (NPSC), Bhubaneswar, 2016, pp. 1-6.

[9] H. A. Sher, and K. E. Addoweesh. Micro-inverter-promising solutions in solar photovoltaics. Energy for Sustainable Development, vol. 16(4), pp. 389-400, 2012.

[10] D. M. Lee, and B. W. Raichle. A side by side comparison of micro and central inverters in shaded and unshaded conditions. World Renewable Energy Forum, V 1, PP 35-39, Denver, USA, 2012.

[11] F. Famosoa, R. Lanzafamea, S.Maenzaa, P. F. Scandura. Performance comparison between micro-inverter and string-inverter. Proceedings of 69th Conference of the Italian Thermal Engineering Association, ATI 2014, Energy Procedia Photovoltaic Systems, vol. 81, pp. 526-539.

[12] E. Kabalci, Y. Kabalci and G. Gokkus. Dual DC-DC converter design for string inverters used in solar plants. Proceedings of International Conference on Renewable Research and Applications (ICRERA), Palermo, 2015, pp. 115-119.

[13] Z. Čorba, B. Popadić, V. Katić, B. Dumnić and D. Milićević. Future of high power PV plants — 1500V inverters. Proceedings of International Symposium on Power Electronics (Ee), Novi Sad, Serbia, 2017, pp. 1-5.

[14] K. D. Papastergiou, P. Bakas and S. Noriega. Photovoltaic string configuration for optimal inverter performance. Proceeding of 8th IEEE International Conference on Power Electronics - ECCE Asia, Jeju, South Korea, 2011, pp. 1632-1636.

[15] Nicola Femia. Power Electronics and Control Techniques for Maximum Energy Harvesting in Photovoltaic Systems. CRC Press Taylor & Francis, London, New York, 2013.

[16] A. Durgadevi, S. Arulselvi and S. P. Natarajan. Study and implementation of Maximum Power Point Tracking (MPPT) algorithm for Photovoltaic systems. Proceeding of 1st International Conference on Electrical Energy Systems, Newport Beach, CA, USA, 2011, pp. 240-245.

[17] Freijedo et al.. Grid synchronisation methods for power converters. Proceedings of IEEE 35th Industrial Electronics Conference (IECON), pp. 522-529, Porto, Portugal, Nov. 2009.

[18] Haitham Abu-Rub, Mariusz Malinowski, Kamal Al-Haddad. Power Electronics for Renewable Energy Systems, Transportation, and Industrial Applications. ISBN: 9781118755501, IEEE Press and John Wiley & Sons Ltd, 2014.

[19] Vu Minh Phap, N. Yamamura, M. Ishida, J. Hirai and N. T. Nga. Design of novel grid-tied solar - Wind hybrid power plant using photovoltaic cell emulating system. Proceedings of IEEE International Conference on Sustainable Energy Technologies (ICSET), Hanoi, Vietnam, 2016, pp. 186-189.

[20] Vu Minh Phap, N. Yamamura, M. Ishida et al. Study on Novel Topology of Solar–Wind Hybrid Power Plant Using Photovoltaic Cell Emulating System. Journal of Electrical Engineering & Technology, Vol 14(2), pp.627-634, 2019..

[21] https://www.ijsr.net/archive/v8i10/ART20201812.pdf.

[22] Kjar, S.B., Pederson, J.K., Blaabjerg, F., A review of simple phase grid-connected inverters for photovoltaic modules. IEE Transcription on Industrial application 41, 1292-1306.

[23] Ying-Tung Hsiao and China-Hong Chen, “Maximum power tracking for photovoltaic power system,” Conference Record of the 2002 IEEE Industry Applications Conference. 37th IAS Annual Meeting (Cat. No.02CH37344), Pittsburgh, PA, USA, 2002, pp. 1035-1040 vol.2, doi: 10.1109/IAS.2002.1042685

[24] https://firstgreenconsulting.wordpress.com/2012/04/25/what-type-of-inverter-systems-used-in-solar-power-plants/

[25] https://www.electronics-notes.com/articles/electronic_components/electrical-electronic-relay/solid-state-relay-switch.php.

[26] Annual report, photovoltaic industry association, EPIA; 2012.

[27] https://documents.worldbank.org/curated/en/868031468161086726/text/667620WP00PUBL005B0SOLAR0GUIDE0BOOK.txt

[28] Modelling of Doubly Fed Induction Generation (DFIG) Converter Controls Lingling Fan, Zhixin Miao, in Modelling and Analysis of Doubly Fed Induction. Generator Wind Energy Systems, 2015.

[29] Kjaer SB, Pedersen JK, Blaabjerg F. A review of single-phase grid-connected inverters for photovoltaic modules. IEEE Trans Ind Appl 2005;41(5).

[30] https://documents.worldbank.org/curated/en/868031468161086726/text/667620WP00PUBL005B0SOLAR0GUIDE0BOOK.txt

[31] Tse KK, Ho MT, Henry, Chung SH, Hui SY. A novel maximum power point tracker for PV panels using switching frequency modulation. IEEE Trans Power Electronics 2002;17(6):980e9.

[32] Veerachary M, SenjyuT, Uezato K. Maximum power point tracking control of IDB converter supplied PV system. IEE Proc Electr Power Appl 2001;148(6):494e502.

[33] Moreno JC, Espí Huerta JM, Gil RG, González SA. A robust predictive current control for three-phase grid-connected inverters. IEEE Trans Ind Electronics October 2009;56(No. 6):1993e2004.

[34] Rodriguez J, Pontt J, Silva CA, Correa P, Lezana P, Cortes P, Ammann U. Predictive current control of a voltage source inverter. IEEE Trans Ind Electronics Feb. 2007;54(No. 1):495e503.

[35] Casaro MM, Martins DC. Behaviour matching technique applied to a three-phase grid-connected PV system. In: Proceedings of IEEE International Conference on Sustainable Energy Technologies. Singapore: ICSET 2008; Nov. 24-27, 2008.

[36] Hua C, Lin J, Shen C. Implementation of a DSP controlled photovoltaic system with peak power tracking. IEEE Trans Ind Electronics Feb 1998;45 (No. 1):99-107.

[37] Femia N, Petrone G, Spagnuolo G, Vitelli M. Optimization of perturb and observe maximum power point tracking method. IEEE Trans Power Electronics July 2005;20(No. 4):963-73.

[38] Hussein KH, Muta I, Hoshino T, Osakada M. Maximum photovoltaic power tracking: an algorithm for rapidly changing atmospheric conditions. IEE Proceedings-Generation, Transm Distribution Jan 1995;142(No. 1):59e64.

[39] Veerachary M, Senjyu T, Uezato K. Voltage-based maximum power point tracking control of PV system. IEEE Trans Aerospace Electronic Syst Jan. 2002; 38(No. 1):262e7.

[40] Tafticht T, Agbossou K, Doumbia ML, Chériti A. An improved maximum power point tracking method for photovoltaic systems. Renewable Energy July 2008; 33(No. 7):1508e16.

[41] Moreno JC, Espí Huerta JM, Gil RG, González SA. A robust predictive current control for three-phase grid-connected inverters. IEEE Trans Ind Electronics October 2009;56(No. 6):1993e2004.

[42] Rodriguez J, Pontt J, Silva CA, Correa P, Lezana P, Cortes P, Ammann U. Predictive current control of a voltage.

[43] Mullane A, Lightbody G, Yacamini R. Wind-turbine fault ride-through enhancement. IEEE Trans Power Syst Nov. 2005;20(No. 4).

[44] Li S, Haskew TA. Transient and steady-state simulation of Decoupled d-q vector control in PWM converter of variable speed wind turbines. In: Proceedings of 33rd Annual Conference of IEEE Industrial electronics. Taipei, Taiwan: IECON 2007; Nov. 5e8, 2007.

[45] Li S, Haskew TA, Jackson J. Power generation characteristic study of integrated DFIG and its frequency converter. Renewable Energy (Elsevier) Jan. 2010; 35(No. 1):42e51.

Chapter 7

[1] UN. Climate change COP26. 2022[cited 2022 15/03.2022].Available from: https//www.un.org/en/climatechange/cop26

[2] Renewablesnow. Kuwait considers 5GW solar project report 2020.

[3] Ghanchangi, Y.N., Ghost, A., Sundaram, S., and Mallick, T.K. Dust and PV Performance in Nigeria: A review Renewable and Sustainable Energy Reviews 2020.121(2020):p.1

[4] Maghamia, M.R., Hizama, H., Gomes, C., Radzi, M. A., Rezadad, M.I., and Hajighorbani.S., Power loss due to soiling on solar panel: A review Renewable and Sustainable Energy Reviews 2016 59(2016):p. 1307-1316 .

[5] Al-Rasheedi. M., Christan, A.G., Mohammad. A., Alaa, I., Jared. A., Hamad.A., Performance evaluation of a utility-scale dual –technology photovoltaic power plant at the Shagaya Renewable Energy Park in Kuwait Renewable and Sustainable Energy Reviews 2020.133:p.110139 .

[6] Zaihidee, F.M., Mekhilef, S., Seyedmahmoudian, M., and Horan. B. Dust as an unalterable deteriorative factor affecting PV panel's efficiency: why and how. Renewable and Sustainable Energy Reviews 2016.65(2016): p 1267=1278.

[7] Gupta, V., Sharma, M., Pachauri, R.K., and Babu, K.N.D. Comprehensive review on effects of dust on solar photovoltaic systems and mitigation techniques, Solar Energy 2019.191(2019):p.592-622

[8] Steensma, G., Roman, R.,Marshall, C.,Bermejo, J., Iyer,K.,Al-Hajraf, S., and Al-Qattan, A. Shagaya renewable energy park project AIP Conference Proceeding , 2019.2126(1):p.040003.

[9] Al-Hemoud, A., et al., Socioeconomic effect of dust storms in Kuwait Arabian Journal of Geosciences.2017.10 (1):p.18.

[10] Ghosh, A., Soiling losses: A Barrier for India's Energy Security Dependency from Photovoltaic Power. Challenges.2020.11 (1):p.9

[11] Lude, S., et al., Optimisation of the Technology Mix for the Shagaya 2 GW Renewable Energy Park in Kuwait. Energy Procedia.2015.69:p.163-16.

[12] GSA. Kuwait 2022{cited 2022; available from: https://globalsalaratlas.info/details?s=29.205142.47.051536&m=bookmark&pv=ground.180.31.10000&c=29.239279.47.97781.13

[13] Chanchangi, Y.N., et al., In-situ assessment of photovoltaic soiling mitigation techniques in northern Nigeria, Energy Conversion and Management. 2021.244:p.114442.